



Towards minimally invasive delivery of large molecules into human T cells by photoporation with polydopamine nanosensitizers and photothermal nanofibers

Dominika Berdecka

Thesis submitted to obtain the degree of
Doctor in Pharmaceutical Sciences at Ghent University
and Doctor in Biomedical Sciences at the University of Antwerp

2023

Promotors

Prof. dr. Kevin Braeckmans (Ghent University)

Prof. dr. ir. Winnok De Vos (University of Antwerp)

Members of the Exam Committee

Prof. dr. Aurélie Crabbé (Chair)	Ghent University
Prof. dr. Koen Raemdonck (Secretary)	Ghent University
Prof. dr. Guy Caljon	University of Antwerp
Prof. dr. Nathalie Cools	University of Antwerp
Prof. dr. Peter Dubrueel	Ghent University
Prof. dr. Alain Labro	Ghent University

TABLE OF CONTENTS

List of abbreviations		1
Aims and outline of this thesis		5
Chapter 1	Non-viral delivery of RNA for therapeutic T cell engineering <i>ex vivo</i>	9
Chapter 2	Delivery of macromolecules in unstimulated T cells by photoporation with polydopamine nanoparticles	89
Chapter 3	Photothermal nanofibers enable macromolecule delivery in unstimulated human T cells	135
Chapter 4	Broader international context, relevance and future perspectives	177
Summary and conclusions		221
Samenvatting en conclusies		225
Curriculum vitae		230

LIST OF ABBREVIATIONS

μVS	Microfluidic vortex shedding
ACT	Adoptive T cell therapy
ALL	Acute lymphoblastic leukemia
AML	Acute myeloid leukemia
APC	Antigen-presenting cell
ASM	Acid sphingomyelinase
ASO	Antisense oligonucleotide
ATP	Adenosine triphosphate
AuNP	Gold nanoparticle
B2M	β-2 microglobulin
BCMA	B-cell maturation antigen
BSA	Bovine serum albumin
CAR	Chimeric antigen receptor
CART	Charge-altering releasable transporter
Cas9	CRISPR-associated 9
CCR-4	CC-chemokine receptor 4
CD	Cluster of differentiation
cGMP	Current good manufacturing practice
CLL	Chronic lymphocytic lymphoma
CRISPR	Clustered regularly interspaced short palindromic repeats
crRNA	CRISPR RNA
CRS	Cytokine release syndrome
CTL	Cytotoxic T lymphocyte
CTLA-4	Cytotoxic T-lymphocyte associated protein 4
CXCR2	C-X-C motif chemokine receptor 2
DAMP	Danger-associated molecular pattern
DC	Dendritic cell
dCas9	Dead Cas9
DLBCL	Diffuse large B-cell lymphoma
DLS	Dynamic light scattering
DNA	Deoxyribonucleic acid
DPBS-	Dulbecco's phosphate-buffered saline without Ca ²⁺ /Mg ²⁺
DSB	Double strand break
e.g.	<i>Exempli gratia</i>
EMA	European medicines agency
FAP	Fibroblast activation protein
FBS	Fetal bovine serum
FD	FITC dextran

FD150	FITC dextran 150 kDa
FD500	FITC dextran 500 kDa
FDA	Food and Drug Administration
FITC	Fluorescein isothiocyanate
GPC-2	Glypican 2
gRNA	Guide RNA
GvHD	Graft-versus-host-disease
HDR	Homology-directed repair
HLA	Human leukocyte antigen
HSPG	Heparan sulfate proteoglycan
ICANS	Immune effector cell-associated neurotoxicity syndrome
ICP-MS/MS	Inductively coupled plasma-tandem mass spectrometry
<i>i.e.</i>	<i>Id est</i>
IFNγ	Interferon γ
IL	Interleukin
IONP	Iron oxide nanoparticle
IMDM	Iscove's modified dulbecco's medium
ITAM	Immunoreceptor tyrosine-based activation motif
ITR	Inverted terminal repeat
IVT	<i>In vitro</i> transcribed
kDa	Kilodalton
LAG-3	Lymphocyte-activation gene 3
LBCL	Large B cell lymphoma
LNP	Lipid nanoparticle
MCL	Mantle cell lymphoma
MFI	Mean fluorescence intensity
MHC	Major histocompatibility complex
MM	Multiple myeloma
mRNA	Messenger RNA
NA	Numerical aperture
NHEJ	Non-homologous end joining
NLS	Nuclear localization sequence
NY-ESO1	New York esophageal squamous cell carcinoma 1
ORF	Open reading frame
P/S	Penicillin/streptomycin
PBAE	Poly(β -amino ester)
PBMC	Peripheral blood mononuclear cell
PCL	Polycaprolactone
PD-1	Programmed cell death protein 1
PD-L1	Programmed death ligand 1
PDDAC	Poly(diallyldimethylammoniumchloride)

pDMAEMA	Poly(2-dimethylaminoethyl methacrylate)
pDNA	Plasmid DNA
PEG	Polyethylene glycol
PEI	Poly(ethyleneimine)
PEN	Photothermal electrospun nanofiber
PM	Plasma membrane
PPR	Pattern recognition receptor
PSMA	Prostate-specific membrane antigen
r/r	Relapsed/refractory
RNA	Ribonucleic acid
RNP	Ribonucleoprotein
rpm	Rotations per minute
RT	Room temperature
saRNA	Self-amplifying mRNA
scFv	Single-chain variable fragment
SD	Standard deviation
SEM	Scanning electron microscopy
sgRNA	Single guide RNA
siRNA	Small interfering RNA
TAA	Tumor associated antigen
TALEN	Transcription activator-like effector nucleases
TCR	T cell receptor
TETAR	T cell expressing two additional receptors
TGFβ	Transforming growth factor β
TIGIT	T cell immunoreceptor with immunoglobulin and ITAM domain
TIL	Tumor-infiltrating lymphocyte
TIM-3	T-cell immunoglobulin and mucin-domain containing 3
TME	Tumor microenvironment
TNFα	Tumor necrosis factor α
TRAC	T cell receptor alpha chain constant
tracrRNA	Trans-activating crRNA
TRUCK	T cell redirected for universal cytokine killing
UTR	Untranslated region
VECT	Volume exchange for convective transfer
VNB	Vapor nanobubble
ZFN	Zinc-finger nuclease

AIMS AND OUTLINE OF THIS THESIS

Cancer represents a heterogeneous group of diseases characterized by the uncontrolled growth of malignant cells that have the potential to spread to distant sites in the body. With over 19 million new cases yearly, cancer ranks as a leading cause of death worldwide, posing a major health and economic concern. Conventional treatment modalities, such as surgery, chemotherapy, radiotherapy and targeted therapy, have been recently reinforced by cancer immunotherapy, which harnesses the power of the immune system to recognize and eliminate malignant cells. Given the central role of T cells in tumor antigen recognition and cell-mediated immunity, adoptive T cell transfer has emerged as an effective strategy to unleash anti-tumor responses. Among engineered T cell therapeutics, chimeric antigen receptor (CAR) T cells represent the most advanced modality, with remarkable clinical responses achieved in patients with certain types of B cell malignancies leading to the regulatory approval of six CAR T cell therapies.

In this approach, T cells are isolated from the patient's peripheral blood and genetically modified to express a tumor antigen-specific receptor before re-infusion in the patient to mediate tumor eradication. Despite the great potential of T cell-based therapies to transform cancer care, *ex vivo* T cell engineering presents unique challenges related to the therapeutic efficacy after adoptive cell transfer, including limited durability of patient response, poor efficacy in solid tumors and toxicities, as well as specific drawbacks of viral-vector based manufacturing, such as safety and regulatory concerns and prohibitive costs. As such, multiple strategies have been developed to modulate CAR T cell potency through the optimization of manufacturing protocols and sophisticated engineering designs, while non-viral transfection approaches have been actively investigated as safe, flexible and sustainable alternatives for the delivery of therapeutic cargo. Among those non-viral technologies, photoporation is an upcoming physical delivery method that combines photo-responsive nanomaterials and laser irradiation to achieve transient membrane permeabilization by distinct photothermal effects, allowing external effector molecules to enter the cell. In this PhD thesis, we investigate the applicability of photoporation for intracellular delivery in unstimulated human T cells.

Compared to their stimulated counterparts, resting T lymphocytes are smaller, non-dividing, displaying lower metabolic rates and generally less susceptible to genetic manipulation, making the activation step a common prerequisite for effective T cell modification for immunotherapies. However, T cell activation triggers their differentiation program, with prolonged *ex vivo* expansion resulting in exhausted phenotypes characterized by impaired anti-tumor activity and limited persistence *in vivo*. In contrast, CAR T cell products enriched in less differentiated subsets are endowed with superior anti-tumor potency, correlating with robust *in vivo* expansion and persistence, thus generating increasing interest in protocols which can retain such minimally differentiated cells. In this study, we compare photoporation performance in resting and pre-activated T cell models. In addition, we study the impact of photoporation treatment on cell phenotype and functionality, in light of future technology translation.

In **Chapter 1**, we provide a general introduction to engineered T cell therapy, giving an overview of the progress made to date and the remaining challenges to increase CAR T cell therapeutic efficacy in a broader range of malignancies, including solid tumors. We describe state-of-the-art CAR T cell manufacturing with viral vectors, pointing out existing limitations that have prompted the growing interest in alternative non-viral T cell engineering approaches. Next, we focus on RNA therapeutics as a safe and versatile tool to modulate T cell phenotype and functionality in next-generation T cell therapies. We first characterize different classes of RNA molecules, highlighting manufacturing advancements enabling their therapeutic applications and existing barriers to effective intracellular delivery. This is followed by an extensive overview of current and emerging delivery technologies for RNA transfection in T cells, including membrane disruption-based and carrier-mediated methods. Finally, we elaborate on specific applications of RNA molecules in preclinical and clinical investigations of engineered T cell therapies.

Traditionally, photoporation has relied on the use of metallic nanoparticles (NPs), with gold nanoparticle (AuNP)-mediated photoporation showing successful delivery of various cargo molecules in immortalized Jurkat cells and primary murine and human lymphocytes. However, AuNPs are known to fragment under intense laser illumination into smaller nanometer-size particles that may intercalate with cellular DNA, thus posing the risk of genotoxicity. In addition, the non-biodegradable nature of AuNPs presents safety and

regulatory hurdles for the clinical translation of nanoparticle-mediated photoporation. To address these concerns, we have developed an alternative nanosensitizer based on biocompatible and biodegradable polydopamine nanoparticles (PDNPs), which can be synthesized from clinically approved precursors and easily functionalized, while exhibiting excellent photothermal conversion properties over a broad spectral range. In **Chapter 2**, we evaluate the applicability of PDNP-sensitized photoporation for intracellular delivery of model FITC-dextran 500 kDa (FD500) in unstimulated and expanded primary human T cells. We first optimize photoporation settings by screening different sizes and concentrations of PDNPs and laser fluences, identifying parameters resulting in optimal delivery yields. For the optimized conditions, we next investigate cell functionality by studying the propensity of quiescent T cells to become activated after photoporation treatment.

As an alternative solution to alleviate the regulatory concerns over cell exposure to free nanoparticles, we developed a photothermal system where iron oxide nanoparticles (IONPs) are embedded in polycaprolactone-based nanofiber meshes fabricated by electrospinning. Laser irradiation of cells collected on such photothermal electrospun nanofiber (PEN) substrates permits the effective transfer of photothermal effects to transiently permeabilize cell membranes to deliver exogenous cargo, while direct exposure of cells to NPs is eliminated. In **Chapter 3**, we evaluate the applicability of PEN photoporation for intracellular delivery of model FITC-dextran 150 kDa (FD150) in unstimulated and pre-activated human T cells. We first investigate potential IONP release from nanofibers using inductively coupled plasma tandem mass spectrometry. Next, we optimize photoporation protocol by testing substrates with varying IONP content and different laser fluences. Finally, we investigate the functional consequences of applying different irradiation parameters by analyzing unstimulated T cell propensity to activation after PEN treatment.

Finally, in **Chapter 4**, we describe the current landscape of T cell-based therapeutics and the remaining challenges that the field needs to address to enable their wider adoption in clinical practice. Next, we discuss potential strategies to augment T cell therapeutic activity by optimizing culturing protocols and combinatorial engineering designs. In the second part, we outline future directions to overcome manufacturing limitations, focusing

on the prospects of non-viral intracellular delivery methods and reflecting on the potential of photoporation technology evaluated in this dissertation.

Chapter 1

Non-viral delivery of RNA for therapeutic

T cell engineering *ex vivo*

An adapted version of this chapter is being prepared for submission as:

Dominika Berdecka^{a,b}, Stefaan C. De Smedt^a, Winnok H. De Vos^b and Kevin Braeckmans^{a,d}.
Non-viral delivery of RNA for therapeutic T cell engineering *ex vivo*.

Prepared for submission in *Advanced Drug Delivery Reviews*.

^a Laboratory of General Biochemistry and Physical Pharmacy, Faculty of Pharmaceutical Sciences, Ghent University

^b Laboratory of Cell Biology and Histology, Department of Veterinary Sciences, University of Antwerp

Author contributions: D.B. performed the literature search, wrote the review article and made the figures. S.D.S., W.D.V. and K.B. reviewed the article.

Table of Contents

Abstract.....	12
1 Introduction.....	13
1.1 Introduction to adoptive T cell therapy	13
1.2 T cell engineering with viral vectors	18
1.3 The potential of RNA to engineer therapeutic T cells.....	20
2 Classes of RNA molecules and manufacturing advancements towards clinical translation.....	21
2.1 Antisense oligonucleotides	21
2.2 Small interfering RNA.....	22
2.3 CRISPR-based gene editing	23
2.4 Aptamers.....	26
2.5 Messenger RNA.....	26
3 Non-viral delivery platforms for RNA therapeutics.....	31
3.1 Membrane-disruption based delivery methods	31
3.1.1 Electroporation	31
3.1.2 Microfluidic cell squeezing.....	35
3.1.3 Solvent-based poration.....	38
3.1.4 Photoporation.....	38
3.1.5 Nanostructures	41
3.2 Carrier-mediated delivery systems	42
3.2.1 Lipid-based nanoparticles.....	43
3.2.2 Polymer-based nanoparticles	46
4 Applications of RNA therapeutics in T cell engineering	48
4.1 Engineering cancer specific T cells	48
4.2 Gene editing for enhancing T cell function	54
4.3 Other strategies to modulate T cell functionality	58
5 Conclusions ant outlook	60
References	64

Abstract

Adoptive T cell transfer has demonstrated remarkable clinical success in the treatment of hematological malignancies, leading to a growing list of FDA-approved chimeric antigen receptor (CAR)-engineered T cell therapies. However, the therapeutic efficacy for solid tumors remains unsatisfactory, highlighting the need for refined T cell engineering strategies and combinatorial approaches. To date, CAR T cell manufacturing relies primarily on gammaretroviral and lentiviral vectors owing to their high transduction efficiency. However, their use is associated with safety concerns, high cost of cGMP-compliant production, regulatory hurdles and restricted cargo capacity, hindering broader application of engineered T cell therapies. To overcome these limitations, non-viral approaches, including membrane permeabilization and carrier-mediated methods, have been investigated as a more versatile and sustainable alternative for next-generation T cell engineering. Non-viral delivery methods can be designed to deliver a broad range of payload molecules, including RNA which enables more controlled and safe modulation of T cell phenotype and functionality. In this chapter, we provide an overview of non-viral delivery of RNA in adoptive T cell therapy. We first define different classes of RNA therapeutics, highlighting manufacturing advancements towards their therapeutic application, after which we discuss the challenges to achieving effective RNA delivery in T cells. Next, we provide an overview of current and emerging delivery technologies for RNA transfection of T cells. Finally, we discuss ongoing preclinical and clinical investigations with RNA-modified T cells.

1 Introduction

1.1 Introduction to adoptive T cell therapy

Cancer is a complex disease characterized by the uncontrolled growth of malignant cells that have the potential to invade neighboring tissues or spread to distant sites in the body. With an estimated 19.3 million new cases in 2020, cancer ranks second among the leading causes of death worldwide, accounting annually for 10 million, or one in six, deaths ¹. Despite the tremendous progress in the field of cancer biology, the genetic and phenotypic diversity of the disease often underlies its resistance to treatment. While conventional treatment strategies, such as surgery, radiation, chemotherapy and targeted therapy have proven highly beneficial in managing primary tumors, treating metastatic or relapsed/refractory (r/r) cancers remains a significant challenge. Over the past years, immunotherapy has instigated a revolution in oncology by exploiting the inherent ability of the immune system to recognize and destroy cancer cells, and has become the fifth pillar of cancer treatment^{2,3}. Several approaches to unleash natural defense responses against immune-evasive cancer cells have been exploited, including cytokine therapies, immune checkpoint inhibition, cancer vaccination and adoptive cell transfer ^{2,4}. In particular, antibody therapies targeting immune checkpoints such as programmed cell death protein 1 (PD-1) and its ligand (PD-L1) or cytotoxic T lymphocyte associated protein 4 (CTLA-4) have proven an effective strategy to overcome peripheral tolerance by removing the breaks on T cell activation and enhancing antigen-specific responses ⁵.

Given the central role of T lymphocytes in tumor antigen recognition and cell-mediated immunity, adoptive T cell transfer has emerged as an alternative treatment modality ⁶. Three main adoptive T cell therapy types can be distinguished: tumor-infiltrating lymphocytes (TILs), T cell receptor (TCR)-engineered T cells and chimeric antigen receptor (CAR)-engineered T cells ⁷⁻⁹. In TIL treatment, lymphocytes that have infiltrated tumor tissue are isolated from a cancer biopsy, expanded *in vitro* and re-infused into the patient in high numbers ¹⁰. Despite initial promising outcomes in patients with metastatic melanoma, TIL therapy has been limited by difficulties with cell isolation, insufficient expansion of cells, and modest antitumor effects due to the scarcity of tumor-reactive T cells and their limited persistence *in vivo* ¹¹⁻¹³. Consequently, the focus has shifted to

genetically engineered approaches, where peripheral blood lymphocytes are first isolated from blood samples in a process called leukapheresis and then reprogrammed *ex vivo* to effectively target cancer cells (**Figure 1**). Besides redirecting T cell specificity by expressing tumor antigen-specific receptors, T cells can be additionally engineered to enhance their antitumor efficacy and improve their safety for potential use in allogeneic applications^{14–17}. Next, the engineered T cells are expanded to achieve therapeutically required doses, while the patient undergoes a lymphodepleting chemotherapy, which eliminates endogenous T cells and increases systemic levels of T cell-stimulating cytokines, augmenting the *in vivo* expansion of subsequently transferred lymphocytes^{18–20}.

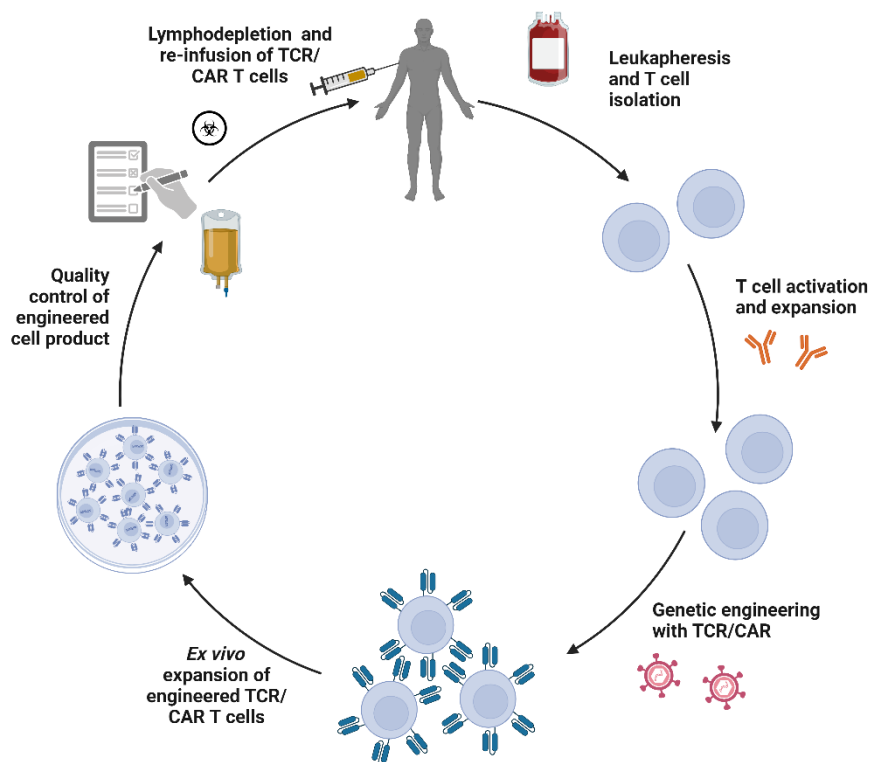


Figure 1. Schematic overview of an autologous adoptive T cell therapy. Leukocytes are isolated from the patient’s blood via leukapheresis and activated with anti-CD3/CD28 antibodies. Next, T cells are engineered to express *e.g.*, a T cell receptor (TCR) or chimeric antigen receptor (CAR) by viral transduction or non-viral transfection. Modified cells are then expanded to therapeutic T cell doses and undergo a quality control. Finally, the patient receives lymphodepleting chemotherapy before being infused with an engineered T cell product.

T cell receptors are heterodimers composed of α and β chains that recognize antigens presented by the major histocompatibility complex (MHC) and subsequently associate with CD3 subunits to form a functional CD3-TCR complex and initiate T cell activation. In engineered T cell therapy, antigen-binding domains of TCR α and β chains are modified to redirect T cell specificity toward an antigen of interest (**Figure 2**)^{9,21}. The repertoire of targetable antigens includes peptides derived from both intracellular and membrane proteins presented by human leukocyte antigen (HLA) class I and class II, respectively. However, since HLA encoding genes are the most polymorphic in the human genome, MHC-matching can be extremely complex and restrict the number of patients who can benefit from a given TCR-engineered T cell therapy²². Another challenge is α/β chain mispairing between transgenic and endogenous TCR chains, leading to nonfunctional complexes or the generation of new TCRs with autoimmune specificity^{23,24}. In addition, competition with mispaired and endogenous TCRs for association with a limited amount of CD3 components may further reduce the expression of engineered TCRs²⁵. Despite their ability to target both intracellular and surface antigens, the number of targets for TCR T cell therapy identified with sufficient safety and efficacy remains limited^{9,26}. Most clinical trials to date have evaluated cancer-testis antigens, with New York esophageal squamous cell carcinoma 1 (NY-ESO1)-targeted T cells demonstrating objective clinical responses in patients with refractory melanoma, synovial cell sarcoma and multiple myeloma²⁷⁻²⁹.

To overcome limitations imposed by the HLA-restriction of TCRs, synthetic CARs have been designed to direct T cell specificity to virtually any target on the surface of malignant cells independently of the MHC presentation. The CAR structure has a modular design consisting of an antigen-binding domain (most often a single-chain variable fragment derived from a monoclonal antibody, scFv), hinge, transmembrane domain and intracellular signaling domain (**Figure 2**). The first generation of CAR T cells comprised an extracellular antibody scFv coupled to a CD3 ζ -signaling domain³⁰⁻³². However, this design proved ineffective in clinical trials due to limited T cell proliferation and cytokine production³³. This led to the incorporation of one or multiple costimulatory molecules such as CD28, 4-1BB (CD137) or OX40 (CD134) in the second and third generation CARs, respectively, providing additional signals necessary for T cell activation³⁴⁻³⁸. Subsequent

generations of CAR T cells feature further modifications aimed at improved anti-tumor efficacy. For instance, fourth generation (TRUCKs or armored CARs) have been engineered to release proinflammatory cytokines such as IL-12 upon CAR engagement in tumor lesions for modulating the immunosuppressive tumor microenvironment ³⁹. The fifth generation construct incorporated truncated cytoplasmic IL-2 receptor domain and STAT-3 binding moiety to promote activation-dependent JAK-STAT signaling and enhance cell proliferation ⁴⁰.

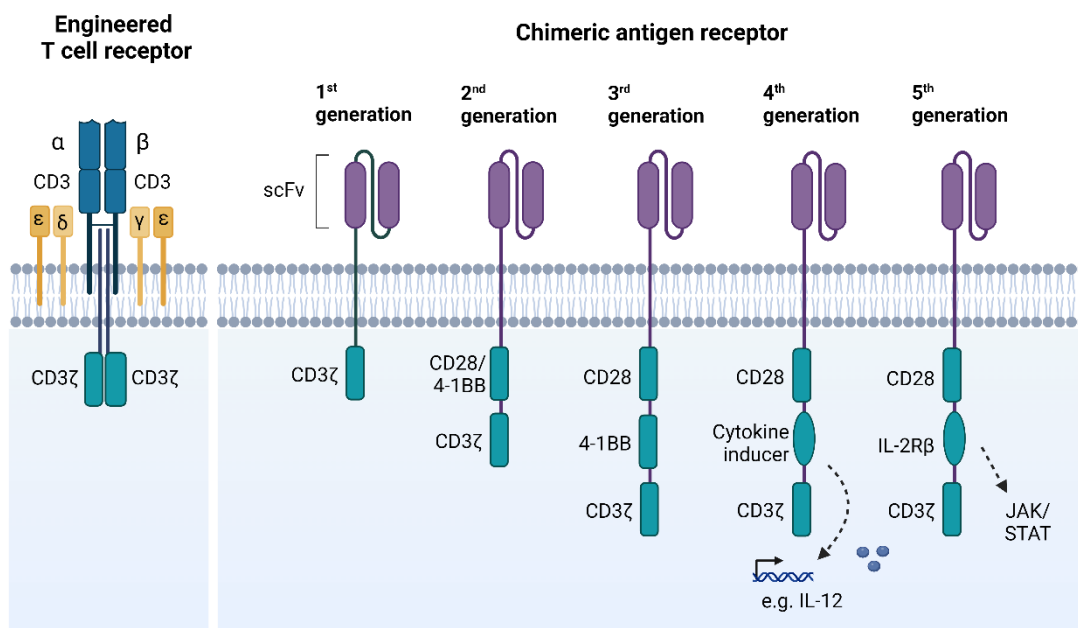


Figure 2. Schematic illustration of an engineered T cell receptor and the evolving designs of chimeric antigen receptors. The TCR complex comprises paired α and β chains which recognize antigens loaded on MHC molecules, and CD3 γ , δ , ϵ and ζ signaling modules. Upon peptide-MHC binding, phosphorylation of immunoreceptor tyrosine-based activation motifs (ITAMs) in the CD3 ζ chains propagates downstream signaling for T cell activation. CAR consists of an extracellular antigen-binding domain (scFv), a hinge, a transmembrane domain and cytoplasmic signaling domain. In early CAR design, the scFv domain was fused with a single CD3 ζ signaling domain only. In the second and third generation CARs, one or two costimulatory domains (*e.g.*, CD28, 4-1BB) were incorporated. The fourth and fifth generation CARs are based on second generation constructs, but additionally contain an inducible cytokine cassette or IL-2 receptor β chain (IL-2R β) fragment for JAK/STAT pathway activation, respectively. scFV- single chain variable fragment.

At the time of writing, six CAR T cell therapies have been approved by the US Food and Drug Administration (FDA) and the European Medicines Agency (EMA), all of which are based on the second generation CAR design. The first CAR T cell product was

tisagenlecleucel (Kymriah[®], Novartis), approved by the FDA in August 2017 for the treatment of r/r B cell acute lymphoblastic leukemia (ALL)⁴¹. Later that year Kite/Gilead received FDA approval for axicabtagene ciloleuce (Yescarta[®]) to treat diffuse B cell lymphoma⁴². These were followed by two more CD19-specific CAR T cells, namely brexucabtagene autoleucel (Tecartus[®], Kite/Gilead)^{43,44} and lisocabtagene maraleucel (Breyanzi[®], Bristol-Myers Squibb)⁴⁵, approved for treating r/r mantle cell lymphoma and large B cell lymphoma, respectively. In April 2021 idecabtagene vicleucel (Abecma[®], Bristol-Myers Squibb) became the first B cell maturation antigen (BCMA)-specific CAR T cell product approved for the treatment of multiple myeloma⁴⁶, while in February 2022 the FDA approval for the first Chinese CAR T cell therapy was obtained, ciltacabtagene autoleucel (Carvykti[®], Legend Biotech/Janssen), which is also BCMA-directed for the same indication⁴⁷.

Despite the remarkable clinical success achieved in certain subsets of B cell leukemias and lymphomas, there are many barriers that limit CAR T cell therapeutic efficacy in other hematological malignancies and solid tumors⁴⁸. A lack of durable clinical responses is attributed to insufficient engraftment and persistence of infused CAR T cells⁴⁹, or development of tumor resistance to single antigen targeting CAR constructs due to loss of target antigen expression on malignant cells, known as antigen escape⁵⁰. For solid tumors, critical challenges include a paucity of specific target tumor antigens and limited T cell trafficking towards and into the tumor bed. In addition, the immunosuppressive tumor microenvironment (TME), characterized by upregulation of inhibitory checkpoints, such as PD-L1 and LAG-3, and the presence of multiple immunosuppressive cell populations (*e.g.*, regulatory T cells, myeloid-derived suppressor cells, M2 macrophages) impairs T cell persistence by inducing T cell exhaustion or anergy^{51,52}. Manufacturing challenges pose another barrier to autologous CAR T cell therapy. For instance, often insufficient numbers and poor quality of lymphocytes are collected from often elderly and heavily pretreated patients, which has sparked interest in allogeneic “off-the-shelf” CAR T cell development⁵³.

It is now widely recognized that further progress in CAR T cell therapy requires combinatorial approaches moving beyond single-target immunotherapy. Such novel engineering strategies center around multiple targeting, checkpoint blockage, *de novo*

cytokine production, improved trafficking with chemokines and remote control CAR designs^{54,55}. To realize such novel approaches, one critical consideration is the choice of genetic engineering tools that should offer safety, high efficiency, cargo flexibility to accommodate different types of payloads and increasingly large CAR constructs, as well as clinical scalability at low cost.

1.2 T cell engineering with viral vectors

Currently, CAR T cell manufacturing relies on the use of gammaretroviral and lentiviral vectors that offer high transduction efficiencies and long-term stable transgene expression. Out of six FDA- and EMA-approved CAR T cell products two use gammaretroviral vectors (Yescarta and Tecartus) and four utilize lentiviral vectors (Kymriah, Breyzani, Abecma, Carvykti). To generate replication-defective vectors, viral sequences coding for genes necessary for additional rounds of virion replication and packaging are removed and replaced by the transgene of interest. Necessary viral sequences encoding capsid proteins, enzymes for reverse transcription/integration and envelope glycoproteins (*i.e.*, gag, pol, env) are provided on separate plasmids⁵⁶. Co-transfection of these plasmids with vector plasmid incorporating the gene of interest provides all the components needed to produce functional viral particles in packaging cell lines such as HEK 293T. Separation of genes required for virion formation prevents progeny virus production while allowing to generate vectors capable of infecting mammalian cells and integrating their genetic material into the host genome⁵⁶.

Gammaretroviral vectors can only transduce dividing cells, while lentiviral vectors are able to infect both dividing and non-dividing cells, though T cell activation is typically required to achieve higher gene transduction efficiencies⁵⁷. Another difference lies in their genomic integration profiles. Gammaretroviral vectors derived from Moloney murine leukemia virus (MLV) show preferential integration near transcriptional start sites and CpG islands, including promoters and enhancers^{58,59}. Such an integration profile carries a risk of oncogenic transformation due to the activation of proto-oncogenes. This concern remained theoretical until MLV use in gene therapy for X-linked severe combined immunodeficiency (SCID-X1) resulted in leukemia development caused by activation of the LMO2 oncogene due to vector integration near LMO2 promoter, prompting careful

monitoring of viral vector safety ever since ⁶⁰. Contrary to retroviruses, human immunodeficiency virus (HIV)-derived lentiviral vectors show preference to integrate in transcriptionally active regions, which is in general considered a safer genomic integration profile ^{61,62}. Even though insertional mutagenesis cannot be excluded, no evidence of oncogenic transformation after T cell transduction with retroviral or lentiviral vectors has been observed to date. Nonetheless, recent reports indicate that the variability of lentiviral vector integration sites in CAR T cells could influence T cell proliferation and clinical responses, highlighting the need to better understand the correlation between vector integration and therapeutic outcomes ^{63,64}.

Viral vector production for clinical applications is performed under current Good Manufacturing Practices (cGMP) in specialized biosafety level 2 facilities and takes 2 to 3 weeks with most of the time being spent on the expansion of HEK 293T producer cells to obtain large quantities of replication-defective vectors ⁵⁶. Compared to gammaretroviral vector manufacturing, lentiviral vector production turned out more challenging to scale up due to the lack of stable vector packaging cell lines and lot-to-lot variations arising from multi-plasmid transient transfection procedures ⁶⁵. Since there is a theoretical potential for generating replication-competent retroviruses or lentiviruses (RCRs/RCLs) during vector manufacturing, the FDA requires extensive testing for RCRs/RCLs in the packaging cell lines and the purified vector product, as well as the final transduced cells before infusion into the patient ⁶⁶. In addition, the FDA recommends patient follow-up for RCRs/RCLs emergence for up to 15 years. Such complex and highly centralized manufacturing processes combined with the need for long-term safety-monitoring results in exceptionally high costs and various logistic challenges, significantly restricting patient accessibility to CAR T cell therapy. Other drawbacks associated with viral vectors are limited cargo capacity of ~8-9 kb and intrinsic risk of immunogenicity ^{67,68}.

The disadvantages of viral vectors have prompted the development of alternative non-viral transfection approaches with a better safety profile and less manufacturing difficulties, resulting in reduced cost and regulatory hurdles, and even facilitating point-of-care CAR T cell production to shorten vein-to-vein time. These techniques will be discussed in more detail in section 3.

1.3 The potential of RNA to engineer therapeutic T cells

Traditionally, T cell modifications for therapeutic applications have been achieved through permanent transgene integration mediated by viral vector transduction. However, RNA moieties have recently emerged as a powerful tool to modulate T cell efficacy in cancer immunotherapy thanks to substantial progress in RNA manufacturing and the development of novel RNA delivery technologies . For instance, T cells can be transfected with mRNA to transiently express tumor antigen-specific receptors. This offers a superior safety profile because the mRNA does not integrate into the genome ⁶⁹ and avoids the risk of insertional mutagenesis. In addition, transient CAR expression in T cells decreases the risk of “on-target off-tumor” toxicity in case target antigens are also expressed in healthy tissues. On the other hand, short-term CAR expression may reduce the T cell’s anti-tumor efficacy, requiring repeated administration of mRNA-modified CAR T cells. Another area of interest is gene editing with designer nucleases, where nuclease delivery in mRNA format results in a narrow time-window of enzyme expression, thus conferring greater control over potential off-target genome editing effects. In addition, RNA therapeutics can also be used to inhibit immunosuppressive receptors and to modulate cytokine expression, which may increase the T cell’s antitumor efficacy. In the next section we will discuss the different classes of RNA molecules, followed by an overview of non-viral transfection technologies and their application in T cell engineering.

2 Classes of RNA molecules and manufacturing advancements towards clinical translation

RNA therapeutics constitute a diverse class of molecules that can regulate the expression of both protein-coding and noncoding genes by acting on proteins, transcripts and genes. A major advantage of RNA-based therapeutics is their ability to target in principle any gene of interest, many of which may be inaccessible to other drug classes like small molecules and antibodies. It was estimated that only 0.05% of the human genome has been drugged by the presently approved protein-targeted therapeutics, since most (98.5%) of the human genome consists of non-protein-coding DNA sequences ⁷⁰. In addition, 85% of human proteins remain difficult to target pharmacologically due to a lack of well-defined pockets for small molecule binding ⁷¹. Yet, most of the human genome is transcribed into RNA, which can be targeted by antisense oligonucleotides (ASOs), small interfering RNA (siRNAs) and microRNAs (miRNAs) based on complementary base-pairing. Thus, by acting on both conventional proteome (protein expression) and the previously undrugged transcriptome (inhibiting expression), RNA molecules can significantly broaden the range of therapeutic targets. The different categories of RNA therapeutics based on their structure and mode of action will be discussed next.

2.1 Antisense oligonucleotides

ASOs are short, synthetic, single-stranded (ss) oligonucleotides (12-25 nt) designed to specifically hybridize to a complementary endogenous pre-mRNA or mRNA through Watson-Crick base-pairing ^{72,73}. The main mechanism of action is the formation of DNA-RNA heteroduplexes, leading to the recruitment of endogenous RNase H and cleavage of the complexes or steric blocking of the ribosomal assembly ^{74,75}. In addition, ASOs can promote alternative splicing by interacting with pre-mRNAs in the nucleus ⁷⁶⁻⁷⁸. Downregulation of the target RNA expression can be achieved by translational arrest upon binding with the 5' untranslated region (UTR) of the mRNAs, cleavage of 5' cap structures or polyadenylation changes ⁷⁹⁻⁸¹. Alternatively, ASO binding to upstream open reading frames (uORFs) and translation inhibitory elements (TIEs) results in increased production of specific proteins encoded by target RNAs ^{82,83}. Finally, ASOs can upregulate the expression of desirable proteins by binding to miRNAs or miRNA-binding sites, thus

inhibiting miRNA-mediated downregulation of gene expression^{84,85}. The therapeutic use of ASOs was first reported by Stephenson and Zamecnik in 1978, who demonstrated that DNA-based ASOs could inhibit Rous sarcoma virus replication *in vitro*⁸⁶. However, these effects were not sustained *in vivo* since unmodified oligonucleotides were prone to nuclease degradation and displayed a poor target affinity. Consequently, in the third generation of ASO therapeutics, numerous chemical modifications such as nucleobase modifications, alternative backbones and bridged nucleic acids have been implemented to improve their stability, target affinity, pharmacokinetics and pharmacodynamics, as extensively reviewed elsewhere^{73,87,88}. Nonetheless, delivery of ASOs remains a hurdle for their broader clinical application.

2.2 Small interfering RNA

RNA interference (RNAi) is a conserved endogenous mechanism used to defend against invading viruses and transposable elements⁸⁹. Gene silencing can be initiated by short double-stranded (ds) RNA sequences such as siRNAs or miRNAs, which mediate sequence-specific mRNA degradation or mRNA translational repression. The endogenous siRNA pathway starts by cleaving long dsRNA molecules into 21-23 nucleotide long siRNAs by the RNase III-type enzyme Dicer. Once incorporated into a multiprotein RNA-induced silencing complex (RISC) in the cytoplasm, siRNA is unwound into the passenger (sense) strand and the guide (anti-sense) strand. The passenger strand is then degraded by Argonaute 2 (AGO2) protein, whereas the guide strand is retained to direct RISC binding to target mRNA to induce AGO2-mediated mRNA cleavage⁹⁰⁻⁹³. Finally, the sliced target mRNA is released and the activated siRNA-RISC complex can be recycled to destroy additional targets, propagating the gene silencing effect⁹⁴. The catalytic activity of siRNA can be sustained for 3 to 7 days in rapidly dividing cells, after which its concentration drops below the therapeutic threshold and repeated administration is required to achieve a persistent effect⁹⁵.

Since its first description in plants and nematodes in the 1990s⁹⁶, the RNAi mechanism has been extensively exploited in fundamental studies of gene function and in developing new therapeutics. Although the first clinical trials using unmodified siRNAs failed due to immune-related toxicities and questionable RNAi effects⁹⁷, further improvements in

chemical design, sequence selection and delivery strategies opened the way for safer and more efficacious RNA compounds ⁹⁸⁻¹⁰⁰.

2.3 CRISPR-based gene editing

Clustered regularly interspaced short palindromic repeats and CRISPR-associated protein 9, aka CRISPR-Cas9, is a part of the bacterial adaptive immune system, which has been transformed into a potent genome editing technology in eukaryotic cells ¹⁰¹. The system relies on a DNA nuclease (Cas9 protein) guided by an RNA sequence that is complementary to the target DNA region (guide RNA or gRNA). In bacteria, native Cas9 requires a guide RNA composed of two associated disparate RNA molecules, being the CRISPR RNA (crRNA) which enables the recognition of the target gene and trans-activating CRISPR RNA (tracrRNA) which facilitates crRNA maturation and Cas9 recruitment. However, for gene editing purposes, both RNA molecules can be linked into a synthetic single guide RNA (sgRNA). Upon gRNA binding to Cas9, a ribonucleoprotein (RNP) complex is formed, whereby recognition of a 20-nucleotide target sequence and protospacer adjacent motif (PAM) engages Cas9 nucleolytic activity, inducing a double-strand break (DSB) ^{102,103}. The latter can be repaired by either non-homologous end joining (NHEJ) or homology-directed repair (HDR). NHEJ is an error-prone process where direct rejoining of the lesion introduces small deletions or insertions, ultimately disrupting the targeted locus (gene knock-out). In contrast, HDR is a more precise mechanism that can be exploited for gene insertion or correction (gene knock-in) in the presence of a donor DNA sequence ^{103,104}.

Over the years, the CRISPR-Cas toolbox has expanded significantly by exploitation of the natural diversity of the CRISPR systems as well as rational engineering. CRISPR-mediated genome editing capabilities were first demonstrated using type II Cas9 DNA endonuclease from the *Streptococcus pyogenes* ¹⁰². The Cas9 nuclease consists of two catalytic domains, HNH and RuvC, which cleave the target and non-target strand, respectively. These domains can be mutated towards the development of base editors and prime editors that operate without inducing a double-strand break, thereby reducing the risk of chromosomal rearrangements ¹⁰⁵. Inactivation of one of the nuclease domains creates a

Cas9 nickase (nCas9) which introduces single-strand cuts, offering better control over off-target effects. Alternatively, inactivation of both nuclease domains generates a dead Cas9 (dCas9), stripped of catalytic activity but still able to recognize and bind to target DNA. The latter can be exploited, for instance, in gene regulation through dCas9 fusion with transcriptional activators or repressors and in epigenetic remodeling via linking with epigenetic effector enzymes ^{105–107}.

Unlike Cas9, most Cas12 nucleases require only crRNA to induce staggered end cuts distal from a 5' T-rich PAM sequence. Cas12a mediates genome editing with a higher specificity than Cas9, which can be related to its lower nuclease activity ¹⁰⁸. In addition, its smaller size and ability to process its own guide RNAs make Cas12 an attractive candidate for multiplex gene engineering ¹⁰⁹. More recently discovered Cas13 nucleases have two HEPN domains and their endonuclease activity is directed toward RNA. Once bound to the target, Cas13 may display a non-specific RNase activity by cleaving bystander RNA molecules in a non-discriminatory manner. This collateral cleavage property has been exploited in nucleic acid detection-based diagnostic technologies, simultaneously raising concerns for therapeutic applications ¹¹⁰. However, a recent screening of Cas13 mutants has identified some high-fidelity variants displaying efficient RNA knockdown activity with minimal collateral damage ¹¹¹.

Despite the robustness and simplicity, the therapeutic application of CRISPR-Cas systems faces challenges related to effective delivery, off-target mutagenesis, genome editing efficiency and immunogenicity. Consequently, several strategies have been developed to enhance Cas specificity. For instance, using paired Cas9 nickases instead of Cas9 nuclease significantly reduces off-target effects without sacrificing the on-target cleavage efficiency ¹¹². In addition, several high-fidelity Cas9 variants have been engineered by rational design or directed evolution. One example is *SpCas9*-HF1 harboring alanine substitution to disrupt the nonspecific contact between *SpCas9* and the phosphate backbone of target DNA ¹¹³. Other approaches rely on the modification of gRNA, including truncated gRNAs ¹¹⁴, engineering secondary structures ¹¹⁵, or addition of cytosine stretches to the 5'-end of the gRNAs as a “safeguard” strategy ¹¹⁶.

Also, chemical modifications optimized for ASOs and siRNAs can be applied to gRNAs to improve their stability against enzymatic degradation, enhance on-target performance and reduce toxicity/ immune recognition. For instance, the incorporation of 2'-O-methyl-3'-phosphonoacetate at specific sites in the ribose-phosphate backbone of gRNAs can significantly reduce off-target cleavage while preserving high on-target activity ¹¹⁷. Similarly, crRNA modification with bridged and locked nucleic acids broadly improves Cas9 cleavage specificity ¹¹⁸. In another study, chemical modifications comprising 2'-O-methyl, 2'-O-methyl 3'-phosphorothioate, or 2'-O-methyl 3'-thioPACE were incorporated at both termini of sgRNAs to enhance genome editing efficiency in primary human T cells and CD34+ hematopoietic stem and progenitor cells ¹¹⁹. Finally, the 5'-hydroxyl modification of gRNA generated by triphosphate group removal helps to evade innate immune responses, leading to efficient Cas RNP-mediated targeted mutagenesis in primary human CD4+ T cells ¹²⁰.

CRISPR-Cas components can be delivered to cells in three formats: DNA vector (either plasmid or viral vector) encoding Cas and gRNA; mRNA encoding Cas protein with a separate guide RNA; or mature CRISPR-Cas ribonucleoprotein. Plasmid-based delivery is a convenient strategy for the co-transfection of multiple components such as Cas, sgRNA(s) and exogenous DNA for HDR, potentially increasing genome editing efficiency ¹²¹. However, it requires nuclear entry and translation and is associated with the risk of host genome integration and off-target effects resulting from prolonged expression ¹²². In addition, exogenous DNA sensing by cellular receptors can trigger innate immune responses ^{123,124}. Compared to plasmids, delivery of Cas-encoding mRNA enables faster onset of genome editing as there is no need for a transcription step before translation commences in the cytoplasm. The transient nature of protein expression can be leveraged to better control the dose and duration of Cas nuclease activity, reducing off-target effects ¹¹⁹. However, due to poor stability and susceptibility to enzymatic degradation, mRNA molecules require chemical modifications and carefully considered delivery mechanisms, as will be discussed further in the next section. Finally, Cas delivery in protein format offers immediate onset of gene editing. Its transient presence translates to reduced off-target effects and toxicity ^{125,126}. However, Cas RNP delivery can be challenging due to the large size and charge of the protein.

2.4 Aptamers

Aptamers are single-stranded oligonucleotides that can bind to various targets with high affinity and selectivity by folding into specific three-dimensional structures. They are produced *in vitro* through a controlled process called Systematic Evolution of Ligands by Exponential Enrichment (SELEX)¹²⁷. Often regarded as a chemical equivalent of antibodies, aptamers have the advantage of being relatively small, more stable, nonimmunogenic and programmable via chemical modifications and conjugation¹²⁸. Aptamer-based therapeutics include antagonist aptamers which disrupt the interaction of disease-associated targets such as protein-protein or receptor-ligand interactions, and agonist aptamers, which can activate target receptors. Furthermore, cell type-specific aptamers serve as carriers to deliver other therapeutic agents to the target cells and tissues. Aptamer-based delivery systems include conjugates with different oligonucleotides and drugs and aptamer-decorated nanomaterials¹²⁸.

2.5 Messenger RNA

Messenger RNA (mRNA), first discovered by Brenner and colleagues in 1961, transfers genetic information from the DNA in the nucleus to the cytoplasmic ribosomes, where it can be translated into proteins¹²⁹. The therapeutic potential of mRNA molecules was first realized in the 1990s, when protein expression was demonstrated by direct injection of *in vitro* transcribed (IVT) mRNA constructs¹³⁰. In another study, Jirikowski *et al.* injected vasopressin mRNA into the hypothalamus of Brattleboro rats to induce the synthesis of vasopressin and (transiently) reverse diabetes insipidus¹³¹. Later, Conry *et al.* injected mRNA constructs encoding a carcinoembryonic antigen in mice to induce an anti-tumoral antibody response¹³². These early demonstrations, coupled with advancements in mRNA design and manufacturing, laid the foundation for a plethora of applications investigated today, including: (1) protein replacement therapy, where exogenous mRNA is administered to replace or supplement endogenous proteins; (2) vaccination, where mRNA encoding specific antigens is introduced to elicit an immune response against infectious diseases or cancer; (3) adoptive cell therapy, where mRNA transfection is used to alter the therapeutic cell's phenotype or function; (4) gene editing, where mRNA enables the transient expression of gene editing nucleases.

mRNA therapeutics offer several advantages compared to DNA-based strategies. First, mRNA does not need to enter the nucleus, thus circumventing the challenge of nuclear delivery and the risk of genomic integration. In addition, as the cytoplasmic site of action makes mRNA independent of cell cycle progression, it is efficacious in both mitotic and non-mitotic cells. The relatively short half-life of mRNA can be advantageous for applications that require only transient protein expression, such as expression of nucleases for gene editing, epitopes in vaccination and transposase in stable non-viral gene transfer. Finally, manufacturing of synthetic mRNA by *in vitro* transcription is relatively simple, fast, scalable, and cost-efficient.

IVT mRNA can be synthesized in a cell-free approach using a phage RNA polymerase (such as SP6, T3, or T7) and a linear DNA template in the presence of nucleotides. The IVT mRNA molecules resemble naturally occurring mature eukaryotic mRNAs and comprise five functional regions: a 5' cap, a 5' untranslated region (UTR), an open reading frame (ORF) encoding the gene of interest, a 3' UTR and a 3' poly(A) tail (**Figure 3**). Each of these structural elements has been modified in recent years to enhance mRNA stability and translation efficiency or to modulate immunogenicity^{133–136}. The 5' cap structure regulates pre-mRNA splicing, nuclear export, mRNA stability against 5'-3' exonuclease-mediated degradation and translation initiation by recruiting eukaryotic initiation factor 4F (eIF4F). The natural eukaryotic 5' cap (cap-0) contains 7-methyl-guanosine connected to the 5' nucleotide through a 5'-5' triphosphate bridge (m7Gppp). Ribose of the first and second nucleotide can be subjected to 2'-O-methylation to generate cap-1 and cap-2, and these methylations have been found to reduce immunogenicity, indicating a role in distinguishing between self and non-self mRNA^{137,138}. In contrast, unmodified mRNA or cap-0 structures can be recognized by cellular pattern recognition receptors (PRRs) such as retinoic acid-inducible gene (RIG)-like receptors (RIG-I and melanoma differentiation-associated protein 5 (MDA-5)), leading to interferon responses and mRNA degradation¹³⁴. In addition, 5' cap structures can be subjected to various chemo-enzymatic modifications to achieve cap analogs with high affinity for eIF4F and low susceptibility for decapping enzymes, or to modulate immunostimulation^{139,140}. Currently, two methods are used to cap IVT mRNA: co-transcriptional capping (CleanCap® technology, TriLink Biotechnologies) and posttranscriptional capping (capping enzymes from vaccinia virus).

Along with the 5' cap, the 3' poly(A) tail regulates mRNA stability and translation efficiency by interaction with poly(A) binding proteins. The length of the poly(A) tail is usually increased to counteract the deadenylation process that eventually leads to mRNA decay, though the optimal length of the poly(A) tail remains controversial^{133,141}. For instance, one study demonstrated that mRNA modification with a poly(A) tail measuring 120 nt increased mRNA stability, translation efficiency and T cell stimulatory capacity of dendritic cells, providing a potential optimization strategy for mRNA vaccine manufacturing¹⁴².

UTRs do not encode proteins but play important roles in regulating translation efficiency, mRNA stability and subcellular localization^{133,143}. The 5' UTR is mainly involved in ribosome recruitment and the initiation of mRNA translation. A strong Kozak sequence is often incorporated after the 5' UTR to improve translation efficiency^{144,145}. The latter can also benefit from eliminating sequences that display an increased propensity towards the formation of stable secondary and tertiary structures, hindering mRNA interactions with ribosomes. The 3' UTR contains miRNA binding sites and governs mRNA stability and half-life¹⁴⁶. For instance, removing miRNA binding sites from 3' UTR can promote encoded protein expression. Alternatively, inserting a tissue-specific miRNA binding site can increase mRNA degradation in off-target tissues upon systemic administration, reducing undesired side effects¹⁴⁷. mRNA translation and half-life can be improved by the incorporation of sequences derived from endogenous long-lived mRNAs, such as alpha and beta globin¹⁴⁵. Furthermore, optimization of the guanine-cytosine content results in enhanced stability and reduced immunogenicity of synthetic mRNA constructs¹⁴⁸.

The ORF coding the sequence of the protein of interest is the core of the IVT mRNA. One approach to increase translatability is codon optimization, where rare codons are replaced with synonymous high-frequency codons to speed up the translation. However, this strategy is controversial since codon replacement may affect protein conformation and give rise to novel peptides with unknown biological activity^{149,150}. Therefore, nucleoside modification appears as the most attractive alternative. The incorporation of modified nucleotides in mRNA, such as pseudouridine (ψ), N1-methylpseudouridine ($m^1\psi$), 5-methoxyuridine (mo^5U), 2-thiouridine (s^2U), 5-methylcytidine (m^5C) and N6-methyladenosine (m^6A) suppresses the activation of TLR receptors, thereby inhibiting the innate immune responses and improving protein translation efficiency^{134,137,151,152}. It is

worth noting that N1-methylpseudouridine modification has been implemented in the development of both Pfizer/BioNTech (comiranty®) and Moderna Therapeutics (spikevax®) SARS-CoV-2 vaccines ¹⁵³.

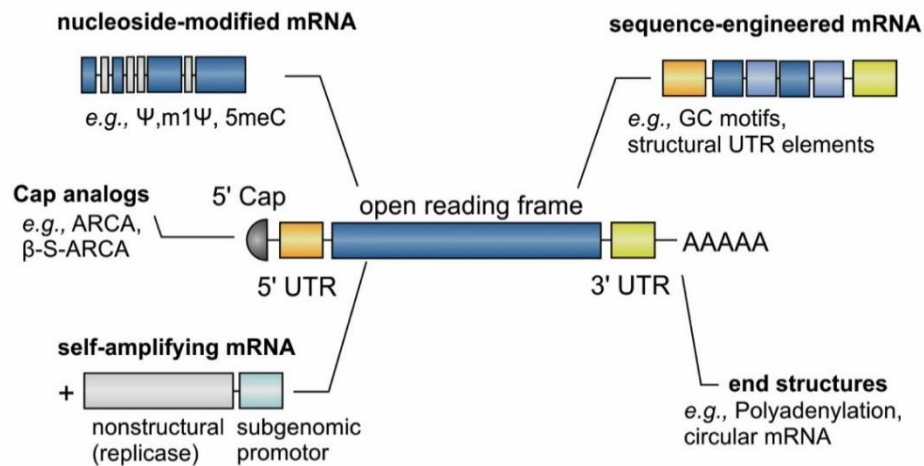


Figure 3. The structure of *in vitro* transcribed (IVT) mRNA. IVT mRNA comprises five functional regions: a 5' cap, 5' and 3' untranslated regions (UTRs), the protein-encoding open reading frame (ORF) and a 3' poly(A) tail. In recent years, each of these elements has been modified to improve mRNA stability and efficiency, or to modulate immunogenicity. Figure adapted from Verbeke *et al.* ¹⁵⁴

Another strategy to reduce the immunostimulatory potential of the IVT mRNA is to perform additional purification steps for removing potentially immunogenic contaminants, such as residual templates, free nucleotides and dsRNA. The most common method to purify IVT mRNA is high performance liquid chromatography (HPLC). For instance, Kariko *et al.* used reversed-phase HPLC to remove dsRNA impurities and demonstrated a remarkable increase in protein expression by 1000-fold, without inducing the production of IFNs or inflammatory cytokines ¹⁵⁵. However, HPLC is not suitable for large scale production of mRNA. Alternative purification methods include oligo(dT)-cellulose chromatography and RNase III specific digestion. The latter has been employed by Foster *et al.* to remove dsRNA byproducts from mRNA encoding CD19 CAR. T cells electroporated with a purified construct displayed decreased expression of checkpoint inhibitors and improved cytotoxicity in a murine leukemia model ¹⁵².

The successful development of COVID-19 mRNA vaccines has fueled further innovations in mRNA engineering aimed at increased stability and more robust expression *in vivo*. In vaccination, achieving adequate antigen expression levels for protection or immunomodulation depends on the number of successfully delivered conventional mRNA transcripts and thus may require large doses or repeated administration. This limitation can be addressed using self-amplifying mRNA (saRNA), based on self-replicating elements derived from the alphavirus genome^{156,157}. Such a construct consists of the alphavirus replication genes, while the structural elements are substituted with the selected gene of interest. As a result of their self-replicative activity, saRNAs can be delivered at lower doses than conventional mRNA to achieve comparable antigen expression^{158,159}. saRNA-based SARS-CoV-2 vaccines have already shown efficiency in inducing high neutralizing antibody titers in animals^{159–161} and several other candidates against infectious diseases and cancer are being tested in clinical trials^{162,163}. However, the substantially larger size of self-amplifying mRNA compared to conventional mRNA (~10 kb vs. ~2-3 kb) may necessitate optimization of delivery formulations.

3 Non-viral delivery platforms for RNA therapeutics

For T cell engineering the RNA molecules need to cross the cell membrane to gain access to the cytosol. However, their hydrophilic nature, macromolecular size and overall strong negative charge preclude cellular entry *via* passive diffusion. Therefore, to facilitate intracellular delivery of RNA, various non-viral strategies have been employed, which can broadly be categorized as membrane disruption-mediated and carrier-mediated methods. Membrane disruption-based technologies enhance the permeability of the plasma membrane mostly *via* physical stimuli, such as electrical fields or mechanical forces, offering direct access to the cytosol. Although considered relatively universal in terms of cell type and cargo molecules to be delivered, such physical methods are often limited to *in vitro* or *ex vivo* applications, being less suited for *in vivo* delivery. In contrast, carrier-based delivery systems designed to condense nucleic acid into compact nanoparticles can be applied both *ex vivo* and *in vivo*. However, these nano-vehicles face specific challenges related to cellular uptake and endosomal escape, as discussed in the next paragraphs. In this section, we provide an overview of both established and emerging technologies for RNA delivery, focusing on *ex vivo* T cell engineering. For each method, the delivery mechanism will be discussed as well as its advantages and disadvantages for therapeutic cell editing.

3.1 Membrane-disruption based delivery methods

3.1.1 Electroporation

Electrical membrane permeabilization, or electroporation in short, is an approach in which cell exposure to high-voltage and low frequency electrical pulses induces a transient increase in plasma membrane (PM) permeability, allowing transmembrane transport of otherwise impermeant exogenous molecules. This phenomenon was first demonstrated in 1982 by Neumann *et al.*, who reported efficient transfection of pDNA into mouse lymphoma cells upon application of strong electric fields¹⁶⁴. Although a comprehensive understanding of the mechanisms of electroporation is still lacking, there is broad consensus that electroporation is best described by the theory of aqueous pore formation that is induced by interfering with the cellular transmembrane potential (TMP)^{165–168}. According to the theory (**Figure 4**), once the applied voltage exceeds a critical

threshold, PM breakdown occurs in two phases: first, water molecules start penetrating the bilayer, forming a water channel; next, the lipids adjacent to the water channel reorient toward the channel with their polar head groups, creating metastable (lasting milliseconds up to several minutes) hydrophilic pores^{166,168,169}. In addition, there is increasing evidence that exposure to electric pulses may cause chemical changes to membrane lipids and modulation of protein function, contributing to the increased permeability of the lipid bilayer^{166,170}.

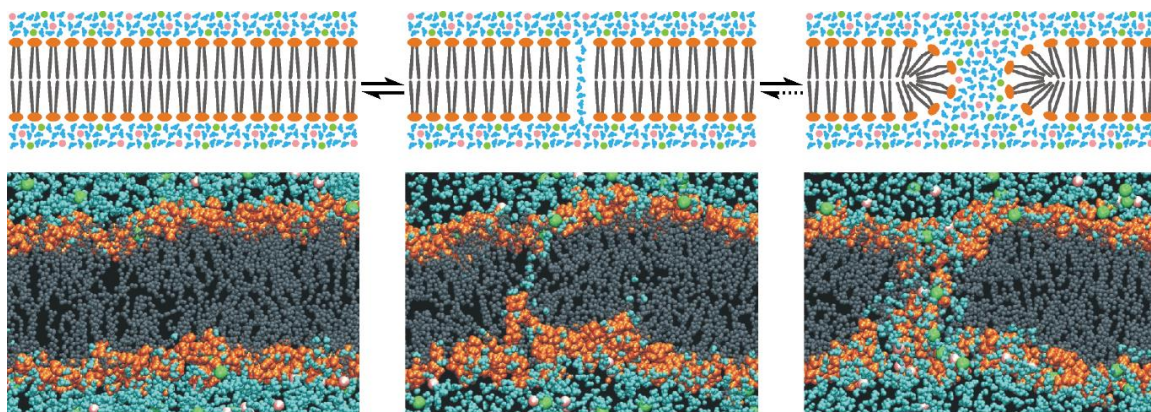


Figure 4. Molecular dynamics of electrically induced membrane permeabilization. Upon lipid bilayer exposure to an external electric field, water molecules (cyan) start penetrating the bilayer, forming an unstable hydrophobic pore. Next, neighboring lipids reorient with their polar headgroups (orange) toward the water molecules, creating a metastable hydrophilic pore and allowing the ions to enter. Adapted from Yarmush *et al.*¹⁶⁵

The extent of membrane permeabilization depends on the magnitude and duration of the applied electric forces^{166,168}. Generally, it is believed that coverage area of pore formation is determined by pulse strength while pore size correlates with pulse duration¹⁶⁷. For instance, application of sub-microsecond pulses induces many small pores (radius ~ 1 nm), whereas longer pulses result in less numerous but larger pores of up to tens of nm¹⁷¹. In addition, high voltage ultrashort pulses in the nanosecond range might be used to target intracellular organelles without disrupting the PM^{172,173}. Pore formation is also influenced by factors such as cell size, membrane curvature, temperature, and osmotic pressure. Generally, smaller cells, such as T lymphocytes, require higher voltages than larger cells to achieve effective PM permeabilization^{168,174}.

Intracellular delivery of exogenous molecules is highly dependent on pore size and cargo properties, such as size, charge and conformational flexibility ^{167,175}. Small neutral molecules enter the cell *via* diffusion through the pores, while transport of charged species such as nucleic acids is facilitated by additional electrophoretic forces present during the pulse ^{176–178}. For instance, siRNA delivery can be mediated by a combination of electrophoretic and/ or diffusive mechanisms depending on the size and lifetime of the pores ^{179,180}. In contrast, transfection of large DNA plasmids is often described as a multistep process involving DNA condensation at the cell membrane, followed by endocytic internalization and a yet poorly understood step of endosomal release in the cytosol and eventual translocation to the nucleus ^{181–183}

To ensure successful intracellular delivery and preservation of cell viability post treatment (*i.e.*, reversible electroporation), several parameters such as field strength, pulse duration and number of pulses need to be optimized for a given combination of cell type and effector molecules ^{184–187}. Moreover, the composition of the electroporation buffer can be adjusted in terms of osmolarity and conductivity to balance transfection efficiency with cytotoxicity ^{188–190}. This flexibility, combined with high delivery efficiencies has established electroporation as one of the leading non-viral transfection technologies for both basic research and clinical applications ¹⁸⁸.

Wide laboratory adoption of electroporation has been supported by the development of several commercial systems such as Gene Pulser™ (Bio-Rad), Nucleofector™ (Lonza), Neon™ (Invitrogen) and NEPA21 electroporator (Nepagene). Clinical manufacturing applications have been facilitated by the introduction of large-scale electroporation platforms, such as MaxCyte's ExPERT family of instruments based on flow electroporation™ technology, CliniMACS® Electroporator from Miltenyi Biotec and CTS Xenon offered by Thermo Fisher Scientific. For example, the MaxCyte GTx™ system can transfect up to 20 billion cells in less than 30 minutes. Such large volume electroporators can be coupled with modules like the CliniMACS Prodigy® platform (Miltenyi) or Cocoon® platform (Lonza) to assemble a fully automated and closed cGMP workflow from cell isolation/activation to genetic engineering and expansion.

Despite being the most established non-viral method for T cell transfections, electroporation comes with certain limitations, not in the least a substantial loss of cell viability post-treatment. Cell damage can be attributed to electrolytic effects such as Joule heating, pH changes and contamination *via* corrosion of electrodes ^{167,191,192}. In addition, cell exposure to strong electric fields has been suggested to trigger lipid peroxidation, protein denaturation, generation of reactive oxygen species and DNA damage ^{166,170,193}. Furthermore, if the PM integrity remains compromised for extended periods of time, it may lead to severe disruption of cell homeostasis, triggering delayed cell death mechanisms ¹⁹⁴. Even when cells survive, they may carry persistent phenotypical alterations, leading to reduced proliferation potential and changes in signaling pathways, activation states and transcriptional responses ^{195–197}. For instance, in an early study by Zhang *et al.*, enhanced transcriptional activity and increased expression of surface activation markers were observed in CD4 T cells treated by nucleofection ¹⁹⁵. Later, DiTommaso *et al.* showed that electroporation induced significant gene expression changes and aberrant cytokine secretion in primary T cells, which translated to functional deficiencies *in vivo* with electroporated T cells failing to demonstrate sustained antigen-specific effector responses and tumor control ¹⁹⁶. It seems, therefore, that the main challenge for electroporation-based T cell engineering lies in long-term survival and functionality rather than the initial delivery efficiency ^{167,198}.

Recent innovations in nanotechnology and microfluidics led to the development of miniaturized electroporation systems such as micro-, nano- and microfluidic-based electroporation, offering more precise control over delivery parameters and electrode-mediated toxicities. One example is the microfluidic continuous-flow electroporation device developed by Lissandrello and colleagues for high-throughput T cell engineering, with a reported mRNA transfection efficiency of up to 95% and a processing rate of 20 million cells per minute ¹⁹⁹. In another study by VanderBurgh *et al.* similar efficiencies were demonstrated for mRNA transfection and CRISPR/Cas9-mediated TCR knockout, while delivery throughput could be scaled up to 256 million cells/min ²⁰⁰. For an extensive overview of such novel designs, we refer the reader to recently published reviews ^{201–203}. Several commercial micro/nano electroporation products are presently being developed by start-up companies, such as by CyteQuest, Kytopen and NAVAN Technologies. It will be

of interest to see how these newer electroporation technologies stack up against the more established bulk electroporation devices for T cell engineering in terms of efficiency, cell viability and functionality.

3.1.2 Microfluidic cell squeezing

As an alternative to electroporation, microfluidic platforms based on rapid mechanical deformation of cells have gained considerable attention. The original implementation of this concept, known as cell squeezing, relies on passing cells in suspension through narrow (smaller than the cell diameter) constrictions in microfluidic channels, leading to mechanical disruption of the PM and facilitating cytosolic delivery of macromolecules present in the surrounding medium (**Figure 5A**)²⁰⁴. A major advantage of this approach is its simplicity, as it only requires a microfluidic chip, reservoirs, and a pressure regulation system to facilitate fluid flow through the chip²⁰⁵. Once microfluidic chip geometry is optimized for a given cell type, scalability through channel parallelization offers high throughput processing of up to 1 million cells per second^{206–208}. Precise control over the membrane disruption process allows for high delivery efficiencies while preserving cell viability and functionality. For example, DiTommaso *et al.* reported that cell squeezing had minimal effect on T cell transcriptional responses, cytokine production *in vitro* and their therapeutic efficacy *in vivo*¹⁹⁶. CellPore™ (StemCell Technologies) is a commercial device that employs CellSqueeze™ technology to deliver RNP complexes for gene editing of non-activated human T cells. Loo *et al.* fabricated a related technology in which cells are quickly squeezed and expanded through a series of constrictions. T cell transfection with mRNA via these ultra-fast physical deformations did not affect T cell proliferation capacity or expression of differentiation and exhaustion surface markers²⁰⁹. This technology is under development at the start-up company CellFe.

While clogging of microchannels with constriction sites by debris or cell clusters is a reported practical disadvantage of the cell squeeze technology, alternative microfluidic designs have emerged in which PM permeabilization is achieved by hydrodynamic forces in relatively wide channels. For instance, Kizer *et al.* developed a clogging-free cross-junction channel design where transient membrane pore formation by rapid hydrodynamic cell shearing permits both diffusive and convective delivery of external

macromolecules into the cytosol ²¹⁰. In another approach called ‘microfluidic vortex shedding’ (μ VS), Jarrell *et al.* constructed a microfluidic chip with an array of equally spaced posts to generate hydrodynamic vortices, which can induce a disruption to the membrane of cells transported by the fluid flow ²⁰⁷. In such a design, spacing between posts was approximately two times larger than the median cell diameter, increasing the tolerance for cell size variability and reducing the risk of channel clogging. The authors reported a very high processing throughput of 2 million cells per second and showed that μ VS-mediated transfection did not impact T cell activation state and proliferation rates for at least seven days after treatment ²⁰⁷. The μ VS technology is presently commercialized by Indee Labs. To address the problem of high cargo consumption, Joo *et al.* designed a strategy that leverages droplet microfluidics with cell mechanical permeabilization (**Figure 5B**) ²¹¹. In this approach, cells and cargo macromolecules are co-encapsulated into droplets, which are then squeezed through a series of narrow constrictions. Upon cell membrane disruption, intracellular delivery occurs by a combination of convection and diffusion-mediated transport. While channel clogging was negligible, loading into droplets significantly reduced the amount of cargo needed.

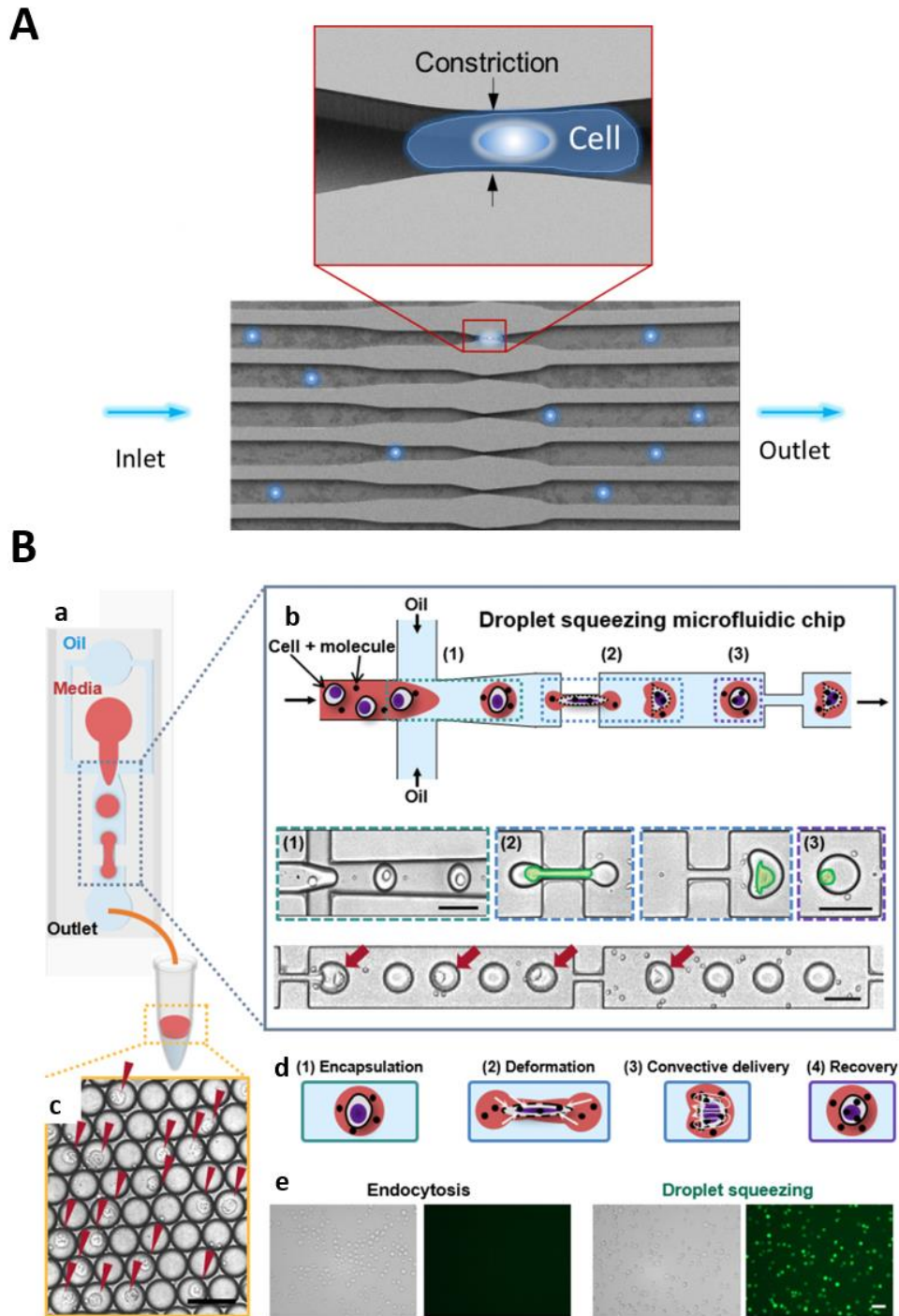


Figure 5. Microfluidic platforms for intracellular delivery. (A) Schematic illustration of the microfluidic cell squeezing principle. Rapid mechanical deformation of cells as they pass through a constriction smaller than their diameter generates transient disruptions in the cell membrane, allowing extracellular molecules dispersed in the surrounding medium to enter the cell. Adapted from Sharei *et al.*²⁰⁴ (B) Droplet squeezing platform. In this approach, cells are first coencapsulated with cargo molecules into water-in-oil droplets. These droplets then flow through a series of narrow constrictions to mechanically disrupt the cell membrane. With cargo molecules present in direct vicinity of membrane pores, intracellular delivery is believed to happen via convective

solution exchange enhanced by recirculation flows in the droplets. An example of FITC dextran delivery in K562 cells is shown. Adapted from Joo *et al.* ²¹¹

3.1.3 Solvent-based poration

Chemicals have also been used to permeabilize the PM. The Solupore[®] technology, currently commercialized by Avectas, uses a proprietary hypotonic permeabilization solution containing a low level of ethanol ²¹². The cargo of interest is mixed with the permeabilization solution and applied to the cells using an atomizer. This leads to local osmotic cell swelling and reversible PM perturbation, enabling cargo molecules to enter the cell by diffusion. After a brief incubation step, a stop solution is added to facilitate membrane resealing. In the initial proof-of-concept study from 2017, O’Dea and co-workers used this technology to demonstrate successful delivery of mRNA, pDNA and proteins in various cell types, including BSA proteins in immortalized Jurkat T cells ²¹². In 2021, the authors reported primary T cell engineering with CD19 CAR mRNA with an average transfection efficiency of 60% and minimal perturbation of immune gene expression and effective CAR-mediated cytotoxicity *in vitro* and *in vivo* ²¹³. Although little literature is available on this technology, press resources provided by the manufacturer indicate a significant potential of the Solupore[®] platform for T cell engineering, which is supported by its simplicity, low cost, high transfection efficiencies with possibility for multiplexing and sequential delivery, and minimal impact on cell phenotype and functionality. The current portfolio of Avectas includes a Solupore Research Grade Tool for feasibility studies and a closed, clinical-grade cell engineering system with a processing scale of 10⁸ cells. A continuous, flow-through system for allogenic cell scale manufacturing of above 10⁹-10¹⁰ cells is currently under development.

3.1.4 Photoporation

Photoporation, also termed optoporation, is an emerging delivery technique that makes use of light energy to transiently permeabilize the cell membrane. In its original form, high-intensity femtosecond laser pulses are focused on the cell membrane to create a pore by photochemical and/or photothermal effects, allowing cytosolic entry of exogenous cargo by diffusion ^{214,215}. Although useful for single-cell transfections, the

general utility of such an approach has been limited by its labor-intensive and inherently slow nature. To enhance photoporation throughput, the process has been combined with photothermal nanomaterials, which efficiently absorb laser light and convert this energy into photothermal effects ²¹⁶. Typically, a nanoparticle-mediated photoporation procedure starts with cell incubation with photothermal nanoparticles to let them adsorb to the cell membrane (**Figure 6A**). Attachment of NPs to the PM can be promoted by NP surface functionalization with positively charged polymers to promote electrostatic interaction or *via* high-affinity ligand-receptor coupling ^{215,217,218}. After removal of unbound NPs by a washing step, the cargo of interest is added and cells are irradiated with a laser to induce membrane permeabilization. By using photosensitizing nanomaterials, the laser energy density required for effective pore formation is substantially reduced as compared to direct laser-induced photoporation. Therefore, a wide laser beam can be used, allowing quick scanning over the cells and significantly enhancing photoporation throughput. For instance, for T cell transfection, processing rates of ~5000 cells per second were reported ²¹⁸.

Depending on the laser energy, PM permeabilization can be mediated by photochemical reactions, local heating, or the generation of water vapor nanobubbles (VNBs). Application of relatively low-intensity laser pulses results in photothermal heating, which induces pore formation by denaturation of integral membrane proteins or local phase transitions of the lipid bilayer ²¹⁹. When NPs are irradiated with sufficiently high laser fluences, typically with pulses shorter than 10 ns, the temperature of the NP increases quickly by several hundreds of degrees, resulting in the evaporation of the surrounding water and formation of fast-expanding vapor nanobubbles. Once the thermal energy of the NPs is consumed, the VNB collapses, leading to local pressure waves that generate transient disruptions in the adjacent cell membrane, providing cytosolic access for external macromolecules ^{214,220,221}.

The applicability of photoporation for T cell editing has been supported by a series of proof-of-concept studies demonstrating successful delivery of various cargo molecules, including model dextrans of up to 500 kDa, siRNA, mRNA and RNP protein complexes in both unstimulated and pre-activated T cells ^{218,222–226}. Although gold NPs have been the most used nanosensitizer, they can be replaced by biocompatible and biodegradable

polydopamine NPs ²²⁵. Interestingly, the polydopamine NP size can be tuned to avoid excessive cell damage and preserve T cell functionality post-treatment ²²⁶. To create larger pores in the cell membrane and to facilitate more efficient transfection of cells with large nucleic acids like mRNA and pDNA, Fraire *et al.* developed optically triggered nanobombs ²²⁷. The nanobombs are composed of a 0.5 μm photothermal core particle surrounded by a corona of smaller inert nanoparticles of 0.1-0.2 μm . Upon absorption of an intense nanosecond laser pulse, the smaller nanoparticles are forcefully expelled by the formation of a VNB from the core particle. It was shown that these nanoparticles can penetrate through the membrane of nearby cells, thus creating large PM pores through which mRNA and pDNA can more easily penetrate. Being relatively gentle to cells, it was demonstrated that the mRNA transfection yield of Jurkat T cells was higher than for electroporation. In another approach, photothermal NPs have been incorporated within electrospun nanofiber substrates (**Figure 6B**), thus avoiding direct Tcell exposure to NPs, and circumventing remaining safety and regulatory concerns ¹⁹⁷. This system was used to transfect human CAR T cells with siRNA to downregulate PD-1 expression, resulting in faster tumor regression in a xenograft mouse model as compared to control CAR T cells. Importantly, it was shown that the functionality of T cells was better preserved as compared to electroporated T cells, resulting in higher cell killing potential. Photoporation with NP sensitizers and photothermal nanofibers is currently being developed by the start-up company Trince, including for T cell engineering.

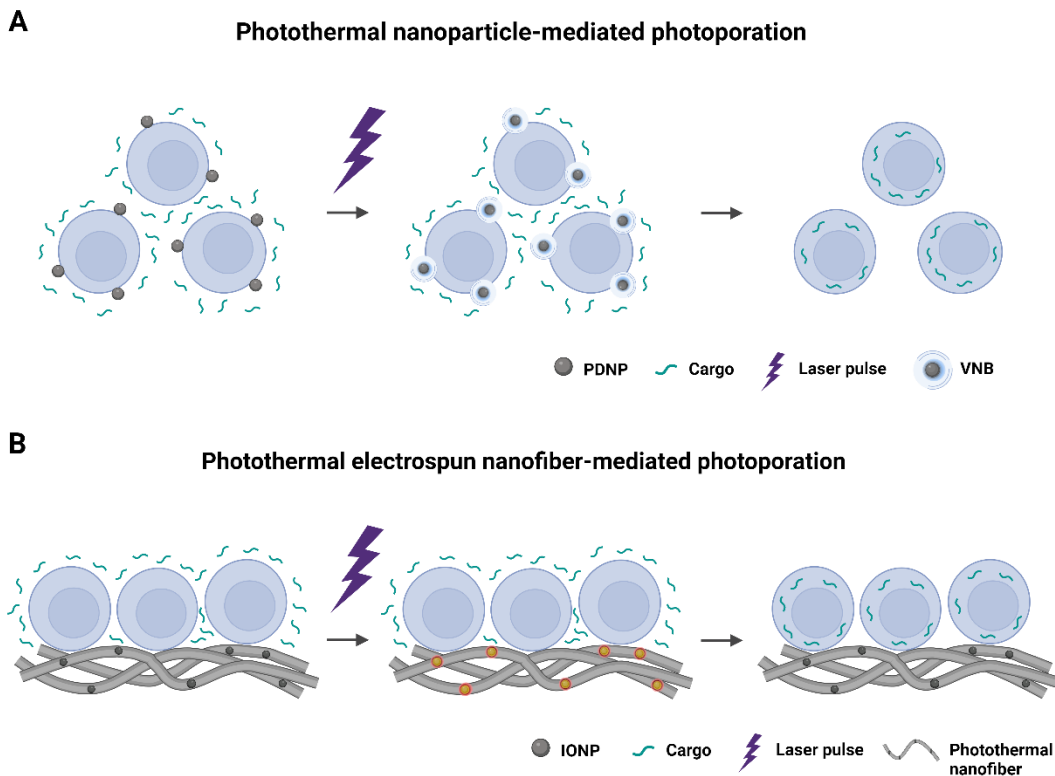


Figure 6. Schematic illustration of two photoporation modalities. (A) In standard nanoparticle-mediated photoporation, cells are first mixed with photothermal NPs, such as gold or polydopamine NPs, to let them adsorb to the cell surface. Next, application of pulsed laser irradiation leads to the generation of transient water vapor nanobubbles around cell-bound NPs. Subsequent expansion and collapse of VNBs cause mechanical membrane disruption, allowing external molecules to diffuse inside the cell. (B) In photothermal electrospun nanofiber-based photoporation, photothermal iron oxide NPs are embedded within nanofiber substrates fabricated by electrospinning. In this way, direct cell exposure to photosensitizing nanoparticles can be eliminated, alleviating safety and regulatory concerns related to the potential presence of nanomaterials in the final cell product. After T cells sedimentation on top of nanofiber mesh, membrane permeabilization occurs via laser-induced photothermal heating.

3.1.5 Nanostructures

Nanowires, nanoneedles and nanostraws are examples of high aspect ratio nanostructures fabricated into vertically aligned arrays to mechanically disrupt cell membranes for intracellular delivery^{167,228,229}. Cargo molecules can be coated at the tip of such structures or added to the cell culture medium. Alternatively, nanostraws, which are hollow versions of nanowires, are used to inject cells with cargo pumped from a fluid reservoir underneath the array. Cell interactions with nanowires rely on passive settling and adhesion, or application of an external force such as centrifugation. The exact

mechanism of nanostructure-mediated penetration and intracellular delivery is a subject of ongoing debate ^{230,231}. It was previously proposed that in the presence of centrifugal forces, the cell membrane undergoes large-scale deformations due to the nanowire indentation, while the cell body volume does not change. In the adhesion-mediated process, cells continue to deform around the nanowires until they adhere to the substrates, inducing localized membrane tension, which eventually causes membrane rupture ²³⁰. Penetration can be optimized by manipulation of needle geometry (density, length and diameter), surface functionalization and interfacing time. For instance, effective intracellular delivery of macromolecules into small immune cells requires nanowires that are longer, sharper and denser compared to structures suitable for larger adherent cells ²³². Transfection with siRNA-coated silicone nanowires demonstrated efficient (77%) gene silencing in resting murine CD4+ T cells without affecting cell viability and post-activation expansion rates, nor inducing innate immune responses ²³². In a follow-up study, the authors employed nanowire-based siRNA delivery to investigate the dynamic regulatory network that controls Th17 differentiation, showcasing the technology potential for efficient engineering of even unstimulated T cells without impacting their phenotype ²³³. More recently, a silicone nanotube-based nanoinjection platform loaded with PCR expression cassette encoding anti-CD19 CAR was used to generate CAR T cells with an average expression efficiency of ~20% and demonstrated CAR-mediated cytotoxicity *in vitro* ²³⁴. As such, nanostructures present an attractive alternative for T cell transfections, though further research on functional consequences of such interfacing and scalable fabrication enabling high throughput treatment are still needed to validate their potential for therapeutic T cell engineering.

3.2 Carrier-mediated delivery systems

As another non-viral strategy, chemical transfection reagents can be used, which mostly rely on endocytic uptake of the complexes that are formed between the RNA and transfection reagent ²³⁵. However, lymphocytes are notoriously hard to transfect with conventional chemical transfection reagents such as cationic lipids and polymers. Although the exact mechanism behind this resistance is not well understood, it is most likely related to specific T cell properties, including their small size, high nucleus-to-cytoplasm ratio, nonphagocytic nature and low rates of endocytosis. For instance, it was

proposed that insufficient uptake of lipoplexes can be explained by relatively low expression levels of heparan sulfate proteoglycans of which the negatively charged sulfate groups are involved in the initial binding of positively charged particles ²³⁶. To increase nanoparticle binding and uptake in lymphocytes, the nanomaterial surface can be functionalized with a receptor-specific ligand that selectively binds to T cells and induces receptor-mediated endocytosis, such as CD3, CD4, CD8, CD7 ^{237–242}, β 7 integrin ²⁴³, PD-1 immune checkpoint ²³⁶ and IL-2 receptor ²⁴⁴.

Another factor that can reduce the efficiency of transfection reagents is the slow acidification rate of endosomes in primary T cells, which is often needed as a release mechanism to let the RNA cargo escape the endosomes ²⁴⁵. Over the years, several strategies to enhance endosomal escape have been reported, including (i) membrane destabilization and membrane fusion-based methods using fusogenic lipids and lipid-polymer nanomaterials, (ii) the proton-sponge effect in the presence of buffering polymers, where the influx of protons and chloride ions leads to endosomal swelling and rupture, (iii) pore formation *via* cell-penetrating peptides and (iv) photochemical and photothermal disruption ^{246–251}. Nevertheless, endosomal escape remains the major rate-limiting step in the delivery of RNA therapeutics by chemical transfection agents, with several studies showing that less than 2% of the internalized cargo reaches the cytoplasm for functional delivery ^{252–254}. Besides enzymatic degradation, nanoparticle excretion from the cell via exocytosis is another mechanism reducing gene delivery efficiency ²⁵³. Also, degradation by cytoplasmic nucleases or clearance by autophagy are factors that reduced transfection efficiency ²⁵⁵.

3.2.1 Lipid-based nanoparticles

Lipid-based formulations, including natural and synthetic lipids and lipid-like materials (lipidoids), represent the most widely used non-viral gene carriers. Early studies focused on cationic lipids such as DOTMA (1,2-di-O-octadecenyl-3-trimethylammonium-propane chloride) and DOTAP (1,2-dioleoyl-3-trimethylammonium propane), which are composed of positively charged polar head groups and hydrophobic tails connected by a linker group ^{256,257}. In an aqueous solution, cationic lipids spontaneously self-assemble into higher-order aggregates and retain their cationic nature in a pH-independent manner. Thanks to

their cationic amino groups, they can electrostatically interact with the negatively charged phosphate groups of mRNAs, leading to the formation of lipoplexes that can shield RNA from nuclease degradation. Lipoplexes obtained by mRNA complexation with cationic liposomes based on DOTMA and helper lipid DOPE were the first lipid-based delivery systems successfully employed for mRNA transfection *in vitro* in 1989²⁵⁸. However, cationic lipoplexes have displayed limitations such as high instability and rapid clearance by phagocytic cells, leading to significant toxicities and inducing proinflammatory immune responses^{259–263}. As such, current research interest has shifted to lipid nanoparticles (LNPs), offering superior stability, structural plasticity and improved gene delivery efficiency^{256,264,265}.

A typical LNP formulation consists of ionizable or cationic lipids, neutral helper lipids, cholesterol and polyethylene glycol (PEG)-lipid (**Figure 7**). Ionizable lipids are positively charged at acidic pH to condense RNAs during LNP formulation but have a neutral charge at physiological pH to minimize toxicity during systemic delivery^{257,265–267}. As such, nanoparticles formulated with pH-responsive lipids demonstrate superior biocompatibility, with prolonged circulation time and reduced off-target accumulation. Following cellular uptake, ionizable lipids can be protonated in the acidic endosomes and interact with anionic endosomal phospholipids to destabilize endosomal membranes and facilitate RNA release in the cytosol. The ionizable lipids are represented by the DLin-MC3-DMA (MC3) lipid included in the formulation of Onpattro® (patisiran), which is the first-ever FDA-approved siRNA drug for the treatment of hereditary transthyretin amyloidosis polyneuropathies²⁶⁸ and biodegradable ionizable lipids, SM-102 and ALC-0315 (**Figure 7c**), used for the formulation of COVID-19 LNP-mRNA vaccines from Moderna (Spikevax®) and Pfizer/ BioNTech (Comirnaty®), respectively²⁵⁶.

Helper lipids such as DSPC (1,2-distearoyl-sn-glycero-3-phosphocholine) or DOPE (1,2-dioleoyl-sn-glycero-3-phosphoethanolamine) can stabilize the membrane structure of LNPs and facilitate endosomal escape²⁶⁹. The cholesterol fraction regulates membrane rigidity and fluidity, promoting particle stabilization by inserting into the inter-phospholipid spaces²⁷⁰. In addition, incorporating cholesterol plays a key role in cell transfection, potentially by promoting membrane fusion and endosomal escape. Although most LNPs are formulated with unmodified cholesterol, hydroxycholesterol

substitution has been recently shown to improve by twofold mRNA delivery to primary human T cells *ex vivo* without altering LNP stability²⁷¹. The hydrophilic PEG-lipid fraction is the lowest of all LNP components (~1-2 mole percentage) but has a considerable impact on their physicochemical properties (size, polydispersity and surface charge), shaping LNP pharmacokinetics upon systemic administration^{272,273}. Incorporation of PEG-lipid increases LNP colloidal stability and prolongs their blood circulation time by reducing serum protein opsonization and clearance by the mononuclear phagocyte system *in vivo*. However, PEGylation can also inhibit cellular internalization and endosomal escape, thus limiting nucleic acid delivery²⁷³.

As mentioned before, the surface of LNPs can be decorated with specific targeting ligands to direct their cell-specific uptake. For example, the Peer group developed a customizable LNP platform for targeted siRNA delivery in lymphocytes²⁷⁴. In this work, LNPs are non-covalently coated with targeting antibodies via a recombinant membrane-anchored lipoprotein that is incorporated in the lipid bilayer and interacts with the antibody Fc domain. Using targeting antibodies directed against CD3, CD4 and CD25, the authors demonstrated efficient delivery and silencing in different murine T cell subsets. In another study, the same research group showed effective lymphocyte targeting with a pan leukocyte β 7 integrin²⁴³.

Current state-of-the-art LNP fabrication strategies rely on microfluidic rapid mixing of the organic phase containing the lipids and mRNA dispersed in the aqueous phase, offering high encapsulation efficiency and good batch-to-batch reproducibility^{275,276}. Such manufacturing process can be scaled-up to meet clinical scale demands, as best exemplified by unprecedentedly large and rapid rollout of COVID-19 LNP-mRNA vaccines.

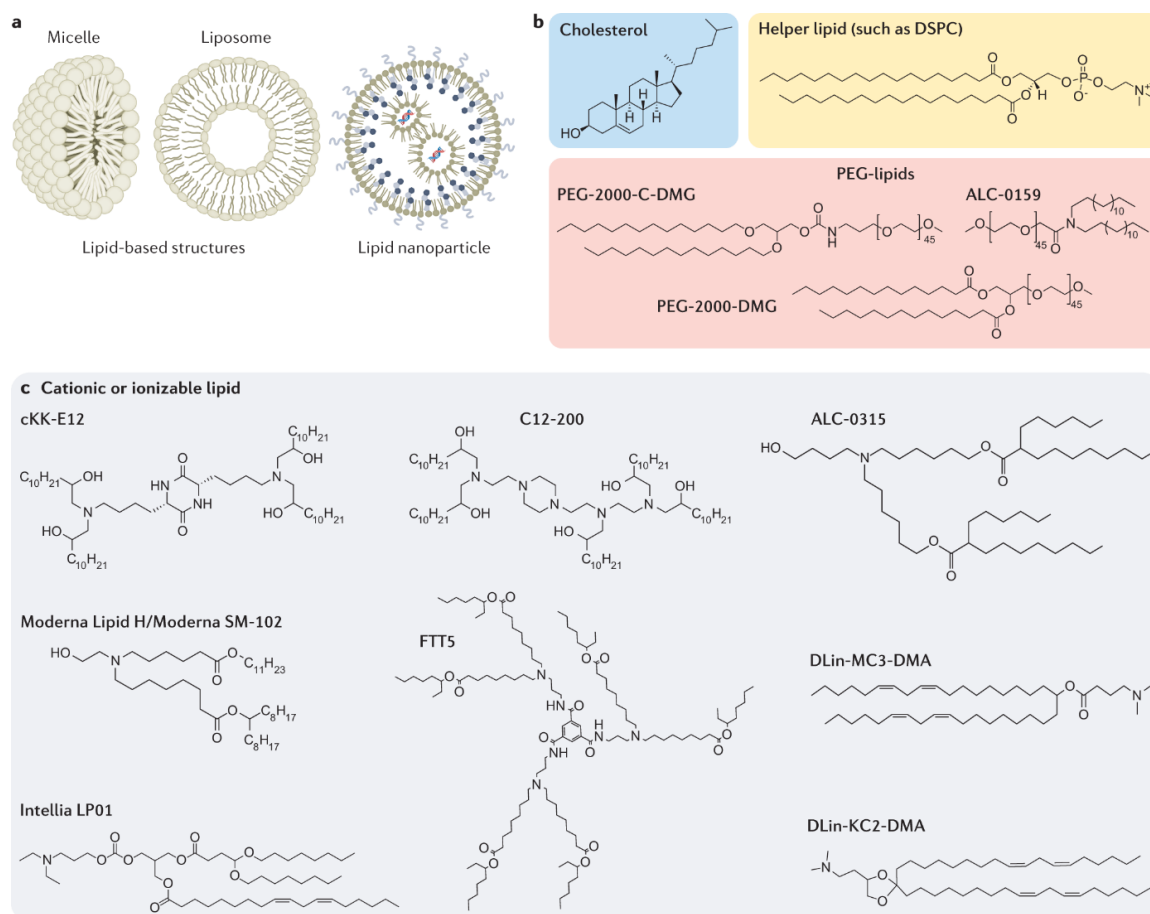


Figure 7. Morphology and major structural components of lipid-based nanoparticles. (a) Schematic representation of different types of lipid-based nanostructures. Micelles consist of a lipid monolayer, while liposomes consist of a lipid layer and an aqueous core. LNPs are composed of multiple lipid layers and a densely packed core encapsulating the nucleic acid cargo. (b-c) Molecular structures of cholesterol, helper lipid DSPC and frequently used PEG-lipids and cationic/ionizable lipids. The latter contain amine groups which become positively charged at low pH, facilitating anionic RNA binding. Figure adapted from Paunovska *et al.*²⁷⁷

3.2.2 Polymer-based nanoparticles

Polymer compounds and their derivatives represent another class of materials explored for gene delivery. Such carriers typically rely on cationic polymers able to complex negatively charged nucleic acids, forming so-called polyplexes. One of the most widely studied polymeric materials is polyethyleneimine (PEI) which offers high transfection efficiencies thanks to its high buffering capacity below physiological pH. Once internalized, protonation of PEI amine groups causes osmotic swelling and endosomal rupture leading to endosomal escape *via* the proton sponge effect²⁷⁸. However, since unmodified PEI is

highly toxic and nonbiodegradable, several strategies, such as shielding or copolymerization, have been proposed to increase its biocompatibility. For instance, PEG-grafted-PEI copolymers have been used to transfect siRNA to primary T cells *in vitro* ²⁷⁹. Alternatively, poly(2-(dimethylamino ethyl methacrylate (PDMAEMA) is a water-soluble cationic polymer known for its pH- and temperature-responsive properties ²⁸⁰. In 2012, Schallon *et al.* reported on PDMAEMA-based star-shaped nanoparticles for siRNA delivery in primary human T cells, reaching around 40% CD4 silencing ²⁸¹. Later, Olden *et al.* evaluated different pHEMA-g-pDMAEMA polymer architectures for mRNA transfection in T cells, reporting transfection efficiencies of up to 50% and 25% in the Jurkat T cell line and primary human T cells, respectively ²⁸². The authors identified reduced cellular uptake and slower endosomal acidification as the major barriers to carrier-mediated T cell transfections ²⁴⁵.

Another interesting class of polymers are biodegradable poly(beta-amino ester)s (PBAEs), synthesized by conjugating amine monomers to diacrylates ²⁸³. The Stephan's group published a series of studies on T cell-targeted gene nanocarriers comprising of i) PBAE polymer matrix to condense the nucleic acid, ii) negatively charged polyglutamic acid (PGA) coating to reduce off-target binding and iii) surface-anchored targeting ligands. Among different examples, such anti-CD3-targeting PBAE-based nanocarriers proved applicable for *ex vivo* T cell engineering with mRNA ²⁸⁴. Transfection of mRNA encoding megaTAL nuclease targeting the TRAC locus resulted in an average TCR knock-out of ~60%. In addition, the authors demonstrated transfection of mRNA encoding FoxO1 transcription factor to promote the generation of central memory T cells which are characterized by superior anti-tumor efficacy ²⁸⁴.

4 Applications of RNA therapeutics in T cell engineering

4.1 Engineering cancer specific T cells

T cells engineered to express tumor specific TCRs and CARs using viral vectors have shown considerable clinical success in adoptive cell therapy for various cancers. Among non-viral approaches, most preclinical and clinical studies have used electroporation for transfecting T cells with mRNA encoding for chimeric antigen receptors.

B cell malignancies were the first hematological malignancies to be effectively targeted with CAR T cells directed against CD19 surface antigen. In 2006, Rabinovich and colleagues were the first to generate CD19 CAR T cells by IVT mRNA electroporation, demonstrating their target-specific cytotoxicity *in vitro* ²⁸⁵. In 2009, the same group showed that such CD19 mRNA modified CD3+CD8+ T cells could inhibit tumor progression in a humanized mouse model of Daudi lymphoma ²⁸⁶. Barrett *et al.* evaluated the cytotoxic potential of CD19-mRNA redirected T cells in a xenograft model of acute lymphoblastic leukemia (ALL), demonstrating T cell migration to distant sites of disseminated tumor with preserved lytic activity and prolonged mice survival ²⁸⁷. In another study, the authors proposed an optimized protocol based on multiple CD19 mRNA CAR T cell infusions combined with interval lymphodepletion to achieve anti-tumor efficacy comparable to that mediated by lentiviral-generated stable CAR T cells ²⁸⁸. Building upon the preclinical success of mRNA-engineered CD19 CAR T cells, as well as the clinical success of lentiviral CD19 CAR T cells in leukemia, the University of Pennsylvania opened a clinical trial in 2014 using CD19-targeted mRNA-engineered T cells in patients with relapsed or refractory classical Hodgkin's lymphoma (NCT02277522 and NCT02624258; **Table 1**). This lymphoma is characterized by scant CD19-negative Hodgkin and Reed-Sternberg (HRS) cells within an immunosuppressive tumor microenvironment, which poses limitations for approaches directly targeting antigens expressed on HRS cells ²⁸⁹. Instead, CAR T cells were targeted against CD19+ B cells in the tumor microenvironment and putative circulating CD19+ HRS cells to disrupt the immunosuppressive milieu, indirectly affecting HRS cell survival. Among four patients administered with mRNA CAR T cells, one patient achieved transient complete response, one showed partial response, one showed stable disease and one

progressed. Owing to the transient CAR mRNA expression, the therapy was well tolerated, with no severe toxicity reported ²⁸⁹.

Beyond CD19, other targets for hematological malignancies have been investigated as well. For instance, Panjwani *et al.* reported on the successful development of canine CD20 mRNA CAR T cells, which induced modest and transient anti-tumor activity in a dog with relapsed B cell lymphoma ²⁹⁰. Since a subset of patients who relapse after CD19 CAR T cell therapy demonstrated outgrowth of CD19-negative tumor cells, Köksal *et al.* evaluated CD37 as an alternative target for CAR-based therapy of B-cell non-Hodgkin lymphoma ²⁹¹. *In vitro* comparison between CD37-targeting and CD19-directed mRNA CAR T cells showed a similar killing efficacy towards human Burkitt's lymphoma cell line BL41 and diffuse large B cell lymphoma cell line U-2932. In addition, CD37 CAR T cells proved as potent as CD19 counterparts in controlling tumor growth in a murine BL-41 xenograft model and outperformed CD19 CAR T cells in treating mice engrafted with U-2932 tumors that contained a CD19-negative population ²⁹¹. Compared to B-cell malignancies for which CAR T cell products have already been approved, identifying a target for CAR T cell therapy in myeloid malignancies such as acute myeloid leukemia (AML) has proven particularly challenging. Since surface antigens expressed on AML cells are usually shared with normal hematopoietic progenitors, targeting them can lead to significant on-target off-tumor toxicity. CD33 and CD123 represent the most commonly investigated markers for CAR T cell engineering in AML treatment. When Kenderian *et al.* evaluated lentiviral CD33 CAR T cells in a xenograft mouse model of AML, effective anti-tumor responses were accompanied by significant hematopoietic toxicity ²⁹². The authors subsequently generated mRNA modified CD33 CAR T cells that displayed potent but transient anti-leukemic activity, thus avoiding previously seen myelotoxicity. Similar findings were reported for lentivirally transduced CD123-redirected CAR T cells in preclinical AML models, with efficient leukemia eradication coming at the cost of severe hematologic toxicity ²⁹³. The same group then assessed mRNA modified CD123 CAR T cells in a MOLM14 xenograft model, demonstrating rapid AML clearance and remission for >6 months ²⁹⁴. In a pilot clinical trial at the University of Pennsylvania (NCT02623582; **Table 1**), mRNA CD123 CAR T cells were tested in patients with relapsed/refractory AML, with the primary objective of showing safety ²⁹⁵. Although the therapy was proven safe, no

anti-tumor efficacy could be demonstrated. The team reported manufacturing difficulties due to the poor quality of patient T cells and a lack of persistence of administered CAR T cells. However, a sufficiently safe profile was established in this study, allowing to proceed with clinical testing of CD123 CAR T cells generated with lentiviral vectors.

B-cell maturation antigen (BCMA) is the most common target for CAR T cell therapy in multiple myeloma (MM). Li *et al.* reported on the development of Descartes-08, an autologous CD8+ T cell-only product modified with anti-BCMA CAR mRNA, demonstrating potent cytolytic activity in MM cells and prolonged host survival in a mouse model of disseminated human myeloma ²⁹⁶. Preliminary results from the phase I/II clinical trial of Descartes-8 in relapsed/ refractory myeloma patients (NCT03448978) indicated good tolerability and durable responses. A phase II clinical trial (NCT04436029) has been initiated to evaluate Descartes-11, a humanized version of Descartes-8, as a consolidative therapy in patients with newly diagnosed, high risk multiple myeloma who have residual disease after induction therapy. Interestingly, BCMA-targeting CAR T cells are also being evaluated in phase I/II clinical trial (NCT04146051) in patients with generalized myasthenia gravis, a neuromuscular autoimmune disease driven by self-reactive antibodies produced by plasma cells. According to a recently published update, Descartes-8 infusions were safe and well-tolerated, resulting in clinically meaningful improvements in disease severity for up to nine months ²⁹⁷.

Beyond targeting hematological malignancies, IVT mRNA-modified CAR T cells have been widely investigated for the treatment of solid tumors, where T cells face additional physical and immune hurdles that impede T cell tumor penetration and persistence at the tumor sites. These include vascular and stromal barriers, tumor antigen heterogeneity and nutrient-poor and immunosuppressive milieu. Some early studies focused on mesothelioma, a type of malignant tumor that occurs in tissues lining the heart, stomach and lungs. Zhao *et al.* designed IVT mRNA CARs targeting mesothelin, a tumor associated antigen (TAA) overexpressed in mesothelioma, ovarian and pancreatic cancers ²⁹⁸. The authors demonstrated that repeated (intratumor) administration of mRNA-modified mesothelin CAR T cells markedly reduced flank mesothelioma tumors in a mouse model. In addition, similar anti-tumor efficacy was observed in a disseminated intraperitoneal tumor model established with patient-derived mesothelioma and treated by multiple

injections of autologous anti-mesothelin CAR T cells, suggesting that autologous T cells can be effectively redirected against TAAs using IVT mRNA. Based on this work, two clinical studies were initiated to evaluate the safety and feasibility of mesothelin-directed mRNA CAR T cell therapy in patients with malignant pleural mesothelioma (NCT01355965) and metastatic pancreatic cancer (NCT01897415). Preliminary analysis of four patients showed that the approach was well tolerated, except for one patient, who developed severe anaphylactic shock after the third CAR T cell infusion received after a four-week treatment interruption ²⁹⁹. It was hypothesized that the anaphylactic event resulted from the induction of IgE antibodies against murine sequences in the CAR construct. The authors adjusted the schedule of infusions, avoiding breaks longer than 10 days in order to prevent further anaphylactic incidences. In a follow-up study, Beatty *et al.* reported on the efficacy of the mesothelin-targeted mRNA CAR T cells in two patients, including the one who had experienced anaphylactic shock ³⁰⁰. Both patients demonstrated a partial response, with evidence of humoral epitope spreading, suggesting the induction of an adaptive immune response. In 2018, Beatty *et al.* published follow-up results from six patients with metastatic pancreatic ductal adenocarcinoma ³⁰¹. None of the patients experienced cytokine release syndrome or neurologic symptoms, nor were dose-limiting toxicities observed. The best overall response achieved with a total of 9 doses of mRNA CAR T cells was stable disease in two patients. One other patient showed a reduction of liver lesions but no effect on the primary pancreatic tumor, suggesting distinct biology between the primary and metastatic disease. The therapy induced a spreading antibody response with increased production of antibodies against multiple proteins, including immunomodulatory molecules such as PD-1, PD-L1 and BCMA. The authors concluded that such antibody responses were consistent with CAR T cell-mediated tumor destruction which lead to the release of self-proteins and their cross-presentation, evoking epitope spreading. It was proposed that mesothelin-directed CAR T cells may serve as a probing tool to investigate the immunobiology of pancreatic tumors and guide further development of effective T cell therapies for this condition.

The example of mesothelin-directed CAR T cells points to the important consideration of the immunogenicity of CAR T cell therapy, which can potentially induce both humoral and cellular anti-CAR responses to non-self components of the CAR construct, resulting in

rapid clearance of administered CAR T cells from the circulation 302,303. Generation of anti-CAR antibodies presents significant concern in case of repeated dosing and in patients receiving CAR T cell products that do not deplete endogenous B cells, like in the case of solid tumors, where a balance between inducing potent endogenous immunity to cancer cells and responses against CAR T cells is desired.

Another target investigated for peritoneal tumors is epithelial cell adhesion molecule (EpCAM), expressed on the normal epithelium and upregulated in peritoneal carcinomatosis from gastrointestinal and gynecological malignancies. Ang *et al.* evaluated EpCAM mRNA CAR T cells in peritoneal dissemination mouse models of human ovarian and colorectal cancers, demonstrating that repeated injections of CAR T delayed tumor growth and prolonged mice survival but were unable to eradicate the disease ³⁰⁴.

GD2 ganglioside and glypican 2 (GPC2) are examples of tumor associated antigens studied for central nervous system tumors. Singh *et al.* compared the efficacy of mRNA-modified and lentivirally-modified GD2 CAR T cells in local and disseminated xenograft models of neuroblastoma ³⁰⁵. While intra-tumoral injection of mRNA GD2 CAR T cells in a localized model resulted in tumor regression, multiple infusions in a disseminated model slowed disease progression and improved survival but could not achieve long-term disease control. Histologic examination showed that, unlike permanently-modified cells, mRNA GD2 CAR T cells were unable to penetrate the tumor environment, implicating that the transient nature of mRNA expression would require local delivery to realize mRNA CAR T cell therapeutic potential. More recently, Foster *et al.* developed GPC2-directed mRNA CAR T cells demonstrating significant cytotoxicity in GPC2-expressing medulloblastoma and high-grade glioblastoma cell lines *in vitro* ³⁰⁶. In addition, repeated locoregional delivery of mRNA GPC2 CAR T cells induced tumor regression in an orthotopic medulloblastoma model and prolonged mice survival in a thalamic diffuse midline glioma xenograft model.

Several TAAs have been investigated for T cell therapy of melanoma, including vascular endothelial growth factor receptor 2 (VEGFR2), gp100 and melanoma-associated chondroitin sulfate proteoglycan (MCSP; or chondroitin sulfate proteoglycan 4, CSPG4) ³⁰⁷⁻³¹⁰. Inoo *et al.* reported that triple administration of mRNA VEGFR2 CAR T cells in a

B16-BL6 murine melanoma model achieved similar tumor growth inhibition as a single transfer of retrovirally-transduced CAR T cells ³¹¹. Another strategy is to use T cells expressing two additional receptors (TETARs) that hold the potential to overcome immune escape due to single antigen loss. Hofflin *et al.* reported on developing mRNA-modified T cells targeting gp100 and a patient-specific, individually mutated antigen ³⁰⁷. These dual-CAR T cells demonstrated specific lytic activity towards target cells loaded with each of their cognate antigens *in vitro*. Uslu *et al.* generated mRNA CD8+ TETARs co-expressing a CAR specific for MCSP antigen and a TCR specific for gp100 antigen, showing antigen-specific cytokine production and killing capacity against A375M and Mel526 melanoma cell lines ³⁰⁸. Of note, TETARs stimulated with both cognate antigens displayed higher cytolytic potential compared to a mixture of monospecific T cells transfected with either a CAR or TCR, indicating that TETARs were indeed able to recognize and target both antigens at the same time.

Hepatocyte growth factor receptor (c-Met) is a TAA expressed in various solid tumors. mRNA-modified c-MET CAR T cells have been evaluated in two clinical trials for the treatment of breast cancer and melanoma (NCT01837602, NCT03060356). Tchou *et al.* first demonstrated that mRNA c-MET CAR T cells elicited potent cytolytic effects in human breast cancer cell lines BT20 and TB129, and suppressed tumor growth in a murine model of human ovarian cancer ³¹². Next, a phase 0 study was initiated to evaluate intratumoral administration of mRNA c-MET CAR T cells in patients with metastatic breast cancer. The treatment was well-tolerated, without significant side effects, but no clinical responses were observed. Histologic examination of excised tumors revealed extensive tumor necrosis, loss of c-MET immunoreactivity and macrophage infiltration, suggesting an inflammatory response evoked by the treatment ³¹². Based on these observations, a phase I study (NCT03060356) was launched to evaluate intravenously administered mRNA c-MET CAR T cells in patients with malignant melanoma and metastatic breast cancer ³¹³. Treatment was safe, with only grade 1 or 2 adverse events observed, but no CRS or grade 3 toxicities. Out of 7 patients, four achieved stable disease while three experienced disease progression. The authors hypothesized that the lack of treatment response could be related to limited trafficking to tumor sites since no mRNA signal was detected in post-infusion tumor tissue.

Although *ex vivo* electroporation remains the most advanced non-viral strategy for therapeutic T cell engineering, alternative approaches based on lipid and polymer nanoformulations have been recently explored for *in vitro* and *in vivo* lymphocyte transfection. For instance, Billingsley *et al.* synthesized a library of 24 ionizable lipids and formulated them into LNPs³¹⁴. The top-performing formulation was then used for CAR mRNA transfection in primary human T cells, achieving CAR expression levels comparable to electroporation and potent cytolytic activity against Nalm-6 acute lymphoblastic leukemia cells *in vitro*.

An overview of clinical trials employing IVT mRNA in adoptive T cell therapy is provided in **Table 1**.

4.2 Gene editing for enhancing T cell function

In addition to introducing exogenous receptors, recent advances in gene editing technologies have opened new avenues to generate T cells with improved phenotypical characteristics, enhanced anti-tumor efficacy and the potential to be used in allogeneic applications. As discussed earlier, CRISPR-Cas9 components can be delivered to cells in various formats, such as plasmid DNA, mRNA and gRNA, or RNP complexes. In particular, delivery of mRNA encoding Cas9 nuclease alongside gRNA alleviates the risk of potential genome integration and, thanks to its transient expression profile, reduces off-target effect probability. Therefore, we mainly focus on studies describing nuclease delivery in such mRNA format. For a more comprehensive overview of CRISPR-Cas applications in T cell engineering, we refer the reader to recently published reviews^{315–319}.

One widely investigated area is to use CRISPR-Cas technology to replace endogenous T-cell receptors with transgenic TCRs to avoid competition in signaling and mispairing between native and transduced TCRs. This strategy can be further extended to generate “off-the-shelf” allogeneic CAR T cell products. Since manufacturing of autologous T cell therapies is often hampered by low yield and poor functionality of lymphocytes collected from elderly and heavily-pretreated patients, collection of allogeneic, healthy donor leukocytes represents an attractive alternative route to produce “universal” tumor-specific T cells with optimized persistence and anti-tumor efficacy^{315,318}. However, one major challenge to allogeneic transplantation is the induction of graft-versus-host-disease

(GvHD), where donor lymphocyte TCRs recognize surface antigens of the patient as foreign (non-self), eliciting an immune response. In addition, alloantigens expressed on transplanted cells, such as human leukocyte antigen (HLA-1), may provoke unwanted host immune responses (allorejection). Therefore, CRISPR-Cas9-mediated knock-out of endogenous TCRs and HLA-1 molecules could improve the compatibility of allogeneic CAR T cells. In particular, the T-cell receptor α constant (TRAC) locus has been extensively investigated as a suitable target for combined gene knockout and CAR knock-in. More specifically, placing the CAR transgene under the control of the endogenous TRAC promoter could drive robust CAR expression comparable to physiological TCR expression levels while simultaneously disrupting the endogenous TCR to eliminate GvHD concerns. For instance, Eyquem *et al.* electroporated Cas9 mRNA and sgRNA to target the TRAC locus and disrupt native TCR expression³²⁰. Subsequent transduction with an AAV vector encoding CD19 CAR DNA was used to induce CAR expression under the transcriptional control of the TRAC promoter. Directing CD19 CAR to the TRAC locus resulted in uniform CAR expression, reduced tonic signaling and delayed T cell differentiation and exhaustion. In a mouse model of acute lymphoblastic leukemia, TRAC-CAR T cells demonstrated potent anti-tumor responses and prolonged median host survival, outperforming conventional retrovirally transduced CARs, with and without TCR knock-out. A similar strategy exploiting cellular homology-directed repair (HDR) mechanism was reported by MacLeod *et al.* who combined an engineered homing nuclease and an AAV donor template for HDR-mediated insertion of the CD19 CAR transgene into the native TCR locus³²¹.

In another study, Georgiadis *et al.* employed a CD19 CAR lentiviral vector with a TRAC-targeting sgRNA sequence incorporated into the 3' long terminal repeat to mitigate potential interference effects³²². Pre-transduced T cells were electroporated with Cas9 mRNA to induce the TRAC locus cleavage and subsequently enriched into a highly homogenous CD19+TCR $\alpha\beta$ - population by magnetic depletion of residual TCR $\alpha\beta$ + cells. In a mouse model of human Daudi B cell leukemia, TCR-negative CD19 CAR T cells demonstrated effective tumor eradication without xenoreactive GvHD and reduced expression of exhaustion markers compared with conventional TCR-expressing CD19 CAR T cells. In 2022, the same group reported on the results of a phase I clinical trial

(NCT04557436) of allogeneic CRISPR-engineered CD19 CAR T cells for the treatment of children with refractory B cell leukemia ³²³. Lymphocytes collected from healthy adult donors were transduced with a CAR19 lentiviral vector incorporating CRISPR guide sequences targeting TRAC and CD52 loci, whose disruption upon Cas9 mRNA delivery by electroporation was intended to prevent GvHD and confer resistance to alemtuzumab used during lymphodepletion. The primary goal of the TT52CAR19 T cell application was to secure molecular remission ahead of programmed allogeneic stem cell transplantation (SCT). Four of six CAR-infused children exhibited cell expansion and achieved remission by day 28, after which they received allo-SCT. Two patients later relapsed and two remained in ongoing remission. Despite reported toxicities, primary safety objectives were met, providing early-stage evidence of feasibility and therapeutic potential of CRISPR-engineered immunotherapy.

To the best of our knowledge, no studies have yet reported on nanoformulation-mediated delivery of Cas9 mRNA specifically to T cells. However, other preclinical and clinical studies have already indicated the potential of nanoparticle-based transfection of gene-editing nucleases. For example, lipid NPs encapsulating Cas9 mRNA and sgRNA targeting transthyretin have been evaluated in a phase I clinical trial for *in vivo* gene editing in patients with hereditary transthyretin amyloidosis (NCT04601051) ³²⁴. In a preclinical study by Moffett *et al.*, polymeric NPs carrying mRNA encoding megaTAL nuclease targeting the TRAC locus demonstrated efficient TCR knock-out in ~60% of T cells ²⁸⁴. NP-mediated gene editing did not affect the efficiency of subsequent lentiviral transduction or the functionality of programmed CAR T cells.

Apart from endogenous TCRs, gene editing has been employed to disrupt inhibitory signals that contribute to T cell exhaustion and reduced anti-tumor efficacy. Many studies have focused on deleting immune checkpoint receptors, such as programmed cell death-1 (PD-1) and cytotoxic T-lymphocyte antigen-4 (CTLA-4). Beane *et al.* reported on PD-1 disruption in melanoma tumor-infiltrating lymphocytes (TILs) via electroporation of zinc finger nuclease mRNA, demonstrating their improved *in vitro* effector function and an increased polyfunctional cytokine profile ³²⁵.

CRISPR-Cas has also been used as an efficient strategy for simultaneous editing of multiple gene loci. Ren *et al.* used Cas9 mRNA electroporation to generate universal CAR T cells with enhanced resistance to apoptosis by disruption of endogenous TCR, HLA-I and CD95/Fas death receptor³²⁶. These triple-negative CAR T cells displayed increased expansion, prolonged survival in the peripheral blood and enhanced tumor control efficacy in a Nalm6 leukemia model. In another study, the same group reported on TRAC, β -2-microglobulin (B2M) and PD-1 disruption in lentivirally transduced CD-19 or prostate stem cell antigen (PSCA) CAR T cells to eliminate GvHD and host-versus-graft effects, and to increase CAR T cell activity³²⁷. HLA-I and TCR double negative T cells showed reduced alloreactivity compared to a single TCR- knock-out, while additional disruption of PD-1 resulted in enhanced anti-tumor activity in a Nalm6-PD-L1 leukemia model, as evidenced by quicker elimination of leukemia cells.

Beyond Cas9, other CRISPR variants have also been explored for multiplex gene editing in T cells. Dai *et al.* used a tracrRNA-independent Cas12a/ Cpf1 nuclease to demonstrate CD22 CAR integration into the TRAC locus combined with PD-1 knock-out³²⁸. Compared to Cas9-edited cells, Cpf1-modified CD22 CAR T cells displayed similar cytokine production and cancer cell killing but reduced expression of exhaustion markers. Webber *et al.* reported on the application of CRISPR base editors delivered by mRNA electroporation to knock-out TRAC, B2M and PD-1 for allogeneic CAR T cell generation³²⁹. Cell modification with base editors reduced DSB induction and translocation frequency compared to Cas9 nuclease-mediated engineering. In addition, the authors noted higher rates of nontarget editing and indel formation when using the RNP format instead of mRNA. In another study by Gaudelli *et al.*, base editors were used to target TRAC, B2M and class II transactivator (CIITA) to reduce the expression of the endogenous TCR and MHC class I and II machinery³³⁰.

Altogether, these studies highlight the potential of mRNA based gene editing technologies to improve the overall efficacy of T cell therapies. Some strategies combining viral vector CAR transduction with TALEN or CRISPR-Cas-enabled modifications have already entered clinical evaluation (**Table 2**), as reviewed in more detail elsewhere^{315,317,318,331}.

4.3 Other strategies to modulate T cell functionality

Effective anti-tumor T cell responses depend on multiple steps such as recognition of tumor-specific antigens, upregulation of activation markers and co-stimulatory molecules, *in vivo* proliferation, trafficking to the tumor site and preserving effector functions in a highly immunosuppressive tumor milieu. Upregulation of inhibitory receptors, downregulation of MHC class I expression on tumor cells and secretion of anti-inflammatory molecules can all contribute to T cell dysfunction, which can be mitigated by approaches based on immunomodulation with cytokines and co-stimulatory ligands and receptors. For instance, mRNA transfection can be employed to temporarily equip T cells with stimulatory receptors, enabling transient activation of inflammatory signaling. Pato *et al.* electroporated TILs from melanoma patients with mRNA encoding constitutively active TLR4 (caTLR4), which resulted in upregulation of CD25 and 4-1BB, increased IFN γ secretion and enhanced anti-melanoma cytolytic activity *in vitro*³³². Similar responses were observed by Levin *et al.* upon TIL electroporation with caCD40 mRNA³³³.

Furthermore, mRNA delivery has been leveraged to provide a transient and localized stimulation with membrane-bound cytokines, circumventing severe toxicities related to high-dose systemic administration. Weinstein-Marom *et al.* reported on electroporation of mRNA encoding membrane-anchored variants of IL-2, IL-12 and IL-15 in human CD8+ T cells and melanoma TILs^{334,335}. Membrane-associated cytokines bound to their corresponding surface receptors mainly *in cis*, thus confining a stimulatory effect to the transfected cells only. The engineered cytokines were found to support the *ex vivo* proliferation of activated T cells to a similar extent as their soluble counterparts. Co-delivery of cytokine mRNA with mRNA encoding for caTLR4 and/or caCD40 mRNA induced IFN gamma secretion, upregulation of T cell activation markers (CD25, CD69, 4-1BB and OX40) and improved the cytotoxicity of TILs against autologous melanoma cells *in vitro*³³⁵. Etxeberria *et al.* engineered tumor-specific CD8+ T cells to transiently express IL-12 and CD137 (4-1BB) ligand, showing that intra-tumoral injection of such modified cells led to epitope spreading and regression of both injected and distant lesions in solid tumor models³³⁶. In addition, patient-derived TILs electroporated with IL-12 mRNA demonstrated significant IFN γ production and anti-tumor efficacy in a patient-derived xenograft mouse model of endometrial cancer, supporting the clinical feasibility of such

an approach. In another study, the same group reported on intracavitary administration of IL-12 mRNA-engineered T cells to eradicate peritoneal metastasis in mouse models ³³⁷. Transient IL-12 expression contributed to a favorable reprogramming of immune cells in the tumor microenvironment, prolonged *in vivo* persistence of transferred T cells and development of more durable immunity after primary tumor eradication.

Finally, other strategies to augment the therapeutic efficacy of T cell-based immunotherapies have focused on improving homing and T cell persistence at tumor sites. For instance, Mitchell *et al.* showed that electroporation of antigen-specific T cells with mRNA encoding chemokine receptor CXCR2 promoted their migration towards glioma-secreted CXCR-2 specific ligands *in vitro* and *in vivo* ³³⁸. Similarly, Almåsbaek *et al.* reported on co-electroporation of mRNA encoding CD19 CAR and chemokine receptors CXCR4 and CCR7 for improved chemotaxis of CAR T cells ³³⁹. Bai *et al.* electroporated CD19 CAR T cells with mRNA encoding for telomerase reverse transcriptase (TERT), demonstrating transiently enhanced telomerase activity and delayed replicative senescence, which translated to improved persistence and long-term anti-tumor efficacy in a mouse xenograft model of B-cell malignancy ³⁴⁰.

Together, these studies demonstrate the utility of RNA therapeutics to enhance T cell functionality towards more efficacious treatment modalities.

5 Conclusions and outlook

Despite remarkable progress seen in CAR T cell therapy in the last decade, several limitations remain to be addressed to move beyond the treatment of specific hematological malignancies and to make it more accessible to a broader population of patients. To mitigate toxicities and unleash CAR T cell potential for solid tumors, more sophisticated engineering approaches will be required to modulate multiple T cell phenotypical characteristics beyond single antigen-specificity. Most likely, such novel designs will necessitate simultaneous introduction and disruption of multiple genes to acquire multi-antigen specificity, reduce GvHD and HvG effects by removing endogenous TCRs and HLAs and overcome TME-imposed immunosuppression by disruption of negative regulators of T cell activation. These new editing strategies must come hand in hand with developing suitable transfection technologies capable of accommodating evolving CAR constructs, genome editing components and/or complementary molecules to modulate T cell functionality upon re-infusion in patients. While viral vectors are still used the most for T cell engineering due to their high efficiency, they come with several safety and practical concerns, such as limited cargo capacity, high cost, specialized facility requirements and regulatory hurdles. Therefore, much research has been devoted to non-viral transfection technologies compatible with the manufacturing of next-generation T cell therapies. Electroporation is the most investigated and clinically advanced non-viral technology, offering high transfection efficiencies, cargo flexibility and compatibility with clinical-grade cell manufacturing systems. However, since it is often associated with substantial cytotoxicity and reduced functionality, alternative physical and carrier-mediated approaches are actively explored, with a focus on preserving cell viability and long-term functionality. Nanostructure arrays, photoporation, chemical poration and microfluidic platforms are all being commercialized, although the latter two have advanced the furthest towards clinical evaluation. Also polymeric but especially lipid based carriers are making rapid progress for T cell engineering, with a promising future towards *in vivo* T cell reprogramming, thus eliminating the need for T cell isolation and *ex vivo* manipulation.

Modification of T cells with IVT mRNA to express specific tumor antigens has demonstrated good tolerability, even though the therapeutic efficacy was limited in

multiple clinical trials. Due to the transient expression of CAR mRNA only lasting up to a few days, repeated administration of CAR T cells is required to achieve meaningful anti-tumor responses. Nonetheless, the superior safety profile of mRNA-engineered T cells offers the opportunity to evaluate the safety of uninvestigated CAR designs before more permanent DNA-based CAR therapies are used for long-term expression. In case of severe adverse events, transient mRNA expression allows to rapidly cease the treatment.

Besides redirecting T cell specificity, genome editing with CRISPR-Cas holds great promise to advance the field, offering high gene-editing efficiency, versatility, and relative simplicity. Delivering Cas nuclease in mRNA format reduces the probability of off-target editing events. Finally, RNA molecules showed the potential to transiently modulate T cell phenotype, for instance, by silencing immune checkpoint receptors or upregulating expression of cytokines to enhance T cell proliferation and persistence upon adoptive cell transfer. Taken together, these studies demonstrate that either alone or more likely in combination with DNA-based permanent changes, RNA molecules will play a significant role in shaping next-generation T cell therapies.

Table 1. Clinical trials using IVT mRNA for adoptive T cell therapy

mRNA	Indication	Sponsor	Opened	Status	ClinicalTrial.gov identifier
anti-CD19 CAR	Hodgkin's lymphoma	University of Pennsylvania	2014	Terminated	NCT02277522
anti-CD123 CAR	Acute myeloid leukemia	University of Pennsylvania	2015	Terminated	NCT02623582
anti-c-MET CAR	Malignant melanoma, breast cancer	University of Pennsylvania	2017	Terminated	NCT03060356
Anti-mutant TGF β II TCR	Metastatic colorectal cancer	Oslo University Hospital	2018	Terminated	NCT03431311
anti-mesothelin CAR	Malignant pleural mesothelioma	University of Pennsylvania	2011	Completed	NCT01355965
anti-mesothelin CAR	Metastatic pancreatic ductal adenocarcinoma	University of Pennsylvania	2013	Completed	NCT01897415
anti-mesothelin CAR	Metastatic breast cancer, triple negative breast cancer	University of Pennsylvania	2013	Completed	NCT01837602
anti-BCMA CAR	Multiple myeloma	Cartesian Therapeutics	2018	Completed	NCT03448978
anti-BCMA CAR	Multiple myeloma	Cartesian Therapeutics	2020	Completed	NCT04436029
anti-BCMA CAR	Multiple myeloma	Cartesian Therapeutics	2019	Active	NCT03994705
anti-BCMA CAR	Multiple myeloma	Cartesian Therapeutics	2021	Active	NCT04816526

Table 2. Clinical trials using electroporation to deliver mRNA encoding gene editing nucleases in T cell therapy

Nuclease (mRNA)/ Target knock-out	Indication	Sponsor	Opened	Status	ClinicalTrial.gov identifier
TALEN mRNA TRAC and CD52 KO	B cell acute lymphoblastic leukemia; Pediatric patients	Institut de Recherches Internationales Servier	2016	Completed	NCT02808442
TALEN mRNA TRAC and CD52 KO	B cell acute lymphoblastic leukemia; Adult patients	Institut de Recherches Internationales Servier	2016	Completed	NCT02746952
Zinc finger nuclease mRNA CCR5 KO	HIV-1	University of Pennsylvania	2015	Completed	NCT02388594
TALEN mRNA CD52 and PD-1 KO	Multiple myeloma	Collectis S.A.	2019	Active	NCT04142619
TALEN mRNA CD52 and PD-1 KO	B cell acute lymphoblastic leukemia	Collectis S.A.	2019	Active	NCT04150497
CRISPR/Cas9 mRNA TRAC KO	Acute myeloid leukemia	Collectis S.A.	2017	Active	NCT03190278
CRISPR/Cas9 mRNA HPK1 KO	B cell malignancies	Xijing Hospital	2019	Active	NCT04037566
CRISPR/Cas9 mRNA CISH KO	Metastatic gastrointestinal epithelial cancer	Intima Bioscience, Inc.	2020	Active	NCT04426669

References

1. Siegel RL, Miller KD, Fuchs HE, Jemal A. Cancer statistics, 2022. *CA Cancer J Clin.* 2022;72(1):7-33.
2. Waldman AD, Fritz JM, Lenardo MJ. A guide to cancer immunotherapy: from T cell basic science to clinical practice. *Nat Rev Immunol.* 2020;20(11):651-668.
3. Singh AK, McGuirk JP. CAR T cells: continuation in a revolution of immunotherapy. *Lancet Oncol.* 2020;21(3):e168-e178.
4. Dobosz P, Dzieciatkowski T. The Intriguing History of Cancer Immunotherapy. *Front Immunol.* 2019;10.
5. Pardoll DM. The blockade of immune checkpoints in cancer immunotherapy. *Nat Rev Cancer.* 2012;12(4):252-264.
6. Rohaan MW, Wilgenhof S, Haanen JBAG. Adoptive cellular therapies: the current landscape. *Virchows Archiv.* 2019;474(4):449-461.
7. Sadelain M. Chimeric antigen receptors: A paradigm shift in immunotherapy. *Annu Rev Cancer Biol.* 2017;1:447-466.
8. June CH, Sadelain M. Chimeric Antigen Receptor Therapy. *New England Journal of Medicine.* 2018;379(1):64-73.
9. Shafer P, Kelly LM, Hoyos V. Cancer Therapy With TCR-Engineered T Cells: Current Strategies, Challenges, and Prospects. *Front Immunol.* 2022;13.
10. Rosenberg SA, Packard BS, Aebersold PM, et al. Use of Tumor-Infiltrating Lymphocytes and Interleukin-2 in the Immunotherapy of Patients with Metastatic Melanoma. *New England Journal of Medicine.* 1988;319(25):1676-1680.
11. Rosenberg SA, Restifo NP, Yang JC, Morgan RA, Dudley ME. Adoptive cell transfer: A clinical path to effective cancer immunotherapy. *Nat Rev Cancer.* 2008;8(4):299-308.
12. Besser MJ, Shapira-Frommer R, Treves AJ, et al. Clinical responses in a phase II study using adoptive transfer of short-term cultured tumor infiltration lymphocytes in metastatic melanoma patients. *Clinical Cancer Research.* 2010;16(9):2646-2655.
13. Rosenberg SA, Yang JC, Sherry RM, et al. Durable complete responses in heavily pretreated patients with metastatic melanoma using T-cell transfer immunotherapy. *Clinical Cancer Research.* 2011;17(13):4550-4557.
14. Kim DW, Cho JY. Recent advances in allogeneic CAR-T cells. *Biomolecules.* 2020;10(2).
15. Fang KKL, Lee J, Khatri I, Na Y, Zhang L. Targeting T-cell malignancies using allogeneic double-negative CD4-CAR-T cells. *J Immunother Cancer.* 2023;11(9).

16. Tipanee J, Samara-Kuko E, Gevaert T, Chuah MK, VandenDriessche T. Universal allogeneic CAR T cells engineered with Sleeping Beauty transposons and CRISPR-CAS9 for cancer immunotherapy. *Molecular Therapy*. 2022;30(10):3155-3175.
17. Martínez Bedoya D, Dutoit V, Migliorini D. Allogeneic CAR T Cells: An Alternative to Overcome Challenges of CAR T Cell Therapy in Glioblastoma. *Front Immunol*. 2021;12.
18. Gattinoni L, Finkelstein SE, Klebanoff CA, et al. Removal of homeostatic cytokine sinks by lymphodepletion enhances the efficacy of adoptively transferred tumor-specific CD8+ T cells. *Journal of Experimental Medicine*. 2005;202(7):907-912.
19. Brentjens RJ, Rivière I, Park JH, et al. Safety and persistence of adoptively transferred autologous CD19-targeted T cells in patients with relapsed or chemotherapy refractory B-cell leukemias. *Blood*. 2011;118(18):4817-4828.
20. Hirayama A V., Gauthier J, Hay KA, et al. The response to lymphodepletion impacts PFS in patients with aggressive non-Hodgkin lymphoma treated with CD19 CAR T cells. *Blood*. 2019;133(17):1876-1887.
21. Sadelain M, Rivière I, Riddell S. Therapeutic T cell engineering. *Nature*. 2017;545(7655):423-431.
22. Robinson J, Halliwell JA, Hayhurst JD, Flicek P, Parham P, Marsh SGE. The IPD and IMGT/HLA database: Allele variant databases. *Nucleic Acids Res*. 2015;43(D1):D423-D431.
23. Govers C, Sebestyén Z, Coccoris M, Willemsen RA, Debets R. T cell receptor gene therapy: strategies for optimizing transgenic TCR pairing. *Trends Mol Med*. 2010;16(2):77-87.
24. Van Loenen MM, De Boer R, Amir AL, et al. Mixed T cell receptor dimers harbor potentially harmful neoreactivity. *Proc Natl Acad Sci U S A*. 2010;107(24):10972-10977.
25. Okamoto S, Mineno J, Ikeda H, et al. Improved expression and reactivity of transduced tumor-specific TCRs in human lymphocytes by specific silencing of endogenous TCR. *Cancer Res*. 2009;69(23):9003-9011.
26. Liu Y, Yan X, Zhang F, et al. TCR-T Immunotherapy: The Challenges and Solutions. *Front Oncol*. 2022;11.
27. Robbins PF, Kassim SH, Tran TLN, et al. A pilot trial using lymphocytes genetically engineered with an NY-ESO-1-reactive T-cell receptor: Long-term follow-up and correlates with response. *Clinical Cancer Research*. 2015;21(5):1019-1027.
28. Ramachandran I, Lowther DE, Dryer-Minnerly R, et al. Systemic and local immunity following adoptive transfer of NY-ESO-1 SPEAR T cells in synovial sarcoma. *J Immunother Cancer*. 2019;7(1).
29. Stadtmauer EA, Fajtg TH, Lowther DE, et al. Long-term safety and activity of NY-ESO-1 SPEAR T cells after autologous stem cell transplant for myeloma. *Blood Adv*. 2019;3(13):2022-2034.

30. Gross G, Waks T, Eshhar Z. Expression of immunoglobulin-T-cell receptor chimeric molecules as functional receptors with antibody-type specificity. *Proceedings of the National Academy of Sciences*. 1989;86(24):10024-10028.
31. Eshhar Z, Waks T, Gross G, Schindler DG. Specific activation and targeting of cytotoxic lymphocytes through chimeric single chains consisting of antibody-binding domains and the gamma or zeta subunits of the immunoglobulin and T-cell receptors. *Proceedings of the National Academy of Sciences*. 1993;90(2):720-724.
32. Kuwana Y, Asakura Y, Utsunomiya N, et al. Expression of chimeric receptor composed of immunoglobulin-derived V regions and T-cell receptor-derived C regions. *Biochem Biophys Res Commun*. 1987;149(3):960-968.
33. Brocker T. *Chimeric Fv-or Fv-Receptors Are Not Sufficient to Induce Activation or Cytokine Production in Peripheral T Cells*. Vol 96.; 2000.
34. Maher J, Brentjens RJ, Gunset G, Rivière I, Sadelain M. Human T-lymphocyte cytotoxicity and proliferation directed by a single chimeric TCR ζ /CD28 receptor. *Nat Biotechnol*. 2002;20(1):70-75.
35. Imai C, Mihara K, Andreansky M, et al. Chimeric receptors with 4-1BB signaling capacity provoke potent cytotoxicity against acute lymphoblastic leukemia. *Leukemia*. 2004;18(4):676-684.
36. Kuhn NF, Purdon TJ, van Leeuwen DG, et al. CD40 Ligand-Modified Chimeric Antigen Receptor T Cells Enhance Antitumor Function by Eliciting an Endogenous Antitumor Response. *Cancer Cell*. 2019;35(3):473-488.e6.
37. Finney HM, Akbar AN, Lawson ADG. Activation of Resting Human Primary T Cells with Chimeric Receptors: Costimulation from CD28, Inducible Costimulator, CD134, and CD137 in Series with Signals from the TCR ζ Chain. *The Journal of Immunology*. 2004;172(1):104-113.
38. Hombach AA, Abken H. Costimulation by chimeric antigen receptors revisited the T cell antitumor response benefits from combined CD28-OX40 signalling. *Int J Cancer*. 2011;129(12):2935-2944.
39. Chmielewski M, Kopecky C, Hombach AA, Abken H. IL-12 release by engineered T cells expressing chimeric antigen receptors can effectively muster an antigen-independent macrophage response on tumor cells that have shut down tumor antigen expression. *Cancer Res*. 2011;71(17):5697-5706.
40. Kagoya Y, Tanaka S, Guo T, et al. A novel chimeric antigen receptor containing a JAK-STAT signaling domain mediates superior antitumor effects. *Nat Med*. 2018;24(3):352-359.
41. Maude SL, Laetsch TW, Buechner J, et al. Tisagenlecleucel in Children and Young Adults with B-Cell Lymphoblastic Leukemia. *New England Journal of Medicine*. 2018;378(5):439-448.

42. Viardot A, Wais V, Sala E, Koerper S. Chimeric antigen receptor (CAR) T-cell therapy as a treatment option for patients with B-cell lymphomas: Perspectives on the therapeutic potential of Axicabtagene ciloleucel. *Cancer Manag Res.* 2019;11:2393-2404.
43. Wang M, Munoz J, Goy A, et al. KTE-X19 CAR T-Cell Therapy in Relapsed or Refractory Mantle-Cell Lymphoma. *New England Journal of Medicine.* 2020;382(14):1331-1342.
44. Shah BD, Ghobadi A, Oluwole OO, et al. KTE-X19 for relapsed or refractory adult B-cell acute lymphoblastic leukaemia: phase 2 results of the single-arm, open-label, multicentre ZUMA-3 study. *The Lancet.* 2021;398(10299):491-502.
45. Ogasawara K, Dodds M, Mack T, Lymp J, Dell'Aringa J, Smith J. Population Cellular Kinetics of Lisocabtagene Maraleucel, an Autologous CD19-Directed Chimeric Antigen Receptor T-Cell Product, in Patients with Relapsed/Refractory Large B-Cell Lymphoma. *Clin Pharmacokinet.* 2021;60(12):1621-1633.
46. Munshi NC, Anderson LD, Shah N, et al. Idecabtagene Vicleucel in Relapsed and Refractory Multiple Myeloma. *New England Journal of Medicine.* 2021;384(8):705-716.
47. Berdeja JG, Madduri D, Usmani SZ, et al. Ciltacabtagene autoleucel, a B-cell maturation antigen-directed chimeric antigen receptor T-cell therapy in patients with relapsed or refractory multiple myeloma (CARTITUDE-1): a phase 1b/2 open-label study. *The Lancet.* 2021;398(10297):314-324.
48. Sterner RC, Sterner RM. CAR-T cell therapy: current limitations and potential strategies. *Blood Cancer J.* 2021;11(4).
49. Singh N, Perazzelli J, Grupp SA, Barrett DM. Early memory phenotypes drive T cell proliferation in patients with pediatric malignancies. *Sci Transl Med.* 2016;8(320).
50. Majzner RG, Mackall CL. Tumor antigen escape from car t-cell therapy. *Cancer Discov.* 2018;8(10):1219-1226.
51. Daei Sorkhabi A, Mohamed Khosroshahi L, Sarkesh A, et al. The current landscape of CAR T-cell therapy for solid tumors: Mechanisms, research progress, challenges, and counterstrategies. *Front Immunol.* 2023;14.
52. Rodriguez-Garcia A, Palazon A, Noguera-Ortega E, Powell DJ, Guedan S. CAR-T Cells Hit the Tumor Microenvironment: Strategies to Overcome Tumor Escape. *Front Immunol.* 2020;11.
53. Poirot L, Philip B, Schiffer-Mannioui C, et al. Multiplex Genome-Edited T-cell Manufacturing Platform for "Off-the-Shelf" Adoptive T-cell Immunotherapies. *Cancer Res.* 2015;75(18):3853-3864.
54. Rafiq S, Hackett CS, Brentjens RJ. Engineering strategies to overcome the current roadblocks in CAR T cell therapy. *Nat Rev Clin Oncol.* 2020;17(3):147-167.

55. Lanitis E, Coukos G, Irving M. All systems go: converging synthetic biology and combinatorial treatment for CAR-T cell therapy. *Curr Opin Biotechnol*. 2020;65:75-87.
56. Levine BL, Miskin J, Wonnacott K, Keir C. Global Manufacturing of CAR T Cell Therapy. *Mol Ther Methods Clin Dev*. 2017;4:92-101.
57. Levine BL. Performance-enhancing drugs: design and production of redirected chimeric antigen receptor (CAR) T cells. *Cancer Gene Ther*. 2015;22(2):79-84.
58. Laufs S, Nagy KZ, Giordano FA, Hotz-Wagenblatt A, Zeller WJ, Fruehauf S. Insertion of retroviral vectors in NOD/SCID repopulating human peripheral blood progenitor cells occurs preferentially in the vicinity of transcription start regions and in introns. *Molecular Therapy*. 2004;10(5):874-881.
59. Cavazza A, Moiani A, Mavilio F. Mechanisms of retroviral integration and mutagenesis. *Hum Gene Ther*. 2013;24(2):119-131.
60. Hacein-Bey-Abina S, Von Kalle C, Schmidt M, et al. LMO2 -Associated Clonal T Cell Proliferation in Two Patients after Gene Therapy for SCID-X1. *Science (1979)*. 2003;302(5644):415-419.
61. Schröder ARW, Shinn P, Chen H, Berry C, Ecker JR, Bushman F. HIV-1 Integration in the Human Genome Favors Active Genes and Local Hotspots. *Cell*. 2002;110(4):521-529.
62. Wang GP, Levine BL, Binder GK, et al. Analysis of lentiviral vector integration in HIV+ study subjects receiving autologous infusions of gene modified CD4+ T cells. *Molecular Therapy*. 2009;17(5):844-850.
63. Fraietta JA, Nobles CL, Sammons MA, et al. Disruption of TET2 promotes the therapeutic efficacy of CD19-targeted T cells. *Nature*. 2018;558(7709):307-312.
64. Nobles CL, Sherrill-Mix S, Everett JK, et al. CD19-targeting CAR T cell immunotherapy outcomes correlate with genomic modification by vector integration. *Journal of Clinical Investigation*. 2020;130(2):673-685.
65. Milone MC, O'Doherty U. Clinical use of lentiviral vectors. *Leukemia*. 2018;32(7):1529-1541.
66. Administration USF and D. Testing of retroviral vector-based human gene therapy products for replication competent retrovirus during product manufacture and patient follow-up. Guidance for industry. *MD: Silver Spring*. Published online 2020.
67. Bulcha JT, Wang Y, Ma H, Tai PWL, Gao G. Viral vector platforms within the gene therapy landscape. *Signal Transduct Target Ther*. 2021;6(1).
68. Lamers CHJ, Willemsen R, Van Elzakker P, et al. Immune responses to transgene and retroviral vector in patients treated with ex vivo-engineered T cells. *Blood*. 2011;117(1):72-82.

69. Sahin U, Karikó K, Türeci Ö. mRNA-based therapeutics-developing a new class of drugs. *Nat Rev Drug Discov*. 2014;13(10):759-780.
70. Hopkins AL, Groom CR. The druggable genome. *Nat Rev Drug Discov*. 2002;1(9):727-730.
71. Neklesa TK, Winkler JD, Crews CM. Targeted protein degradation by PROTACs. *Pharmacol Ther*. 2017;174:138-144.
72. Bennett CF. Therapeutic antisense oligonucleotides are coming of age. *Annu Rev Med*. 2019;70:307-321.
73. Ramasamy T, Ruttala HB, Munusamy S, Chakraborty N, Kim JO. Nano drug delivery systems for antisense oligonucleotides (ASO) therapeutics. *Journal of Controlled Release*. 2022;352(April):861-878.
74. Liang XH, Sun H, Nichols JG, Crooke ST. RNase H1-Dependent Antisense Oligonucleotides Are Robustly Active in Directing RNA Cleavage in Both the Cytoplasm and the Nucleus. *Molecular Therapy*. 2017;25(9):2075-2092.
75. Dias N, Dheur S, Nielsen PE, et al. Antisense PNA tridecamers targeted to the coding region of Ha-ras mRNA arrest polypeptide chain elongation. *J Mol Biol*. 1999;294(2):403-416.
76. Wilton SD, Lloyd F, Carville K, et al. Specific removal of the nonsense mutation from the mdx dystrophin mRNA using antisense oligonucleotides. *Neuromuscular Disorders*. 1999;9(5):330-338.
77. Disterer P, Kryczka A, Liu Y, et al. Development of therapeutic splice-switching oligonucleotides. *Hum Gene Ther*. 2014;25(7):587-598.
78. Lim KH, Han Z, Jeon HY, et al. Antisense oligonucleotide modulation of non-productive alternative splicing upregulates gene expression. *Nat Commun*. 2020;11(1).
79. Melton DA. Injected anti-sense RNAs specifically block messenger RNA translation in vivo. *Proc Natl Acad Sci U S A*. 1985;82(1):144-148.
80. Baker BF, Lot SS, Kringel J, et al. Oligonucleotide-europium complex conjugate designed to cleave the 5' cap structure of the ICAM-1 transcript potentiates antisense activity in cells. *Nucleic Acids Res*. 1999;27(6):1547-1551.
81. Vickers TA, Wyatt JR, Burckin T, Bennett CF, Freier SM. Fully modified 2' MOE oligonucleotides redirect polyadenylation. *Nucleic Acids Res*. 2001;29(6):1293-1299.
82. Liang XH, Shen W, Sun H, Migawa MT, Vickers TA, Crooke ST. Translation efficiency of mRNAs is increased by antisense oligonucleotides targeting upstream open reading frames. *Nat Biotechnol*. 2016;34(8):875-880.
83. Liang XH, Sun H, Shen W, et al. Antisense oligonucleotides targeting translation inhibitory elements in 5' UTRs can selectively increase protein levels. *Nucleic Acids Res*. 2017;45(16):9528-9546.

84. Gebert LFR, Rebhan MAE, Crivelli SEM, Denzler R, Stoffel M, Hall J. Miravirsen (SPC3649) can inhibit the biogenesis of miR-122. *Nucleic Acids Res.* 2014;42(1):609-621.
85. Khorkova O, Stahl J, Joji A, Volmar CH, Wahlestedt C. Amplifying gene expression with RNA-targeted therapeutics. *Nat Rev Drug Discov.* Published online 2023.
86. Zamecnik PC, Stephenson ML. Inhibition of Rous sarcoma virus replication and cell transformation by a specific oligodeoxynucleotide. *Proc Natl Acad Sci U S A.* 1978;75(1):280-284.
87. Crooke ST, Liang X hai, Crooke RM, Baker BF, Geary RS. Antisense drug discovery and development technology considered in a pharmacological context. *Biochem Pharmacol.* 2021;189(July 2020):114196.
88. Shadid M, Badawi M, Abulrob A. Antisense oligonucleotides: absorption, distribution, metabolism, and excretion. *Expert Opin Drug Metab Toxicol.* 2021;17(11):1281-1292.
89. Plasterk RHA. RNA Silencing: The Genome's Immune System. *Science (1979).* 2002;296(5571):1263-1265.
90. Jinek M, Doudna JA. A three-dimensional view of the molecular machinery of RNA interference. *Nature.* 2009;457(7228):405-412.
91. Whitehead KA, Langer R, Anderson DG. Knocking down barriers: Advances in siRNA delivery. *Nat Rev Drug Discov.* 2009;8(2):129-138.
92. Hu B, Zhong L, Weng Y, et al. Therapeutic siRNA: state of the art. *Signal Transduct Target Ther.* 2020;5(1).
93. Iwakawa H oki, Tomari Y. Life of RISC: Formation, action, and degradation of RNA-induced silencing complex. *Mol Cell.* 2022;82(1):30-43.
94. Hutvágner G, Zamore PD. A microRNA in a Multiple-Turnover RNAi Enzyme Complex. *Science (1979).* 2002;297(5589):2056-2060.
95. Bartlett DW, Davis ME. Insights into the kinetics of siRNA-mediated gene silencing from live-cell and live-animal bioluminescent imaging. *Nucleic Acids Res.* 2006;34(1):322-333.
96. Fire A, Xu S, Montgomery MK, Kostas SA, Driver SE, Mello CC. Potent and specific genetic interference by double-stranded RNA in *Caenorhabditis elegans*. *Nature.* 1998;391(6669):806-811.
97. Kleinman ME, Yamada K, Takeda A, et al. Sequence- and target-independent angiogenesis suppression by siRNA via TLR3. *Nature.* 2008;452(7187):591-597.
98. Dar SA, Thakur A, Qureshi A, Kumar M. SiRNAmoD: A database of experimentally validated chemically modified siRNAs. *Sci Rep.* 2016;6(December 2015):1-8.
99. Foster DJ, Brown CR, Shaikh S, et al. Advanced siRNA Designs Further Improve In Vivo Performance of GalNAc-siRNA Conjugates. *Molecular Therapy.* 2018;26(3):708-717.

100. Winkle M, El-Daly SM, Fabbri M, Calin GA. Noncoding RNA therapeutics — challenges and potential solutions. *Nat Rev Drug Discov.* 2021;20(8):629-651.
101. Doudna JA. The promise and challenge of therapeutic genome editing. *Nature.* 2020;578(7794):229-236.
102. Jinek M, Chylinski K, Fonfara I, Hauer M, Doudna JA, Charpentier E. A Programmable Dual-RNA-Guided DNA Endonuclease in Adaptive Bacterial Immunity. *Science (1979).* 2012;337(6096):816-821.
103. Doudna JA, Charpentier E. The new frontier of genome engineering with CRISPR-Cas9. *Science (1979).* 2014;346(6213).
104. Xue C, Greene EC. DNA Repair Pathway Choices in CRISPR-Cas9-Mediated Genome Editing. *Trends in Genetics.* 2021;37(7):639-656.
105. Anzalone A V., Koblan LW, Liu DR. Genome editing with CRISPR-Cas nucleases, base editors, transposases and prime editors. *Nat Biotechnol.* 2020;38(7):824-844.
106. Qi LS, Larson MH, Gilbert LA, et al. Repurposing CRISPR as an RNA-guided platform for sequence-specific control of gene expression. *Cell.* 2013;152(5):1173-1183.
107. Wang H, La Russa M, Qi LS. CRISPR/Cas9 in Genome Editing and beyond. *Annu Rev Biochem.* 2016;85:227-264.
108. Kim D, Kim J, Hur JK, Been KW, Yoon SH, Kim JS. Genome-wide analysis reveals specificities of Cpf1 endonucleases in human cells. *Nat Biotechnol.* 2016;34(8):863-868.
109. Zetsche B, Heidenreich M, Mohanraju P, et al. Multiplex gene editing by CRISPR-Cpf1 using a single crRNA array. *Nat Biotechnol.* 2017;35(1):31-34.
110. Bot JF, van der Oost J, Geijsen N. The double life of CRISPR-Cas13. *Curr Opin Biotechnol.* 2022;78:102789.
111. Tong H, Huang J, Xiao Q, et al. High-fidelity Cas13 variants for targeted RNA degradation with minimal collateral effects. *Nat Biotechnol.* 2023;41(1):108-119.
112. Ran FA, Hsu PD, Lin CY, et al. Double Nicking by RNA-Guided CRISPR Cas9 for Enhanced Genome Editing Specificity. *Cell.* 2013;154(6):1380-1389.
113. Kleinstiver BP, Pattanayak V, Prew MS, et al. High-fidelity CRISPR-Cas9 nucleases with no detectable genome-wide off-target effects. *Nature.* 2016;529(7587):490-495.
114. Fu Y, Sander JD, Reyon D, Cascio VM, Joung JK. Improving CRISPR-Cas nuclease specificity using truncated guide RNAs. *Nat Biotechnol.* 2014;32(3):279-284.
115. Kocak DD, Josephs EA, Bhandarkar V, Adkar SS, Kwon JB, Gersbach CA. Increasing the specificity of CRISPR systems with engineered RNA secondary structures. *Nat Biotechnol.* 2019;37(6):657-666.

116. Kawamata M, Suzuki HI, Kimura R, Suzuki A. Optimization of Cas9 activity through the addition of cytosine extensions to single-guide RNAs. *Nat Biomed Eng.* 2023;7(May).
117. Ryan DE, Taussig D, Steinfeld I, et al. Improving CRISPR-Cas specificity with chemical modifications in single-guide RNAs. *Nucleic Acids Res.* 2018;46(2):792-803.
118. Cromwell CR, Sung K, Park J, et al. Incorporation of bridged nucleic acids into CRISPR RNAs improves Cas9 endonuclease specificity. *Nat Commun.* 2018;9(1):1-11.
119. Hendel A, Bak RO, Clark JT, et al. Chemically modified guide RNAs enhance CRISPR-Cas genome editing in human primary cells. *Nat Biotechnol.* 2015;33(9):985-989.
120. Kim S, Koo T, Jee HG, et al. CRISPR RNAs trigger innate immune responses in human cells. *Genome Res.* 2018;28(3):367-373.
121. Ran FA, Hsu PD, Wright J, Agarwala V, Scott DA, Zhang F. Genome engineering using the CRISPR-Cas9 system. *Nat Protoc.* 2013;8(11):2281-2308.
122. Fu Y, Foden JA, Khayter C, et al. High-frequency off-target mutagenesis induced by CRISPR-Cas nucleases in human cells. *Nat Biotechnol.* 2013;31(9):822-826.
123. Hiroaki Hemmi, Osamu Takeuchi*, Taro Kawai, et al. A Toll-like receptor recognizes bacterial DNA. *Nature.* 2000;408(September):740-745.
124. Ewaisha R, Anderson KS. Immunogenicity of CRISPR therapeutics—Critical considerations for clinical translation. *Front Bioeng Biotechnol.* 2023;11(February):1-15.
125. Kim S, Kim D, Cho SW, Kim J, Kim JS. Highly efficient RNA-guided genome editing in human cells via delivery of purified Cas9 ribonucleoproteins. *Genome Res.* 2014;24(6):1012-1019.
126. Liang X, Potter J, Kumar S, et al. Rapid and highly efficient mammalian cell engineering via Cas9 protein transfection. *J Biotechnol.* 2015;208:44-53.
127. Tuerk C, Gold L. Systematic Evolution of Ligands by Exponential Enrichment: RNA Ligands to Bacteriophage T4 DNA Polymerase. *Science (1979).* 1990;249(4968):505-510.
128. Zhou J, Rossi J. Aptamers as targeted therapeutics: current potential and challenges. *Nat Rev Drug Discov.* 2017;16(3):181-202.
129. BRENNER S, JACOB F, MEELSON M. An Unstable Intermediate Carrying Information from Genes to Ribosomes for Protein Synthesis. *Nature.* 1961;190(4776):576-581.
130. Wolff JA, Malone RW, Williams P, et al. Direct Gene Transfer into Mouse Muscle in Vivo. *Science (1979).* 1990;247(4949):1465-1468.
131. Jirikowski GF, Sanna PP, Maciejewski-Lenoir D, Bloom FE. Reversal of Diabetes Insipidus in Brattleboro Rats: Intrahypothalamic Injection of Vasopressin mRNA. *Science (1979).* 1992;255(5047):996-998.

132. Conry RM, LoBuglio AF, Wright M, et al. Characterization of a Messenger RNA Polynucleotide Vaccine Vector. *Cancer Res.* 1995;55(7):1397-1400.
133. Jia L, Qian SB. Therapeutic mRNA Engineering from Head to Tail. *Acc Chem Res.* 2021;54(23):4272-4282.
134. Liu A, Wang X. The Pivotal Role of Chemical Modifications in mRNA Therapeutics. *Front Cell Dev Biol.* 2022;10(July):1-11.
135. von der Haar T, Mulrone TE, Hedayioglu F, et al. Translation of in vitro-transcribed RNA therapeutics. *Front Mol Biosci.* 2023;10(February):1-10.
136. Leppek K, Byeon GW, Kladwang W, et al. Combinatorial optimization of mRNA structure, stability, and translation for RNA-based therapeutics. *Nat Commun.* 2022;13(1):1536.
137. Karikó K, Buckstein M, Ni H, Weissman D. Suppression of RNA recognition by Toll-like receptors: The impact of nucleoside modification and the evolutionary origin of RNA. *Immunity.* 2005;23(2):165-175.
138. Drazkowska K, Tomecki R, Warminski M, et al. 2'-O-Methylation of the second transcribed nucleotide within the mRNA 5' cap impacts the protein production level in a cell-specific manner and contributes to RNA immune evasion. *Nucleic Acids Res.* 2022;50(16):9051-9071.
139. van Dülmen M, Muthmann N, Rentmeister A. Chemo-Enzymatic Modification of the 5' Cap Maintains Translation and Increases Immunogenic Properties of mRNA. *Angewandte Chemie - International Edition.* 2021;60(24):13280-13286.
140. Bollu A, Peters A, Rentmeister A. Chemo-Enzymatic Modification of the 5' Cap To Study mRNAs. *Acc Chem Res.* 2022;55(9):1249-1261.
141. Passmore LA, Collier J. Roles of mRNA poly(A) tails in regulation of eukaryotic gene expression. *Nat Rev Mol Cell Biol.* 2022;23(2):93-106.
142. Holtkamp S, Kreiter S, Selmi A, et al. Modification of antigen-encoding RNA increases stability, translational efficacy, and T-cell stimulatory capacity of dendritic cells. *Blood.* 2006;108(13):4009-4017.
143. Jia L, Mao Y, Ji Q, Dersh D, Yewdell JW, Qian SB. Decoding mRNA translatability and stability from the 5' UTR. *Nat Struct Mol Biol.* 2020;27(9):814-821.
144. Kozak M. An analysis of 5'-noncoding sequences from 699 vertebrate messenger RNAs. *Nucleic Acids Res.* 1987;15(20):8125-8148.
145. Zarghampoor F, Azarpira N, Khatami SR, Behzad-Behbahani A, Foroughmand AM. Improved translation efficiency of therapeutic mRNA. *Gene.* 2019;707(February):231-238.
146. Friedman RC, Farh KKH, Burge CB, Bartel DP. Most mammalian mRNAs are conserved targets of microRNAs. *Genome Res.* 2009;19(1):92-105.

147. Jain R, Frederick JP, Huang EY, et al. MicroRNAs Enable mRNA Therapeutics to Selectively Program Cancer Cells to Self-Destruct. *Nucleic Acid Ther.* 2018;28(5):285-296.
148. Zeng C, Hou X, Yan J, et al. Leveraging mRNA Sequences and Nanoparticles to Deliver SARS-CoV-2 Antigens In Vivo. *Advanced Materials.* 2020;32(40):2004452.
149. Mauro VP, Chappell SA. A critical analysis of codon optimization in human therapeutics Optimizing codon usage for increased protein expression. *Trends Mol Med.* 2014;20(11):604-613.
150. Hia F, Takeuchi O. The effects of codon bias and optimality on mRNA and protein regulation. *Cellular and Molecular Life Sciences.* 2021;78(5):1909-1928.
151. Kormann MSD, Hasenpusch G, Aneja MK, et al. Expression of therapeutic proteins after delivery of chemically modified mRNA in mice. *Nat Biotechnol.* 2011;29(2):154-157.
152. Foster JB, Choudhari N, Perazzelli J, et al. Purification of mRNA Encoding Chimeric Antigen Receptor Is Critical for Generation of a Robust T-Cell Response. *Hum Gene Ther.* 2019;30(2):168-178.
153. Morais P, Adachi H, Yu YT. The Critical Contribution of Pseudouridine to mRNA COVID-19 Vaccines. *Front Cell Dev Biol.* 2021;9(November):1-9.
154. Verbeke R, Lentacker I, De Smedt SC, Dewitte H. The dawn of mRNA vaccines: The COVID-19 case. *Journal of Controlled Release.* 2021;333:511-520.
155. Karikó K, Muramatsu H, Ludwig J, Weissman D. Generating the optimal mRNA for therapy: HPLC purification eliminates immune activation and improves translation of nucleoside-modified, protein-encoding mRNA. *Nucleic Acids Res.* 2011;39(21):e142-e142.
156. Tews BA, Meyers G. Self-Replicating RNA. In: *Methods in Molecular Biology.* Vol 1499. ; 2017:15-35.
157. Lundstrom K. Self-Replicating RNA Viruses for RNA Therapeutics. *Molecules.* 2018;23(12):3310.
158. Vogel AB, Lambert L, Kinnear E, et al. Self-Amplifying RNA Vaccines Give Equivalent Protection against Influenza to mRNA Vaccines but at Much Lower Doses. *Molecular Therapy.* 2018;26(2):446-455.
159. Rappaport AR, Hong SJ, Scallan CD, et al. Low-dose self-amplifying mRNA COVID-19 vaccine drives strong protective immunity in non-human primates against SARS-CoV-2 infection. *Nat Commun.* 2022;13(1):3289.
160. McKay PF, Hu K, Blakney AK, et al. Self-amplifying RNA SARS-CoV-2 lipid nanoparticle vaccine candidate induces high neutralizing antibody titers in mice. *Nat Commun.* 2020;11(1):3523.

161. de Alwis R, Gan ES, Chen S, et al. A single dose of self-transcribing and replicating RNA-based SARS-CoV-2 vaccine produces protective adaptive immunity in mice. *Molecular Therapy*. 2021;29(6):1970-1983.
162. Bloom K, van den Berg F, Arbuthnot P. Self-amplifying RNA vaccines for infectious diseases. *Gene Ther*. 2021;28(3-4):117-129.
163. Blakney AK, Ip S, Geall AJ. An Update on Self-Amplifying mRNA Vaccine Development. *Vaccines (Basel)*. 2021;9(2):97.
164. Neumann E, Schaefer-Ridder M, Wang Y, Hofschneider PH. Gene transfer into mouse lyoma cells by electroporation in high electric fields. *EMBO J*. 1982;1(7):841-845.
165. Yarmush ML, Golberg A, Serša G, Kotnik T, Miklavčič D. Electroporation-Based Technologies for Medicine: Principles, Applications, and Challenges. *Annu Rev Biomed Eng*. 2014;16(1):295-320.
166. Kotnik T, Rems L, Tarek M, Miklavčič D. Membrane Electroporation and Electropermeabilization: Mechanisms and Models. *Annu Rev Biophys*. 2019;48(1):63-91.
167. Stewart MP, Langer R, Jensen KF. Intracellular Delivery by Membrane Disruption: Mechanisms, Strategies, and Concepts. *Chem Rev*. 2018;118(16):7409-7531.
168. Campelo SN, Huang PH, Buie CR, Davalos R V. Recent Advancements in Electroporation Technologies: From Bench to Clinic. *Annu Rev Biomed Eng*. 2023;25(1):77-100.
169. Gurunian A, Dean DA. Multiple conductance states of lipid pores during Voltage-Clamp electroporation. *Bioelectrochemistry*. 2023;151(December 2022):108396.
170. Rems L, Viano M, Kasimova MA, Miklavčič D, Tarek M. The contribution of lipid peroxidation to membrane permeability in electropermeabilization: A molecular dynamics study. *Bioelectrochemistry*. 2019;125:46-57.
171. Son RS, Smith KC, Gowrishankar TR, Vernier PT, Weaver JC. Basic Features of a Cell Electroporation Model: Illustrative Behavior for Two Very Different Pulses. *J Membr Biol*. 2014;247(12):1209-1228.
172. Napotnik TB, Wu YH, Gundersen MA, Miklavčič D, Vernier PT. Nanosecond electric pulses cause mitochondrial membrane permeabilization in Jurkat cells. *Bioelectromagnetics*. 2012;33(3):257-264.
173. Nuccitelli R. Application of Pulsed Electric Fields to Cancer Therapy. *Bioelectricity*. 2019;1(1):30-34.
174. Agarwal A, Zudans I, Weber EA, Olofsson J, Orwar O, Weber SG. Effect of Cell Size and Shape on Single-Cell Electroporation. *Anal Chem*. 2007;79(10):3589-3596.
175. Shinoda W. Permeability across lipid membranes. *Biochimica et Biophysica Acta (BBA) - Biomembranes*. 2016;1858(10):2254-2265.

176. Puc M, Kotnik T, Mir LM, Miklavčič D. Quantitative model of small molecules uptake after in vitro cell electropermeabilization. *Bioelectrochemistry*. 2003;60(1-2):1-10.
177. Sözer EB, Pocetti CF, Vernier PT. Transport of charged small molecules after electropermeabilization — drift and diffusion. *BMC Biophys*. 2018;11(1):4.
178. Casciola M, Tarek M. A molecular insight into the electro-transfer of small molecules through electropores driven by electric fields. *Biochim Biophys Acta Biomembr*. 2016;1858(10):2278-2289.
179. Paganin-Gioanni A, Bellard E, Escoffre JM, Rols MP, Teissié J, Golzio M. Direct visualization at the single-cell level of siRNA electrotransfer into cancer cells. *Proc Natl Acad Sci U S A*. 2011;108(26):10443-10447.
180. Breton M, Delemotte L, Silve A, Mir LM, Tarek M. Transport of siRNA through lipid membranes driven by nanosecond electric pulses: An experimental and computational study. *J Am Chem Soc*. 2012;134(34):13938-13941.
181. Pavlin M, Kandušer M. New Insights into the Mechanisms of Gene Electrotransfer – Experimental and Theoretical Analysis. *Sci Rep*. 2015;5(1):9132.
182. Rosazza C, Deschout H, Buntz A, Braeckmans K, Rols MP, Zumbusch A. Endocytosis and Endosomal Trafficking of DNA After Gene Electrotransfer In Vitro. *Mol Ther Nucleic Acids*. 2016;5(February):e286.
183. Rosazza C, Haberl Meglic S, Zumbusch A, Rols MP, Miklavcic D. Gene Electrotransfer: A Mechanistic Perspective. *Curr Gene Ther*. 2016;16(2):98-129.
184. Jordan ET, Collins M, Terefe J, Ugozzoli L, Rubio T. Optimizing electroporation conditions in primary and other difficult-to-transfect cells. *Journal of Biomolecular Techniques*. 2008;19(5):328-334.
185. Haberl S, Kandušer M, Flisar K, et al. Effect of different parameters used for in vitro gene electrotransfer on gene expression efficiency, cell viability and visualization of plasmid DNA at the membrane level. *J Gene Med*. 2013;15(5):169-181.
186. Zhang Z, Qiu S, Zhang X, Chen W. Optimized DNA electroporation for primary human T cell engineering. *BMC Biotechnol*. 2018;18(1):4.
187. Potočnik T, Sachdev S, Polajžer T, Maček Lebar A, Miklavčič D. Efficient Gene Transfection by Electroporation—In Vitro and In Silico Study of Pulse Parameters. *Applied Sciences*. 2022;12(16):8237.
188. Ruzgys P, Jakutavičiūtė M, Šatkauskienė I, Čepurnienė K, Šatkauskas S. Effect of electroporation medium conductivity on exogenous molecule transfer to cells in vitro. *Sci Rep*. 2019;9(1):1436.

189. Sherba JJ, Hogquist S, Lin H, Shan JW, Shreiber DI, Zahn JD. The effects of electroporation buffer composition on cell viability and electro-transfection efficiency. *Sci Rep.* 2020;10(1):3053.
190. Novickij V, Rembialkowska N, Staigvila G, Kulbacka J. Effects of extracellular medium conductivity on cell response in the context of sub-microsecond range calcium electroporation. *Sci Rep.* 2020;10(1):3718.
191. Olaiz N, Signori E, Maglietti F, et al. Tissue damage modeling in gene electrotransfer: The role of pH. *Bioelectrochemistry.* 2014;100:105-111.
192. Li Y, Wu M, Zhao D, et al. Electroporation on microchips: the harmful effects of pH changes and scaling down. *Sci Rep.* 2015;5(1):17817.
193. Pakhomova ON, Khorokhorina VA, Bowman AM, et al. Oxidative effects of nanosecond pulsed electric field exposure in cells and cell-free media. *Arch Biochem Biophys.* 2012;527(1):55-64.
194. Batista Napotnik T, Polajžer T, Miklavčič D. Cell death due to electroporation – A review. *Bioelectrochemistry.* 2021;141:107871.
195. Zhang M, Ma Z, Selliah N, et al. The impact of Nucleofection® on the activation state of primary human CD4 T cells. *J Immunol Methods.* 2014;408(1):123-131.
196. DiTommaso T, Cole JM, Cassereau L, et al. Cell engineering with microfluidic squeezing preserves functionality of primary immune cells in vivo. *Proceedings of the National Academy of Sciences.* 2018;115(46):E10907-E10914.
197. Xiong R, Hua D, Van Hoeck J, et al. Photothermal nanofibres enable safe engineering of therapeutic cells. *Nat Nanotechnol.* 2021;16(11):1281-1291.
198. Houthaeve G, De Smedt SC, Braeckmans K, De Vos WH. The cellular response to plasma membrane disruption for nanomaterial delivery. *Nano Conver.* 2022;9(1):6.
199. Lissandrello CA, Santos JA, Hsi P, et al. High-throughput continuous-flow microfluidic electroporation of mRNA into primary human T cells for applications in cellular therapy manufacturing. *Sci Rep.* 2020;10(1):1-16.
200. VanderBurgh JA, Corso TN, Levy SL, Craighead HG. Scalable continuous-flow electroporation platform enabling T cell transfection for cellular therapy manufacturing. *Sci Rep.* 2023;13(1):6857.
201. Kar S, Loganathan M, Dey K, et al. Single-cell electroporation: current trends, applications and future prospects. *Journal of Micromechanics and Microengineering.* 2018;28(12):123002.
202. Morshedi Rad D, Alsadat Rad M, Razavi Bazaz S, Kashaninejad N, Jin D, Ebrahimi Warkiani M. A Comprehensive Review on Intracellular Delivery. *Advanced Materials.* 2021;33(13):2005363.

203. Choi SE, Khoo H, Hur SC. Recent Advances in Microscale Electroporation. *Chem Rev.* 2022;122(13):11247-11286.
204. Sharei A, Zoldan J, Adamo A, et al. A vector-free microfluidic platform for intracellular delivery. *Proceedings of the National Academy of Sciences.* 2013;110(6):2082-2087.
205. Sharei A, Cho N, Mao S, et al. Cell squeezing as a robust, microfluidic intracellular delivery platform. *J Vis Exp.* 2013;(81):1-7.
206. Saung MT, Sharei A, Adalsteinsson VA, et al. A Size-Selective Intracellular Delivery Platform. *Small.* 2016;12(42):5873-5881.
207. Jarrell JA, Twite AA, Lau KHWJ, et al. Intracellular delivery of mRNA to human primary T cells with microfluidic vortex shedding. *Sci Rep.* 2019;9(1):3214.
208. Park JC, Bernstein H, Loughhead S, et al. Cell Squeeze: driving more effective CD8 T-cell activation through cytosolic antigen delivery. *Immuno-Oncology and Technology.* 2022;16(C):100091.
209. Loo J, Sicher I, Goff A, et al. Microfluidic transfection of mRNA into human primary lymphocytes and hematopoietic stem and progenitor cells using ultra-fast physical deformations. *Sci Rep.* 2021;11(1):21407.
210. Kizer ME, Deng Y, Kang G, Mikael PE, Wang X, Chung AJ. Hydroporator: a hydrodynamic cell membrane perforator for high-throughput vector-free nanomaterial intracellular delivery and DNA origami biostability evaluation. *Lab Chip.* 2019;19(10):1747-1754.
211. Joo B, Hur J, Kim GB, Yun SG, Chung AJ. Highly Efficient Transfection of Human Primary T Lymphocytes Using Droplet-Enabled Mechanoporation. *ACS Nano.* 2021;15(8):12888-12898.
212. O'Dea S, Annibaldi V, Gallagher L, et al. Vector-free intracellular delivery by reversible permeabilization. Omri A, ed. *PLoS One.* 2017;12(3):e0174779.
213. Kavanagh H, Dunne S, Martin DS, et al. A novel non-viral delivery method that enables efficient engineering of primary human T cells for ex vivo cell therapy applications. *Cytotherapy.* 2021;23(9):852-860.
214. Xiong R, Samal SK, Demeester J, Skirtach AG, De Smedt SC, Braeckmans K. Laser-assisted photoporation: fundamentals, technological advances and applications. *Adv Phys X.* 2016;1(4):596-620.
215. Ramon J, Xiong R, De Smedt SC, Raemdonck K, Braeckmans K. Vapor nanobubble-mediated photoporation constitutes a versatile intracellular delivery technology. *Curr Opin Colloid Interface Sci.* 2021;54:101453.
216. Xiong R, Sauvage F, Fraire JC, Huang C, De Smedt SC, Braeckmans K. Photothermal Nanomaterial-Mediated Photoporation. *Acc Chem Res.* 2023;56(6):631-643.

217. Xiong R, Raemdonck K, Peynshaert K, et al. Comparison of Gold Nanoparticle Mediated Photoporation: Vapor Nanobubbles Outperform Direct Heating for Delivering Macromolecules in Live Cells. *ACS Nano*. 2014;8(6):6288-6296.
218. Raes L, Van Hecke C, Michiels J, et al. Gold Nanoparticle-Mediated Photoporation Enables Delivery of Macromolecules over a Wide Range of Molecular Weights in Human CD4+ T Cells. *Crystals (Basel)*. 2019;9(8):411.
219. Urban AS, Fedoruk M, Horton MR, Rädler JO, Stefani FD, Feldmann J. Controlled Nanometric Phase Transitions of Phospholipid Membranes by Plasmonic Heating of Single Gold Nanoparticles. *Nano Lett*. 2009;9(8):2903-2908.
220. Lukianova-Hleb E, Hu Y, Latterini L, et al. Plasmonic Nanobubbles as Transient Vapor Nanobubbles Generated around Plasmonic Nanoparticles. *ACS Nano*. 2010;4(4):2109-2123.
221. Maheshwari S, van der Hoef M, Prosperetti A, Lohse D. Dynamics of Formation of a Vapor Nanobubble Around a Heated Nanoparticle. *The Journal of Physical Chemistry C*. 2018;122(36):20571-20580.
222. Wayteck L, Xiong R, Braeckmans K, De Smedt SC, Raemdonck K. Comparing photoporation and nucleofection for delivery of small interfering RNA to cytotoxic T cells. *Journal of Controlled Release*. 2017;267:154-162.
223. Raes L, Stremersch S, Fraire JC, et al. Intracellular Delivery of mRNA in Adherent and Suspension Cells by Vapor Nanobubble Photoporation. *Nanomicro Lett*. 2020;12(1):1-17.
224. Raes L, Pille M, Harizaj A, et al. Cas9 RNP transfection by vapor nanobubble photoporation for ex vivo cell engineering. *Mol Ther Nucleic Acids*. 2021;25(September):696-707.
225. Harizaj A, Wels M, Raes L, et al. Photoporation with Biodegradable Polydopamine Nanosensitizers Enables Safe and Efficient Delivery of mRNA in Human T Cells. *Adv Funct Mater*. 2021;31(28):2102472.
226. Berdecka D, Harizaj A, Goemaere I, et al. Delivery of macromolecules in unstimulated T cells by photoporation with polydopamine nanoparticles. *Journal of Controlled Release*. 2023;354:680-693.
227. Fraire JC, Shaabani E, Sharifiaghdam M, et al. Light triggered nanoscale biolistics for efficient intracellular delivery of functional macromolecules in mammalian cells. *Nat Commun*. 2022;13(1).
228. He G, Hu N, Xu AM, Li X, Zhao Y, Xie X. Nanoneedle Platforms: The Many Ways to Pierce the Cell Membrane. *Adv Funct Mater*. 2020;30(21):1909890.
229. Tay A. The Benefits of Going Small: Nanostructures for Mammalian Cell Transfection. *ACS Nano*. 2020;14(7):7714-7721.

230. Xie X, Xu AM, Angle MR, Tayebi N, Verma P, Melosh NA. Mechanical model of vertical nanowire cell penetration. *Nano Lett.* 2013;13(12):6002-6008.
231. Zou J, Li J, Chen T, Li X. Penetration mechanism of cells by vertical nanostructures. *Phys Rev E.* 2020;102(5):052401.
232. Shalek AK, Gaublomme JT, Wang L, et al. Nanowire-Mediated Delivery Enables Functional Interrogation of Primary Immune Cells: Application to the Analysis of Chronic Lymphocytic Leukemia. *Nano Lett.* 2012;12(12):6498-6504.
233. Yosef N, Shalek AK, Gaublomme JT, et al. Dynamic regulatory network controlling TH17 cell differentiation. *Nature.* 2013;496(7446):461-468.
234. Chen Y, Mach M, Shokouhi AR, et al. Efficient non-viral CAR-T cell generation via silicon-nanotube-mediated transfection. *Materials Today.* 2023;63(March):8-17.
235. Charpentier JC, King PD. Mechanisms and functions of endocytosis in T cells. *Cell Communication and Signaling.* 2021;19(1):92.
236. Nie W, Wei W, Zuo L, et al. Magnetic Nanoclusters Armed with Responsive PD-1 Antibody Synergistically Improved Adoptive T-Cell Therapy for Solid Tumors. *ACS Nano.* 2019;13(2):1469-1478.
237. Smith TT, Stephan SB, Moffett HF, et al. In situ programming of leukaemia-specific T cells using synthetic DNA nanocarriers. *Nat Nanotechnol.* 2017;12(8):813-820.
238. Kheiriloomoom A, Kare AJ, Ingham ES, et al. In situ T-cell transfection by anti-CD3-conjugated lipid nanoparticles leads to T-cell activation, migration, and phenotypic shift. *Biomaterials.* 2022;281(December 2021):121339.
239. Tombácz I, Laczkó D, Shahnawaz H, et al. Highly efficient CD4+ T cell targeting and genetic recombination using engineered CD4+ cell-homing mRNA-LNPs. *Molecular Therapy.* 2021;29(11):3293-3304.
240. Ramishetti S, Kedmi R, Goldsmith M, et al. Systemic Gene Silencing in Primary T Lymphocytes Using Targeted Lipid Nanoparticles. *ACS Nano.* 2015;9(7):6706-6716.
241. Schmid D, Park CG, Hartl CA, et al. T cell-targeting nanoparticles focus delivery of immunotherapy to improve antitumor immunity. *Nat Commun.* 2017;8(1):1747.
242. Kumar P, Ban HS, Kim SS, et al. T Cell-Specific siRNA Delivery Suppresses HIV-1 Infection in Humanized Mice. *Cell.* 2008;134(4):577-586.
243. Ramishetti S, Hazan-Halevy I, Palakuri R, et al. A Combinatorial Library of Lipid Nanoparticles for RNA Delivery to Leukocytes. *Advanced Materials.* 2020;32(12):1-8.
244. Frick SU, Domogalla MP, Baier G, et al. Interleukin-2 Functionalized Nanocapsules for T Cell-Based Immunotherapy. *ACS Nano.* 2016;10(10):9216-9226.

245. Olden BR, Cheng E, Cheng Y, Pun SH. Identifying key barriers in cationic polymer gene delivery to human T cells. *Biomater Sci.* 2019;7(3):789-797.
246. Varkouhi AK, Scholte M, Storm G, Haisma HJ. Endosomal escape pathways for delivery of biologicals. *Journal of Controlled Release.* 2011;151(3):220-228.
247. Dowdy SF. Overcoming cellular barriers for RNA therapeutics. *Nat Biotechnol.* 2017;35(3):222-229.
248. Smith SA, Selby LI, Johnston APR, Such GK. The Endosomal Escape of Nanoparticles: Toward More Efficient Cellular Delivery. *Bioconjug Chem.* 2019;30(2):263-272.
249. Vermeulen LMP, Brans T, Samal SK, et al. Endosomal Size and Membrane Leakiness Influence Proton Sponge-Based Rupture of Endosomal Vesicles. *ACS Nano.* 2018;12(3):2332-2345.
250. Degors IMS, Wang C, Rehman ZU, Zuhorn IS. Carriers break barriers in drug delivery: endocytosis and endosomal escape of gene delivery vectors. *Acc Chem Res.* 2019;52(7):1750-1760.
251. Fraire JC, Houthaeve G, Liu J, et al. Vapor nanobubble is the more reliable photothermal mechanism for inducing endosomal escape of siRNA without disturbing cell homeostasis. *Journal of Controlled Release.* 2020;319(December 2019):262-275.
252. Gilleron J, Querbes W, Zeigerer A, et al. Image-based analysis of lipid nanoparticle-mediated siRNA delivery, intracellular trafficking and endosomal escape. *Nat Biotechnol.* 2013;31(7):638-646.
253. Sahay G, Querbes W, Alabi C, et al. Efficiency of siRNA delivery by lipid nanoparticles is limited by endocytic recycling. *Nat Biotechnol.* 2013;31(7):653-658.
254. Brown CR, Gupta S, Qin J, et al. Investigating the pharmacodynamic durability of GalNAc-siRNA conjugates. *Nucleic Acids Res.* 2020;48(21):11827-11844.
255. Abildgaard MH, Brynjólfsson SH, Frankel LB. The Autophagy-RNA Interplay: Degradation and Beyond. *Trends Biochem Sci.* 2020;45(10):845-857.
256. Tenchov R, Bird R, Curtze AE, Zhou Q. Lipid Nanoparticles from Liposomes to mRNA Vaccine Delivery, a Landscape of Research Diversity and Advancement. *ACS Nano.* 2021;15(11):16982-17015.
257. Sun D, Lu ZR. Structure and Function of Cationic and Ionizable Lipids for Nucleic Acid Delivery. *Pharm Res.* 2023;40(1):27-46.
258. Malone RW, Felgner PL, Verma IM. Cationic liposome-mediated RNA transfection. *Proceedings of the National Academy of Sciences.* 1989;86(16):6077-6081.
259. Aramaki Y, Takano S, Arima H, Tsuchiya S. Induction of apoptosis in WEHI 231 cells by cationic liposomes. *Pharm Res.* 2000;17(5):515-520.

260. Lv H, Zhang S, Wang B, Cui S, Yan J. Toxicity of cationic lipids and cationic polymers in gene delivery. *Journal of Controlled Release*. 2006;114(1):100-109.
261. Kedmi R, Ben-Arie N, Peer D. The systemic toxicity of positively charged lipid nanoparticles and the role of Toll-like receptor 4 in immune activation. *Biomaterials*. 2010;31(26):6867-6875.
262. Knudsen KB, Northeved H, Kumar EK P, et al. In vivo toxicity of cationic micelles and liposomes. *Nanomedicine*. 2015;11(2):467-477.
263. Cui S, Wang Y, Gong Y, et al. Correlation of the cytotoxic effects of cationic lipids with their headgroups. *Toxicol Res (Camb)*. 2018;7(3):473-479.
264. Hou X, Zaks T, Langer R, Dong Y. Lipid nanoparticles for mRNA delivery. *Nat Rev Mater*. 2021;6(12):1078-1094.
265. Zhang YQ, Guo RR, Chen YH, et al. Ionizable drug delivery systems for efficient and selective gene therapy. *Mil Med Res*. 2023;10(1):1-29.
266. Bailey AL, Cullis PR. Modulation of Membrane Fusion by Asymmetric Transbilayer Distributions of Amino Lipids. *Biochemistry*. 1994;33(42):12573-12580.
267. Cullis PR, Hope MJ. Lipid Nanoparticle Systems for Enabling Gene Therapies. *Molecular Therapy*. 2017;25(7):1467-1475.
268. Adams D, Gonzalez-Duarte A, O’Riordan WD, et al. Patisiran, an RNAi Therapeutic, for Hereditary Transthyretin Amyloidosis. *New England Journal of Medicine*. 2018;379(1):11-21.
269. Cheng X, Lee RJ. The role of helper lipids in lipid nanoparticles (LNPs) designed for oligonucleotide delivery. *Adv Drug Deliv Rev*. 2016;99:129-137.
270. Nakhaei P, Margiana R, Bokov DO, et al. Liposomes: Structure, Biomedical Applications, and Stability Parameters With Emphasis on Cholesterol. *Front Bioeng Biotechnol*. 2021;9(September):1-23.
271. Patel SK, Billingsley MM, Frazee C, et al. Hydroxycholesterol substitution in ionizable lipid nanoparticles for mRNA delivery to T cells. *Journal of Controlled Release*. 2022;347(November 2021):521-532.
272. Suk JS, Xu Q, Kim N, Hanes J, Ensign LM. PEGylation as a strategy for improving nanoparticle-based drug and gene delivery. *Adv Drug Deliv Rev*. 2016;99(6):28-51.
273. Tenchov R, Sasso JM, Zhou QA. PEGylated Lipid Nanoparticle Formulations: Immunological Safety and Efficiency Perspective. *Bioconjug Chem*. Published online 2023.
274. Kedmi R, Veiga N, Ramishetti S, et al. A modular platform for targeted RNAi therapeutics. *Nat Nanotechnol*. 2018;13(3):214-219.

275. Evers MJW, Kulkarni JA, van der Meel R, Cullis PR, Vader P, Schiffelers RM. State-of-the-Art Design and Rapid-Mixing Production Techniques of Lipid Nanoparticles for Nucleic Acid Delivery. *Small Methods*. 2018;2(9):1700375.
276. Duan Y, Dhar A, Patel C, et al. A brief review on solid lipid nanoparticles: Part and parcel of contemporary drug delivery systems. *RSC Adv*. 2020;10(45):26777-26791.
277. Paunovska K, Loughrey D, Dahlman JE. Drug delivery systems for RNA therapeutics. *Nat Rev Genet*. 2022;23(5):265-280.
278. Akinc A, Thomas M, Klibanov AM, Langer R. Exploring polyethylenimine-mediated DNA transfection and the proton sponge hypothesis. *Journal of Gene Medicine*. 2005;7(5):657-663.
279. Weber ND, Merkel OM, Kissel T, Muñoz-Fernández MÁ. PEGylated poly(ethylene imine) copolymer-delivered siRNA inhibits HIV replication in vitro. *Journal of Controlled Release*. 2012;157(1):55-63.
280. Agarwal S, Zhang Y, Maji S, Greiner A. PDMAEMA based gene delivery materials. *Materials Today*. 2012;15(9):388-393.
281. Schallon A, Synatschke C V., Jérôme V, Müller AHE, Freitag R. Nanoparticulate Nonviral Agent for the Effective Delivery of pDNA and siRNA to Differentiated Cells and Primary Human T Lymphocytes. *Biomacromolecules*. 2012;13(11):3463-3474.
282. Olden BR, Cheng Y, Yu JL, Pun SH. Cationic polymers for non-viral gene delivery to human T cells. *Journal of Controlled Release*. 2018;282(December 2017):140-147.
283. Karlsson J, Rhodes KR, Green JJ, Tzeng SY. Poly(beta-amino ester)s as gene delivery vehicles: challenges and opportunities. *Expert Opin Drug Deliv*. 2020;17(10):1395-1410.
284. Moffett HF, Coon ME, Radtke S, et al. Hit-and-run programming of therapeutic cytoreagents using mRNA nanocarriers. *Nat Commun*. 2017;8(1).
285. Rabinovich PM, Komarovskaya ME, Ye ZJ, et al. Synthetic Messenger RNA as a Tool for Gene Therapy. *Hum Gene Ther*. 2006;17(10):1027-1035.
286. Rabinovich PM, Komarovskaya ME, Wrzesinski SH, et al. Chimeric receptor mRNA transfection as a tool to generate antineoplastic lymphocytes. *Hum Gene Ther*. 2009;20(1):51-61.
287. Barrett DM, Zhao Y, Liu X, et al. Treatment of Advanced Leukemia in Mice with mRNA Engineered T Cells. *Hum Gene Ther*. 2011;22(12):1575-1586.
288. Barrett DM, Liu X, Jiang S, June CH, Grupp SA, Zhao Y. Regimen-Specific Effects of RNA-Modified Chimeric Antigen Receptor T Cells in Mice with Advanced Leukemia. *Hum Gene Ther*. 2013;24(8):717-727.
289. Svoboda J, Rheingold SR, Gill SI, et al. Nonviral RNA chimeric antigen receptor–modified T cells in patients with Hodgkin lymphoma. *Blood*. 2018;132(10):1022-1026.

290. Panjwani MK, Smith JB, Schutsky K, et al. Feasibility and safety of RNA-transfected CD20-specific chimeric antigen receptor T cells in dogs with spontaneous B cell lymphoma. *Molecular Therapy*. 2016;24(9):1602-1614.
291. Köksal H, Dillard P, Josefsson SE, et al. Preclinical development of CD37CAR T-cell therapy for treatment of B-cell lymphoma. *Blood Adv*. 2019;3(8):1230-1243.
292. Kenderian SS, Ruella M, Shestova O, et al. CD33-specific chimeric antigen receptor T cells exhibit potent preclinical activity against human acute myeloid leukemia. *Leukemia*. 2015;29(8):1637-1647.
293. Gill S, Tasian SK, Ruella M, et al. Preclinical targeting of human acute myeloid leukemia and myeloablation using chimeric antigen receptor–modified T cells. *Blood*. 2014;123(15):2343-2354.
294. Tasian SK, Kenderian SS, Shen F, et al. Optimized depletion of chimeric antigen receptor T cells in murine xenograft models of human acute myeloid leukemia. *Blood*. 2017;129(17):2395-2407.
295. Cummins KD, Frey N, Nelson AM, et al. Treating Relapsed / Refractory (RR) AML with Biodegradable Anti-CD123 CAR Modified T Cells. *Blood*. 2017;130:1359.
296. Lin L, Cho SF, Xing L, et al. Preclinical evaluation of CD8+ anti-BCMA mRNA CAR T cells for treatment of multiple myeloma. *Leukemia*. 2021;35(3):752-763.
297. Granit V, Benatar M, Kurtoglu M, et al. *Safety and Clinical Activity of Autologous RNA Chimeric Antigen Receptor T-Cell Therapy in Myasthenia Gravis (MG-001): A Prospective, Multicentre, Open-Label, Non-Randomised Phase 1b/2a Study*. Vol 22.; 2023.
298. Zhao Y, Moon E, Carpenito C, et al. Multiple Injections of Electroporated Autologous T Cells Expressing a Chimeric Antigen Receptor Mediate Regression of Human Disseminated Tumor. *Cancer Res*. 2010;70(22):9053-9061.
299. Maus M V., Haas AR, Beatty GL, et al. T Cells Expressing Chimeric Antigen Receptors Can Cause Anaphylaxis in Humans. *Cancer Immunol Res*. 2013;1(1):26-31.
300. Beatty GL, Haas AR, Maus M V, et al. Mesothelin-Specific Chimeric Antigen Receptor mRNA-Engineered T Cells Induce Antitumor Activity in Solid Malignancies. *Cancer Immunol Res*. 2014;2(2):112-120.
301. Beatty GL, O’Hara MH, Lacey SF, et al. Activity of Mesothelin-Specific Chimeric Antigen Receptor T Cells Against Pancreatic Carcinoma Metastases in a Phase 1 Trial. *Gastroenterology*. 2018;155(1):29-32.
302. Wagner DL, Fritsche E, Pulsipher MA, et al. Immunogenicity of CAR T cells in cancer therapy. *Nat Rev Clin Oncol*. 2021;18(6):379-393.
303. Khan AN, Chowdhury A, Karulkar A, et al. Immunogenicity of CAR-T Cell Therapeutics: Evidence, Mechanism and Mitigation. *Front Immunol*. 2022;13.

304. Ang WX, Li Z, Chi Z, et al. Intraperitoneal immunotherapy with T cells stably and transiently expressing anti-EpCAM CAR in xenograft models of peritoneal carcinomatosis. *Oncotarget*. 2017;8(8):13545-13559.
305. Singh N, Liu X, Hulitt J, et al. Nature of Tumor Control by Permanently and Transiently Modified GD2 Chimeric Antigen Receptor T Cells in Xenograft Models of Neuroblastoma. *Cancer Immunol Res*. 2014;2(11):1059-1070.
306. Foster JB, Griffin C, Rokita JL, et al. Development of GPC2-directed chimeric antigen receptors using mRNA for pediatric brain tumors. *J Immunother Cancer*. 2022;10(9):1-14.
307. Höfflin S, Prommersberger S, Uslu U, et al. Generation of CD8+ T cells expressing two additional T-cell receptors (TETARs) for personalised melanoma therapy. *Cancer Biol Ther*. 2015;16(9):1323-1331.
308. Uslu U, Schuler G, Dörrie J, Schaft N. Combining a chimeric antigen receptor and a conventional T-cell receptor to generate T cells expressing two additional receptors (TETARs) for a multi-hit immunotherapy of melanoma. *Exp Dermatol*. 2016;25(11):872-879.
309. Simon B, Harrer DC, Schuler-Thurner B, Schuler G, Uslu U. Arming T cells with a gp100-specific TCR and a CSPG4-specific CAR using combined DNA-and RNA-based receptor transfer. *Cancers (Basel)*. 2019;11(5).
310. Wiesinger M, März J, Kummer M, et al. Clinical-scale production of car-t cells for the treatment of melanoma patients by mrna transfection of a cspg4-specific car under full gmp compliance. *Cancers (Basel)*. 2019;11(8):1-18.
311. Inoo K, Inagaki R, Fujiwara K, et al. Immunological quality and performance of tumor vessel-targeting CAR-T cells prepared by mRNA-EP for clinical research. *Mol Ther Oncolytics*. 2016;3(May):16024.
312. Tchou J, Zhao Y, Levine BL, et al. Safety and efficacy of intratumoral injections of chimeric antigen receptor (CAR) T cells in metastatic breast cancer. *Cancer Immunol Res*. 2017;5(12):1152-1161.
313. Shah PD, Huang AC, Xu X, et al. Phase I Trial of Autologous RNA-electroporated cMET-directed CAR T Cells Administered Intravenously in Patients with Melanoma and Breast Carcinoma. *Cancer Research Communications*. 2023;3(5):821-829.
314. Billingsley MM, Singh N, Ravikumar P, Zhang R, June CH, Mitchell MJ. Ionizable Lipid Nanoparticle-Mediated mRNA Delivery for Human CAR T Cell Engineering. *Nano Lett*. 2020;20(3):1578-1589.
315. Depil S, Duchateau P, Grupp SA, Mufti G, Poirot L. 'Off-the-shelf' allogeneic CAR T cells: development and challenges. *Nat Rev Drug Discov*. 2020;19(3):185-199.
316. Dimitri A, Herbst F, Fraietta JA. Engineering the next-generation of CAR T-cells with CRISPR-Cas9 gene editing. *Mol Cancer*. 2022;21(1).

317. Khan A, Sarkar E. CRISPR/Cas9 encouraged CAR-T cell immunotherapy reporting efficient and safe clinical results towards cancer. *Cancer Treat Res Commun.* 2022;33.
318. Qasim W. Genome-edited allogeneic donor “universal” chimeric antigen receptor T cells. *Blood.* 2023;141(8):835-845.
319. Atsavapranee ES, Billingsley MM, Mitchell MJ. Delivery technologies for T cell gene editing: Applications in cancer immunotherapy. *EBioMedicine.* 2021;67.
320. Eyquem J, Mansilla-Soto J, Giavridis T, et al. Targeting a CAR to the TRAC locus with CRISPR/Cas9 enhances tumour rejection. *Nature.* 2017;543(7643):113-117.
321. MacLeod DT, Antony J, Martin AJ, et al. Integration of a CD19 CAR into the TCR Alpha Chain Locus Streamlines Production of Allogeneic Gene-Edited CAR T Cells. *Molecular Therapy.* 2017;25(4):949-961.
322. Georgiadis C, Preece R, Nickolay L, et al. Long Terminal Repeat CRISPR-CAR-Coupled “Universal” T Cells Mediate Potent Anti-leukemic Effects. *Molecular Therapy.* 2018;26(5):1215-1227.
323. Ottaviano G, Georgiadis C, Soragia †, et al. *Phase 1 Clinical Trial of CRISPR-Engineered CAR19 Universal T Cells for Treatment of Children with Refractory B Cell Leukemia.*; 2022.
324. Gillmore JD, Gane E, Taubel J, et al. CRISPR-Cas9 In Vivo Gene Editing for Transthyretin Amyloidosis. *New England Journal of Medicine.* 2021;385(6):493-502.
325. Beane JD, Lee G, Zheng Z, et al. Clinical Scale Zinc Finger Nuclease-mediated Gene Editing of PD-1 in Tumor Infiltrating Lymphocytes for the Treatment of Metastatic Melanoma. *Molecular Therapy.* 2015;23(8):1380-1390.
326. Ren J, Zhang X, Liu X, et al. *A Versatile System for Rapid Multiplex Genome-Edited CAR T Cell Generation.* Vol 8.; 2017.
327. Ren J, Liu X, Fang C, Jiang S, June CH, Zhao Y. Multiplex genome editing to generate universal CAR T cells resistant to PD1 inhibition. *Clinical Cancer Research.* 2017;23(9):2255-2266.
328. Dai X, Park JJ, Du Y, et al. One-step generation of modular CAR-T cells with AAV–Cpf1. *Nat Methods.* 2019;16(3):247-254.
329. Webber BR, Lonetree C lin, Kluesner MG, et al. Highly efficient multiplex human T cell engineering without double-strand breaks using Cas9 base editors. *Nat Commun.* 2019;10(1).
330. Gaudelli NM, Lam DK, Rees HA, et al. Directed evolution of adenine base editors with increased activity and therapeutic application. *Nat Biotechnol.* 2020;38(7):892-900.
331. Ghaffari S, Khalili N, Rezaei N. CRISPR/Cas9 revitalizes adoptive T-cell therapy for cancer immunotherapy. *Journal of Experimental and Clinical Cancer Research.* 2021;40(1).

332. Pato A, Eisenberg G, Machlenkin A, et al. Messenger RNA encoding constitutively active Toll-like receptor 4 enhances effector functions of human T cells. *Clin Exp Immunol*. 2015;182(2):220-229.
333. Levin N, Weinstein-Marom H, Pato A, et al. Potent Activation of Human T Cells by mRNA Encoding Constitutively Active CD40. *The Journal of Immunology*. 2018;201(10):2959-2968.
334. Weinstein-Marom H, Pato A, Levin N, et al. Membrane-attached Cytokines Expressed by mRNA Electroporation Act as Potent T-Cell Adjuvants. *Journal of Immunotherapy*. 2016;39(2):60-70.
335. Weinstein-Marom H, Levin N, Pato A, et al. Combined Expression of Genetic Adjuvants Via mRNA Electroporation Exerts Multiple Immunostimulatory Effects on Antitumor T Cells. *Journal of Immunotherapy*. 2019;42(2):43-50.
336. Etxeberria I, Bolaños E, Quetglas JI, et al. Intratumor Adoptive Transfer of IL-12 mRNA Transiently Engineered Antitumor CD8+ T Cells. *Cancer Cell*. 2019;36(6):613-629.
337. Di Trani CA, Cirella A, Arrizabalaga L, et al. Intracavitary adoptive transfer of IL-12 mRNA-engineered tumor-specific CD8+ T cells eradicates peritoneal metastases in mouse models. *Oncoimmunology*. 2023;12(1):1-16.
338. Mitchell DA, Karikari I, Cui X, Xie W, Schmittling R, Sampson JH. Selective modification of antigen-specific T cells by RNA electroporation. *Hum Gene Ther*. 2008;19(5):511-521.
339. Almåsbak H, Rian E, Hoel HJ, et al. Transiently redirected T cells for adoptive transfer. *Cytotherapy*. 2011;13(5):629-640.
340. Bai Y, Kan S, Zhou S, et al. Enhancement of the in vivo persistence and antitumor efficacy of CD19 chimeric antigen receptor T cells through the delivery of modified TERT mRNA. *Cell Discov*. 2015;1(1).

Chapter 2

Delivery of macromolecules in unstimulated T cells by photoporation with polydopamine nanoparticles

This chapter has been published as:

Dominika Berdecka^{a,b}, Aranit Harizaj^a, Ilia Goemaere^{a,b}, Deep Punj^a, Glenn Goetgeluk^c, Stijn De Munter^c, Herlinde De Keersmaecker^{a,d}, Veerle Boterberg^e, Peter Dubruel^e, Bart Vandekerckhove^c, Stefaan C. De Smedt^a, Winnok H. De Vos^b and Kevin Braeckmans^{a,d}. Delivery of macromolecules in unstimulated T cells by photoporation with polydopamine nanoparticles. *Journal of Controlled Release*. 2023; 354: 680–93.

^a Laboratory of General Biochemistry and Physical Pharmacy, Faculty of Pharmaceutical Sciences, Ghent University

^b Laboratory of Cell Biology and Histology, Department of Veterinary Sciences, University of Antwerp

^c Department of Diagnostic Sciences, Faculty of Medicine and Health Sciences, Ghent University Hospital

^d Ghent Light Microscopy Core, Ghent University

^e Polymer Chemistry and Biomaterials Group, Department of Organic and Macromolecular Chemistry, Ghent University

Author contributions: D.B. performed T cell isolation, photoporation experiments, functional T cell experiments and data analysis. In addition, D.B. made the figures and wrote the article. A.H. and I.G. performed the PDNP synthesis and characterization. D.P. assisted with the VNB generation threshold. G.G and S.D.M. provided initial assistance with T cell assays. H.D.K. provided assistance for microscopy. V.B assisted with the PDNP coating analysis. P.D., B.V., S.D.S., W.D.V. and K.B. reviewed the article.

Table of Contents

Abstract.....	92
1 Introduction.....	93
2 Materials and methods	97
2.1 Human T cell isolation and culture	97
2.2 Visualization of unstimulated and expanded T cells by confocal microscopy....	97
2.3 Synthesis and physicochemical characterization of polydopamine nanoparticles.....	98
2.4 Determination of VNB generation threshold.....	101
2.5 Photoporation for the delivery of FITC-dextran 500 kDa	101
2.6 T cell activation after photoporation of unstimulated T cells	102
2.7 Evaluation of cell viability with Cell Titer Glo assay	103
2.8 Cell counting with Trypan Blue	104
2.9 Quantification of cytokines in cell culture supernatants	104
2.10 Statistical analysis	104
3 Results.....	105
3.1 Characterization of unstimulated and activated T cells by confocal microscopy	105
3.2 Synthesis and physicochemical characterization of polydopamine nanoparticles.....	106
3.3 Intracellular delivery of FD500 in unstimulated T cells.....	111
3.4 Intracellular delivery of FD500 in expanded T cells	113
3.5 Evaluation of T cell functionality after pre-treatment by photoporation	115
4 Discussion	121
5 Conclusion	124
References	125
Supplementary Information	132

Abstract

Ex vivo modification of T cells with exogenous cargo is a common prerequisite for the development of T cell therapies, such as chimeric antigen receptor therapy. Despite the clinical success and FDA approval of several such products, T cell manufacturing presents unique challenges related to therapeutic efficacy after adoptive cell transfer and several drawbacks of viral transduction-based manufacturing, such as high cost and safety concerns. To generate cellular products with optimal potency, engraftment potential and persistence *in vivo*, recent studies have shown that minimally differentiated T cell phenotypes are preferred. However, genetic engineering of quiescent T cells remains challenging. Photoporation is an upcoming alternative non-viral transfection method which makes use of photothermal nanoparticles, such as polydopamine nanoparticles (PDNPs), to induce transient membrane permeabilization by distinct photothermal effects upon laser irradiation, allowing exogenous molecules to enter cells. In this study, we analyzed the capability of PDNP-photoporation to deliver large model macromolecules (FITC-dextran 500 kDa, FD500) in unstimulated and expanded human T cells. We compared different sizes of PDNPs (150, 250 and 400 nm), concentrations of PDNPs and laser fluences and found an optimal condition that generated high delivery yields of FD500 in both T cell phenotypes. A multiparametric analysis of cell proliferation, surface activation markers and cytokine production, revealed that unstimulated T cells photoporated with 150 nm and 250 nm PDNPs retained their propensity to become activated, whereas those photoporated with 400 nm PDNPs did less. Our findings show that PDNP-photoporation is a promising strategy for transfection of quiescent T cells, but that PDNPs should be small enough to avoid excessive cell damage.

1 Introduction

Intracellular delivery of plasma membrane-impermeable molecules, such as contrast agents or nucleic acids, is not only a common requirement for cell biological research, but also for the development of engineered cell-based therapies¹. One of the most prominent examples of the latter is adoptive T cell transfer where T cells are genetically modified to express a chimeric antigen receptor (CAR) or T cell receptor (TCR) to increase their potency to recognize and kill tumor cells²⁻⁴. CAR T cell immunotherapy demonstrated durable clinical responses in relapsed and refractory B cell malignancies, leading to the regulatory approval of several CD19-specific CAR T cell therapies⁵⁻⁹.

At present, 6 CAR T cell products are FDA approved for the treatment of hematological malignancies. To extend its possibilities towards the treatment of solid tumors, vast research efforts are aimed at improving CAR T cell potency and *in vivo* persistence. In this context, several preclinical and clinical studies demonstrated that intrinsic T cell properties, such as differentiation status, may be a critical determinant of patient response to treatment. Superior anti-tumor responses were observed for T cells with less differentiated phenotypes, such as naïve or central memory cells, correlating with robust *in vivo* expansion and persistence¹⁰⁻¹⁶. In contrast, prolonged *in vitro* culture drives cells towards terminal differentiation with increased expression of exhaustion markers and inhibitory receptors¹⁰.

Generation of cellular products with optimal potency, engraftment potential and persistence can be achieved by shortening culture time, optimizing culture conditions (culture medium, cell density, cytokine supplementation, *etc.*), or modulation of metabolic pathways. Importantly, Ghassemi *et al.* previously showed that reducing the time of *ex vivo* culture to 3-5 days resulted in less differentiated CAR T cells with superior leukemia control at low cell doses when compared to cells expanded for 9 days¹⁷. Recent reports even try to completely eliminate the activation and *ex vivo* expansion steps in order to maximize the therapeutic potential of CAR T cells^{18,19}. For instance, Ghassemi and Milone demonstrated that functional CAR T cells can be generated from quiescent cells within 24 h of T cell collection by lentiviral transduction under optimized culture conditions. Importantly, these non-activated CAR T cells exhibited potent anti-leukemic *in*

vivo activity at cell doses lower than those effective for activated CAR T cells produced using a standard 9-day protocol ¹⁸. Nonetheless, genetic engineering of quiescent T cells remains challenging and is only reported in a very limited number of publications ^{20–22}.

At present, the CAR T cell manufacturing process predominantly relies on retro- or lentiviral transduction to deliver the transgene into pre-activated T cells, followed by their *in vitro* expansion to achieve therapeutically required doses. Despite its satisfactory performance for the current generation of approved T cell therapies, viral vectors remain associated with several limitations ^{23–25}. GMP-compliant viral vector production for clinical applications is a lengthy and costly process, requiring stringent quality control testing for the presence of replication-competent viruses in the final cell product. Furthermore, viral vectors carry an intrinsic risk of immunogenicity or insertional oncogenesis while offering limited cargo capacity, which may become problematic with the evolving CAR design. These challenges have spurred a growing interest in safer non-viral gene delivery technologies with a simpler and more cost-effective manufacturing process. This would result in greater availability and reduced vein-to-vein time for the benefit of patients, especially for those with rapidly progressing disease ^{26–28}.

For genetic modification of T cells, techniques that physically induce membrane permeabilization have proven especially promising. These techniques use a physical stimulus to transiently permeabilize the cell membrane, allowing cargo molecules to enter the cytosol. Electroporation is the best-known example, but it can induce high levels of acute toxicity and long-term adverse effects, diminishing the therapeutic potential of the final cell product ^{29–32}. In recent years, newer and gentler membrane permeabilization technologies have emerged which have much less impact on normal T cell functioning. Examples are cell squeezing ³², microneedles ³¹ and most recently, nanofiber-based photoporation ³³.

In its traditional form, photoporation or optoporation is a physical delivery method based on laser irradiation of photothermal nanoparticles (NPs) that can attach to the cell membrane ^{34,35}. Depending on the applied laser energy, membrane permeabilization can be achieved by distinct photothermal effects (**Figure 1**). Application of a relatively low laser fluence results in direct heating of NPs that triggers local phase transitions in the

lipid bilayer and glycoprotein denaturation³⁶. When sufficiently high laser fluences are used, the NP temperature rises above the critical temperature of the surrounding liquid causing its almost instantaneous evaporation and formation of vapor nanobubbles (VNBs). Rapid expansion and collapse of VNBs lead to high-pressure waves and fluid shear stress that can generate transient pores in the plasma membrane^{34,37,38}. The technology typically makes use of metallic nanoparticles, such as gold nanoparticles (AuNPs). AuNP-mediated photoporation has been successfully used to deliver various molecules such as siRNA, mRNA and Cas9 ribonucleoprotein (RNP) complexes in both murine and human T lymphocytes^{39–41}. However, AuNPs in an aqueous environment are known to fragment under intense laser irradiation into smaller particles of a few nanometers. This represents a potential safety risk since very small AuNPs have been shown to intercalate with cellular DNA, potentially leading to genotoxic effects^{42–46}. Moreover, the non-biodegradable nature of AuNPs presents safety and regulatory hurdles for the clinical translation of NP-mediated photoporation. To address these limitations, we have recently developed an alternative system based on biocompatible and biodegradable polydopamine nanoparticles (PDNPs). PDNPs can be optically stimulated over the entire visible range, can be easily synthesized in a broad range of sizes, and their surface can be readily functionalized in a variety of ways⁴⁷. Using PDNPs of about 0.5 μm in size as photoporation sensitizers we could successfully transfect activated and expanded human T cells with mRNA⁴⁸.

It remains unknown whether PDNP photoporation is equally suited to deliver macromolecules in quiescent T cells and to what extent it impacts their fitness and functionality. Therefore, we have here compared macromolecule delivery by PDNP-photoporation in unstimulated and expanded T cells. Since unstimulated T cells are substantially smaller than activated T cells, we decided to test smaller sizes of PDNPs than before. PDNPs of three different nominal sizes were first synthesized (150 nm, 250 nm and 400 nm), after which the PDNP concentration and laser fluence was determined which leads to the best intracellular delivery yield of FITC-dextran 500 kDa as a model macromolecule. For the optimized conditions, we investigated cell functionality by testing the propensity of quiescent cells to become activated after PDNP-photoporation. T cell

activation was determined by analyzing cell proliferation, expression of surface activation markers and secretion of effector cytokines.

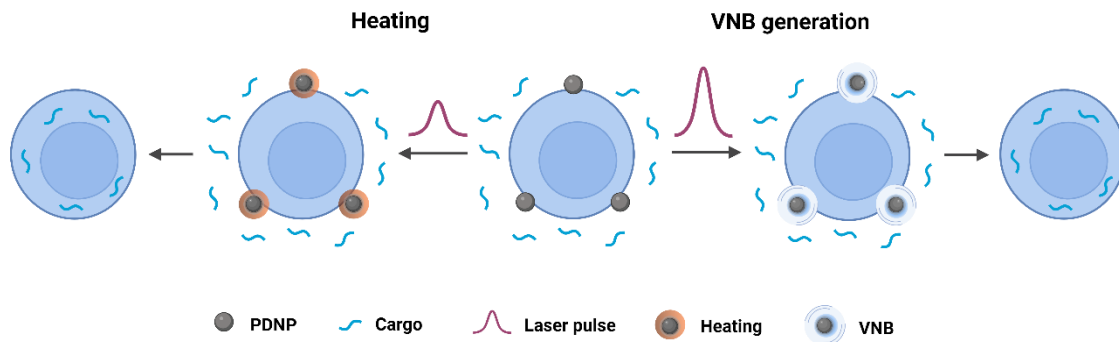


Figure 1. Overview of PDNP photoporation procedure for intracellular delivery of macromolecules in T cells. First, BSA-coated polydopamine nanoparticles (PDNPs) and macromolecules of interest are added to the cells. Depending on the applied laser energy, transient cell membrane permeabilization can be achieved either by photothermal heating or the generation of vapor nanobubbles (VNBs), allowing the exogenous cargo to diffuse into the cell cytoplasm. Created with BioRender.com

2 Materials and methods

2.1 Human T cell isolation and culture

Healthy donor buffy coats were obtained from the Red Cross Flanders Biobank (Ghent, Belgium) and used following the guidelines of the Medical Ethical Committee of Ghent University Hospital (Ghent, Belgium). Peripheral blood mononuclear cells (PBMCs) were isolated *via* density gradient centrifugation with Lymphoprep (Stem Cell Technologies, Vancouver, Canada). Next, human pan CD3⁺ T cells were isolated by a magnetic negative selection using the EasySep Human T cell enrichment Kit (Stem Cell Technologies, Vancouver, Canada) according to the manufacturer's protocol. Unstimulated cells were maintained in Iscove's modified Dulbecco's medium (IMDM) GlutaMAX (Gibco, Merelbeke, Belgium), supplemented with 10% heat-inactivated fetal bovine serum (FBS, Biowest), 100 U/mL penicillin and 100 µg/mL streptomycin (P/S, Gibco, Merelbeke, Belgium) and treated by photoporation on the day of isolation. Alternatively, T cells were stimulated with ImmunoCult Human CD3/CD28 T cell Activator (Stem Cell Technologies, Vancouver, Canada) according to the manufacturer's instructions. Activated cells were supplemented with 10 ng/mL IL-2 (PeproTech, United Kingdom) and kept in culture for 7 days before the photoporation treatment.

2.2 Visualization of unstimulated and expanded T cells by confocal microscopy

Unstimulated and expanded T cells were stained with Hoechst 33342 (Invitrogen, Belgium) and CellMask Deep Red Plasma membrane stain (Invitrogen, Belgium). Samples were visualized with a Nikon A1R HD confocal laser scanning microscope (Nikon Benelux, Belgium) with a 60x water immersion lens (SR plan apo IR 60X WI, NA 1.3, WD 180µm). 408 nm and 633 nm laser lines were used for Hoechst and Cy5/Deep red (Cell Mask), respectively. Fluorescence was detected through a 450/50 nm (MHE57010) and 700/75nm (MHE57070) emission filter on a Multi-Alkali PMT (A1-DUG-2 GaAsP Multi Detector Unit, Nikon), respectively. A galvano scanner was used for unidirectional scanning to acquire the channels sequentially at a scan speed of 0.5 FPS with 2X line averaging. The pinhole was set to 1.2 AU. The pixel size was set to 90 nm/pixel. ImageJ (FIJI) software⁴⁹ was used to process the images and average T cell sizes were determined by manual measurement of cell diameter (minimum 100 cells per cell phenotype).

2.3 Synthesis and physicochemical characterization of polydopamine nanoparticles

The synthesis of polydopamine nanoparticles (PDNPs) was based on a protocol originally reported by Ju *et al.*⁵⁰, and later adapted by Harizaj *et al.*⁴⁸. Briefly, dopamine hydrochloride powder (Sigma-Aldrich) was dissolved in HyClone water (HyPure, Cell Culture Grade, VWR) at a concentration of 3.5 mg/mL at 50°C. Next, 1M NaOH solution was added under vigorous stirring at a fixed molar ratio of 1:0.8, turning the solution pale yellow first, and eventually dark brown. The solution was left to stir for approximately 7 h and the hydrodynamic diameter of the particles was monitored every hour by dynamic light scattering (DLS, Zetasizer Nano ZS, Malvern Instruments Co., Ltd). To reduce potential particle aggregation, the suspensions were sonicated at 10% amplitude for 30 seconds with a tip sonicator (Branson Digital Sonifier, Danbury, USA). Once the desired hydrodynamic diameter was achieved, nanoparticles were retrieved by centrifugation and were washed several times with HyClone water. For 150 nm PDNPs, the NP suspension was transferred to 1.5 mL Eppendorf tubes and PDNPs were washed with HyClone water by centrifugation (21.000 rcf, 20 minutes). For 250 nm PDNPs, the suspension was collected in 50 mL conical tubes and the PD NPs were washed with HyClone water by centrifugation (4.000 rcf, 20 minutes). 400 nm PDNPs were also collected in 50 mL conical tubes and were washed with HyClone water by centrifugation (4.000 rcf, 10 minutes).

Next, to increase the colloidal stability of PDNPs in suspension a functionalization with bovine serum albumin (BSA, Biotechnology grade, VWR Chemicals, USA) was performed. The uncoated PDNP suspension was mixed with a 10 mg/mL BSA solution in DPBS at a 1:1 volume ratio. The mixture was then allowed to react by vigorous stirring overnight and the remaining unbound BSA was removed by several washing steps with HyClone water. The following centrifugation speeds were used for different sizes: 150 nm PDNPs (21.000 rcf, 20 minutes), 250 nm PDNPs (4000 rcf, 20 minutes) and 400 nm PDNPs (4000 rcf, 10 minutes). The resulting BSA-coated PD NPs were dispersed in HyClone water and stored at 4°C.

To provide additional evidence for successful BSA coating, 400 nm PDNPs were coated with albumin–fluorescein isothiocyanate conjugate (FITC-BSA, Sigma-Aldrich) as described for the coating with standard BSA. PDNP dilutions (at 5.6×10^8 NPs/mL) were

added to wells of a glass-bottom 96-well plate and left to dry overnight at 37°C. Next, ProLong™ Diamond antifade mountant (Invitrogen, Belgium) was added and samples were allowed to cure for 24 h at room temperature. Samples were visualized with a Nikon A1R HD confocal laser scanning microscope (Nikon Benelux, Belgium) with a 60x oil immersion lens (plan apo λ 60X oil, NA 1.4, WD 130 μ m). The PDNP core particles were visualized in light scattering mode using a 80/20 beam splitter, while the FITC-BSA coating was visualized in the green fluorescent channel using a 525/50nm emission filter (MHE57030, Nikon). A galvano scanner was used for unidirectional scanning to acquire the channels sequentially. Scan speed was set to 0.125 FPS with 16X line averaging. The pinhole was set to 1.2 AU. The pixel size was set to 110 nm/pixel. ImageJ (FIJI) was used to process the images.

Additionally, relative fluorescence intensities of uncoated and FITC-BSA-coated PDNP dilutions were measured using a VICTOR3 1420 Multilabel Counter® (Perkin Elmer) with excitation at 485 nm and emission at 535 nm.

To visualize the particles by scanning electron microscopy (SEM), BSA-coated PDNPs were dried on silicon wafers one day before the measurement. SEM images were acquired with a FEI Quanta 200F microscope (Thermo Fisher) operating at a voltage of 20 kV. Dynamic light scattering (DLS, Zetasizer Nano ZS, Malvern Instruments Co., Ltd.) was used to measure the hydrodynamic diameter and nanoparticle tracking analysis (NTA, NanoSight LM10, Malvern Panalytical, UK) was performed to determine nanoparticle concentrations⁵¹⁻⁵³. NTA was performed in scattering mode with a 488 nm laser.

To estimate the mass concentration of PDNPs administered to cells, a spherical shape of nanoparticles was assumed with a PDNP density of 1.52 g/cm³ as previously reported in the literature⁵⁴. For spherical nanoparticles, the volume is $V=4/3\pi r^3$, where r is the radius of the sphere (based on NP diameters measured from SEM images). Next, the mass of single NP was calculated by multiplying NP volume by polydopamine density, from which the mass concentrations are finally obtained. The conversion between PDNP number [NPs/mL] and mass [mg/mL] concentrations is reported in **Table 1** below.

Table 1. Estimated conversion between PDNP number [NPs/mL] and mass [mg/mL] concentrations. To estimate the mass of PDNPs administered to cells, a spherical shape of nanoparticles was assumed and a PDNP density of 1.52 g/cm³ previously reported in the literature. For spherical nanoparticles, the volume is $V=4/3\pi r^3$, where r is the radius of the sphere (based on NP diameters measured from SEM images). Next, the mass of single NP can be calculated by multiplying NP volume by polydopamine density, from which finally the mass concentration is obtained.

Nominal size	Diameter (SEM)	Single NP volume [cm ³]	Single NP mass [mg]	Concentration NPs/mL [x10 ¹⁰]	Concentration [mg/mL]
150 nm	141 nm	1.47 x10 ⁻¹⁵	0.22 x10 ⁻¹¹	4	0.09
				8	0.18
				16	0.36
				32	0.71
				64	1.43
				128	2.86
				256	5.71
				512	11.42
250 nm	238 nm	7.06 x10 ⁻¹⁵	1.07 x10 ⁻¹¹	0.25	0.03
				0.5	0.05
				1	0.11
				2	0.21
				4	0.43
				8	0.86
				16	1.72
				32	3.43
400 nm	385 nm	29.88 x10 ⁻¹⁵	4.54 x10 ⁻¹¹	0.0625	0.03
				0.125	0.06
				0.25	0.11
				0.5	0.23
				1	0.45
				2	0.91
				4	1.82

2.4 Determination of VNB generation threshold

For the generation and detection of VNBs, an in-house developed setup equipped with a 3 ns pulsed 532 nm laser (Cobolt Tor™ Series, Cobolt AB, Solna, Sweden) was used to illuminate the PDNPs. The stocks of PDNPs were first diluted in ddH₂O to a concentration of $\sim 1 \times 10^9$ NPs/mL, next samples were transferred to 50 mm γ -irradiated glass bottom dishes (MatTek Corporation, Ashland, MA, USA) and particles were allowed to sediment on the bottom. Lasers pulses were generated using a 25 MHz pulse generator (TGP3121, Aim-TTi, Huntingdon, UK), with control over the pulse energy being provided by an adjustable DC power supply (HQ Power PS23023, Velleman Group, Gavere, Belgium). The VNBs were visualized using dark field microscopy, where the increased scatter of VNBs resulted in bright white spots on a black background. The number of VNBs visible within the irradiated region was quantified for increasing laser pulse fluences. These VNB numbers were then plotted in the function of laser pulse fluence and a Boltzmann sigmoid curve was fitted to determine the threshold, defined as the laser fluence at which there is a 90% probability of a given particle generating a VNB.

2.5 Photoporation for the delivery of FITC-dextran 500 kDa

FITC-dextran of 500 kDa (FD500, Sigma-Aldrich, Bornem, Belgium) was used as a model macromolecule for measuring delivery efficiency and optimizing photoporation parameters. FD500 delivery was performed in either unstimulated or activated and expanded human T cells. Opti-MEM was selected as the transfection buffer of choice. The cells were first washed three times by centrifugation (300xg, 5 min) with Opti-MEM to remove any residual cell culture medium with FBS. After the final washing step, cells were resuspended in Opti-MEM and transferred to a flat-bottom 96-well plate (1×10^6 cells per well). Next, a series of PDNP dilutions was prepared in Opti-MEM and added to cell suspensions to reach concentrations specified in the results. Finally, FD500 was added to the mixture to reach a final concentration of 1 mg/mL. The plate was quickly spun down to let the cells sediment to the bottom of the plate. Photoporation was then performed with an in-house developed setup with a nanosecond laser (3 ns pulse duration, 532 nm wavelength) and equipped with a galvano scanner, enabling irradiation in high throughput (3-4 s per well). Immediately after laser treatment, cells were washed three times by

centrifugation (300xg, 5 min), resuspended in fresh culture medium, and incubated at 37°C, 5% CO₂ until the moment of analysis of delivery efficiency and cell viability.

To evaluate the delivery efficiency of FD500 (*i.e.*, the percentage of FITC-positive cells), T cells were washed once with DPBS- (300xg, 5 min) and resuspended in flow buffer (DPBS- with 1% BSA, 0.1% Sodium Azide) with TO-PRO3 iodide (Invitrogen, Belgium) as cell viability dye. Flow cytometry was performed using a MACSQuant Analyzer 16 (Miltenyi Biotec, Germany) and a minimum of 40 000 cells were analyzed per sample. FITC and TO-PRO-3/APC were excited with 488 and 640 nm lasers and detected with 525/50 and 655-730 nm filters, respectively. FD500-positive cells were gated on singlet living (TO-PRO-3-negative) cells. FlowJo™ software (Treestar Inc.) was used for data analysis and an example gating strategy is displayed in Figure S4 in the Supplementary Information.

2.6 T cell activation after photoporation of unstimulated T cells

To determine to which extent quiescent T cells can still be stimulated after being treated with photoporation, unstimulated T cells were treated by photoporation as described before but in the absence of cargo molecules. This allows assessing the influence of the photoporation treatment alone, excluding potential confounding effects due to the intracellularly delivered cargo molecules. After laser treatment, the cells were rested overnight at 37°C, 5% CO₂. The next day, cells were stimulated with ImmunoCult Human CD3/CD28 T cell Activator (Stem Cell Technologies, Vancouver, Canada) according to the manufacturer's protocol. Briefly, T cells (1x10⁶/mL) were seeded in 24-well plates in complete IMDM supplemented with 10 ng/mL IL-2 and 25 uL of CD3/CD28 Activator was added per well. Cultures were split and supplemented with fresh medium on day 3, day 5 and day 7.

As a control, T cells were mixed with PDNPs but without applying laser irradiation. After exposure to PDNPs, cells were activated as described above.

For the analysis of surface activation markers by flow cytometry, the following anti-human monoclonal antibodies were used: CD3 FITC (StemCell Technologies, Vancouver, Canada), CD3 PE/Cy7 (Biolegend, USA), CD154 FITC (Biolegend, USA), CD137 PE (Biolegend, USA), HLA-DR PerCP (Biolegend, USA), PD-1 APC (Biolegend, USA) and PD-1 PE (Miltenyi Biotec,

Germany). Briefly, cells were washed with DPBS, resuspended in flow buffer and incubated with the indicated antibodies for 30 min at 4°C. LIVE/DEAD™ Fixable Aqua Stain (Invitrogen, Belgium) or TO-PRO™-3 iodide (Invitrogen, Belgium) were included in the staining panels to distinguish between live and dead cell populations. After two washing steps, samples were measured on a MACSQuant Analyzer 16 (Miltenyi Biotec, Germany). LIVE/DEAD™ Aqua Stain and TO-PRO-3/ APC were excited with 405 and 640 nm lasers and detected with 525/50 and 655-730 nm filters, respectively. FITC, PE, PerCP and PE-Cy7 were excited with a 488 nm laser and collected with the respective filters of 525/50 nm, 585/40 nm, 655-730 nm, and 750 nm LP. FlowJo software (Treestar Inc.) was used for data analysis.

2.7 Evaluation of cell viability with Cell Titer Glo assay

The CellTiter Glo® luminescent cell viability assay (Promega, Belgium) was used according to the manufacturer's instructions to assess cell viability after photoporation or to monitor T cells stimulated after pre-treatment by photoporation. In this assay, the number of viable cells is determined by quantitation of the ATP present, as an indicator of metabolically active cells. Briefly, T cells in complete culture medium were supplemented with an equal volume of CellTiter Glo® reagent and shaken on an orbital shaker (120 rpm) for 10 min at room temperature. Next, the cell lysates were transferred to an opaque 96-well plate and the luminescent signal was measured using a GloMax® microplate reader (Promega, Belgium) with a detection wavelength range of 350 to 650 nm. Cell viability was calculated relative to the non-treated control.

The cell viability readout was then combined with delivery efficiency measured by flow cytometry to obtain the delivery yield, a parameter representing the viable and successfully transfected fraction compared to the initial cell population. The delivery yield percentage can be calculated by multiplying the percentage of FD500-positive cells and the percentage of viable cells:

$$\text{Delivery yield [\%]} = (\text{delivery efficiency [\%]} \times \text{cell viability [\%]}) / 100$$

2.8 Cell counting with Trypan Blue

To monitor cell viability and proliferation of T cells activated after photoporation treatment, cells were counted manually using a Bürker counting chamber (Brand GMBH, Germany) and trypan blue exclusion staining (0.4%, Sigma-Aldrich, Belgium). Cell number changes were normalized to the starting seeding density of 1×10^6 cells/mL on day 1 and corrected for culture dilutions at the previously indicated time points.

2.9 Quantification of cytokines in cell culture supernatants

Cell culture supernatants were collected at the indicated time points and stored at -80°C . The production of interferon gamma and Tumor Necrosis Factor alpha was determined using the Human IFN gamma ELISA kit (Invitrogen, Belgium) and the Human TNF alpha ELISA kit (Invitrogen, Belgium), according to the manufacturer's protocols. The absorbance was measured at 450 nm with a VICTOR3 1420 Multilabel Counter[®] (Perkin Elmer). The results are presented both without normalization and normalized to cell numbers.

2.10 Statistical analysis

All data are shown as mean \pm standard deviation (SD). Statistical differences were analyzed using GraphPad Prism 8 software (La Jolla, USA). Two-way ANOVA with Tukey's multiple comparisons test was used to compare maximal FD500 delivery yields achieved with different PDNP sizes and laser fluences, and to analyze cell proliferation rates in cultures pre-treated by photoporation. Expression of surface activation markers and cytokine production were evaluated using Kruskal-Wallis nonparametric test with Dunn's multiple comparisons test. Asterisks are used to illustrate statistical significance (* $p < 0.05$; ** $p < 0.01$; *** $p < 0.001$; **** $p < 0.0001$).

3 Results

3.1 Characterization of unstimulated and activated T cells by confocal microscopy

In this study, we aimed to investigate the applicability of PDNP-photoporation for the intracellular delivery in unstimulated and expanded T cells. As it is well known that activated T cells are larger than quiescent T cells^{55,56}, we reasoned that it would be of interest to evaluate different sizes of PDNPs. To better understand the morphological differences between these two cell phenotypes and guide the selection of photothermal NP sizes, we first visualized unstimulated and pre-activated T cells by confocal microscopy after nuclear and cell membrane staining (**Figure 2**). The average cell diameters quantified from confocal images were $7 \pm 0.5 \mu\text{m}$ for the unstimulated (**Figure 2C**) and $12.6 \pm 2 \mu\text{m}$ for the activated T cells (**Figure 2D**).

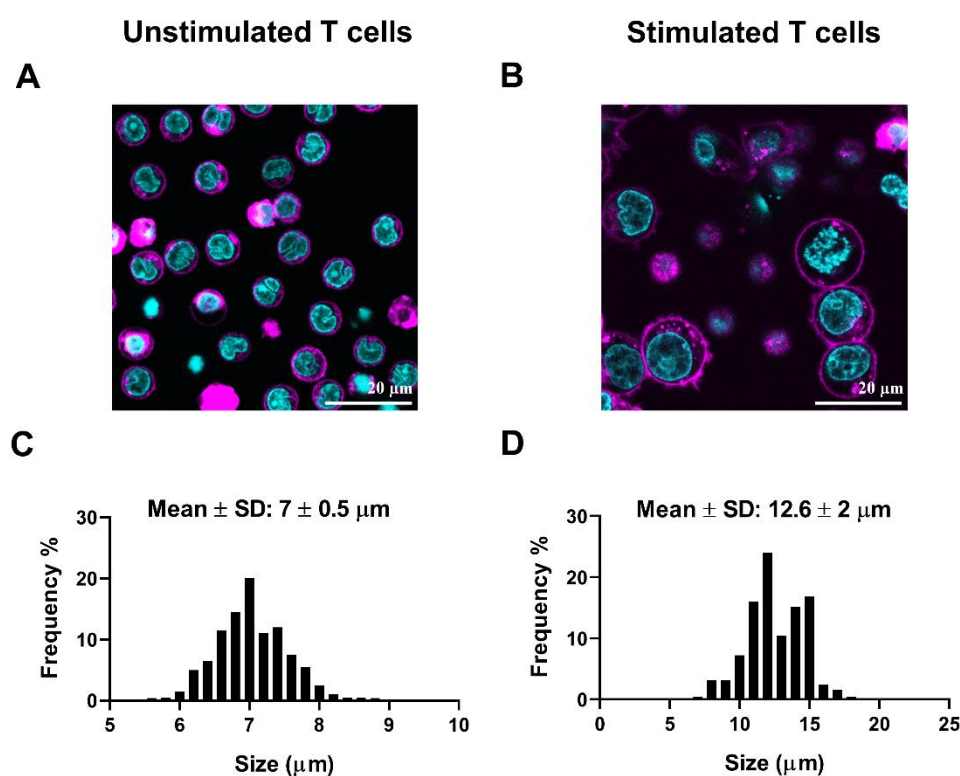


Figure 2. Visualization of unstimulated and activated T cells by confocal microscopy. (A, B) Representative confocal images of unstimulated (A) and activated (B) T cells. T cell nuclei and cell membranes were stained with Hoechst 33342 (cyan) and CellMask Deep Red stain (magenta), respectively. The scale bar represents 20 μm. (C, D) Size distribution of unstimulated (C) and activated (D) T cells, as derived from the confocal images.

3.2 Synthesis and physicochemical characterization of polydopamine nanoparticles

The synthesis of polydopamine nanoparticles (PDNPs) was performed according to the protocol adapted by Harizaj *et al.* ⁴⁸ and is based on the neutralization of dopamine hydrochloride with NaOH, followed by spontaneous air oxidation (cfr. M&M) ⁵⁰. The size of particles is affected by various synthesis parameters, such as reaction temperature, pH and dopamine concentration ^{50,57}. Using a dopamine hydrochloride/NaOH ratio of 1:0.8 and a reaction temperature of 50°C, a gradual growth of PDNPs was achieved. Size was monitored at regular time intervals by dynamic light scattering (DLS). Sonication was applied to remove any remaining agglomerates as previously reported by Harizaj *et al.* ⁴⁸. Once the desired size was reached, the reaction was terminated and the PDNPs were retrieved by centrifugation.

The uncoated PDNPs displayed excellent colloidal stability in water but tended to aggregate in Opti-MEM (**Figure 3** and **Table 2**), calling for an extra functionalization step to ensure good stability in transfection media that are typically used in cell experiments. Serum albumins have been widely used in biomedical applications such as the synthesis of multifunctional nanoparticles for drug delivery and bioimaging or ultrathin coatings of nanostructures to enhance their immune compatibility ⁵⁸⁻⁶⁰. In the present study we opted for PDNP functionalization with bovine serum albumin (BSA), which is based on a Schiff base type or Michael addition reaction between amine groups of albumin and catechol/ quinone groups of polydopamine and can be achieved by overnight incubation of PDNPs with BSA solution ⁶¹⁻⁶³. After PDNP functionalization, an increase in hydrodynamic diameter from 493 ± 3 nm to 522 ± 3 nm was observed (**Table 2**), providing a first indication of successful coating. This observation was in agreement with other studies reporting BSA coatings with a thickness in the nanometer scale ^{60,64,65}. In addition, the zeta-potential turned slightly negative after the coating procedure (**Table 3**), similar to what was previously reported by Harizaj *et al.* ⁴⁸.

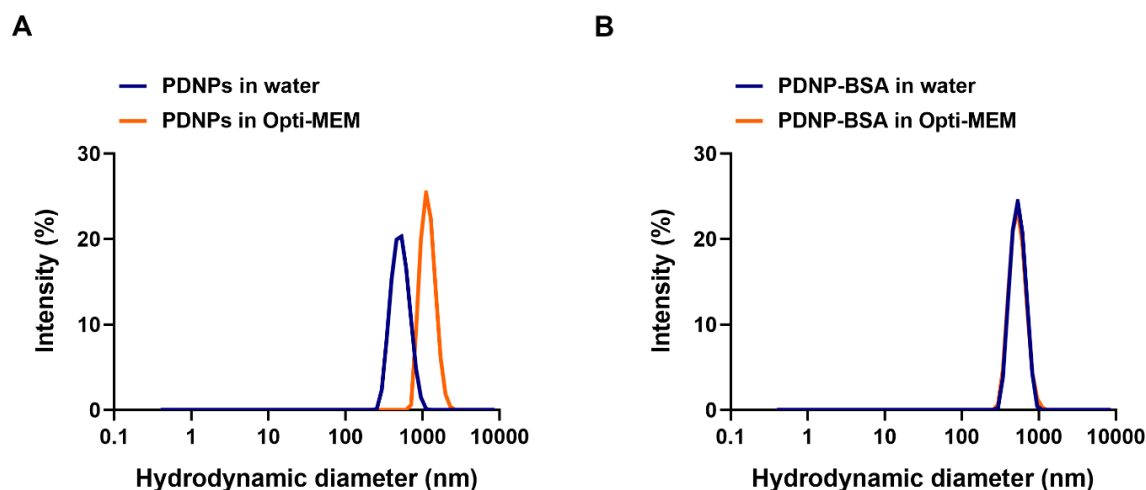


Figure 3. Characterization of pristine (uncoated) and BSA-coated PDNPs by DLS. Representative intensity size distributions of uncoated (A) and BSA-coated (B) 400 nm PDNPs measured in water (blue curve) and Opti-MEM (orange curve).

Table 2. Characterization of representative pristine (uncoated) and BSA-coated 400 nm PDNPs by DLS.

Sample	Hydrodynamic diameter in water [nm]	PDI in water	Hydrodynamic diameter in Opti-MEM [nm]	PDI in Opti-MEM	Zeta potential in water [mV]
Uncoated	493 ± 3	0.066 ± 0.039	1216 ± 4	0.232 ± 0.094	-9.29 ± 0.7
BSA-coated	522 ± 3	0.023 ± 0.007	520 ± 10	0.031 ± 0.016	-12 ± 0.3

Table 3. Characterization of BSA-coated PDNPs by DLS.

PDNP nominal size	Hydrodynamic diameter in water [nm]	PDI in water	Hydrodynamic diameter in Opti-MEM [nm]	PDI in Opti-MEM	Zeta potential in water [mV]
150 nm PDNPs	145 ± 1	0.015 ± 0.010	149 ± 1	0.021 ± 0.024	-32.5 ± 0.6
250 nm PDNPs	237 ± 5	0.013 ± 0.009	255 ± 4	0.018 ± 0.023	-19.1 ± 0.6
400 nm PDNPs	471 ± 1	0.018 ± 0.004	460 ± 6	0.026 ± 0.037	-37.8 ± 0.9

To provide further evidence for effective BSA coating, PDNPs were functionalized with FITC-conjugated BSA and visualized by confocal microscopy (**Figure 4**). The PDNP core particles were visualized by in light scattering mode, while the FITC-BSA coating was visualized in the green fluorescent channel. We were able to successfully detect fluorescence for FITC-BSA-coated particles, which was not the case for the uncoated PDNPs. These results were finally complemented with a spectrometric analysis of relative fluorescence intensities of FITC-BSA-coated and uncoated PDNPs (**Figure S1**, Supplementary Information). Together these data show that a BSA coating could be successfully applied to the PDNPs.

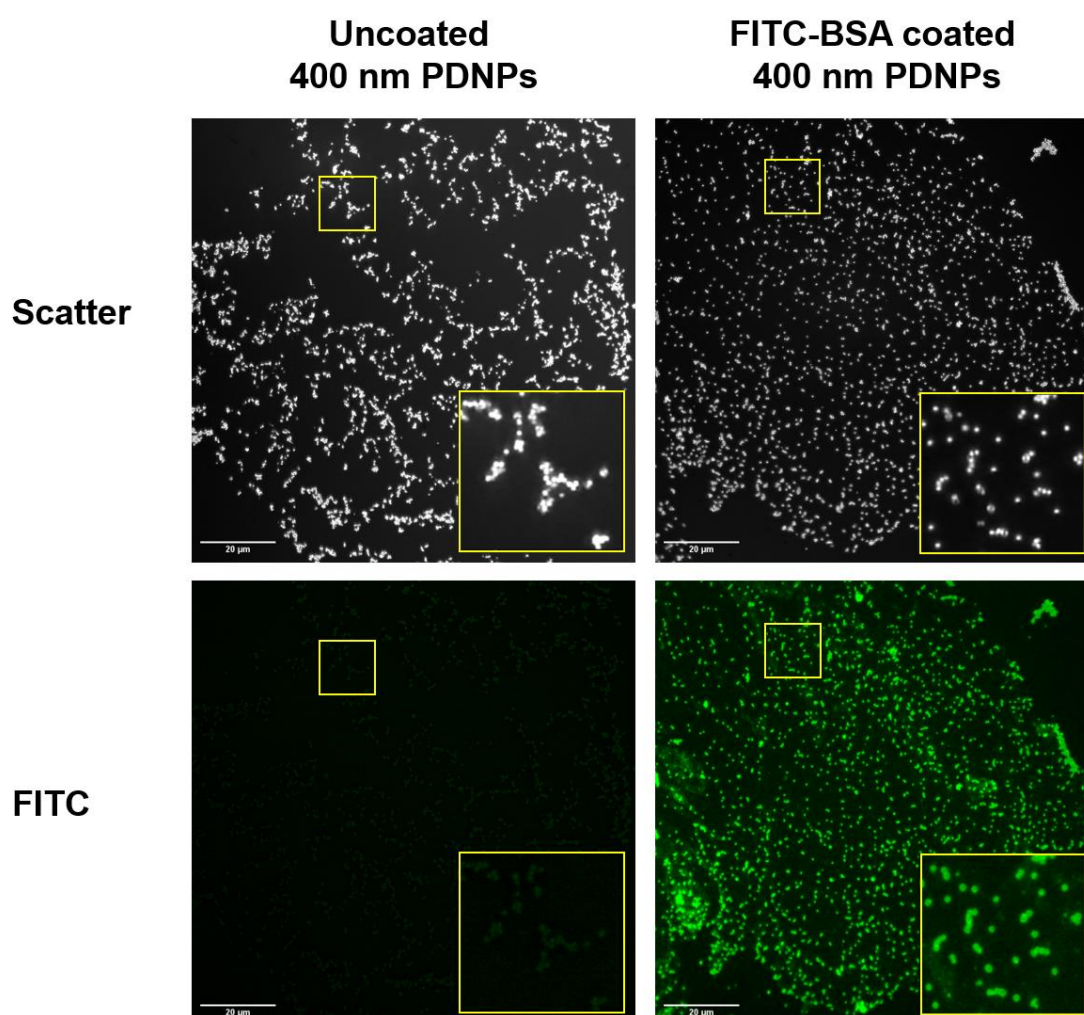
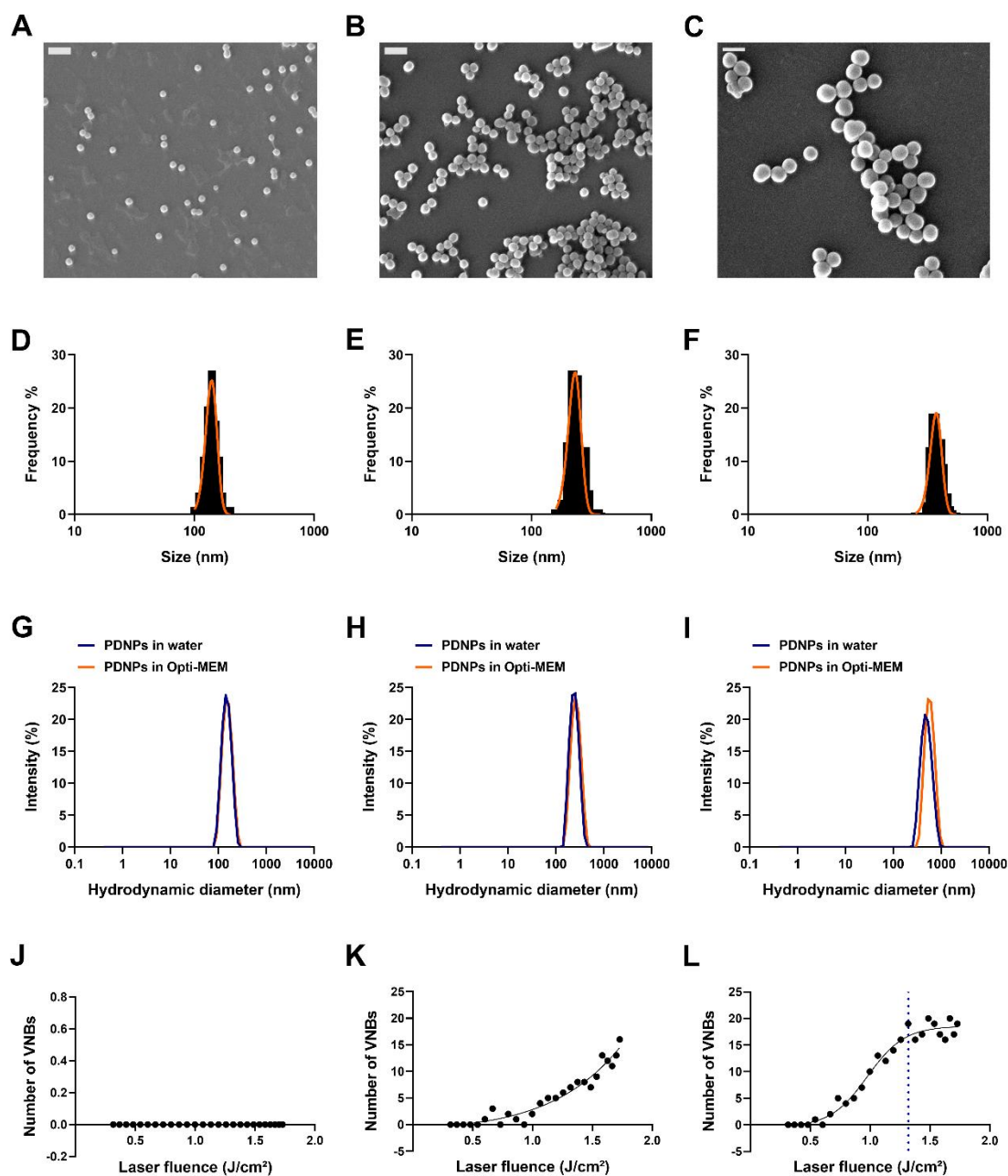


Figure 4. Visualization of uncoated and FITC-BSA-coated 400 nm PDNPs by confocal microscopy. Signals from the scattering mode (PDNP core particles) and FITC channel (FITC-BSA coating) are color coded in grey and green, respectively. The scale bar represents 20 µm.

BSA-coated PDNPs of three different dimensions were created, of which the size and morphology was analyzed by SEM (**Figure 5A, 5B, 5C**). Each formulation showed a near-spherical shape of fairly uniform size. Using image analysis, we measured respective PDNP diameters of 141 ± 18 nm (**Figure 5D**), 238 ± 34 nm (**Figure 5E**) and 385 ± 42 nm (**Figure 5F**). For ease of reference, we will refer to those particles as 150 nm, 250 nm and 400 nm PDNPs, respectively. The hydrodynamic diameter of the PDNPs was additionally assessed by DLS in water and Opti-MEM, of which representative intensity size distributions are displayed in **Figure 5G, 5H** and **5I**. The average hydrodynamic size was respectively 145 ± 1 nm, 237 ± 5 nm and 471 ± 1 nm in water, and 149 ± 1 nm, 255 ± 4 nm and 460 ± 6 nm in Opti-MEM (**Table 3**). All formulations were characterized by quite low polydispersity index (PDI) values in both water and Opti-MEM, indicating relatively narrow size distributions^{66,67}. This shows that PDNPs are stable in Opti-MEM which is used to add them to cells. In addition, the BSA-PDNP size was determined after mixing with FD500, which is a model cargo molecule used in the present study. As can be seen in **Figure S2**, no change in size was observed, showing that BSA-PDNPs do not aggregate in the presence of FD500.

While the hydrodynamic size measured by DLS corresponded well with the particle diameters measured with SEM, 400 nm PDNPs appeared larger when measured with DLS. This may be due to the presence of spurious aggregates (dimers or small agglomerates) that cannot be discriminated from individual particles with DLS. Nevertheless, overall, there was a good correspondence between SEM and DLS size measurements. Next, we investigated whether differently sized PDNPs can generate VNBs when irradiated with pulsed laser light (**Figure 5J, 5K, 5L**). VNBs can be visualized by dark field microscopy as they intensely scatter light during their lifetime. By counting the number of VNBs as a function of the applied laser fluence and by fitting the plotted data with a Boltzmann function, the VNB threshold can be determined, which is defined as the laser fluence at which 90% of the NPs present in the irradiated region generate VNBs. For 400 nm PDNPs, the threshold laser fluence was determined to be 1.32 J/cm². 250 nm PDNPs generated bubbles when illuminated with higher laser fluences, however, no saturation of the VNB formation could be reached within the range of fluences available on our optical setup, hence no threshold could be determined. Lastly, for 150 nm PDNPs, no VNBs were detected, even at the highest available laser fluence. These results are in agreement with

the observations of Harizaj *et al.*⁴⁸, who previously reported an increasing VNB threshold for decreasing PDNP sizes.



(Caption continues on the next page)

Figure 5. Physicochemical characterization of BSA-coated polydopamine nanoparticles (PDNPs) of different sizes. (A-C) Representative SEM images of 150 nm (A), 250 nm (B), and 400 nm (C) PDNPs. The scale bar corresponds to 500 nm. (D-F) Size distribution of 150 nm (D), 250 nm (E), and 400 nm (F) PDNPs, as derived from the SEM images. (G-I) Representative intensity size distributions of BSA-coated PDNPs of 150 nm (G), 250 nm (H), and 400 nm (I) as measured by DLS in water (blue curve) and Opti-MEM (orange curve). (J-L) Determination of vapor nanobubble

(VNB) generation threshold for 150 nm (J), 250 nm (K) and 400 nm (L) PDNPs. The number of bubbles was determined for increasing laser pulse fluences using dark field microscopy. The VNB threshold is deduced using a Boltzmann fit (solid line) and is defined as the laser pulse fluence at which 90% of the asymptotic value of the Boltzmann fit is obtained (blue dotted line).

3.3 Intracellular delivery of FD500 in unstimulated T cells

To evaluate the efficiency of intracellular delivery by PDNP photoporation in unstimulated human T cells, FD500 was selected as a model compound. The procedure of isolating unstimulated T cells from blood samples and application of the photoporation procedure is schematically depicted in **Figure 6A**. For each particle size, T cells were incubated with a range of PDNP concentrations and irradiated with three different laser fluences, *i.e.*, 0.56 J/cm², 1.06 J/cm² and 1.45 J/cm², the latter being close to the highest fluence that can be reached on the photoporation setup used in this study. The percentage of FD500+ cells (readout for delivery efficiency), as quantified by flow cytometry, gradually increased with PDNP concentration, gradually approaching near 100% positive cells (**Figure 6B, 6C, 6D**). The increase in delivery efficiency was associated with decreasing cell viability, which was assessed two hours after photoporation using a Cell Titer Glo assay. The delivery yield, the percentage of FD500+ cells which are alive, was unique to PDNP size (**Figure 6E, 6F, 6G**). For 150 nm PDNPs the most optimal PDNP concentration was consistently 256×10¹⁰ NPs/mL, while it was 8×10¹⁰ NPs/mL for 250 nm PDNPs and 2×10¹⁰ NPs/mL for 400 nm PDNPs. The delivery efficiency for those concentrations was higher for higher laser fluences, but due to a proportionally higher cytotoxicity, the optimal yield values were not significantly different for different laser fluences. Finally, the delivery yield increased with decreasing PDNP size, with the yields being statistically different for treatment with 150 nm PDNPs compared to 400 nm PDNPs ($p < 0.001$ for treatment with 1.06 J/cm²; $p < 0.01$ for 0.56 J/cm² and 1.45 J/cm²).

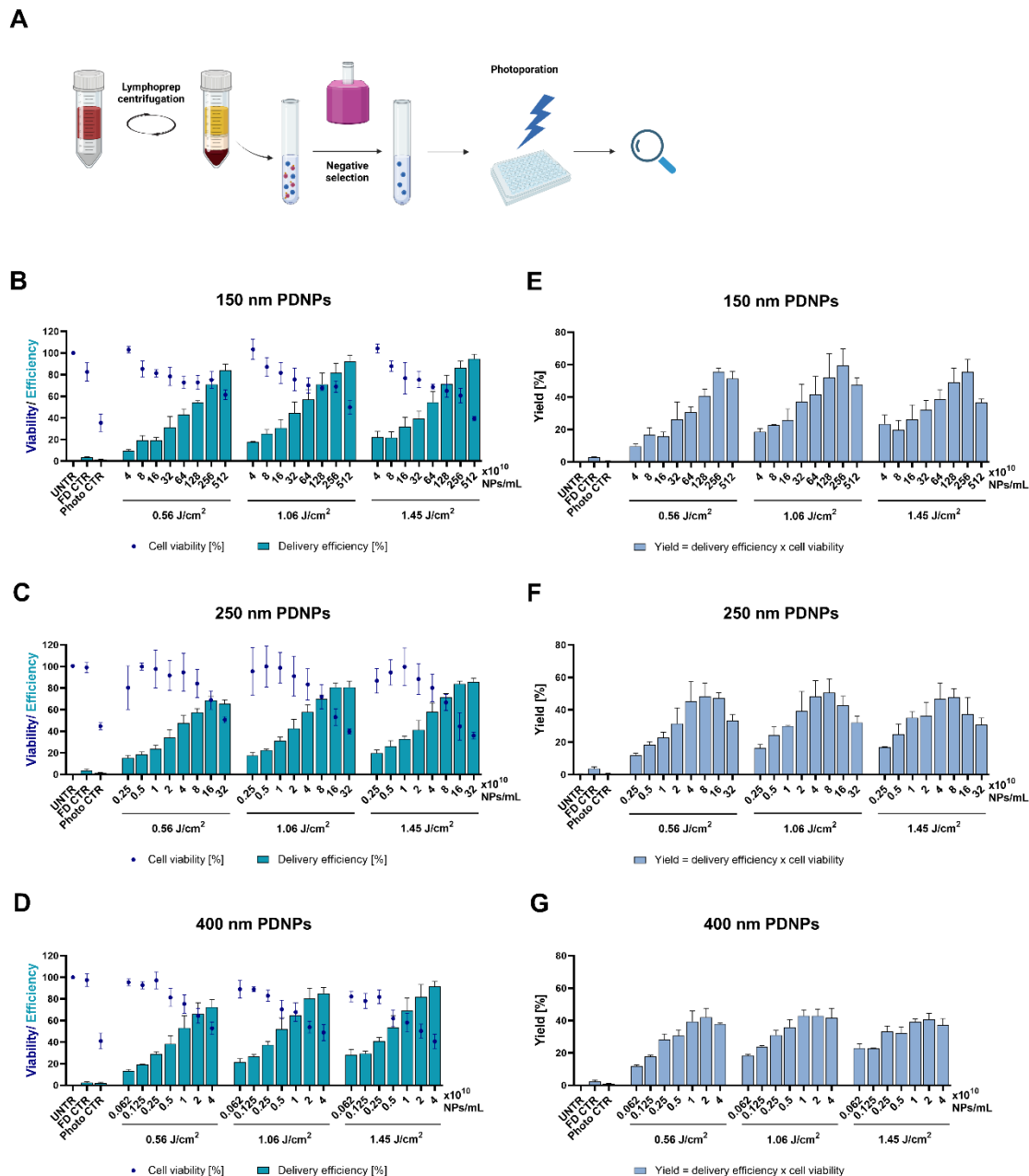


Figure 6. Intracellular delivery of FD500 in unstimulated human T cells by PDNP photoporation. (A) Schematic overview of the experimental procedure. Unstimulated T cells were treated by photoporation for the intracellular delivery of FD500 on the day of isolation. T cells were mixed with increasing concentrations of PDNPs of different sizes and irradiated with three laser fluences of 0.56, 1.06 and 1.45 J/cm². Untreated cells (UNTR), cells incubated with FD500 (FD CTR), cells incubated with FD500 and PDNPs (PDNPs + FD) and cells mixed with NPs and irradiated in the absence of cargo (photo CTR) served as control conditions. (B-D) Delivery efficiency of FD500 (bars) was measured by flow cytometry and cell viability (dots) was determined by a Cell Titer Glo assay 2 hours after the treatment. (E-G) Delivery yield represents the viable and transfected fraction of the initial cell population and was calculated as the product of delivery efficiency and cell viability. Data represent the mean \pm SD of at least four different donors tested per PDNP size.

3.4 Intracellular delivery of FD500 in expanded T cells

Next, we performed the same experiment on expanded T cells. In this case, as schematically shown in **Figure 7A**, lymphocytes were activated with anti-CD3 and anti-CD28 antibodies and cultured in the presence of IL-2 for 7 days before being treated by photoporation in exactly the same manner as before. Again, higher percentages of FD500+ cells (delivery efficiency) could be observed with increasing PDNP concentration, at the expense of cell viability (**Figure 7B, 7C, 7D**). Again, higher laser fluence led to higher delivery efficiency, but due to higher toxicity there was no appreciable difference in the optimal delivery yield. For 150 nm PDNPs, the optimal PDNP concentration was 128-256×10¹⁰ NPs/mL, similar as for unstimulated T cells. For 250 nm PDNPs the optimal concentration was 8-16×10¹⁰ NPs/mL, again close to what was found for unstimulated T cells. For 400 nm PDNPs the optimal concentration varied between 0.25 and 1×10¹⁰ NPs/mL due to a relatively high variability between donors. This is slightly lower than for unstimulated T cells. But, considering high variability between donors, we conclude that the optimal PDNP concentration is very similar for unstimulated or expanded T cells. When looking at the effect of particle size, PDNPs of 250 nm produced the highest yield, although the difference with other sizes was not statistically significant. Therefore, PDNP size had less influence on photoporation efficiency of expanded T cells. While the exact reason for this remains elusive, it may be related to the fact that unstimulated T cells are smaller than activated T cells (**Figure 2**) and, therefore, may be more sensitive to the size of PDNP (and of the induced membrane pores).

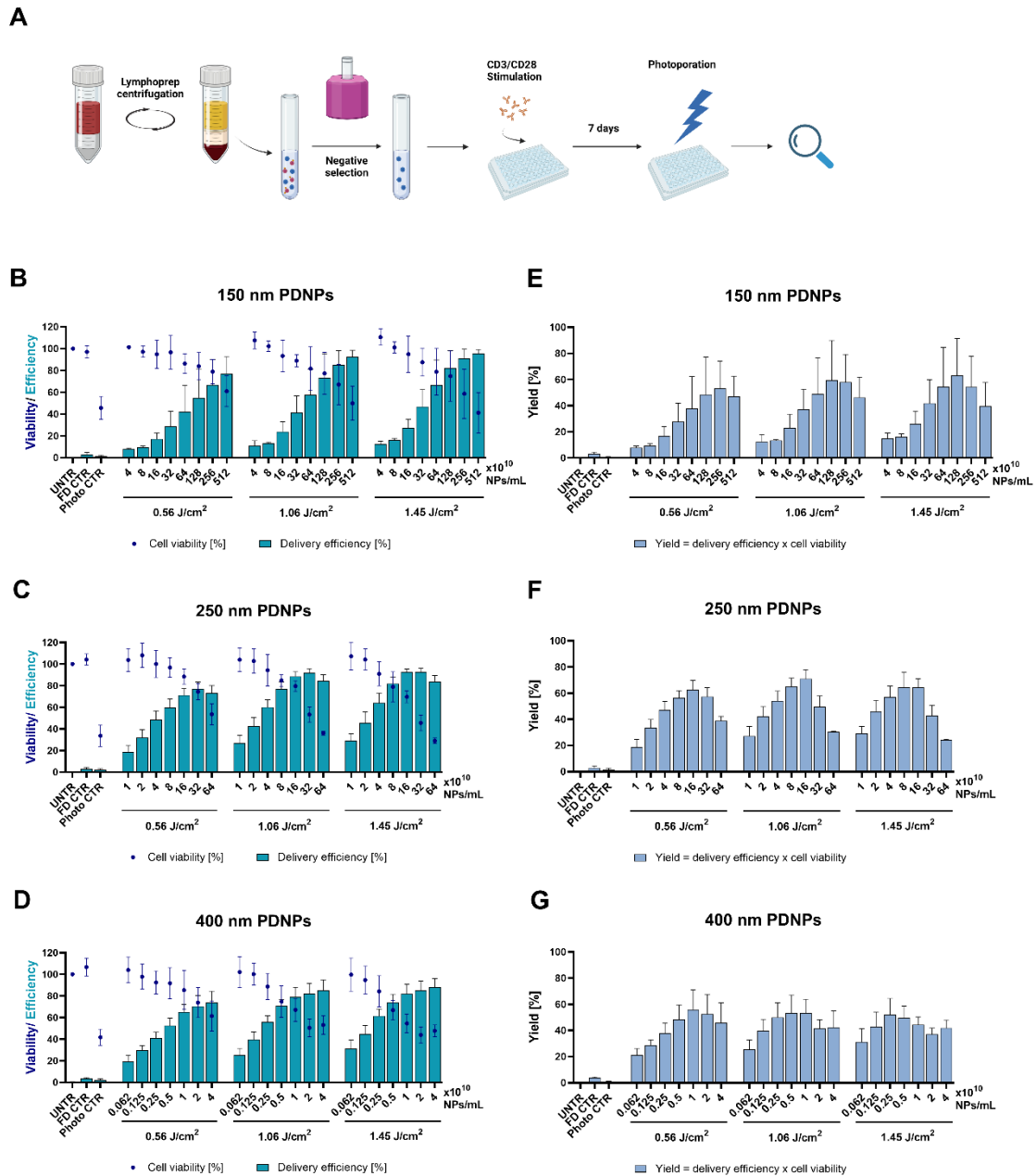


Figure 7. Intracellular delivery of FD500 in expanded human T cells by PDNP photoporation. (A) Schematic overview of the experimental procedure. T cells were stimulated with ImmunoCult CD3/CD28 Activator and cultured for 7 days before photoporation treatment. Cells were mixed with increasing concentrations of PDNPs of different sizes and irradiated with three laser fluences of 0.56, 1.06 and 1.45 J/cm². Untreated cells (UNTR), cells incubated with FD500 (FD CTR), cells incubated with FD500 and PDNPs (PDNPs + FD) and cells mixed with NPs and irradiated in the absence of cargo (photo CTR) served as control conditions. (B-D) Delivery efficiency of FD500 (bars) was measured by flow cytometry and cell viability (dots) was determined by a Cell Titer Glo assay 2 hours after the treatment. (E-G) Delivery yield represents the viable and transfected fraction of the initial cell population and was calculated as the product of delivery efficiency and cell viability. Data represent the mean \pm SD of at least four different donors tested per PDNP size.

3.5 Evaluation of T cell functionality after pre-treatment by photoporation

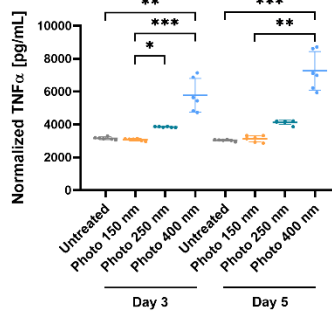
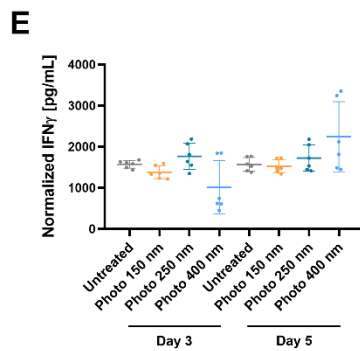
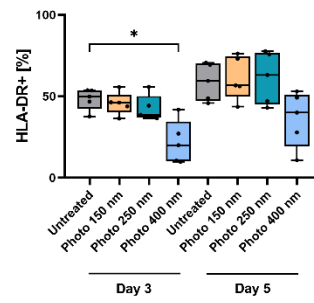
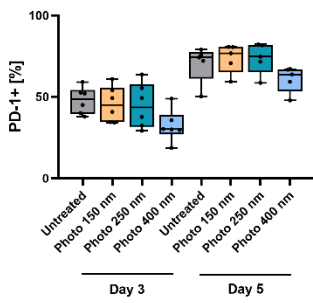
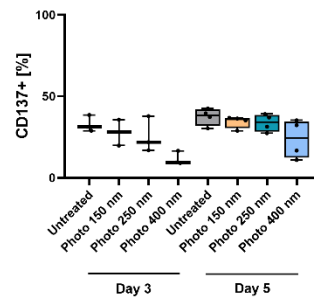
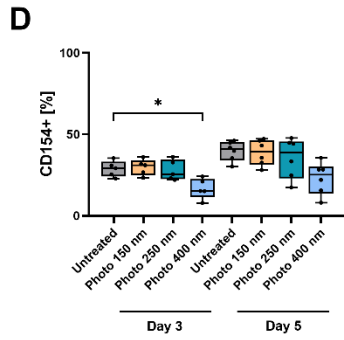
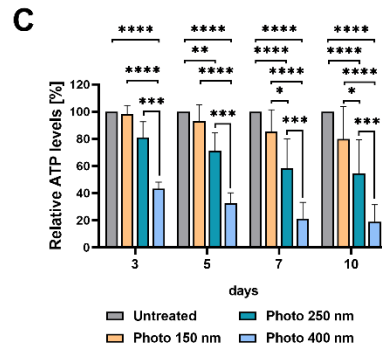
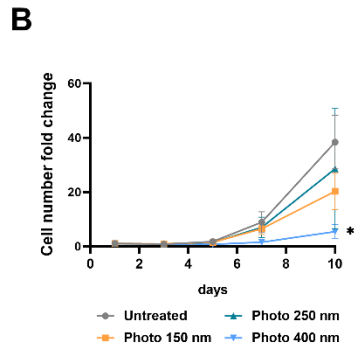
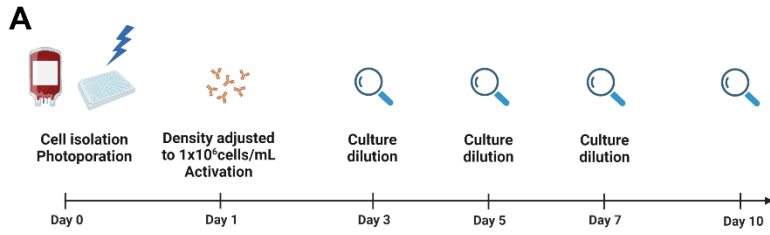
Delivery efficiency and cell viability are the two most common success metrics in the assessment of intracellular delivery methods. However, for cell-based therapies, it is of critical importance to understand the impact of the applied transfection method on cell phenotype and function after treatment. T cell activation is one of the central events in the adaptive immune response, necessary for the generation of cellular and humoral immunity. Having optimized the photoporation parameters, we sought to investigate the functionality of cells irradiated with differently sized PDNPs by assessing their activation propensity after laser exposure. To this end, we measured cell proliferation, upregulation of activation markers and cytokine production (**Figure 8A and Figure S3**). Unstimulated T cells were first exposed to photoporation in the absence of cargo using optimized PDNP concentrations, *i.e.*, 256×10^{10} NPs/mL (150 nm PDNPs), or 8×10^{10} NPs/mL (250 nm PDNPs), or 2×10^{10} NPs/mL (400 nm PDNPs), hereafter referred to as *photo 150*, *photo 250* and *photo 400*, respectively. Laser irradiation was performed at an intermediate laser fluence of 1.06 J/cm^2 and cells were then rested overnight. Before stimulation with CD3/CD28 tetrameric antibody complexes and IL-2, the cell density was adjusted to 1×10^6 cells/mL in each experimental group to compensate for cell loss. Unstimulated cells cultured in a plain medium without activating agents were additionally included as a control condition (**Figure S3**). To evaluate T cell expansion, we measured cell proliferation for up to 10 days by manual cell counting and a spectrophotometric metabolic (ATP quantification) assay. Based on cell counting, a statistically significant ($p < 0.05$) decreased proliferation potential was only observed at day 10 for photo 400-treated cells when compared to the untreated culture, whereas there were no statistically significant differences for the other conditions (**Figure 8B**). The ATP levels of photo 150-treated T cells remained comparable to the untreated ones throughout the whole culture period (**Figure 8C**). However, for photo 250-treated T cells, a significant decrease in viable cell numbers was noticed from day 5 on, stabilizing at $55 \pm 24\%$ at day 10. Photo 400-treated T cells turned out to be more heavily affected, with ATP rates being significantly lower than in the untreated culture and other conditions ($p < 0.001$), dropping to $\sim 20\text{-}30\%$ at the end of culture. Next, we evaluated the expression of well-established surface activation markers, including CD154 (CD40L), CD137 (4-1BB), HLA-DR and activation/exhaustion marker PD-1 (**Figure 8D**). Since these antigens are known to display different kinetics of expression

upon T cell stimulation⁶⁸⁻⁷⁰, they were analyzed at two different time points: day 3 and day 5. Significantly diminished expression of CD154 and HLA-DR was observed at day 3 for photo 400-treated cells but not for photo 150- or photo 250-treated cells. No significant differences in expression profiles of CD137 and PD-1 were found.

Finally, the production of key effector cytokines such as IFN γ and TNF α was analyzed (**Figure S5 and 8E**). In line with proliferation readouts, a heavily diminished secretion of IFN γ was observed at day 3 and 5 for T cells irradiated with 400 nm PDNPs, but not for the other photoporated groups. Also, a reduced TNF α production could be noted for 400 nm PDNPs at day 3 (**Figure S5**). The lower levels of cytokines are obviously biased by the lower cell density. Hence, we normalized the ELISA readouts to the cell numbers as determined by manual cell counting (**Figure 8E**). After doing so, IFN γ levels in untreated and photoporated cultures were relatively similar, while the production of TNF α had increased for photo 400-treated cells, which may render T cells more susceptible to activation-induced cell death⁷¹.

Importantly, the exposure to PDNPs without laser treatment had no measurable influence on cell proliferation and expression of activation markers (**Figure 9**), showing that the PDNPs by themselves do not affect T cell functionality.

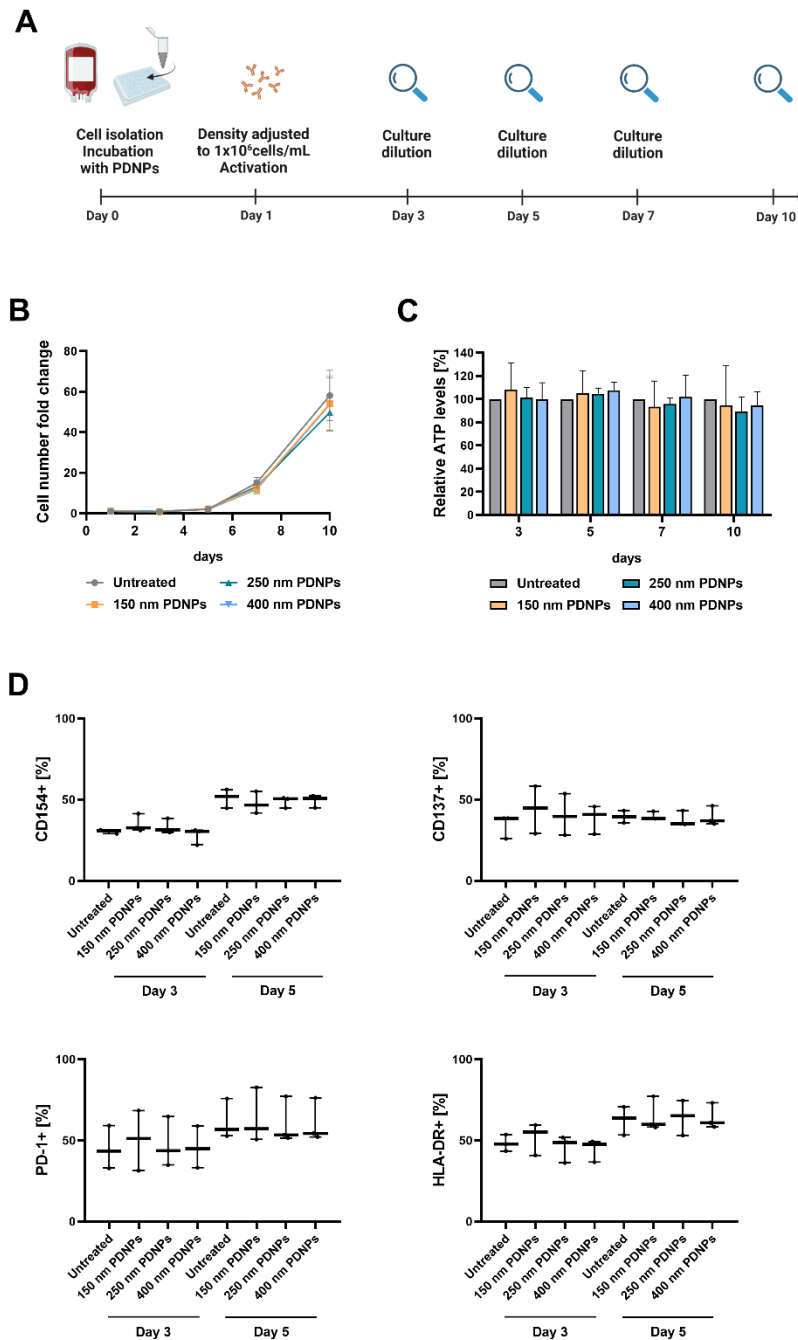
Together, these data point to persistent phenotypic alterations of photo 400-treated T cells, resulting in diminished proliferation rates and aberrant expression of activation markers. On the contrary, T cells irradiated with smaller PDNPs preserved their propensity to become activated much better.



(Caption on the next page)

Figure 8. Evaluation of T cell functionality after pre-treatment by PDNP photoporation.

(A) Schematic overview of the experimental setup and timeline. Unstimulated T cells were treated by photoporation in the absence of FD500 on the day of isolation (day 0). The cells were then allowed to rest overnight. The next day (day 1), the cell density of every experimental group was adjusted to 1×10^6 cells/mL to ensure the optimal stimulation with ImmunoCult CD3/CD28 T cell Activator, as per the manufacturer's instructions. Cultures were diluted at day 3, 5 and 7 and various experimental readouts were assayed at different time points. (B) Cell number fold changes in T cell cultures pre-treated with different PDNP sizes as assessed by cell counting with Trypan blue staining. The normalized cell growth was calculated relative to the seeding density at day 1. Data are represented as the mean \pm SD of cultures of four different donors. Statistical analysis was performed using Two-way ANOVA with Tukey's multiple comparisons test (* $p < 0.05$). (C) Viability of T cell cultures was monitored using Cell Titer Glo assay. The values were calculated relative to the non-treated control at every time point. Data are represented as the mean \pm SD of cultures of five different donors. Statistical analysis was performed using Two-way ANOVA with Tukey's multiple comparisons test (* $p < 0.05$; ** $p < 0.01$; *** $p < 0.001$; **** $p < 0.0001$). (D) The expression of surface activation markers CD154, CD137, PD-1 and HLA-DR was evaluated by flow cytometry at day 3 and day 5 after the photoporation. Data are represented as boxes-and-whiskers showing the minimum to maximum results of cultures of at least three different donors. Statistical analysis was performed using Kruskal-Wallis nonparametric test with Dunn's multiple comparisons test (* $p < 0.05$). (E) The production of IFN γ and TNF α was determined using an ELISA assay. Cell culture supernatants were collected at day 3 and day 5 after the laser treatment. Results were normalized to the cell numbers determined by manual cell counting. Data are represented as the mean (center bar) \pm SD of cultures of three different donors. Statistical analysis was performed using Kruskal-Wallis nonparametric test with Dunn's multiple comparisons test (* $p < 0.05$; ** $p < 0.01$; *** $p < 0.001$).



(Caption continues on the next page)

Figure 9. Evaluation of T cell functionality after pre-treatment with PDNPs of different sizes. (A) Schematic overview of the experimental setup and timeline. Unstimulated T cells were briefly incubated with PDNPs similar as for photoporation, but without applying laser irradiation (day 0). Next, cells were washed and allowed to rest overnight. The next day (day 1), the cell density of every experimental group was adjusted to 1×10^6 cells/mL to ensure optimal stimulation with ImmunoCult CD3/CD28 T cell Activator, as per the manufacturer's instructions. Cultures were diluted at day 3, 5 and 7 and various experimental readouts were assayed at different time points. (B) Cell number fold changes in T cell cultures pre-treated with different PDNP sizes as assessed by cell counting with Trypan blue staining. The normalized cell growth was calculated relative to

the seeding density at day 1. Data are represented as the mean \pm SD of cultures of three different donors. Statistical analysis was performed using Two-way ANOVA with Tukey's multiple comparisons test (no significant differences were detected). (C) Viability of T cell cultures was monitored using a Cell Titer Glo assay. The values were calculated relative to the non-treated control at every time point. Data are represented as the mean \pm SD of cultures of three different donors. Statistical analysis was performed using Two-way ANOVA with Tukey's multiple comparisons test (no significant differences were detected). (D) The expression of surface activation markers CD154, CD137, PD-1 and HLA-DR was evaluated by flow cytometry at day 3 and day 5 after incubation with PDNPs. Data are represented as boxes-and-whiskers showing the minimum to maximum results of cultures of three different donors. Statistical analysis was performed using Kruskal-Wallis nonparametric test with Dunn's multiple comparisons test (not significant).

4 Discussion

NP-mediated photoporation is a promising physical intracellular delivery technology, offering tunability and high throughput. Since it is a laser-activated method, it can deliver compounds in a spatiotemporally defined manner, even with single cell precision^{72,73}. It has proven successful in the delivery of a wide range of molecules such as fluorescent markers^{74,75}, nucleic acids or proteins into various cell types including primary neurons⁷³ and T lymphocytes³⁹⁻⁴¹. Recently, we demonstrated successful photoporation of cells using synthetic melanin-like nanoparticles as biodegradable replacement of the more commonly used inorganic nanoparticles, such as AuNPs⁴⁸. These polydopamine nanoparticles (PDNPs) offer some unique advantages such as biocompatibility, biodegradability, synthesis from clinically approved precursors and excellent photothermal conversion properties over a broad spectral region⁷⁶⁻⁸⁰.

In the field of CAR T cell therapies, vast research efforts have been directed towards increasing T cell potency and persistence *in vivo*. Recent evidence suggests that less differentiated cell phenotypes are preferred¹⁰⁻¹⁶, so that *ex vivo* transfection of quiescent cells would be highly advantageous. It is, therefore, of crucial importance to select a delivery technology that minimally impacts the phenotype and functionality of T cells^{26,81}. For instance, it was demonstrated that electroporation of T cells pushes them to an exhausted and therapeutically inferior phenotype^{29,32,82}, which is not the case for newer and gentler delivery technologies, such as microfluidic cell squeezing³² and nanofiber-based photoporation³³.

To assess the value of PDNP photoporation for T cell engineering, it is, therefore, of importance to further investigate to which extent it can be used to deliver macromolecules in unstimulated T cells without affecting the cell's phenotype. As activated T cells are larger than quiescent T cells (**Figure 2**), we reasoned that it would be of interest to evaluate different sizes of PDNPs. Therefore, we synthesized PDNPs with an average size of approximately 150 nm, 250 nm and 400 nm, which were coated with BSA as before⁴⁸ to achieve good colloidal stability of PDNPs in Opti-MEM. Importantly, human serum albumin and bovine serum albumin (BSA) share several characteristics, such as high solubility in water, long half-life in blood, similar molecular weight, and a similar number of amino acid residues. Therefore, for (pre-clinical) research purposes, both types of

albumins have been widely applied, with no noticeable differences in properties of such nanomaterials, suggesting that BSA can be substituted by serum albumin extracted from human blood at later stages of technology translation ⁵⁸⁻⁶⁰.

Next, we optimized photoporation parameters for both unstimulated and expanded T cells by extensive screening of PDNP concentrations and laser fluences. As a model cargo, we selected FD500, which corresponds to a hydrodynamic diameter of 31 nm and falls in the size range of some therapeutically relevant molecules, such as transcription factors, antibodies and genome-editing nucleases ¹. In unstimulated T cells, we observed an inverse correlation between maximal delivery yields and increasing PDNP sizes. 150 nm PDNPs significantly outperformed the largest 400 nm PD formulation, mainly due to inducing less toxicity for a similar delivery efficiency. Importantly, optimal photoporation conditions for both 150 and 250 nm PDNPs were associated with favorable viability above 70% and delivery efficiencies between 70 and 85%, resulting in a delivery yield of 50-60%. However, when unstimulated cells were irradiated with 400 nm PDNPs, cell viability dropped to ~55%, resulting in the lowest delivery yield among all tested formulations. In the case of CD3/CD28 activated T cells, the overall best performance was obtained with 250 nm PDNPs, where high delivery efficiency (~90%) was combined with relatively low toxicity, resulting in an excellent yield of ~70%. The delivery yield for both 150 and 400 nm PDNPs was slightly less, although differences were not statistically significant. Altogether, slightly higher delivery yields were achieved in pre-activated cells when compared to unstimulated T cells. This was somehow expected and in agreement with previous studies on AuNP-mediated photoporation which demonstrated that the efficiency of intracellular delivery increases with increasing cell size ⁸³. Nonetheless, the delivery yield for both T cell models clearly exceeded those described previously for FD500 delivery by AuNP-mediated photoporation in Jurkat cells (~20%) ⁸⁴ and PDNP-photoporation with 500 nm PDNPs in expanded T cells (~30%) ⁴⁸. This shows that, if PDNP size is optimized for a given cell (pheno)type, they are excellent sensitizers for photoporation, resulting in high delivery yields.

However, as discussed above, delivery efficiency alone is insufficient in the context of adoptive T cell therapy, since also T cell fitness is a critical determinant of therapeutic efficacy. Therefore, to better understand the functional implications of PDNP

photoporation, we studied T cell propensity to activation after laser exposure. We observed no significant changes to proliferation of photo 150-treated cells, indicating that T cells remained highly functional after treatment. Some impact on growth rates could be noted after subculturing of photo 250-treated cells. However, expression of activation markers and secretion of IFN γ and TNF α remained comparable to the untreated control. In contrast, photo 400- treated T cells could not recover in terms of proliferation and surface phenotype. These observations are in line with the ranking of PDNP size according to their maximal delivery yields (150 nm > 250 nm > 400 nm), underscoring the importance of tailoring the size of the photosensitizer to a specific cell (pheno)type to ensure optimal delivery and cell phenotype preservation.

The reason why larger PDNPs have a bigger impact on small quiescent T cells can be due to two reasons. First of all, for the laser fluences used in this study, the 150 nm PDNPs did not generate VNB, meaning that membrane pore formation was due to direct heating. Instead, 400 nm PDNPs did form VNB, in which case pores are generated by a different mechanism (mechanical perturbation). Therefore, it could be that VNB formation by larger PDNPs, and the mechanical pressure waves that result from that, inflict more damage to cells as compared to mere heating at the plasma membrane. A second reason could be that VNB formation by large PDNPs results in larger membrane pores, which could be more difficult to repair by small cells like unstimulated T cells^{85,86}. In any case, whatever the underlying reason, this perturbation resulted in immediate cell loss as demonstrated by ATP measurements performed 2 hours after laser treatment. Additionally, the surviving cell population carried some persistent phenotype alterations which manifested themselves in reduced proliferation rates during *in vitro* expansion. Moreover, we observed an aberrant cytokine production, similar to what was reported before for the treatment by electroporation^{32,33}.

Having identified PDNP sizes that have a minimal impact on T cell activation propensity, in future work it will be of interest to determine delivery efficiency in different T cell subsets, such as naïve or memory cells and analyze the impact of photoporation treatment on the respective subpopulations, for instance by single cell sequencing. Such phenotypical analysis could reveal more about the impact of PDNP photoporation on T cell differentiation. Lastly, the investigation of T cell functionality may be strengthened by

the assessment of antigen specific cytolytic activity of photoporated CAR-T cells as has been done before for nanofiber photoporation [33]. Nonetheless, the multiparametric *in vitro* analysis performed in this study provides valuable insights for further optimization of PDNP photoporation towards genetic engineering of highly functional human T cells.

5 Conclusion

In summary, we optimized PDNP photoporation for macromolecule delivery in both unstimulated and expanded human T cells. A systematic screening of photosensitizer sizes revealed that laser treatment of quiescent cells with small 150 nm PDNPs generates favorable delivery yields with a minimal impact on T cell functionality. Our findings highlight the need for tailoring the size of photothermal NPs to cell (pheno)type and the importance of careful evaluation the effect of the delivery method on phenotype and functionality. The observations made in this study will be helpful to further develop photoporation as an intracellular delivery method for the genetic engineering of clinically relevant immune cells.

References

1. Stewart MP, Langer R, Jensen KF. Intracellular Delivery by Membrane Disruption: Mechanisms, Strategies, and Concepts. *Chem Rev*. 2018;118(16):7409-7531.
2. Sadelain M, Rivière I, Riddell S. Therapeutic T cell engineering. *Nature*. 2017;545(7655):423-431.
3. Majzner RG, Mackall CL. Clinical lessons learned from the first leg of the CAR T cell journey. *Nat Med*. 2019;25(9):1341-1355.
4. Waldman AD, Fritz JM, Lenardo MJ. A guide to cancer immunotherapy: from T cell basic science to clinical practice. *Nat Rev Immunol*. 2020;20(11):651-668.
5. Maude SL, Frey N, Shaw PA, et al. Chimeric Antigen Receptor T Cells for Sustained Remissions in Leukemia. *New England Journal of Medicine*. 2014;371(16):1507-1517.
6. Park JH, Rivière I, Gonen M, et al. Long-Term Follow-up of CD19 CAR Therapy in Acute Lymphoblastic Leukemia. *New England Journal of Medicine*. 2018;378(5):449-459.
7. Maude SL, Laetsch TW, Buechner J, et al. Tisagenlecleucel in Children and Young Adults with B-Cell Lymphoblastic Leukemia. *New England Journal of Medicine*. 2018;378(5):439-448.
8. Neelapu SS, Locke FL, Bartlett NL, et al. Axicabtagene Ciloleucel CAR T-Cell Therapy in Refractory Large B-Cell Lymphoma. *New England Journal of Medicine*. 2017;377(26):2531-2544.
9. Locke FL, Ghobadi A, Jacobson CA, et al. Long-term safety and activity of axicabtagene ciloleucel in refractory large B-cell lymphoma (ZUMA-1): a single-arm, multicentre, phase 1–2 trial. *Lancet Oncol*. 2019;20(1):31-42.
10. Gattinoni L, Klebanoff CA, Palmer DC, et al. Acquisition of full effector function in vitro paradoxically impairs the in vivo antitumor efficacy of adoptively transferred CD8+ T cells. *Journal of Clinical Investigation*. 2005;115(6):1616-1626.
11. Klebanoff CA, Gattinoni L, Torabi-Parizi P, et al. Central memory self/tumor-reactive CD8+ T cells confer superior antitumor immunity compared with effector memory T cells. *Proc Natl Acad Sci U S A*. 2005;102(27):9571-9576.
12. Hinrichs CS, Borman ZA, Cassard L, et al. Adoptively transferred effector cells derived from naïve rather than central memory CD8 + T cells mediate superior antitumor immunity. *Proceedings of the National Academy of Sciences*. 2009;106(41):17469-17474.
13. Gattinoni L, Lugli E, Ji Y, et al. A human memory T cell subset with stem cell–like properties. *Nat Med*. 2011;17(10):1290-1297.
14. Fraietta JA, Nobles CL, Sammons MA, et al. Disruption of TET2 promotes the therapeutic efficacy of CD19-targeted T cells. *Nature*. 2018;558(7709):307-312.

15. Fraietta JA, Lacey SF, Orlando EJ, et al. Determinants of response and resistance to CD19 chimeric antigen receptor (CAR) T cell therapy of chronic lymphocytic leukemia. *Nat Med*. 2018;24(5):563-571.
16. Arcangeli S, Falcone L, Camisa B, et al. Next-Generation Manufacturing Protocols Enriching TSCM CAR T Cells Can Overcome Disease-Specific T Cell Defects in Cancer Patients. *Front Immunol*. 2020;11(June).
17. Ghassemi S, Nunez-Cruz S, O'Connor RS, et al. Reducing ex vivo culture improves the antileukemic activity of chimeric antigen receptor (CAR) T cells. *Cancer Immunol Res*. 2018;6(9):1100-1109.
18. Ghassemi S, Durgin JS, Nunez-Cruz S, et al. Rapid manufacturing of non-activated potent CAR T cells. *Nat Biomed Eng*. 2022;6(2):118-128.
19. de Macedo Abdo L, Barros LRC, Saldanha Viegas M, et al. Development of CAR-T cell therapy for B-ALL using a point-of-care approach. *Oncoimmunology*. 2020;9(1).
20. Liu L, Johnson C, Fujimura S, Teque F, Levy JA. Transfection optimization for primary human CD8+ cells. *J Immunol Methods*. 2011;372(1-2):22-29.
21. Seki A, Rutz S. Optimized RNP transfection for highly efficient CRISPR/Cas9-mediated gene knockout in primary T cells. *Journal of Experimental Medicine*. 2018;215(3):985-997.
22. Aksoy P, Aksoy BA, Czech E, Hammerbacher J. Viable and efficient electroporation-based genetic manipulation of unstimulated human T cells. *bioRxiv*. 2018;(Cm):1-34.
23. Vormittag P, Gunn R, Ghorashian S, Veraitch FS. A guide to manufacturing CAR T cell therapies. *Curr Opin Biotechnol*. 2018;53:164-181.
24. Eyles JE, Vessillier S, Jones A, Stacey G, Schneider CK, Price J. Cell therapy products: focus on issues with manufacturing and quality control of chimeric antigen receptor T-cell therapies. *Journal of Chemical Technology and Biotechnology*. 2019;94(4):1008-1016.
25. Levine BL, Miskin J, Wonnacott K, Keir C. Global Manufacturing of CAR T Cell Therapy. *Mol Ther Methods Clin Dev*. 2017;4:92-101.
26. Raes L, De Smedt SC, Raemdonck K, Braeckmans K. Non-viral transfection technologies for next-generation therapeutic T cell engineering. *Biotechnol Adv*. 2021;49(April):107760.
27. Moretti A, Ponzo M, Nicolette CA, Tcherepanova IY, Biondi A, Magnani CF. The Past, Present, and Future of Non-Viral CAR T Cells. *Front Immunol*. 2022;13(June):1-25.
28. Wagner DL, Koehl U, Chmielewski M, Scheid C, Stripecke R. Review: Sustainable Clinical Development of CAR-T Cells – Switching From Viral Transduction Towards CRISPR-Cas Gene Editing. *Front Immunol*. 2022;13(June):1-13.
29. Huerfano S, Ryabchenko B, Forstová J. Nucleofection of Expression Vectors Induces a Robust Interferon Response and Inhibition of Cell Proliferation. *DNA Cell Biol*. 2013;32(8):467-479.

30. Cromer MK, Vaidyanathan S, Ryan DE, et al. Global Transcriptional Response to CRISPR/Cas9-AAV6-Based Genome Editing in CD34+ Hematopoietic Stem and Progenitor Cells. *Molecular Therapy*. 2018;26(10):2431-2442.
31. Tay A, Melosh N. Transfection with Nanostructure Electro-Injection is Minimally Perturbative. *Adv Ther (Weinh)*. 2019;2(12):1900133.
32. DiTommaso T, Cole JM, Cassereau L, et al. Cell engineering with microfluidic squeezing preserves functionality of primary immune cells in vivo. *Proceedings of the National Academy of Sciences*. 2018;115(46):E10907-E10914.
33. Xiong R, Hua D, Van Hoeck J, et al. Photothermal nanofibres enable safe engineering of therapeutic cells. *Nat Nanotechnol*. 2021;16(11):1281-1291.
34. Xiong R, Samal SK, Demeester J, Skirtach AG, De Smedt SC, Braeckmans K. Laser-assisted photoporation: fundamentals, technological advances and applications. *Adv Phys X*. 2016;1(4):596-620.
35. Ramon J, Xiong R, De Smedt SC, Raemdonck K, Braeckmans K. Vapor nanobubble-mediated photoporation constitutes a versatile intracellular delivery technology. *Curr Opin Colloid Interface Sci*. 2021;54:101453.
36. Urban AS, Fedoruk M, Horton MR, Rädler JO, Stefani FD, Feldmann J. Controlled Nanometric Phase Transitions of Phospholipid Membranes by Plasmonic Heating of Single Gold Nanoparticles. *Nano Lett*. 2009;9(8):2903-2908.
37. Xiong R, Raemdonck K, Peynshaert K, et al. Comparison of Gold Nanoparticle Mediated Photoporation: Vapor Nanobubbles Outperform Direct Heating for Delivering Macromolecules in Live Cells. *ACS Nano*. 2014;8(6):6288-6296.
38. Lukianova-Hleb E, Hu Y, Latterini L, et al. Plasmonic Nanobubbles as Transient Vapor Nanobubbles Generated around Plasmonic Nanoparticles. *ACS Nano*. 2010;4(4):2109-2123.
39. Wayteck L, Xiong R, Braeckmans K, De Smedt SC, Raemdonck K. Comparing photoporation and nucleofection for delivery of small interfering RNA to cytotoxic T cells. *Journal of Controlled Release*. 2017;267:154-162.
40. Raes L, Stremersch S, Fraire JC, et al. Intracellular Delivery of mRNA in Adherent and Suspension Cells by Vapor Nanobubble Photoporation. *Nanomicro Lett*. 2020;12(1):1-17.
41. Raes L, Pille M, Harizaj A, et al. Cas9 RNP transfection by vapor nanobubble photoporation for ex vivo cell engineering. *Mol Ther Nucleic Acids*. 2021;25(September):696-707.
42. Bongiovanni G, Olshin PK, Yan C, Voss JM, Drabbels M, Lorenz UJ. The fragmentation mechanism of gold nanoparticles in water under femtosecond laser irradiation. *Nanoscale Adv*. 2021;3(18):5277-5283.

43. González-Rubio G, Guerrero-Martínez A, Liz-Marzán LM. Reshaping, Fragmentation, and Assembly of Gold Nanoparticles Assisted by Pulse Lasers. *Acc Chem Res.* 2016;49(4):678-686.
44. Ziefuss AR, Reich S, Reichenberger S, Levantino M, Plech A. In situ structural kinetics of picosecond laser-induced heating and fragmentation of colloidal gold spheres. *Physical Chemistry Chemical Physics.* 2020;22(9):4993-5001.
45. Tsoli M, Kuhn H, Brandau W, Esche H, Schmid G. Cellular uptake and toxicity of Au55 clusters. *Small.* 2005;1(8-9):841-844.
46. Pan Y, Neuss S, Leifert A, et al. Size-dependent cytotoxicity of gold nanoparticles. *Small.* 2007;3(11):1941-1949.
47. Ryu JH, Messersmith PB, Lee H. Polydopamine Surface Chemistry: A Decade of Discovery. *ACS Appl Mater Interfaces.* 2018;10(9):7523-7540.
48. Harizaj A, Wels M, Raes L, et al. Photoporation with Biodegradable Polydopamine Nanosensitizers Enables Safe and Efficient Delivery of mRNA in Human T Cells. *Adv Funct Mater.* 2021;31(28):2102472.
49. Schindelin J, Arganda-Carreras I, Frise E, et al. Fiji: an open-source platform for biological-image analysis. *Nat Methods.* 2012;9(7):676-682.
50. Ju KY, Lee Y, Lee S, Park SB, Lee JK. Bioinspired polymerization of dopamine to generate melanin-like nanoparticles having an excellent free-radical-scavenging property. *Biomacromolecules.* 2011;12(3):625-632.
51. Filipe V, Hawe A, Jiskoot W. Critical evaluation of nanoparticle tracking analysis (NTA) by NanoSight for the measurement of nanoparticles and protein aggregates. *Pharm Res.* 2010;27(5):796-810.
52. Boyd RD, Pichaimuthu SK, Cuenat A. New approach to inter-technique comparisons for nanoparticle size measurements; using atomic force microscopy, nanoparticle tracking analysis and dynamic light scattering. *Colloids Surf A Physicochem Eng Asp.* 2011;387(1-3):35-42.
53. Shang J, Gao X. Nanoparticle counting: towards accurate determination of the molar concentration. *Chem Soc Rev.* 2014;43(21):7267-7278.
54. Nishizawa N, Kawamura A, Kohri M, Nakamura Y, Fujii S. Polydopamine Particle as a Particulate Emulsifier. *Polymers (Basel).* 2016;8(3):62.
55. Wolf T, Jin W, Zoppi G, et al. Dynamics in protein translation sustaining T cell preparedness. *Nat Immunol.* 2020;21(8):927-937.
56. Howden AJM, Hukelmann JL, Brenes A, et al. Quantitative analysis of T cell proteomes and environmental sensors during T cell differentiation. *Nat Immunol.* 2019;20(11):1542-1554.

57. Wang X, Chen Z, Yang P, Hu J, Wang Z, Li Y. Size control synthesis of melanin-like polydopamine nanoparticles by tuning radicals. *Polym Chem.* 2019;10(30):4194-4200.
58. Liu Z, Chen X. Simple bioconjugate chemistry serves great clinical advances: albumin as a versatile platform for diagnosis and precision therapy. *Chem Soc Rev.* 2016;45(5):1432-1456.
59. An FF, Zhang XH. Strategies for Preparing Albumin-based Nanoparticles for Multifunctional Bioimaging and Drug Delivery. *Theranostics.* 2017;7(15):3667-3689.
60. Ghalandari B, Yu Y, Ghorbani F, et al. Polydopamine nanospheres coated with bovine serum albumin permit enhanced cell differentiation: fundamental mechanism and practical application for protein coating formation. *Nanoscale.* 2021;13(47):20098-20110.
61. Lee H, Rho J, Messersmith PB. Facile Conjugation of Biomolecules onto Surfaces via Mussel Adhesive Protein Inspired Coatings. *Advanced Materials.* 2009;21(4):431-434.
62. Liu J, Xu H, Tang X, et al. Simple and tunable surface coatings via polydopamine for modulating pharmacokinetics, cell uptake and biodistribution of polymeric nanoparticles. *RSC Adv.* 2017;7(26):15864-15876.
63. Singh N, Nayak J, Patel K, Sahoo SK, Kumar R. Electrochemical impedance spectroscopy reveals a new mechanism based on competitive binding between Tris and protein on a conductive biomimetic polydopamine surface. *Physical Chemistry Chemical Physics.* 2018;20(40):25812-25821.
64. Raghuwanshi VS, Yu B, Browne C, Garnier G. Reversible pH Responsive Bovine Serum Albumin Hydrogel Sponge Nanolayer. *Front Bioeng Biotechnol.* 2020;8(June):1-10.
65. Purohit R, Vallabani NS, Shukla RK, Kumar A, Singh S. Effect of gold nanoparticle size and surface coating on human red blood cells. *Bioinspired, Biomimetic and Nanobiomaterials.* 2016;5(3):121-131.
66. Mudalige T, Qu H, Van Haute D, Ansar SM, Paredes A, Ingle T. Characterization of Nanomaterials. In: *Nanomaterials for Food Applications.* Elsevier; 2019:313-353.
67. Danaei M, Dehghankhold M, Ataei S, et al. Impact of Particle Size and Polydispersity Index on the Clinical Applications of Lipidic Nanocarrier Systems. *Pharmaceutics.* 2018;10(2):57.
68. Caruso A, Licenziati S, Corulli M, et al. Flow cytometric analysis of activation markers on stimulated T cells and their correlation with cell proliferation. *Cytometry.* 1997;27(1):71-76.
69. Reddy M, Eirikis E, Davis C, Davis HM, Prabhakar U. Comparative analysis of lymphocyte activation marker expression and cytokine secretion profile in stimulated human peripheral blood mononuclear cell cultures: An in vitro model to monitor cellular immune function. *J Immunol Methods.* 2004;293(1-2):127-142.

70. Shipkova M, Wieland E. Surface markers of lymphocyte activation and markers of cell proliferation. *Clinica Chimica Acta*. 2012;413(17-18):1338-1349.
71. Popescu I, Snyder ME, Isella CJ, et al. CD4 + T-Cell Dysfunction in Severe COVID-19 Disease Is Tumor Necrosis Factor- α /Tumor Necrosis Factor Receptor 1–Dependent. *Am J Respir Crit Care Med*. 2022;205(12):1403-1418.
72. Xiong R, Drullion C, Verstraelen P, et al. Fast spatial-selective delivery into live cells. *Journal of Controlled Release*. 2017;266:198-204.
73. Xiong R, Verstraelen P, Demeester J, et al. Selective labeling of individual neurons in dense cultured networks with nanoparticle-enhanced photoporation. *Front Cell Neurosci*. 2018;12(March):1-11.
74. Xiong R, Joris F, Liang S, et al. Cytosolic Delivery of Nanolabels Prevents Their Asymmetric Inheritance and Enables Extended Quantitative in Vivo Cell Imaging. *Nano Lett*. 2016;16(10):5975-5986.
75. Liu J, Xiong R, Brans T, et al. Repeated photoporation with graphene quantum dots enables homogeneous labeling of live cells with extrinsic markers for fluorescence microscopy. *Light Sci Appl*. 2018;7(1):47.
76. Ku SH, Park CB. Human endothelial cell growth on mussel-inspired nanofiber scaffold for vascular tissue engineering. *Biomaterials*. 2010;31(36):9431-9437.
77. Liu Y, Ai K, Liu J, Deng M, He Y, Lu L. Dopamine-melanin colloidal nanospheres: An efficient near-infrared photothermal therapeutic agent for in vivo cancer therapy. *Advanced Materials*. 2013;25(9):1353-1359.
78. Liu X, Cao J, Li H, et al. Mussel-inspired polydopamine: A biocompatible and ultrastable coating for nanoparticles in vivo. *ACS Nano*. 2013;7(10):9384-9395.
79. Poinard B, Lam SAE, Neoh KG, Kah JCY. Mucopenetration and biocompatibility of polydopamine surfaces for delivery in an Ex Vivo porcine bladder. *Journal of Controlled Release*. 2019;300(February):161-173.
80. Carmignani A, Battaglini M, Sinibaldi E, et al. In Vitro and Ex Vivo Investigation of the Effects of Polydopamine Nanoparticle Size on Their Antioxidant and Photothermal Properties: Implications for Biomedical Applications. *ACS Appl Nano Mater*. 2022;5(1):1702-1713.
81. Houthaeve G, De Smedt SC, Braeckmans K, De Vos WH. The cellular response to plasma membrane disruption for nanomaterial delivery. *Nano Converg*. 2022;9(1):6.
82. Zhang M, Ma Z, Selliah N, et al. The impact of Nucleofection[®] on the activation state of primary human CD4 T cells. *J Immunol Methods*. 2014;408(1):123-131.
83. Schomaker M, Killian D, Willenbrock S, et al. Biophysical effects in off-resonant gold nanoparticle mediated (GNOME) laser transfection of cell lines, primary- and stem cells using fs laser pulses. *J Biophotonics*. 2015;8(8):646-658.

84. Raes L, Van Hecke C, Michiels J, et al. Gold Nanoparticle-Mediated Photoporation Enables Delivery of Macromolecules over a Wide Range of Molecular Weights in Human CD4+ T Cells. *Crystals (Basel)*. 2019;9(8):411.
85. Jimenez AJ, Perez F. Plasma membrane repair: the adaptable cell life-insurance. *Curr Opin Cell Biol*. 2017;47:99-107.
86. Zhen Y, Radulovic M, Vietri M, Stenmark H. Sealing holes in cellular membranes. *EMBO J*. 2021;40(7):1-13.

Supplementary Information

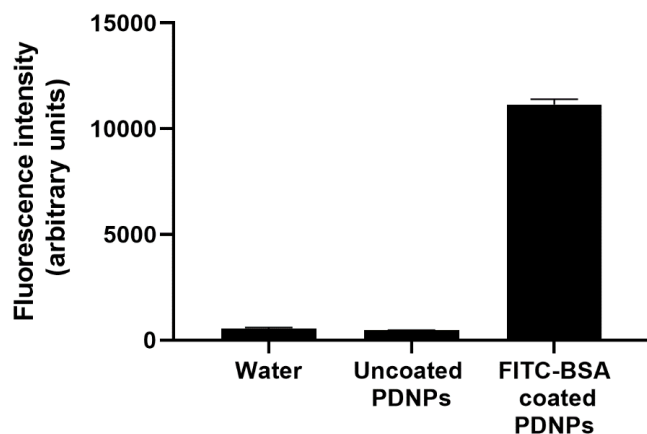


Figure S1. Fluorometric analysis of uncoated and FITC-BSA-coated 400 nm PDNPs.

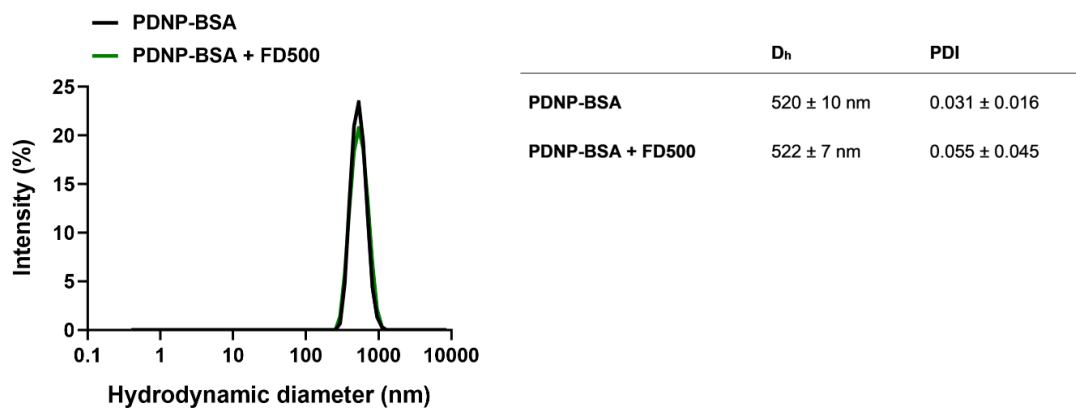


Figure S2. Characterization of PDNP interaction with FITC dextran 500 kDa (FD500) as measured by DLS in Opti-MEM. The highest concentration of BSA-coated 400 nm PDNPs tested in this study, *i.e.*, 4×10^{10} NPs/mL, was used.

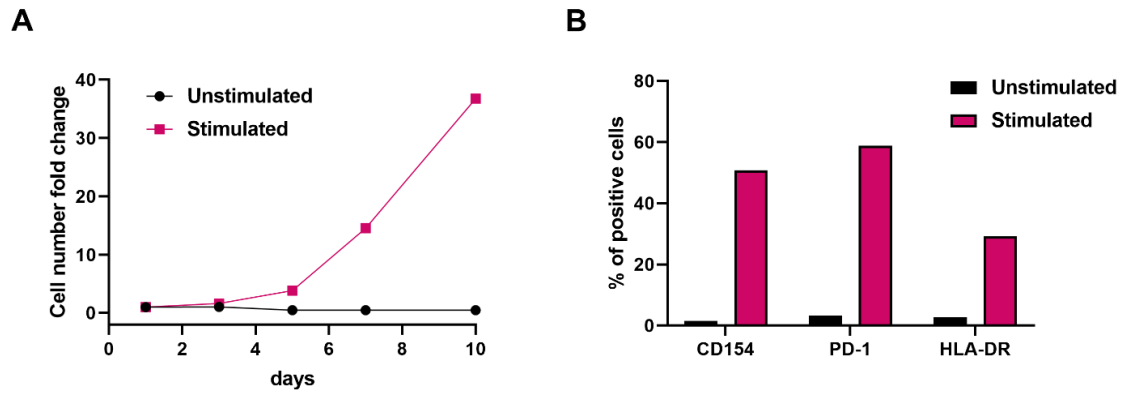


Figure S3. Activation of human T cells stimulated with ImmunoCult™ Human CD3/CD28 T cell Activator. (A) T cells were stimulated with ImmunoCult and maintained in complete IMDM medium supplemented with IL-2. Viable cells were counted on day 3, 5, 7 and 10. (B) The expression of surface activation markers was analyzed by flow cytometry after 48 h of stimulation. One representative donor is shown.

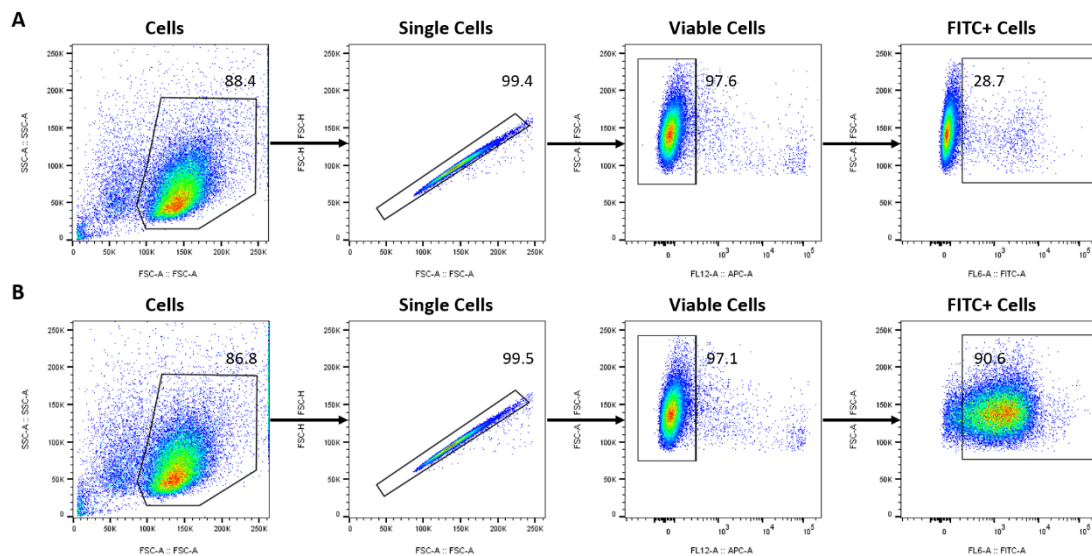


Figure S4. Flow cytometry gating strategy used to determine delivery efficiency of FD500 in stimulated T cells. Cells were first gated using forward scatter area (FSC-A) and side scatter area (SSC-A). Next, singlets were gated using FSC-A and FSC-height. From this population, living cells were defined based on negative TO-PRO3 staining (APC-signal). Finally, FITC (FD500)-positive cells were determined based on their FITC-area signal. (A) Stimulated T cells incubated with FD500 without laser irradiation. (B) Stimulated T cells mixed with 150 nm PDNPs at a concentration of $128 \times 10^{10}/\text{mL}$ and FD500 and irradiated with 1.06 J cm^{-2} .

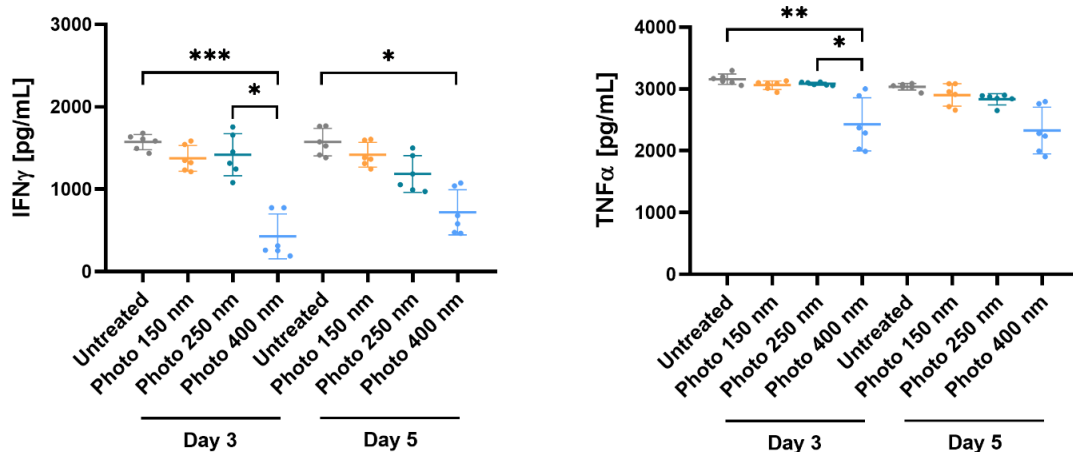


Figure S5. The production of IFN γ and TNF α as determined by an ELISA assay. Cell culture supernatants were collected at day 3 and day 5 after the laser treatment. Data are represented as the mean (center bar) \pm SD of cultures of three different donors. Statistical analysis was performed using Kruskal-Wallis nonparametric test with Dunn's multiple comparisons test (*p < 0.05; **p < 0.01; ***p < 0.001).

Chapter 3

Photothermal nanofibers enable macromolecule delivery in unstimulated human T cells

This chapter will be submitted for publication as:

Dominika Berdecka^{a,b}, Manon Minsart^c, Tao Lu^a, Deep Punj^a, Riet De Rycke^d, Mina Nikolić^e, Eduardo Bolea-Fernandez^{e,f}, Frank Vanhaecke^e, Ranhua Xiong^g, Stefaan C. De Smedt^{a,g}, Peter Dubruel^c, Winnok H. De Vos^b and Kevin Braeckmans^a. Photothermal nanofibers enable macromolecule delivery in unstimulated human T cells.

^a Laboratory of General Biochemistry and Physical Pharmacy, Faculty of Pharmaceutical Sciences, Ghent University

^b Laboratory of Cell Biology and Histology, Department of Veterinary Sciences, University of Antwerp

^c Polymer Chemistry and Biomaterials Group, Department of Organic and Macromolecular Chemistry, Ghent University

^d VIB Bioimaging Core and Department of Biomedical Molecular Biology, VIB Center for Inflammation Research

^e Atomic and Mass Spectrometry Research Group, Department of Chemistry, Ghent University

^f Aragón Institute of Engineering Research (I3A), Department of Analytical Chemistry, University of Zaragoza, Spain

^g Joint Laboratory of Advanced Biomedical Materials (Nanjing Forestry University–Ghent University), College of Chemical Engineering, Nanjing Forestry University, China

Author contributions: D.B. performed the nanofiber fabrication, T cell isolation, photoporation experiments, functional T cell experiments and data analysis. In addition, D.B. made the figures and wrote the article. M.M. and T.L. contributed to the nanofiber fabrication. D.P. assisted with the VNB generation analysis. R.D.R. performed the electron microscopy analysis. M.N. and E.B.F. performed the ICP-MS/MS analysis. R.X. was involved in the conceptualization and provided technical guidance on PEN photoporation. F.V., R.X., S.D.S., P.D., W.D.V. and K.B. reviewed the article.

Table of Contents

Abstract.....	138
1 Introduction.....	139
2 Materials and methods	142
2.1 Fabrication of photothermal nanofibers by electrospinning.....	142
2.2 Preparation of PEN substrates for suspension cells	142
2.3 Electron microscopy.....	143
2.4 Dark and bright field microscopy for detection of vapor nanobubbles	143
2.5 Quantification of Fe release by ICP-MS/MS.....	143
2.6 Human T cell isolation and culture	145
2.7 PEN photoporation for the delivery of FITC-dextran 150 kDa.....	145
2.8 Evaluation of FD150 delivery by flow cytometry and confocal microscopy.....	146
2.9 T cell activation after PEN photoporation of unstimulated T cells	147
2.10 Analysis of T cell phenotype after stimulation.....	147
2.11 Cytokine secretion analysis	147
2.12 Evaluation of cell viability with Cell Titer Glo assay	148
2.13 Cell counting with Trypan Blue	148
2.14 Statistical analysis	148
3 Results.....	149
3.1 Synthesis and characterization of PEN substrates.....	149
3.2 Intracellular delivery of FD150 in unstimulated vs. expanded T cells	154
3.3 Evaluation of T cell functionality after PEN treatment	159
4 Discussion	163
5 Conclusion	166
References	167
Supplementary Information	172

Abstract

Cell therapies such as adoptive T cell transfer require *ex vivo* modification of cells with exogenous cargo to modulate their phenotype (*e.g.*, to express a synthetic antigen receptor) for optimal therapeutic efficacy upon reinfusion in a patient. Several studies have shown superior anti-tumor activity of minimally differentiated T cell subsets over their activated counterparts. Therefore, developing techniques for safe and efficient manipulation of these quiescent cells is important for both clinical applications and fundamental studies of T cell biology. Photoporation with photothermal electrospun nanofibers (PEN) is an efficient and minimally perturbing non-viral intracellular delivery technique for activated and expanded T cells. However, the technique has not yet been applied to unstimulated T cells. Here, we investigated the potential of PEN photoporation for the delivery of macromolecules into these cells. First, we confirmed with inductively coupled plasma tandem mass spectrometry that there was no significant iron release from fibers after laser activation of PEN substrates for laser fluences up to 0.36 J cm^{-2} . Next, we demonstrated successful intracellular delivery of 150 kDa FITC-dextran as a model macromolecule in resting and pre-activated lymphocytes with 55-60% delivery efficiency. By analyzing metabolic activity, activation surface marker presentation and extracellular cytokine release, we found that PEN treatment had no effect on cell proliferation and a limited impact on T cell activation propensity for all tested irradiation energies. Thus, our findings show that PEN photoporation holds promise as a safe and efficient delivery strategy, paving the way for its use in the genetic modification of minimally differentiated T cells.

1 Introduction

Intracellular delivery of exogenous macromolecules has been instrumental for fundamental biological research and the development of novel therapeutics, with numerous applications, including precision gene editing, drug delivery, cell imaging/tracking, immunotherapy, and regenerative medicine ^{1,2}. Intracellular delivery can be achieved with carrier-mediated ^{3,4} and membrane-disruption-based approaches ^{5,6}. To date, viral vectors remain the most clinically advanced carrier-based option, offering highly efficient and specific transduction, such as for generating chimeric antigen receptor (CAR)-modified T cells for cancer therapy ^{7,8}. Nonetheless, challenges related to their potential immunogenicity, safety concerns over off-target effects, limited cargo capacity, and complex and expensive manufacturing processes have instigated the development of non-viral delivery methods ^{9–11}. Non-viral vectors, such as liposomes, cationic polymers, or inorganic nanoparticles are considered relatively safe but often suffer from unsatisfactory delivery efficiency, especially in primary and post-mitotic cells. When it comes to treating cells *in vitro* or *ex vivo*, membrane disruption-based technologies are considered more versatile as they are less dependent on the type of cargo and cell. They mostly use physical triggers (*e.g.*, mechanical ^{12,13}, electrical ^{14–16}, magnetic ¹⁷, optical, or thermal ^{18,19}) to transiently increase the permeability of the cell membrane, allowing external cargo to enter the cytosol.

Combining laser illumination with photo-responsive nanomaterials, photoporation has recently emerged as a potent membrane disruption-based delivery technology ^{20,21}. Typically, cells are first incubated with photothermal nanoparticles (NPs) to let them adsorb to the cell membrane. Upon (pulsed) laser irradiation, NPs efficiently convert light energy into thermal energy, producing distinct photothermal effects that induce local pore formation in the cell membrane ^{20,22}. Depending on the applied laser fluence, plasma membrane permeabilization can be achieved by photochemical reactions, local heating and mechanical forces ^{23–25}. The technology typically uses inorganic photosensitizers, including gold NPs ^{18,26–28}, iron oxide NPs (IONPs) ^{29,30}, carbon black NPs ^{31–33}, reduced graphene oxide ³⁴ and graphene quantum dots ³⁵. However, when it comes to clinical translation, direct exposure of engineered cells to poorly degradable inorganic NPs leads

to safety and regulatory concerns when the modified cells are to be used for treating patients. Despite the increasing presence of nanomaterials in biomedicine, their regulation remains hampered by a lack of standardized procedures to determine their safety^{36,37}.

To address these issues and pave the way for the use of photoporation in clinical applications, we have recently developed a new photothermal system where IONPs are embedded in polycaprolactone fiber meshes fabricated by electrospinning. Laser irradiation of cells present on a substrate of photothermal electrospun nanofibers (PEN) allows efficiently permeabilizing cells to deliver an exogenous cargo. After photoporation, cells can be conveniently collected from the PEN substrate while sensitizing NPs remain safely embedded within the nanofibers, thus ensuring a final cell product that is nanoparticle-free³⁸. PEN photoporation proved successful in delivering model molecules of up to 500 kDa in cell lines, and effector molecules such as CRISPR-Cas9 ribonucleoprotein complexes in human embryonic stem cells and expanded T cells³⁸. Importantly, contrary to electroporation, PEN photoporation was demonstrated to have minimal impact on cell homeostasis and functionality. For instance, when applied to expanded T cells, PEN photoporation did not affect cell proliferation, expression of exhaustion markers, or cytokine release. Consequently, CAR T cells exposed to photoporation had a significantly higher cytolytic potential than electroporated CAR T cells.

In the present work, we extended our investigation on PEN photoporation to deliver cargo molecules in highly challenging unstimulated T lymphocytes, which has been explored only in a limited number of publications^{39–41}. Compared to their stimulated counterparts, resting T cells are smaller in size, non-dividing and display lower metabolic rates maintained mainly through oxidative phosphorylation rather than glycolysis^{42,43}. Unstimulated T cells are generally less susceptible to genetic manipulation than pre-activated cells. Among several factors, this is attributed to a reduced membrane fluidity, which restricts the penetration of carrier-based transfection reagents⁴⁴. Moreover, low expression of surface receptors involved in endocytosis may limit the efficiency of viral and non-viral carrier-based methods. Not surprisingly, T cell activation has, therefore, been a standard prerequisite for T cell engineering for immunotherapies. However,

lymphocyte activation triggers their differentiation program, with prolonged *ex vivo* culture resulting in an exhausted phenotype^{45,46}. Several studies have demonstrated superior anti-tumor activity of less differentiated T cell subsets, thus, there is increasing interest in protocols that can retain such naïve and memory phenotypes^{47–55}.

Here, we hypothesized that PEN photoporation, being a physical delivery method, may overcome the previously described difficulties of carrier-based approaches for delivering cargo in unstimulated T cells. We first optimized PEN photoporation parameters (IONP concentration and laser fluence) resulting in optimal intracellular delivery of FITC-dextran 150 kDa as a model macromolecule in unstimulated T cells. In addition, we investigated to which extent embedded IONPs are released from the nanofibers upon laser stimulation. Next, we studied the functional consequences of applying different irradiation settings by investigating the proliferation potential and propensity of unstimulated T cells to activation after PEN photoporation by analyzing surface activation marker expression and cytokine production.

2 Materials and methods

2.1 Fabrication of photothermal nanofibers by electrospinning

Poly- ϵ -caprolactone (PCL, $M_W \approx 80,000 \text{ g mol}^{-1}$), N, N-Dimethylformamide (DMF), tetrahydrofuran (THF, reagent grade, stabilized with 0.025% BHT inhibitor) and iron oxide (II, III) nanopowder (#637106, 50-100 nm particle size) were purchased from Sigma-Aldrich (Belgium). 15 wt% PCL solutions doped with 0-10 wt% iron oxide nanoparticles (IONPs) were prepared by dispersing PCL pellets and iron oxide nanopowder in a 1:1 mixture of DMF and THF and magnetic stirring overnight. Directly before the electrospinning, the solution was sonicated in an ultrasonic bath (Branson Ultrasonics™, Thermo Fisher Scientific) for 1 hour at RT. The electrospinning was performed using a Fluidnatek® LE-50 electrospinning/ electro spraying machine equipped with a drying heating unit (Bioinicia S.L., Paterna, Spain) to control the temperature and relative humidity within the electrospinning chamber. Fibers were collected on microscope glass slides (#1000912, Marienfeld) mounted on a rotating drum collector (diameter 100 mm) with an injector-to-collector distance of 12 cm. Solution flow rate was set to 1.5 mL/h, voltage applied on the injector was 8 kV and the collector was polarized with -2 kV. The emitter was operated with lateral movement of 50 mm/s within a range of 200 mm, whereas the rotation speed of the collector was 200 rpm. The temperature and relative humidity in the electrospinning chamber were adjusted to 26°C and 30%, respectively. Nanofiber collection was terminated after 30 min.

2.2 Preparation of PEN substrates for suspension cells

PEN wells were created using eight-well Press-to-Seal™ Silicone Isolators with Adhesive, 9 mm diameter, 1.0 mm deep (P24744, Thermo Fisher). After removing the protective sealing, spacers were gently stuck on the nanofiber mesh and samples were immersed in DI water for 3 min to easily remove nanofibers from the glass slide (**Figure S1-1**). Next, samples were dried and turned upside down with silicone spacers facing down and fibers facing up (**Figure S1-2**). Round high-precision cover glasses (#0117500, thickness No. 1.5H, 10 mm diameter, Marienfeld) were placed on top of each well (**Figure S1-3**) and finally secured in place with an adhesive seal (#AB0580, Thermo Fisher) (**Figure S1-4**). Next, samples were manually cut into smaller pieces so that they can be placed in wells of *e.g.*

a 24-well plate (**Figure S1-5**). These home-made PEN wells were sterilized by UV irradiation for 45 min in a laminar flow cabinet before being used for cell culture. Finally, to make the nanofiber surface more hydrophilic and facilitate uniform spreading of the cell suspension over the entire PEN well area, substrates were hydrated by immersion in sterile 0.1 M NaOH overnight at 4 °C. After incubation, samples were rinsed and stored in DPBS until further use in cell experiments.

2.3 Electron microscopy

SEM images were acquired with an FEI Quanta 200F microscope (Thermo Fisher) at 20 kV using an EDT detector under a high vacuum. The average fiber diameter of each sample was quantified from the SEM images using ImageJ (FIJI) software⁵⁶ by measuring fibers at 100 random positions.

2.4 Dark and bright field microscopy for detection of vapor nanobubbles

For the generation and detection of VNBs, an in-house developed setup equipped with a 3 ns pulsed 532 nm laser (Cobolt Tor™ Series, Cobolt AB, Solna, Sweden) and a galvano scanner (Thorlabs, GVS002-2D Galvo System), enabling irradiation in high throughput, was used to illuminate PEN wells covered with a drop of DI water. The galvo scanner scans the laser beam (approx. 50 μm diameter at the sample) across the nanofiber surface such that each location essentially receives a single laser pulse (with some overlap between adjacent pulses). The formation of water vapor nanobubbles (VNBs) was visualized for increasing laser pulse fluences using dark field microscopy (Nikon, C-DD Dark Field Condenser Dry), where the increased scattered light of VNBs resulted in bright white spots on a black background. Afterwards, bright field images of irradiated PEN substrates were recorded using a Nikon A1R HD confocal laser scanning microscope (Nikon Benelux, Belgium) with a 10x lens (plan apo 10X, NA 0.45). For the quantification of VNB, image analysis was performed as previously reported by Houthaeye *et al.*⁵⁷

2.5 Quantification of Fe release by ICP-MS/MS

Potential release of IONPs from nanofibers upon laser irradiation was determined by inductively coupled plasma-tandem mass spectrometry (ICP-MS/MS)⁵⁸. For ICP-MS/MS analysis, only high-purity reagents were used. Purified water (resistivity 18.2 MΩ cm) was

obtained from a Milli-Q Element water purification system (Millipore, France). Pro-analysis purity level 14 M HNO₃ (Chem-Lab, Belgium) further purified by sub-boiling distillation and ultra-pure 9.8 M H₂O₂ (Sigma Aldrich, Belgium) were chosen for sample digestion. Appropriate dilutions of 1 g L⁻¹ single element standard solutions (Inorganic Ventures, USA) were used for method development, optimization, and calibration purposes. For quantitative element determination, external calibration was relied on (0, 1, 2.5, 5, 10 and 20 µg L⁻¹ Fe), with Ga as the internal standard (5 µg L⁻¹).

Samples were prepared by adding Milli-Q water to the PEN substrates (50 µL per well), performing laser irradiation at increasing laser pulse fluences, and collecting the Milli-Q water into metal-free tubes (VWR, Belgium) after laser irradiation. To estimate the maximal amount of Fe that could be potentially released, intact nanofiber substrates (corresponding to the area of a single PEN well) were included as positive controls. Next, samples were digested *via* acid digestion in Teflon Savillex beakers, pre-cleaned with HNO₃ and HCl and rinsed with Milli-Q water. A mixture of 1 mL of 14 M HNO₃ and 0.5 mL of 9.8 M H₂O₂ was added to each sample and the procedure was completed after heating at 110 °C on a hot plate for approx. 18 h. The samples were evaporated until dryness and re-dissolved in 2 mL of 0.35 M HNO₃. Prior to ICP-MS/MS analysis, the samples were 1.25-, 10-, 100- and 1000- fold diluted with 0.35 M HNO₃.

(Ultra-)trace element determination of Fe was carried out using an Agilent 8800 ICP-MS/MS instrument (ICP-QQQ, Agilent Technologies, Japan). The sample introduction system comprises a concentric nebulizer (400 µL min⁻¹) mounted onto a Peltier-cooled (2 °C) Scott-type spray chamber. This instrument is equipped with a tandem mass spectrometry configuration consisting of two quadrupole units (Q1 and Q2) and a collision-reaction cell (CRC) located in-between both quadrupole mass filters (Q1-CRC-Q2). The MS/MS mode provides additional means to deal with spectral overlap in a more straightforward way compared to traditional single-quadrupole ICP-MS instrumentation. In this work, the CRC was pressurized with a mixture of NH₃/He (10% NH₃ in He) to overcome spectral interferences seriously hampering (ultra-)trace element determination of Fe, *e.g.*, overlap between the signals of polyatomic interferences, such as ⁴⁰ArO⁺ and ⁴⁰CaO⁺, and ⁵⁶Fe⁺ ions (mass-to-charge – m/z – 56 amu). The introduction of 3 mL min⁻¹ of NH₃/He allows the conversion of ⁵⁶Fe⁺ ions into ⁵⁶Fe(NH₃)₂⁺ reaction product ions that can

be detected free from spectral interferences at a different m/z ratio (90 amu). This approach is often referred to as mass-shift and relies on the adequate selection of the best-suited reaction product ion formed upon reaction between the analyte ion and the reaction gas by using the product ion scanning tool. To correct for instrument instability, signal drift and matrix effects, $^{71}\text{Ga}^+$ was monitored on-mass. A methodological quantification limit of $2.50 \mu\text{g L}^{-1}$ was calculated as 10 times the standard deviation of 10 measurements of a blank solution divided by the slope of the calibration curve.

2.6 Human T cell isolation and culture

Healthy donor buffy coats were obtained from the Red Cross Flanders Biobank (Ghent, Belgium) after informed consent and approval, and used following the guidelines of the Medical Ethical Committee of Ghent University Hospital (Ghent, Belgium). Peripheral blood mononuclear cells (PBMCs) were isolated *via* density gradient centrifugation with Lymphoprep (Stem Cell Technologies, Vancouver, Canada). Next, CD3-positive T cells were separated by a magnetic negative selection using the EasySep Human T cell enrichment Kit (Stem Cell Technologies, Vancouver, Canada) according to the manufacturer's instructions. Unstimulated cells were maintained in Iscove's modified Dulbecco's medium (IMDM) GlutaMAX (Gibco, Merelbeke, Belgium), supplemented with 10% heat-inactivated fetal bovine serum (FBS, Biowest), 100 U/mL penicillin and 100 $\mu\text{g/mL}$ streptomycin (P/S, Gibco, Merelbeke, Belgium) and treated by PEN photoporation on the day of isolation. To obtain stimulated T cells, T cells were stimulated with ImmunoCult Human CD3/CD28 T cell Activator (Stem Cell Technologies, Vancouver, Canada) according to the manufacturer's protocol. Activated cells were cultured in the presence of 10 ng/mL IL-2 (PeproTech, United Kingdom) for 7 days before PEN photoporation treatment.

2.7 PEN photoporation for the delivery of FITC-dextran 150 kDa

FITC-dextran of 150 kDa (FD150, Sigma-Aldrich, Bornem, Belgium) was used as a model macromolecule for measuring delivery efficiency and optimizing PEN photoporation parameters. FD150 delivery was performed in either unstimulated or activated and expanded human T cells. The cells were first washed three times by centrifugation (300xg, 5 min) with Opti-MEM to remove any residual cell culture medium with FBS. After the

final washing step, cells were resuspended in Opti-MEM at a density of 1×10^6 cells per 25 μL . Next, the cell suspension was mixed 1:1 with 2 mg/mL FD150 dilution in Opti-MEM (final concentration: 1 mg/mL) and a total of 50 μL (*i.e.*, 1×10^6 cells) was used per single PEN well. Cells were allowed to sediment on the fiber mesh for 5 min before starting the laser treatment.

Photoporation was then performed with an in-house developed setup with a nanosecond laser (3 ns pulse duration, 532 nm wavelength) and equipped with a galvano scanner. For some experiments, cells were repeatedly irradiated, in which case cells were resuspended within the PEN well between each laser scan to reposition cells across the nanofiber surface. Once laser treatment was completed, cells were collected into Eppendorf tubes and PEN substrates were washed twice with PBS to recover any remaining cells. Finally, cells were washed three times by centrifugation (300xg, 5 min), resuspended in fresh culture medium, and incubated at 37°C, 5% CO₂, until further analysis.

2.8 Evaluation of FD150 delivery by flow cytometry and confocal microscopy

To evaluate the delivery efficiency of FD150 (*i.e.*, the percentage of FITC-positive cells), T cells were washed once with DPBS⁻ (300xg, 5 min) and resuspended in flow buffer (DPBS⁻, 1% bovine serum albumin, 0.1% sodium azide) with TO-PRO3 iodide (Invitrogen, Belgium) as cell viability indicator. Flow cytometry was performed using a MACSQuant Analyzer 16 (Miltenyi Biotec, Germany) and analysis was based on a minimum of 30 000 cells per sample. FITC and TO-PRO-3/ APC were excited by 488 and 640 nm lasers and detected with 525/50 and 655-730 nm filters, respectively. FlowJo™ software (Treestar Inc.) was used for data analysis. FD150-positive cells were gated on singlet living (TO-PRO-3-negative) cells and the mean fluorescence intensity (MFI) of each sample was expressed relative to cells that were incubated with FD150 without laser irradiation (CTR).

FD150 uptake was additionally confirmed by confocal microscopy. T cells were stained with Hoechst 33342 (Invitrogen, Belgium) and visualized with a Nikon A1R HD confocal laser scanning microscope (Nikon Benelux, Belgium) with a 40x objective lens (plan apo λ 40X, NA 0.9, WD 250 μm). Hoechst and FD150 were excited sequentially with 408 nm and 488 nm laser lines and detected with 450/50 and 525/50 nm emission filters, respectively. ImageJ (FIJI) software was used to process the images ⁵⁶.

2.9 T cell activation after PEN photoporation of unstimulated T cells

To evaluate to which extent quiescent T cells preserve their activation propensity after being treated with PEN photoporation, unstimulated T cells were laser irradiated after collection on a 1 wt% IONP substrate as described before, but in the absence of cargo molecules. This allows assessing the impact of the photoporation treatment alone, excluding potential confounding effects of cargo molecules. After laser treatment, the cells were rested overnight at 37°C, 5% CO₂. The next day, cells were seeded at a density of 1x10⁶/mL in 24-well plates in complete IMDM supplemented with 10 ng/mL IL-2 and stimulated with ImmunoCult Human CD3/CD28 T cell Activator (Stem Cell Technologies, Vancouver, Canada) according to the manufacturer's protocol. Cultures were split and supplemented with fresh medium on day 3, day 5 and day 7. Unstimulated cells maintained in a plain culture medium without activating agents were preserved as a control condition.

2.10 Analysis of T cell phenotype after stimulation

To analyze the activation status of T cells pre-treated by PEN photoporation and stimulated with ImmunoCult Activator for 48 h, the following anti-human monoclonal antibodies were used: CD25 FITC, CD69 FITC, CD154 FITC, CD137 PE, HLA-DR PerCP/Cy5, PD-1 FITC (all from BioLegend, USA) and PD-1 PE (Miltenyi Biotec, Germany). Briefly, cells were washed with DPBS, resuspended in flow buffer and incubated with the indicated antibodies for 30 min at 4°C. LIVE/DEAD™ Fixable Aqua Stain (Invitrogen, Belgium) or TO-PRO-3 iodide (Invitrogen, Belgium) stainings were used to distinguish between live and dead cell populations. After two washing steps, samples were analyzed with a MACSQuant Analyzer 16 (Miltenyi Biotec, Germany), and FlowJo software (Treestar Inc.) was used for data analysis.

2.11 Cytokine secretion analysis

Cell culture supernatants were collected after 24 and 48 h of T cell stimulation and stored at -80°C. Secretion of several cytokines, including IL-5, IL-6, IL-9, IL-10, IL-13, IL-17A, IL-22, IFN-γ and TNF-α was quantified using a multiplex bead assay (LEGENDplex™, BioLegend, Belgium), according to the manufacturer's protocol. Samples were measured using a

CytoFlex (Beckman Coulter, Suarlée, Belgium) flow cytometer and the LEGENDplex™ Data Analysis Software was used for data analysis.

2.12 Evaluation of cell viability with Cell Titer Glo assay

The CellTiter Glo® luminescent cell viability assay (G7571, Promega, Belgium), which is based on the quantitation of the cell's ATP content, was used to evaluate cell viability after PEN photoporation or to monitor growth rates of T cells stimulated after PEN photoporation. Briefly, T cells in complete culture medium were supplemented with an equal volume of CellTiter Glo® reagent and shaken on an orbital shaker (120 rpm) for 10 min at room temperature. Next, cell lysates were transferred to an opaque 96-well plate and the luminescent signal was measured using a GloMax® microplate reader (Promega, Belgium).

The cell viability readout was multiplied with the FD150 delivery efficiency analyzed by flow cytometry (gated on living cells) to estimate the overall delivery yield, which is the percentage of viable and successfully transfected cells compared to the initial number of cells.

2.13 Cell counting with Trypan Blue

To assess cell viability and proliferation of T cells stimulated after the PEN photoporation, cells were counted manually using a Bürker counting chamber (Brand GMBH, Germany) with trypan blue exclusion staining (0.4%, Sigma-Aldrich, Belgium). Cell number changes were normalized to the starting seeding density and corrected for culture dilutions at each time point.

2.14 Statistical analysis

All data are shown as mean \pm standard deviation (SD). Statistical differences were analyzed using GraphPad Prism 8 software (La Jolla, USA). Two-way ANOVA with Tukey's multiple comparisons test was used to compare maximal FD150 delivery yields achieved with PEN substrates with varying IONP wt% and different laser pulse fluences, and to analyze T cell proliferation rates, expression of surface activation markers and cytokine production. Statistical differences with a p value <0.05 were considered significant.

3 Results

3.1 Synthesis and characterization of PEN substrates

Photothermal nanofibers were fabricated by electrospinning of poly- ϵ -caprolactone solutions doped with various weight percentages of IONPs, as reported previously⁵⁹. Home-made cell culture wells were prepared with a nanofiber mesh positioned at the bottom so that cells would sediment on the nanofiber mesh when added to the well. Using scanning electron microscopy (SEM), we confirmed the presence of IONPs within the nanofibers (**Figure 1A**), with increasing IONP density for substrates with a higher weight percentage of IONPs. After applying a gold coating to the nanofibers for enhanced SEM contrast, we quantified the nanofiber diameter, which ranged from 0.5 μm to 2.5 μm , irrespective of the IONP concentration (**Figure 1B-C**).

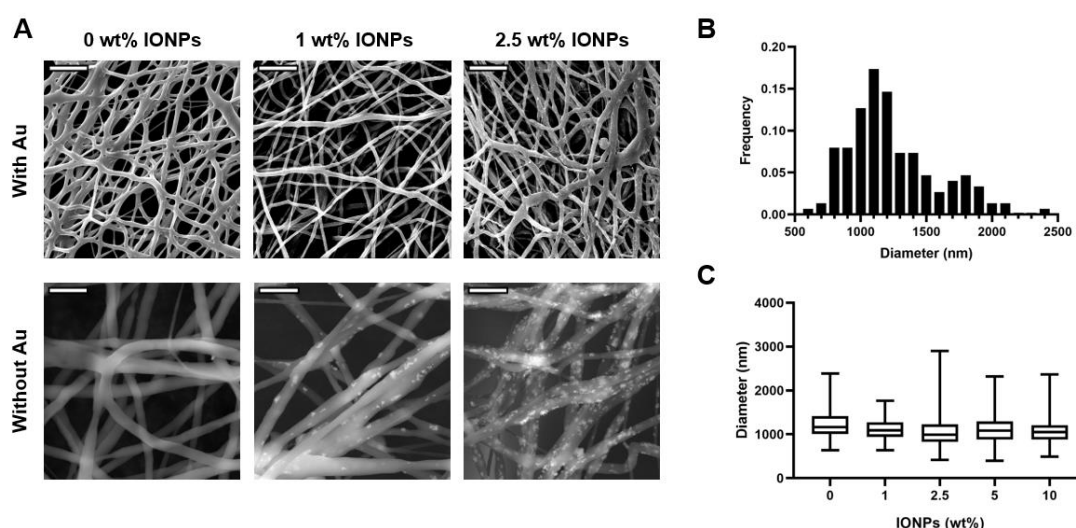


Figure 1. Characterization of photothermal electrospun nanofibers. (A) SEM images of nanofiber meshes containing 0, 1 and 2.5 % IONPs, recorded with or without gold coating. Scale bars correspond to 20 μm (top images) and 5 μm (bottom images). (B) Histogram of nanofiber diameter without IONPs as derived from the SEM images of gold coated nanofibers. (C) Average nanofiber diameter for increasing concentrations of IONPs. Box plots with whiskers ranging from minimum to maximum.

To validate the nanofibers' photothermal properties, we next determined water vapor nanobubble (VNB) formation for increasing laser pulse fluences using dark field microscopy. We detected VNBs in PEN substrates with 1% IONP starting from laser pulse

fluences of 0.36 J cm^{-2} (**Figure 2**). Interestingly, image analysis revealed that increasing the fluence to 0.50 J cm^{-2} resulted in less numerous but larger bubbles (**Figure 2C**). When inspecting the nanofiber meshes after laser irradiation with brightfield microscopy, stable (at least up to 3 h) micrometer-sized bubbles could still be seen, which likely stem from the coalescence of the original VNBs. For higher IONP concentrations of 5 to 10 wt%, single VNBs were already detected from a laser pulse fluence of 0.10 J cm^{-2} , which became more numerous and prominent at a fluence of 0.28 J cm^{-2} (**Figure 3**), again leading to stable micro-meter bubbles (**Figure S2**). Nanofiber irradiation with 0.28 J cm^{-2} also showed that bubbles became less numerous for increasing IONP content but larger or more heterogenous in size (**Figure 3B**).

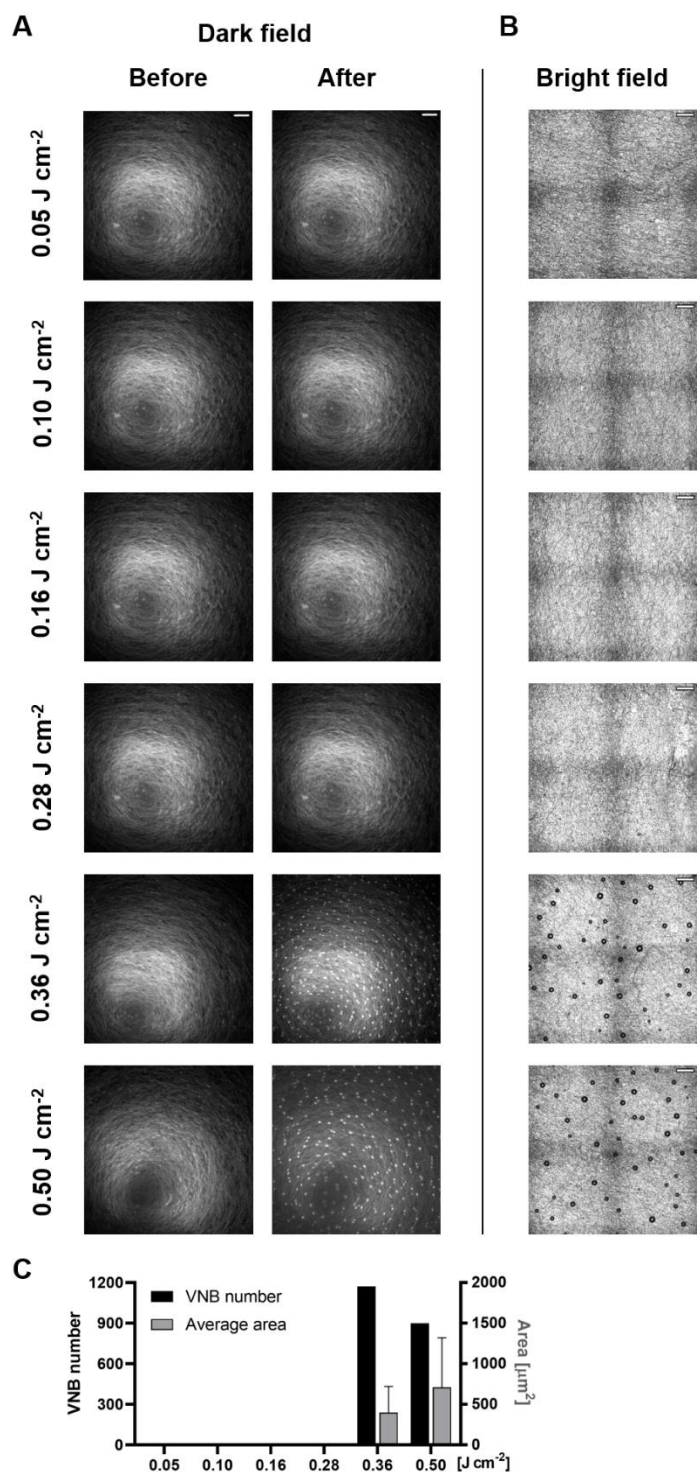


Figure 2. Visualization of vapor (nano)bubble generation on substrates with 1 wt% IONPs. (A) Dark field images of PEN substrates with 1 wt% IONPs before and immediately after irradiation with a laser pulse of increasing fluence. Water vapor nanobubbles are visible starting from a laser fluence of 0.36 J cm⁻². Scale bar 200 μm. (B) Bright field images of PEN surfaces, showing stable microbubbles after irradiation for laser pulse fluences above 0.36 J cm⁻². Scale bar 200 μm. (C) Quantification of VNB number and average area (μm²) as derived from the dark field images.

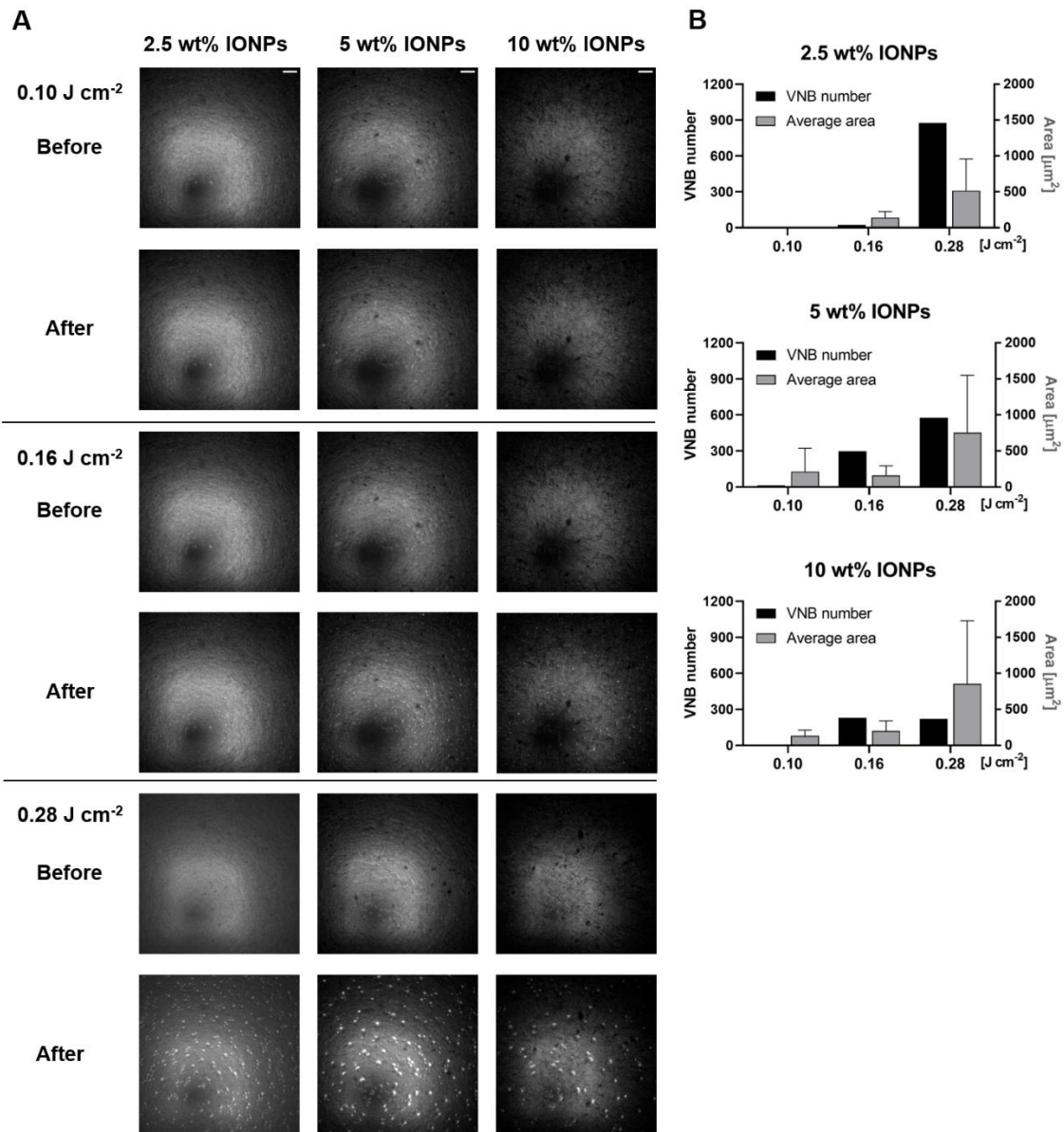


Figure 3. Visualization of vapor (nano)bubble generation. (A) Dark field images of PEN substrates containing 2.5, 5 and 10 wt% IONPs before and immediately after irradiation with a laser pulse of increasing fluence. Scale bar 200 μm. (B) Quantification of VNB number and average area (μm²) as derived from the dark field images.

While VNBs are often considered beneficial in traditional nanoparticle-mediated photoporation with suspended NPs, their high energy may have disadvantages for PEN photoporation as it could damage the nanofibers and trigger the release of the embedded IONPs. Therefore, we next analyzed potential iron release from the PEN substrates by ICP-MS/MS using a 32x improved quantification limit of 0.0025 mg L⁻¹ as compared to our

previous work⁵⁹ (**Figure 4**). As positive controls, nanofiber meshes corresponding to the area of a PEN well were subjected to acid digestion to release all embedded IONPs. As a negative control, (laser-irradiated) PEN substrates without IONPs were used. The iron content in water collected from the nonirradiated controls and PEN substrates without IONPs remained below the limit of quantification (LoQ). Thus, to determine which laser pulse fluences resulted in potentially significant iron release, we used a one-sample t-test to compare the results to the LoQ. A small amount of iron was systematically found in the nanofiber samples with 2.5% to 10% IONPs irradiated with high laser pulse fluences of 0.36 J cm⁻² and 1.56 J cm⁻². Iron release was significant for 2.5% and 10% IONPs, but not for 5% IONPs due to a higher variability of the individual measurement points. Note that, even at the highest laser fluence (~10× higher than the fluence for which VNB generation was first observed for these IONP wt%) only a limited percentage of the total IONP content was released. In contrast, for PEN substrates with 1% IONPs, no significant iron release was observed irrespective of the laser pulse intensity. This correlates with our finding that larger bubbles are formed for nanofibers with higher IONP content, which may be more damaging to the nanofibers. Thus, we conclude that IONP release can be avoided from PEN substrates with 1% IONPs upon laser irradiation with fluences up to 1.56 J cm⁻², which is the highest setting available on our photoporation setup.

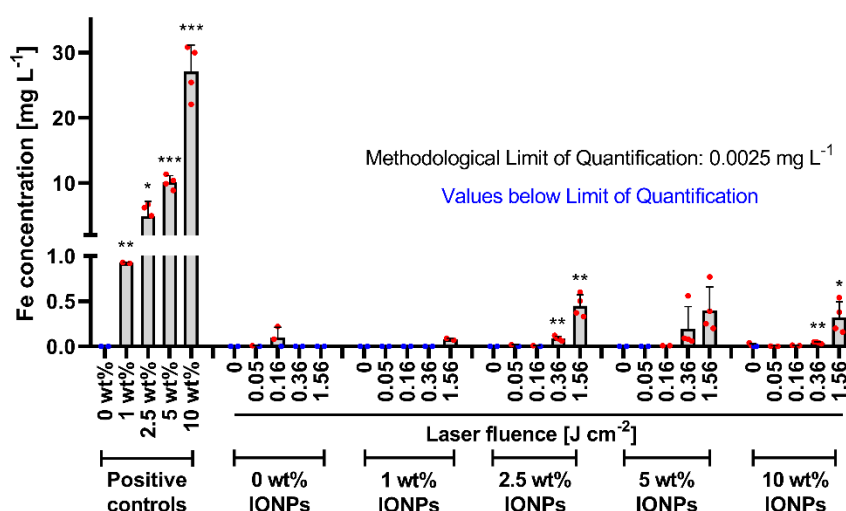


Figure 4. Analysis of potential IONP leakage from laser-activated PEN substrates by ICP-MS/MS. The iron concentration was measured in DI water collected from PEN substrates (with 0-10 wt% IONPs) after laser irradiation with the indicated laser pulse fluences. Nanofibers digested in acid

are included as positive controls. One sample t-test was used to determine whether the measured mean Fe concentration was statistically different from the LoQ of 0.0025 mg L⁻¹ (* p < 0.05; ** p < 0.01; *** p < 0.001; **** p < 0.0001).

3.2 Intracellular delivery of FD150 in unstimulated vs. expanded T cells

To test the applicability of PEN photoporation for the intracellular delivery of macromolecules in unstimulated human T cells, we used FITC-dextran with a molecular weight of 150 kDa (FD150) as a model molecule. We chose this size as it is in the range of therapeutically relevant proteins such as genome-editing nucleases. Cells were applied to homemade PEN wells with increasing IONP content and irradiated a single time with a range of laser pulse fluences up to 0.50 J cm⁻² (**Figure 5** and **Figure S3**). In addition, repeated laser irradiation (2x, 3x, 4x) was tested for a low fluence of 0.10 J cm⁻² at which no IONPs are released. In the latter case, cells were resuspended in PEN wells between each laser scan to allow a random repositioning of cells for each irradiation step. The delivery efficiency (= the percentage of FD150-positive cells gated on singlet viable cells) was quantified by flow cytometry (**Figure 5A-H**). Irrespective of the IONP content, the delivery efficiency increased with laser fluence, reaching ~55-60% for the highest tested fluence (**Figure 5A-D**). Confocal microscopy images visually confirmed that more cells became FD150-positive as laser fluence increased (**Figure 5I**). Also, the amount of FD150 per cell increased with laser fluence, here expressed as the relative mean fluorescence intensity (rMFI) compared to cells that were incubated with FD150 without laser irradiation (**Figure S4**). However, higher delivery efficiencies were accompanied by comparable decreases in cell viability, resulting in a maximal delivery yield (*i.e.*, the percentage of living FD150-positive cells compared to the initial cell population) of around 30%. For instance, for T cells photoporated on fibers with 1 wt% IONPs, the maximal delivery yield was obtained for irradiation with 0.28 J cm⁻², after which no further improvement could be achieved by increasing the laser fluence (**Figure 5E**). For the same reason, repeated photoporation at a fluence of 0.10 J cm⁻² could not increase the delivery yield further. Finally, delivery yields were not statistically different between PEN substrates with different IONP content for a given fluence. No enhanced delivery or cytotoxicity was observed when cells were irradiated on PEN substrates without photo-responsive IONPs (**Figure S3**). Independently of the applied laser fluence, the percentages

of FD150+ cells remained comparable to the controls incubated with FD150 without laser irradiation.

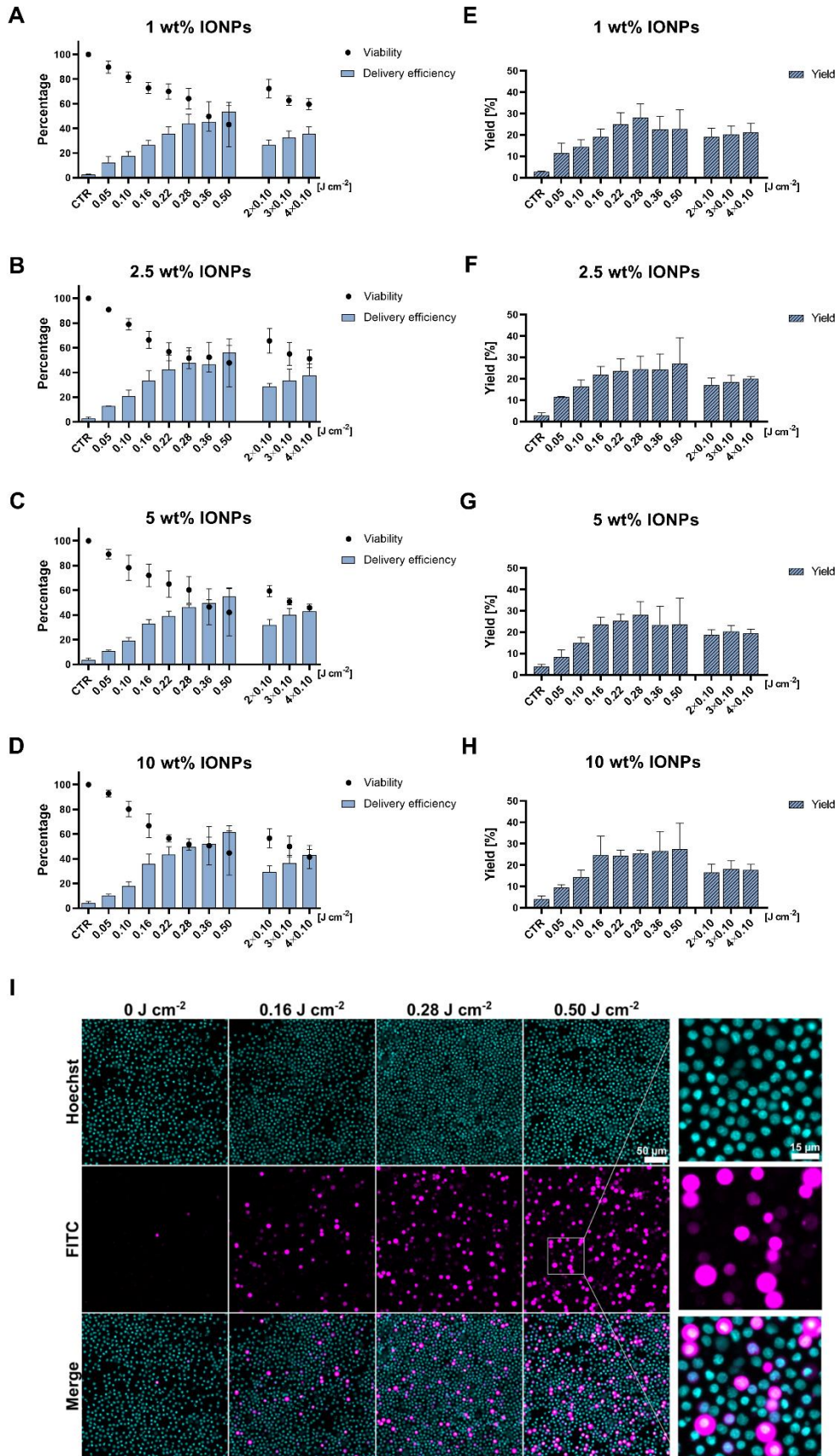


Figure 5. Intracellular delivery of FD150 in unstimulated human T cells by PEN photoporation. FD150 was delivered in unstimulated T cells by PEN photoporation. T cells were applied to PEN substrates with increasing IONP content and irradiated with the indicated laser fluences. All samples were irradiated one time, except for samples irradiated with a laser pulse fluence of 0.10 J cm^{-2} which were subsequently irradiated up to 4 \times . Cells incubated with FD without applying laser irradiation (CTR) served as a control for any spontaneous uptake. (A-D) Delivery efficiency of FD150 (bars) was measured by flow cytometry (gated on viable cells) and cell viability (dots) was determined by a Cell Titer Glo assay. (E-H) Delivery yield was calculated by multiplying the delivery efficiency (flow cytometry) and cell viability (Cell Titer Glo), representing the percentage of viable and transfected cells compared to the initial cell population. Data represent the mean \pm SD of at least four different donors tested per each IONP wt%. (I) Confocal microscopy images of T cells photoporated on PEN substrates with 1 wt% IONPs. Signals from the nuclear staining with Hoechst 33342 and FITC channel are color-coded in cyan and magenta, respectively. The scale bar represents $50 \mu\text{m}$.

To compare the delivery efficiency of PEN photoporation in unstimulated T cells, we performed an analogous evaluation on stimulated T cells. Lymphocytes were activated with anti-CD3 and anti-CD28 antibodies and expanded in the presence of IL-2 before PEN photoporation on day 7. Overall, while similar trends were found as for unstimulated T cells, some differences were seen. First, cell viability decreased more rapidly for increasing laser fluences as for unstimulated T cells (**Figure 6A-D**). As delivery efficiency was comparable, this resulted in overall lower delivery yields (**Figure 6E-H**). Also, the amount of FD150 per cell was markedly lower for stimulated compared to unstimulated T cells (**Figure S5**). Second, repeating photoporation a second time (0.1 J cm^{-2}) now resulted in a significant increase in delivery yield for PEN substrates with 2.5 wt% ($p < 0.0001$), 1 wt% ($p < 0.001$) and 10 wt% ($p < 0.05$) IONPs, even outperforming a single treatment with higher laser fluences. However, repeating PEN photoporation a 3rd and 4th time did not result in a significant further improvement in delivery yield. Overall, the most optimal delivery yields in stimulated T cells were obtained using fibers with 2.5 wt% IONPs irradiated two times with a laser fluence of 0.10 J cm^{-2} . This finding was qualitatively supported by confocal microscopy (**Figure 6I**).

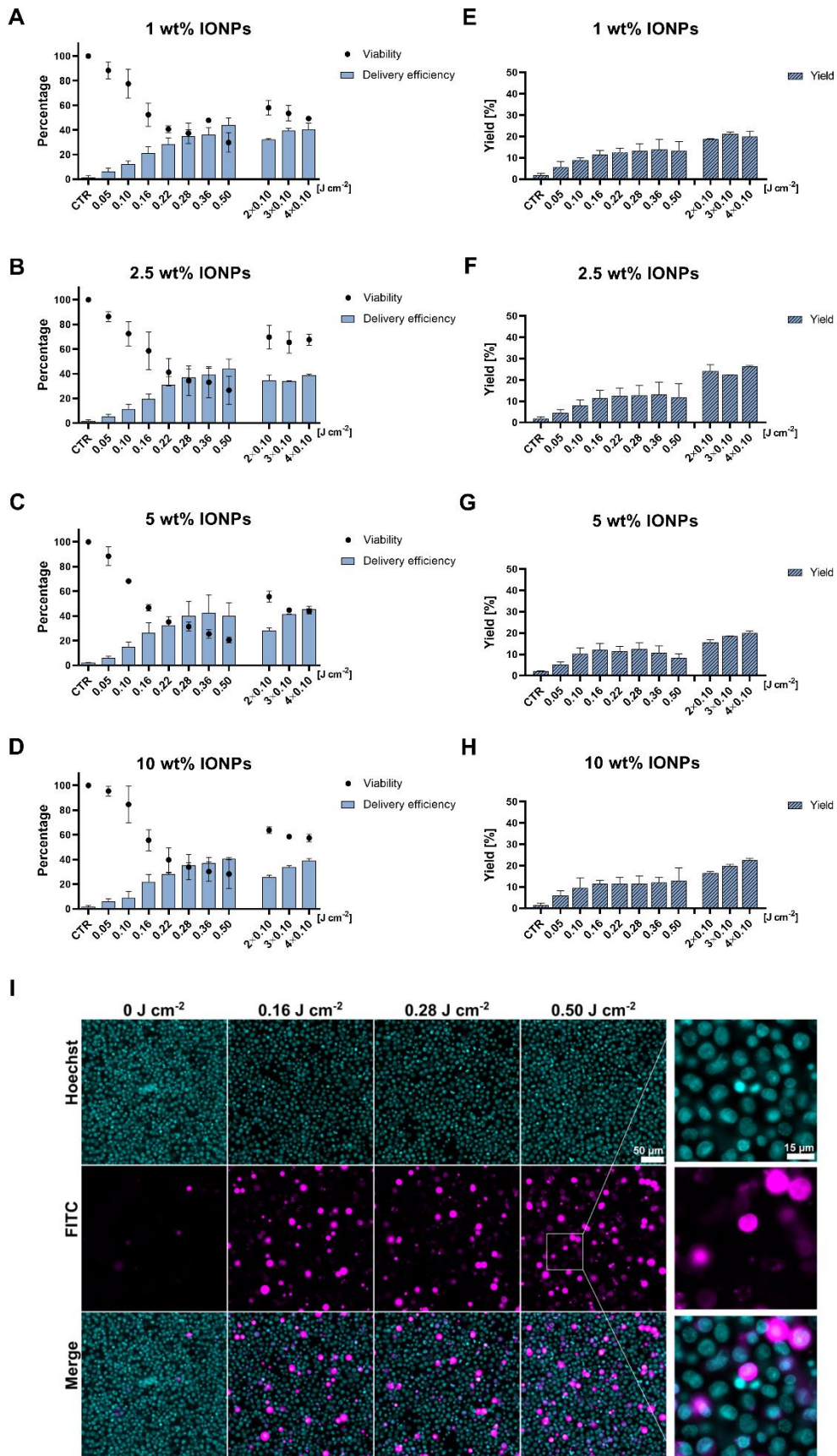


Figure 6. Intracellular delivery of FD150 in expanded human T cells by PEN photoporation. T cells were stimulated with ImmunoCult CD3/CD28 Activator and cultured for 7 days before applying PEN photoporation. All samples were irradiated one time, except for samples irradiated with a laser pulse fluence of 0.10 J cm^{-2} which were subsequently irradiated up to 4×. Cells incubated with FD150 without applying laser irradiation (CTR) served as a control for any spontaneous uptake. (A-D) Delivery efficiency of FD150 (bars) was measured by flow cytometry (gated on viable cells) and cell viability (dots) was determined by a Cell Titer Glo assay. (E-H) Delivery yield was calculated by multiplying the delivery efficiency (flow cytometry) and cell viability (Cell Titer Glo), representing the percentage of viable and transfected cells compared to the initial cell population. Data represent the mean \pm SD of at least four different donors tested per each IONP wt%. (I) Confocal microscopy images of T cells photoporated on PEN substrates with 1 wt% IONPs. Signals from the nuclear staining with Hoechst 33342 and FITC channel are color-coded in cyan and magenta, respectively. The scale bar represents 50 μm .

3.3 Evaluation of T cell functionality after PEN treatment

Apart from delivery yield, retention of T cell fitness is arguably an even more critical determinant for selecting a transfection method. Therefore, we investigated the activation potential of unstimulated T cells after PEN photoporation. Since we did not observe any significant impact of IONP content on the delivery yields for unstimulated T cells, we opted to continue working with PEN substrates with 1 wt% IONPs. Furthermore, considering that ICP-MS showed a limited IONP release above 0.36 J cm^{-2} , laser irradiation was further limited to fluences up to 0.28 J cm^{-2} . To unambiguously investigate the effects by PEN photoporation, unstimulated T cells were treated in the absence of cargo and rested overnight. The following day, cell densities were equalized between all experimental groups to compensate for potential cell loss and ensure a uniform stimulation protocol. T cell activation status was then assessed by analysis of activation marker expression, cytokine production and proliferation.

We first focused on the short-term effects of PEN photoporation on the T cell phenotype. A panel of well-established plasma membrane markers that become upregulated in response to T cell activation comprised both early activation markers, such as CD69, CD25 and CD154, and molecules appearing at late stages of activation, like CD137 or HLA-DR, as well as a checkpoint receptor PD-1 (**Figure 7A**). After 48h, these molecules were significantly upregulated in all experimental groups stimulated with anti-CD3/CD28 antibodies, compared to the unstimulated control ($p < 0.0001$). Importantly, no significant

differences in expression profiles of untreated and PEN-photoporation-treated cells were found, irrespective of the applied laser fluence, confirming that photoporation does not negatively affect the activation potential of unstimulated T cells.

Next, we validated the effects of PEN photoporation on the production of inflammatory cytokines after 24 and 48 h of stimulation (**Figure 7B**). For most anti-inflammatory (IL-10, IL-13) and pro-inflammatory (TNF- α , IL-5) cytokines, no significant alterations were found compared to untreated T cells. A significantly diminished secretion of proinflammatory IL-6 and IL-17A was observed in all PEN-treated groups, independent of the irradiation settings. IL-9 levels were significantly reduced after 24 h for the higher laser fluences, but recovered to the control levels after 48h, except for the highest fluence of 0.28 J cm⁻². IFN- γ production was significantly reduced for the highest laser fluence after 24 h, which was resolved after 48h. Also, for IL-22 two irradiated samples had a significant reduction after 24 h, but this again restored to baseline levels as observed for the untreated group after 48 h.

Finally, we evaluated cell proliferation as another hallmark of activation, critical for mounting an effective immune response. T cell expansion was monitored for up to 10 days by manual cell counting and ATP quantification with a Cell Titer Glo assay (**Figure 7C-D**). PEN photoporated T cells displayed similar growth kinetics to untreated cells, independently of the applied laser settings (**Figure 7C**). Likewise, the ATP levels of all experimental groups remained comparable throughout the culture period (**Figure 7D**). Hence, despite modulating a subset of pro-inflammatory cytokines, no detrimental effects of PEN treatment on the long-term proliferation capacity of the bulk CD3⁺ T cell population were observed.

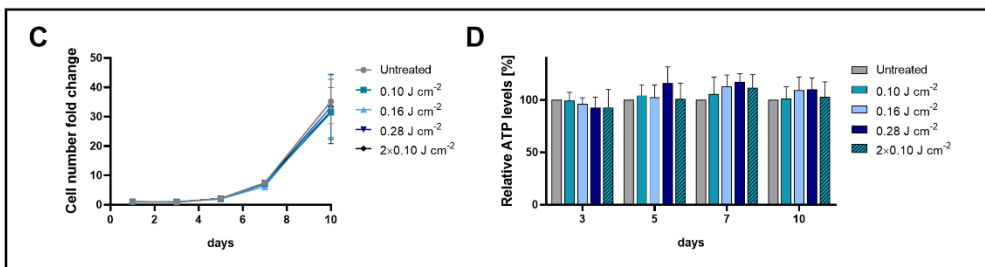
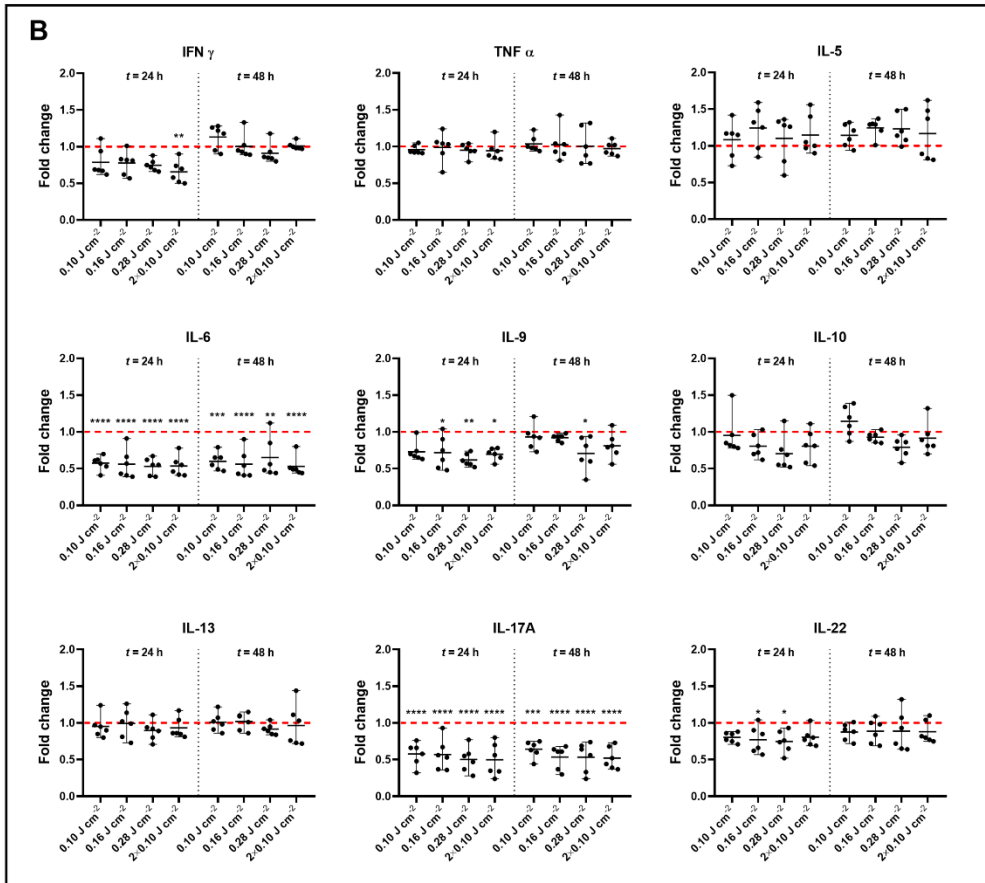
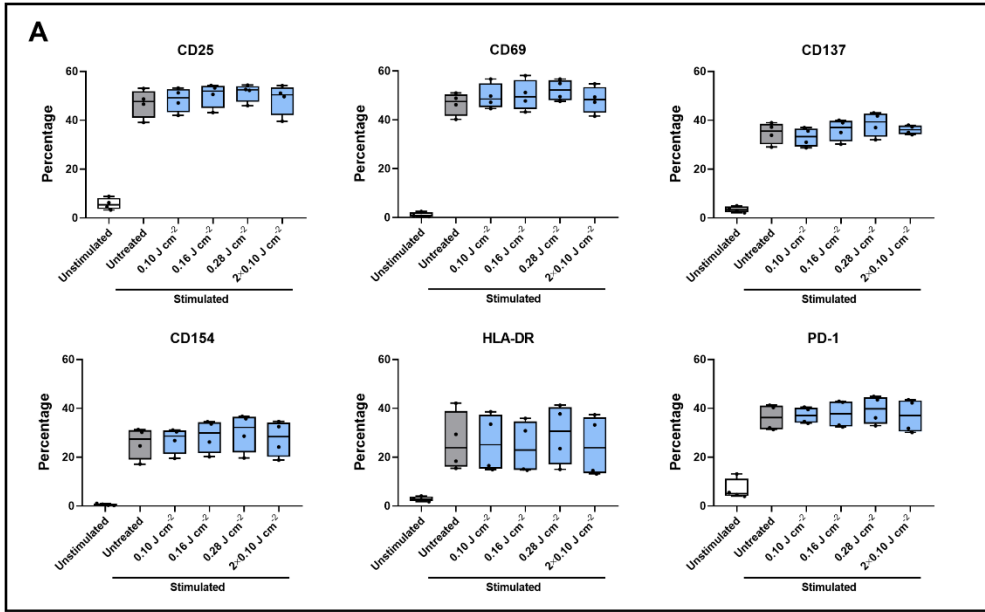


Figure 7. Evaluation of T cell propensity to activation after pre-treatment by PEN photoporation.

Unstimulated T cells were irradiated on PEN substrates with 1 wt% IONPs in the absence of cargo on the day of isolation. The next day, cell density of every experimental group was adjusted to 1×10^6 cells/mL and stimulation with ImmunoCult CD3/CD28 T cell Activator was initiated. (A) The expression of surface activation markers was evaluated by flow cytometry after 48 h of stimulation. Data are represented as boxes-and-whiskers showing the minimum to maximum results of cultures of four different donors. Statistical analysis was performed using Two-way ANOVA with Tukey's multiple comparisons test. (B) Cytokine secretion of several key inflammatory cytokines was measured in culture supernatant collected 24 and 48 h after stimulation. Values are expressed relative (fold change) to the untreated control (red dashed line). Data represent the mean (center bar) \pm SD of cultures of four different donors. Statistical analysis was performed using Two-way ANOVA with Tukey's multiple comparisons test (* $p < 0.05$; ** $p < 0.01$; *** $p < 0.001$; **** $p < 0.0001$). (C) Cell number fold changes in T cell cultures irradiated with different laser fluences as assessed by cell counting with Trypan blue staining. The normalized cell growth was calculated relative to the seeding density at day 1. Data are represented as the mean \pm SD of cultures of four different donors. Statistical analysis was performed using Two-way ANOVA with Tukey's multiple comparisons test. (D) The ATP content of T cell cultures was monitored using a Cell Titer Glo assay. The values were calculated relative to the untreated control at every time point. Data are represented as the mean \pm SD of cultures of four different donors. Statistical analysis was performed using Two-way ANOVA with Tukey's multiple comparisons test.

4 Discussion

Efficient and safe introduction of exogenous cargo inside cells lies at the heart of *ex vivo* cell engineering for immunotherapy and regenerative medicine, fueling a quest for improved intracellular delivery/transfection technologies. In the context of adoptive T cell transfer, several studies have demonstrated superior antitumor efficacy of cellular products enriched in minimally differentiated T cell subsets, making *ex vivo* manipulation of quiescent T cells of interest for both clinical applications and more fundamental studies of T cell biology. However, resting lymphocytes remain overly reluctant to standard transfection reagents. A limited number of reports use instead a physical stimulus, such as electrical or mechanical, to transiently permeabilize the T cell membrane for an influx of effector molecules. Here we proposed PEN photoporation as a gentle physical method for intracellular delivery in unstimulated human T cells.

In line with the core goal of preventing direct exposure of cells to sensitizing NPs which are used in photoporation, we first investigated potential iron release from the fibers upon laser irradiation. ICP-MS/MS confirmed that no significant Fe release occurred from the fibers with 1% IONPs even when illuminated with the maximal available fluence of 1.56 J cm^{-2} . However, for PEN substrates containing 2.5-10% IONPs, small amounts of iron were detected upon irradiation with laser pulse fluences of 0.36 J cm^{-2} and 1.56 J cm^{-2} . This can be explained by our observation that PEN substrates with 1% IONPs only started to generate VNBs starting from a laser pulse fluence of 0.36 J cm^{-2} . However, at higher IONP content, the fluence threshold at which bubbles were first observed was $0.10\text{-}0.16 \text{ J cm}^{-2}$. Moreover, the bubbles tended to become bigger for higher IONP content, which may be more destabilizing to the nanofiber structure and promote the release of IONPs. Instead, at low laser pulse fluences the predominant photothermal effect is mere heating, which does not lead to IONP release.

Next, we studied how these photothermal effects can be exploited for intracellular delivery of FD150 as a model macromolecule in unstimulated human T cells. We demonstrated delivery efficiencies of up to 55-60% for increasing laser pulse fluences, which translated to overall delivery yields of about 30% after accounting for cytotoxicity. To put these values into perspective, our group previously reported very comparable

delivery yields for gold NP-mediated photoporation in immortalized Jurkat cells²⁷ and expanded primary human T cells²⁸. However, photoporation with polydopamine NPs was more efficient in stimulated and unstimulated human T cells with yields up to 50-60% even with FITC-dextran of 500 kDa^{60,61}.

The results of this study revealed some differences in FD150 delivery yields between unstimulated and expanded T cells. For the same PEN photoporation settings (*i.e.*, IONP content and laser pulse fluence), we noted more toxicity of pre-stimulated cells compared to their resting counterparts. Although a specific mechanism behind these observations remains uncertain, we can envision that the delivery outcomes are defined by an interplay of cell characteristics (*e.g.*, size), nanofiber diameter, IONP distribution and mesh porosity, dictating the extent of plasma membrane (PM) exposure to photothermal effects. Furthermore, a particular phenotype's mechanical properties (*e.g.*, membrane fluidity and stress-bearing properties of the cytoskeleton) can influence cell susceptibility to permeabilization and subsequent membrane resealing. For instance, it is known that A-type lamins are upregulated in response to TCR activation, enhancing F-actin polymerization and T cell stiffening⁶²⁻⁶⁴. Although the relationship between membrane tension, cytoskeleton rigidity and force required for membrane disruption is complex, we can speculate that smaller and less stiff unstimulated T cells are more efficient in resealing PM wounds inflicted by PEN treatment compared to their larger stimulated counterparts, translating to better preservation of cell viability in unstimulated cultures. Lastly, we observed a small benefit of repeated photoporation on FD150 delivery yields in stimulated T cells. This can be possibly explained by previous findings of a potentiated response to PM injury, where cells that have been subjected to a first insult are primed to deal more efficiently with a second insult, for instance by resealing the membrane damage more quickly than the initial wound⁶⁵.

Overall, although reasonable delivery efficiencies were achieved in unstimulated T cells using PEN photoporation, at present there is a limit to intracellular delivery with photo-responsive substrates that cannot be mitigated by enhancing the laser irradiation settings. As goes for any intracellular delivery technology, there seems to be a threshold above which increased delivery efficiency is counteracted by cytotoxicity, halting further improvement in delivery yields. However, delivery efficiency is only half the story. Indeed,

it is increasingly being realized that the long-term impact of the delivery technology on cell phenotype and functionality should be considered as well. Therefore, we here investigated the functional consequences of PEN photoporation by evaluating the propensity of unstimulated T cells to activation after treatment by PEN photoporation. We did not observe any significant changes in the surface marker expression profile of PEN-treated cells, regardless of the applied laser pulse fluence. However, we noted a reduced secretion of a specific subset of pro-inflammatory cytokines (IL-6, IL-9, and IL-17), even though there was no impact on the production of IL-5, TNF- α , IFN- γ , or selected anti-inflammatory molecules. To explain these findings, it is necessary to reflect on the PM role as a major platform for T cell signaling, integrating signals that control processes such as activation, proliferation, and response to cytokines. Clearly, a disruption to PM composition and spatiotemporal organization may cause alterations to signal transduction and eventually affect T cell functionality. For instance, lowering glycosphingolipids levels in CD4+ T cells by pharmacological inhibitors or gene disruption specifically inhibited T cell differentiation to the IL-17-producing helper lineage ⁶⁶. Furthermore, it has been shown that T cell activation and differentiation is regulated by the activity of acid sphingomyelinase (ASM), which mediates the hydrolysis of sphingomyelin to ceramide, an important lipid messenger in intracellular signaling ^{67,68}. In CD4+ T cells, ASM inhibition led to a diminished TCR signal transduction, accompanied by impaired polarization into Th1, Th2 or Th17 phenotypes, measured by decreased levels of IFN- γ , IL-4 and IL-17 cytokine production, respectively ⁶⁹.

An additional consideration is that membrane repair may alter the organization and abundance of cell surface receptors, and hence cell functionality. In macrophages, for instance, membrane shedding in response to pore-forming toxins can lead to the removal of cytokine receptors from the cell surface resulting in immune suppression ⁷⁰. In B cells, endocytosis-mediated removal of PM wounds has been shown to disrupt B cell receptor signaling by interfering with their lipid raft-dependent internalization ⁷¹. These examples illustrate the significance of the complete recovery of PM functionality, going beyond the initial resealing of wounded areas. Therefore, for membrane disruption-based technologies like photoporation it is important to understand whether such transient permeabilization induces any persistent phenotypical alterations that may impair cell

functionality ⁷². In this study we observed a modulation of a subset of proinflammatory cytokines within 48 h of stimulation, possibly related to a Th17 phenotype. However, how persistent these changes are and their exact implications on cell functionality remain to be investigated further. Nevertheless, at the CD3+ total population level, these changes did not impact the surface activation marker profile or long-term proliferation capacity of PEN-treated cells.

5 Conclusion

In summary, we demonstrated that PEN photoporation, which enables intracellular delivery without direct exposure of cells to the sensitizing NPs, can be effectively used to deliver macromolecules in unstimulated human T cells, with limited impact on their activation propensity and proliferation. Combined with unique safety and regulatory advantage, this system paves the way for future translation of photoporation technology towards the production of engineered cell products.

References

1. Stewart MP, Sharei A, Ding X, Sahay G, Langer R, Jensen KF. In vitro and ex vivo strategies for intracellular delivery. *Nature*. 2016;538(7624):183-192.
2. Morshedi Rad D, Alsadat Rad M, Razavi Bazaz S, Kashaninejad N, Jin D, Ebrahimi Warkiani M. A Comprehensive Review on Intracellular Delivery. *Advanced Materials*. 2021;33(13):2005363.
3. Mitchell MJ, Billingsley MM, Haley RM, Wechsler ME, Peppas NA, Langer R. Engineering precision nanoparticles for drug delivery. *Nat Rev Drug Discov*. 2021;20(2):101-124.
4. Butt MH, Zaman M, Ahmad A, et al. Appraisal for the Potential of Viral and Nonviral Vectors in Gene Therapy: A Review. *Genes (Basel)*. 2022;13(8).
5. Stewart MP, Langer R, Jensen KF. Intracellular Delivery by Membrane Disruption: Mechanisms, Strategies, and Concepts. *Chem Rev*. 2018;118(16):7409-7531.
6. Qu Y, Zhang Y, Yu Q, Chen H. Surface-Mediated Intracellular Delivery by Physical Membrane Disruption. *ACS Appl Mater Interfaces*. 2020;12(28):31054-31078.
7. Sadelain M, Rivière I, Riddell S. Therapeutic T cell engineering. *Nature*. 2017;545(7655):423-431.
8. June CH, Sadelain M. Chimeric Antigen Receptor Therapy. *New England Journal of Medicine*. 2018;379(1):64-73.
9. Moretti A, Ponzio M, Nicolette CA, Tcherepanova IY, Biondi A, Magnani CF. The Past, Present, and Future of Non-Viral CAR T Cells. *Front Immunol*. 2022;13(June):1-25.
10. Wagner DL, Koehl U, Chmielewski M, Scheid C, Stripecke R. Review: Sustainable Clinical Development of CAR-T Cells – Switching From Viral Transduction Towards CRISPR-Cas Gene Editing. *Front Immunol*. 2022;13(June):1-13.
11. Labbé RP, Vessillier S, Rafiq QA. Lentiviral Vectors for T Cell Engineering: Clinical Applications, Bioprocessing and Future Perspectives. *Viruses*. 2021;13(8):1528.
12. DiTommaso T, Cole JM, Cassereau L, et al. Cell engineering with microfluidic squeezing preserves functionality of primary immune cells in vivo. *Proceedings of the National Academy of Sciences*. 2018;115(46):E10907-E10914.
13. Joo B, Hur J, Kim GB, Yun SG, Chung AJ. Highly Efficient Transfection of Human Primary T Lymphocytes Using Droplet-Enabled Mechanoporation. *ACS Nano*. 2021;15(8):12888-12898.
14. Zhang Z, Qiu S, Zhang X, Chen W. Optimized DNA electroporation for primary human T cell engineering. *BMC Biotechnol*. 2018;18(1):1-9.
15. Tay A, Melosh N. Transfection with Nanostructure Electro-Injection is Minimally Perturbative. *Adv Ther (Weinh)*. 2019;2(12):1900133.
16. Cao Y, Ma E, Cestellos-Blanco S, et al. Nontoxic nanopore electroporation for effective intracellular delivery of biological macromolecules. *Proc Natl Acad Sci U S A*. 2019;116(16):7899-7904.

17. Zuvin M, Kuruoglu E, Kaya VO, et al. Magnetofection of green fluorescent protein encoding DNA-bearing polyethyleneimine-coated superparamagnetic iron oxide nanoparticles to human breast cancer cells. *ACS Omega*. 2019;4(7):12366-12374.
18. Xiong R, Raemdonck K, Peynshaert K, et al. Comparison of Gold Nanoparticle Mediated Photoporation: Vapor Nanobubbles Outperform Direct Heating for Delivering Macromolecules in Live Cells. *ACS Nano*. 2014;8(6):6288-6296.
19. Tang H, Wang J, Yu L, et al. Ultrahigh Efficiency and Minimalist Intracellular Delivery of Macromolecules Mediated by Latent-Photothermal Surfaces. *ACS Appl Mater Interfaces*. 2021;13(10):12594-12602.
20. Xiong R, Samal SK, Demeester J, Skirtach AG, De Smedt SC, Braeckmans K. Laser-assisted photoporation: fundamentals, technological advances and applications. *Adv Phys X*. 2016;1(4):596-620.
21. Xiong R, Sauvage F, Fraire JC, Huang C, De Smedt SC, Braeckmans K. Photothermal Nanomaterial-Mediated Photoporation. *Acc Chem Res*. 2023;56(6):631-643.
22. Ramon J, Xiong R, De Smedt SC, Raemdonck K, Braeckmans K. Vapor nanobubble-mediated photoporation constitutes a versatile intracellular delivery technology. *Curr Opin Colloid Interface Sci*. 2021;54:101453.
23. Lapotko D. Plasmonic nanoparticle-generated photothermal bubbles and their biomedical applications. *Nanomedicine*. 2009;4(7):813-845.
24. Lukianova-Hleb E, Hu Y, Latterini L, et al. Plasmonic Nanobubbles as Transient Vapor Nanobubbles Generated around Plasmonic Nanoparticles. *ACS Nano*. 2010;4(4):2109-2123.
25. Maheshwari S, van der Hoef M, Prosperetti A, Lohse D. Dynamics of Formation of a Vapor Nanobubble Around a Heated Nanoparticle. *The Journal of Physical Chemistry C*. 2018;122(36):20571-20580.
26. Wayteck L, Xiong R, Braeckmans K, De Smedt SC, Raemdonck K. Comparing photoporation and nucleofection for delivery of small interfering RNA to cytotoxic T cells. *Journal of Controlled Release*. 2017;267:154-162.
27. Raes L, Van Hecke C, Michiels J, et al. Gold Nanoparticle-Mediated Photoporation Enables Delivery of Macromolecules over a Wide Range of Molecular Weights in Human CD4+ T Cells. *Crystals (Basel)*. 2019;9(8):411.
28. Raes L, Pille M, Harizaj A, et al. Cas9 RNP transfection by vapor nanobubble photoporation for ex vivo cell engineering. *Mol Ther Nucleic Acids*. 2021;25(September):696-707.
29. Wang L, Wu J, Hu Y, et al. Using porous magnetic iron oxide nanomaterials as a facile photoporation nanoplatfrom for macromolecular delivery. *J Mater Chem B*. 2018;6(27):4427-4436.
30. Harizaj A, Van Hauwermeiren F, Stremersch S, et al. Nanoparticle-sensitized photoporation enables inflammasome activation studies in targeted single cells. *Nanoscale*. 2021;13(13):6592-6604.

31. Chakravarty P, Qian W, El-Sayed MA, Prausnitz MR. Delivery of molecules into cells using carbon nanoparticles activated by femtosecond laser pulses. *Nat Nanotechnol.* 2010;5(8):607-611.
32. Sengupta A, Kelly SC, Dwivedi N, Thadhani N, Prausnitz MR. Efficient intracellular delivery of molecules with high cell viability using nanosecond-pulsed laser-activated carbon nanoparticles. *ACS Nano.* 2014;8(3):2889-2899.
33. Chakravarty P, Lane CD, Orlando TM, Prausnitz MR. Parameters affecting intracellular delivery of molecules using laser-activated carbon nanoparticles. *Nanomedicine.* 2016;12(4):1003-1011.
34. Liu J, Li C, Brans T, et al. Surface Functionalization with Polyethylene Glycol and Polyethyleneimine Improves the Performance of Graphene-Based Materials for Safe and Efficient Intracellular Delivery by Laser-Induced Photoporation. *Int J Mol Sci.* 2020;21(4):1540.
35. Liu J, Xiong R, Brans T, et al. Repeated photoporation with graphene quantum dots enables homogeneous labeling of live cells with extrinsic markers for fluorescence microscopy. *Light Sci Appl.* 2018;7(1):47.
36. Siegrist S, Cörek E, Detampel P, Sandström J, Wick P, Huwylar J. Preclinical hazard evaluation strategy for nanomedicines. *Nanotoxicology.* 2019;13(1):73-99.
37. Foulkes R, Man E, Thind J, Yeung S, Joy A, Hoskins C. The regulation of nanomaterials and nanomedicines for clinical application: current and future perspectives. *Biomater Sci.* 2020;8(17):4653-4664.
38. Xiong R, Hua D, Van Hoeck J, et al. Photothermal nanofibres enable safe engineering of therapeutic cells. *Nat Nanotechnol.* 2021;16(11):1281-1291.
39. Liu L, Johnson C, Fujimura S, Teque F, Levy JA. Transfection optimization for primary human CD8+ cells. *J Immunol Methods.* 2011;372(1-2):22-29.
40. Seki A, Rutz S. Optimized RNP transfection for highly efficient CRISPR/Cas9-mediated gene knockout in primary T cells. *Journal of Experimental Medicine.* 2018;215(3):985-997.
41. Aksoy P, Aksoy BA, Czech E, Hammerbacher J. Viable and efficient electroporation-based genetic manipulation of unstimulated human T cells. *bioRxiv.* 2018;(Cm).
42. Howden AJM, Hukelmann JL, Brenes A, et al. Quantitative analysis of T cell proteomes and environmental sensors during T cell differentiation. *Nat Immunol.* 2019;20(11):1542-1554.
43. Wolf T, Jin W, Zoppi G, et al. Dynamics in protein translation sustaining T cell preparedness. *Nat Immunol.* 2020;21(8):927-937.
44. Robinson GA, Waddington KE, Pineda-Torra I, Jury EC. Transcriptional regulation of T-cell lipid metabolism: Implications for plasma membrane lipid rafts and T-cell function. *Front Immunol.* 2017;8(NOV):1-10.
45. Gattinoni L, Klebanoff CA, Palmer DC, et al. Acquisition of full effector function in vitro paradoxically impairs the in vivo antitumor efficacy of adoptively transferred CD8+ T cells. *Journal of Clinical Investigation.* 2005;115(6):1616-1626.

46. Gumber D, Wang LD. Improving CAR-T immunotherapy: Overcoming the challenges of T cell exhaustion. *EBioMedicine*. 2022;77:103941.
47. Klebanoff CA, Gattinoni L, Torabi-Parizi P, et al. Central memory self/tumor-reactive CD8+ T cells confer superior antitumor immunity compared with effector memory T cells. *Proc Natl Acad Sci U S A*. 2005;102(27):9571-9576.
48. Hinrichs CS, Borman ZA, Cassard L, et al. Adoptively transferred effector cells derived from naïve rather than central memory CD8 + T cells mediate superior antitumor immunity. *Proceedings of the National Academy of Sciences*. 2009;106(41):17469-17474.
49. Gattinoni L, Lugli E, Ji Y, et al. A human memory T cell subset with stem cell-like properties. *Nat Med*. 2011;17(10):1290-1297.
50. Fraietta JA, Nobles CL, Sammons MA, et al. Disruption of TET2 promotes the therapeutic efficacy of CD19-targeted T cells. *Nature*. 2018;558(7709):307-312.
51. Fraietta JA, Lacey SF, Orlando EJ, et al. Determinants of response and resistance to CD19 chimeric antigen receptor (CAR) T cell therapy of chronic lymphocytic leukemia. *Nat Med*. 2018;24(5):563-571.
52. Arcangeli S, Falcone L, Camisa B, et al. Next-Generation Manufacturing Protocols Enriching TSCM CAR T Cells Can Overcome Disease-Specific T Cell Defects in Cancer Patients. *Front Immunol*. 2020;11(June).
53. Ghassemi S, Nunez-Cruz S, O'Connor RS, et al. Reducing ex vivo culture improves the antileukemic activity of chimeric antigen receptor (CAR) T cells. *Cancer Immunol Res*. 2018;6(9):1100-1109.
54. de Macedo Abdo L, Barros LRC, Saldanha Viegas M, et al. Development of CAR-T cell therapy for B-ALL using a point-of-care approach. *Oncoimmunology*. 2020;9(1).
55. Ghassemi S, Durgin JS, Nunez-Cruz S, et al. Rapid manufacturing of non-activated potent CAR T cells. *Nat Biomed Eng*. 2022;6(2):118-128.
56. Schindelin J, Arganda-Carreras I, Frise E, et al. Fiji: an open-source platform for biological-image analysis. *Nat Methods*. 2012;9(7):676-682.
57. Houthaeve G, Xiong R, Robijns J, et al. Targeted perturbation of nuclear envelope integrity with vapor nanobubble-mediated photoporation. *ACS Nano*. 2018;12(8):7791-7802.
58. Bolea-Fernandez E, Balcaen L, Resano M, Vanhaecke F. Overcoming spectral overlap via inductively coupled plasma-tandem mass spectrometry (ICP-MS/MS). A tutorial review. *J Anal At Spectrom*. 2017;32(9):1660-1679.
59. Xiong R, Hua D, Van Hoeck J, et al. Photothermal nanofibres enable safe engineering of therapeutic cells. *Nat Nanotechnol*. 2021;16(11):1281-1291.
60. Harizaj A, Wels M, Raes L, et al. Photoporation with Biodegradable Polydopamine Nanosensitizers Enables Safe and Efficient Delivery of mRNA in Human T Cells. *Adv Funct Mater*. 2021;31(28):2102472.

61. Berdecka D, Harizaj A, Goemaere I, et al. Delivery of macromolecules in unstimulated T cells by photoporation with polydopamine nanoparticles. *Journal of Controlled Release*. 2023;354:680-693.
62. González-Granado JM, Silvestre-Roig C, Rocha-Perugini V, et al. Nuclear Envelope Lamin-A Couples Actin Dynamics with Immunological Synapse Architecture and T Cell Activation. *Sci Signal*. 2014;7(322):1-14.
63. Walling BL, Murphy PM. Protean Regulation of Leukocyte Function by Nuclear Lamins. *Trends Immunol*. 2021;42(4):323-335.
64. Jung P, Zhou X, Iden S, Bischoff M, Qu B. T cell stiffness is enhanced upon formation of immunological synapse. *Elife*. 2021;10:1-13.
65. Togo T. Disruption of the plasma membrane stimulates rearrangement of microtubules and lipid traffic toward the wound site. *J Cell Sci*. 2006;119(13):2780-2786.
66. Sengupta S, Karsalia R, Morrissey A, Bamezai AK. Cholesterol-dependent plasma membrane order (Lo) is critical for antigen-specific clonal expansion of CD4+ T cells. *Sci Rep*. 2021;11(1):13970.
67. Bai A, Guo Y. Acid sphingomyelinase mediates human CD4+ T-cell signaling: potential roles in T-cell responses and diseases. *Cell Death Dis*. 2017;8(7):e2963-e2963.
68. Pinto C, Sousa D, Ghilas V, Dardis A, Scarpa M, Macedo MF. Acid sphingomyelinase deficiency: A clinical and immunological perspective. *Int J Mol Sci*. 2021;22(23).
69. Bai A, Kokkotou E, Zheng Y, Robson SC. Role of acid sphingomyelinase bioactivity in human CD4+ T-cell activation and immune responses. *Cell Death Dis*. 2015;6(7):1-9.
70. Bhattacharjee P, Keyel PA. Cholesterol-dependent cytolysins impair pro-inflammatory macrophage responses. *Sci Rep*. 2018;8(1):1-15.
71. Miller H, Castro-Gomes T, Corrotte M, et al. Lipid raft-dependent plasma membrane repair interferes with the activation of B lymphocytes. *Journal of Cell Biology*. 2015;211(6):1193-1205.
72. Houthaev G, De Smedt SC, Braeckmans K, De Vos WH. The cellular response to plasma membrane disruption for nanomaterial delivery. *Nano Converg*. 2022;9(1):6.

Supplementary Information

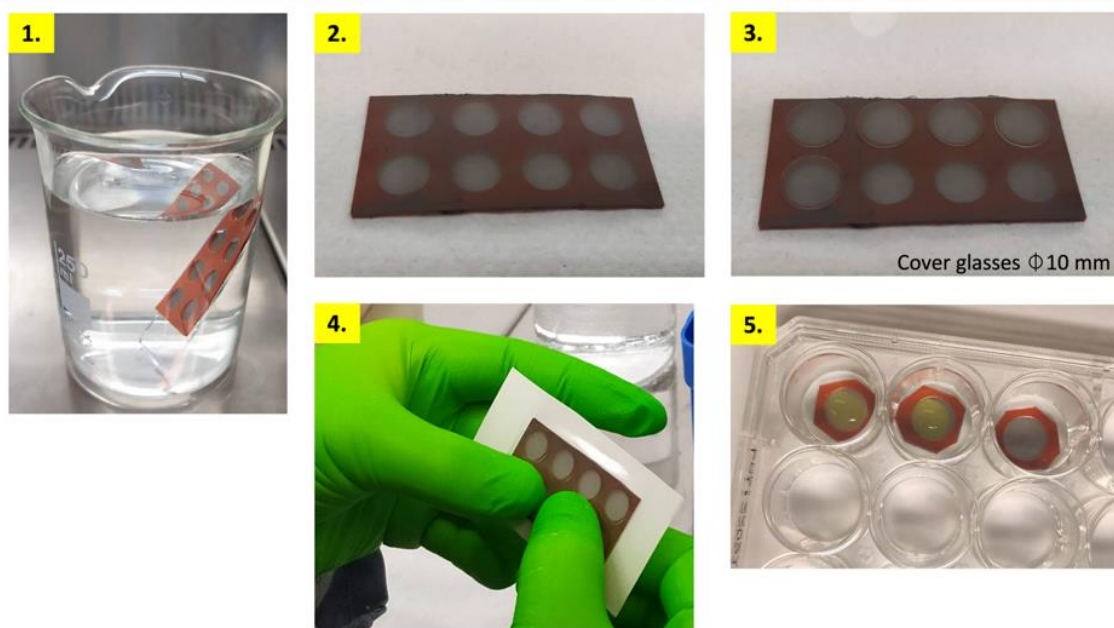


Figure S1. Preparation of PEN wells for the treatment of suspension cells. (1) After removing the protective sealing, eight-well Press-to-Seal™ Silicone Isolators were gently stuck on the nanofiber mesh and samples were immersed in DI water to easily remove nanofibers from the glass slide. (2) Next, samples were dried, turned upside down with silicone spacers facing down. (3) Round cover glasses are placed on the top surface for each well. (4) Cover slips are held in place with a transparent adhesive seal. (5) Finally, samples are manually cut into smaller pieces, with a single PEN well per piece for positioning in a 24-well titre plate.

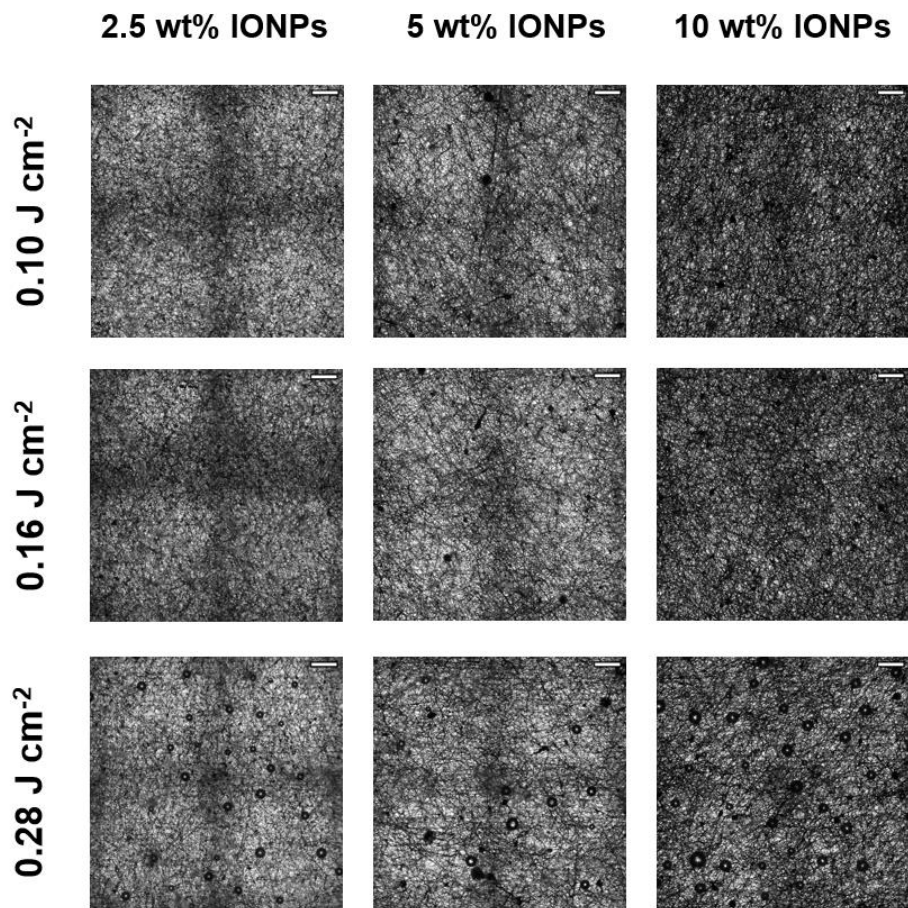


Figure S2. Bright field images of PEN substrates containing 2.5, 5 and 10 wt% IONPs after laser irradiation. Scale bar 200 μm .

Table S1. Fe concentrations measured by ICP-MS analysis in Mili-Q water collected from PEN substrates after laser activation or fiber digestion only (LoQ = Limit of Quantification).

Substrate	Laser fluence [J cm ⁻²]	Sample type	Fe concentration [mg L ⁻¹]			
			sample 1	sample 2	sample 3	sample 4
0 wt% IONPs	0	Mili-Q H ₂ O	<LoQ	<LoQ		
	0.05		<LoQ	0.010		
	0.16		0.076	<LoQ	0.218	
	0.36		<LoQ	<LoQ		
	1.56		<LoQ	<LoQ		
	0	Fiber	<LoQ	<LoQ		
1 wt% IONPs	0	Mili-Q H ₂ O	<LoQ	<LoQ		
	0.05		<LoQ	<LoQ		
	0.16		<LoQ	<LoQ		
	0.36		<LoQ	<LoQ		
	1.56		0.085	0.068		
	0	Fiber	0.929	0.922		
2.5 wt% IONPs	0	Mili-Q H ₂ O	<LoQ	<LoQ		
	0.05		<LoQ	0.019		
	0.16		0.006	<LoQ		
	0.36		0.124	0.058	0.093	0.078
	1.56		0.370	0.332	0.501	0.598
	0	Fiber	6.220	4.970	1.694	6.715
5 wt% IONPs	0	Mili-Q H ₂ O	<LoQ	<LoQ		
	0.05		<LoQ	<LoQ		
	0.16		0.011	0.008		
	0.36		0.083	0.090	0.063	0.557
	1.56		0.253	0.199	0.771	0.388
	0	Fiber	10.400	8.880	11.326	9.903
10 wt% IONPs	0	Mili-Q H ₂ O	0.038	0.006	<LoQ	<LoQ
	0.05		<LoQ	0.004		
	0.16		0.010	0.013		
	0.36		0.034	0.042	0.049	0.050
	1.56		0.199	0.160	0.540	0.379
	0	Fiber	30.800	25.400	22.044	29.965

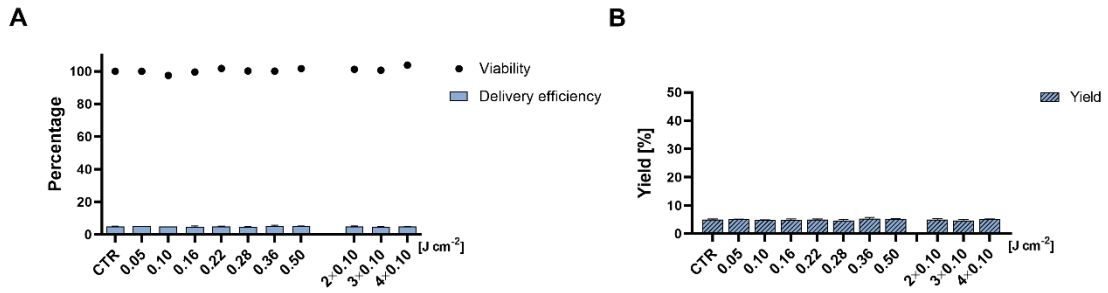


Figure S3. Intracellular delivery of FD150 in unstimulated human T cells by PEN photoporation with PEN substrates without IONPs. All samples were irradiated one time, except for samples irradiated with a laser pulse fluence of $0.10\ J\ cm^{-2}$ which were subsequently irradiated up to 4x. Cells incubated with FD without applying laser irradiation (CTR) served as a control for any spontaneous uptake. (A) Delivery efficiency of FD150 (bars) was measured by flow cytometry (gated on viable cells) and cell viability (dots) was determined by a Cell Titer Glo assay. (B) Delivery yield was calculated by multiplying the delivery efficiency and cell viability, representing the percentage of viable and transfected cells compared to the initial cell population. Data represent the mean \pm SD (n=3) of one donor.

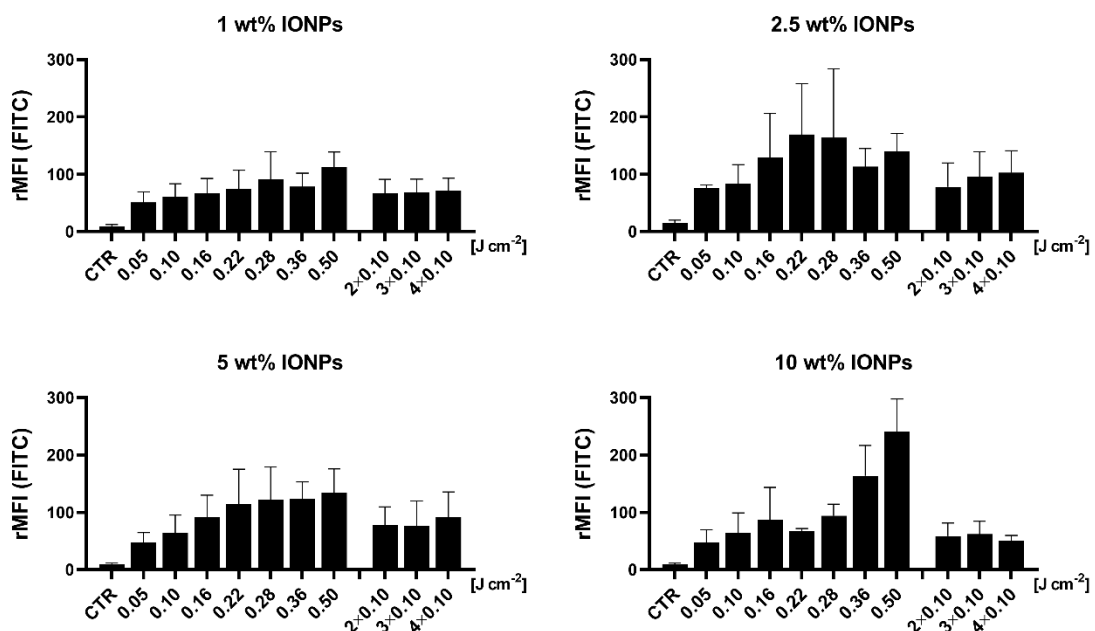


Figure S4. Intracellular delivery of FD150 in unstimulated T cells: relative mean fluorescence intensity of FITC-positive cells after PEN photoporation. Data represent the mean \pm SD of at least four different donors tested per each IONP wt%.

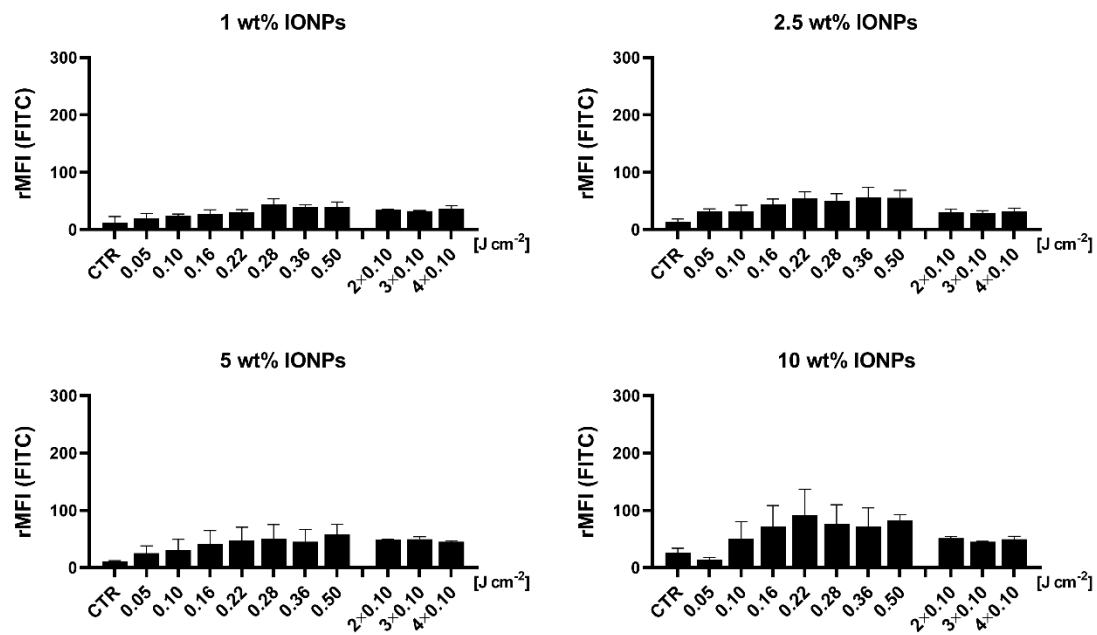


Figure S5. Intracellular delivery of FD150 in expanded T cells: relative mean fluorescence intensity of FITC-positive cells after PEN photoporation. Data represent the mean \pm SD of at least four different donors tested per each IONP wt%.

Chapter 4

Broader international context, relevance and future perspectives

Table of Contents

Abstract.....	180
1 Engineered T cell therapies: progress and challenges	181
2 Overcoming therapeutic limitations of engineered T cells	188
2.1 Optimization of T cell manufacturing protocols to increase T cell fitness	188
2.2 Novel CAR designs to improve efficacy and mitigate toxicity.....	193
3 Overcoming manufacturing bottleneck to increase accessibility to T cell therapies	198
3.1 Non-viral T cell engineering	198
3.2 Shifting paradigm in T cell manufacturing: towards automation and decentralization	202
3.3 Off-the-shelf CAR T cells.....	204
Conclusions and outlook.....	205
References	206

Abstract

Adoptive T cell therapies have demonstrated remarkable clinical responses in certain hematological malignancies, leading to the regulatory approval of six CAR T cell therapies to date. However, their efficacy for the treatment of solid tumors remains limited, while complex and extremely costly manufacturing process have restricted patient accessibility to this novel treatment. In this final chapter, we will first describe the current landscape of T cell based therapeutics and point out the remaining challenges to their wider adoption, related to cell biological potency or manufacturing limitations. We will discuss the relevance of the optimization of T cell manufacturing protocols to preserve T cell fitness, giving a broader context for our interest in the engineering of minimally manipulated quiescent T cells in this PhD thesis. Next, we will provide examples of novel CAR designs to increase CAR T cell efficacy in the immunosuppressive tumor microenvironment and mitigating on-target off-tumor toxicities. In the second part, we will focus on the strategies to overcome the current limitations of autologous CAR T cell manufacturing, highlighting the potential of non-viral transfection methods as a safe, flexible and cost-efficient alternative to viral vector-based production. Finally, we will discuss the importance of automation and decentralization for a wider adoption of engineered T cell therapies, and the emergence of allogeneic approaches as an off-the-shelf alternative for patients who could not benefit from autologous therapy.

1 Engineered T cell therapies: progress and challenges

According to the World Health Organization (WHO), cancer is a leading cause of death worldwide, with 10 million cancer related deaths reported in 2020 and estimated 27.5 million new cases to be added to the global cancer burden by the end of 2040, exerting tremendous strain on the affected individuals and national healthcare systems ¹. Engineered T cell therapies hold significant transformative potential as a new type of cancer treatment that harnesses the immune system to fight cancer. In particular, chimeric antigen receptor (CAR)-engineered cell therapies that rely on genetic modification with a recombinant receptor to redirect T cells to recognize and eliminate tumor cells expressing a specific target surface antigen have demonstrated notable clinical success in the treatment of hematological malignancies and currently dominate the field of adoptive cell therapy. For example, pediatric and young adult patients with refractory or relapsed (r/r) acute lymphoblastic leukemia (ALL) have achieved overall remission rates of up to 90% after treatment with autologous anti-CD19 CAR T cells ^{2,3}. These unprecedented response rates resulted in the tisagenlecleucel (Kymriah™) approval by the U.S. Food and Drug Administration (FDA) in 2017, marking a significant milestone in cancer immunotherapy and fueling further research into the potential of engineered T cell therapies for other tumor types. According to a recent report, CAR T cells represented more than 50% of 2756 active cell therapy agents in the global immunoncology pipeline in 2022 (**Figure 1**), highlighting that it continues to be the most investigated and promising modality in adoptive cell transfer ⁴. Out of an estimated 850 ongoing clinical trials of CAR T cell therapies in 2022, approximately 40% investigated CAR T cell efficacy in solid tumors, reflecting the field's pursuit of moving beyond the treatment of certain hematological malignancies. For blood cancers, the most-pursued target antigens are CD19, BCMA, CD22, CD20 and CD123, while in solid tumors, frequently targeted proteins include HER2, mesothelin, glypican 2 and EGFR ⁴.

To date, six CAR T cell therapies have been approved by the FDA and European Medicines Agency (EMA). Following tisagenlecleucel approval for the treatment of pediatric and young adult ALL, three more CD19-specific CAR T cell therapies obtained market authorization for the treatment of different B cell malignancies, namely axicabtagene

ciloleucel (Yescarta™), brexucabtagene autoleucel (Tecartus™) and lisocabtagene maraleucel (Breyanzi™). In April 2021 and February 2022, two BCMA-directed CAR T cell therapies were approved by the FDA for the treatment of multiple myeloma, namely idecabtagene vicleucel (Abecma™) and ciltacabtagene autoleucel (Carvykti™). A detailed overview of the approved CAR T cell therapies is provided in **Table 1**.

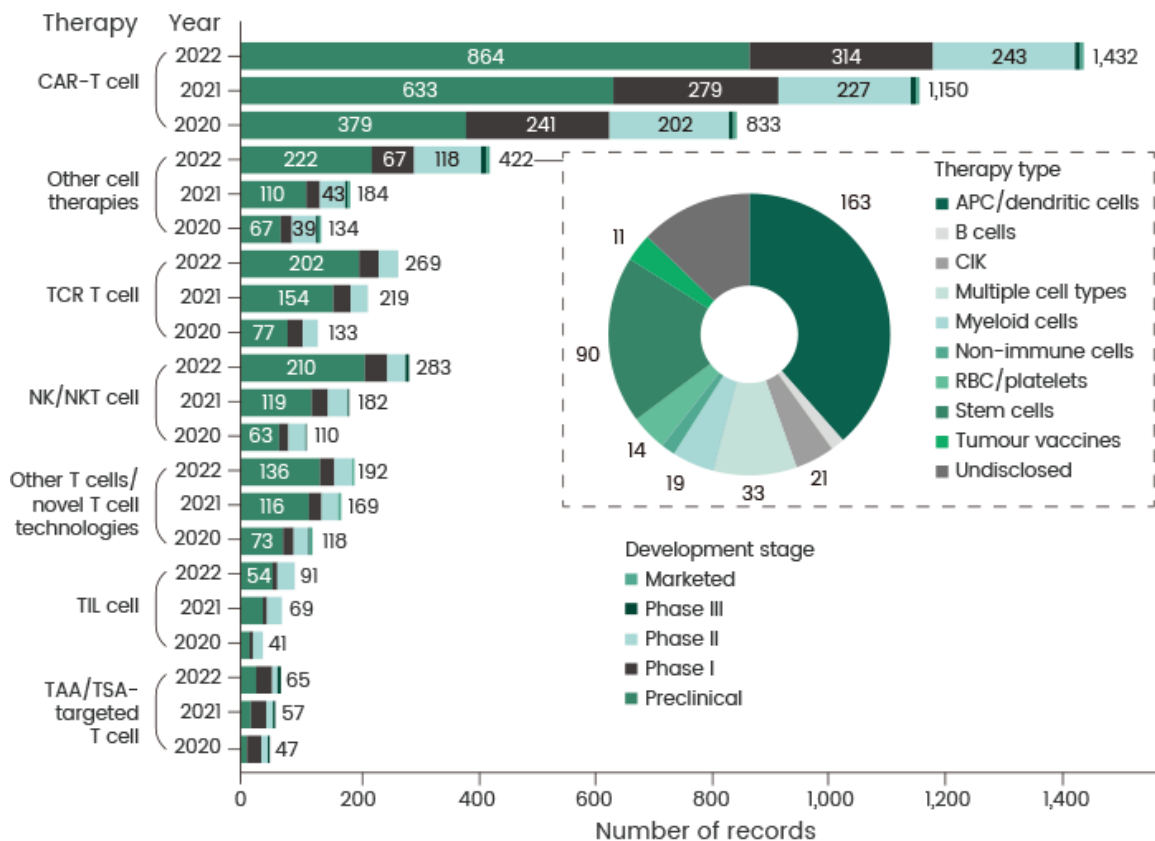


Figure 1. Overview of different cell therapy types in the global cancer cell therapy pipeline from 2020 to 2022. APC: antigen-presenting cell, CIK: cytokine-induced killer, NK: natural killer, RBC: red blood cell, TAA: tumor-associated antigen, TCR: T cell receptor, TIL: tumor-infiltrating lymphocyte, TSA: tumor-specific antigen. The pie chart illustrates the composition of the 'other cell therapies' category in 2022. Adapted from ⁴.

Given the increasing number of clinical trials and product approvals, the CAR T cell therapy market is projected to grow significantly in the upcoming decade. For instance, according to a recent study by Towards Healthcare, the CAR T cell therapy segment is estimated to expand from USD 3.8 billion in 2022 to USD 88.5 billion in 2032 (**Figure 2**).

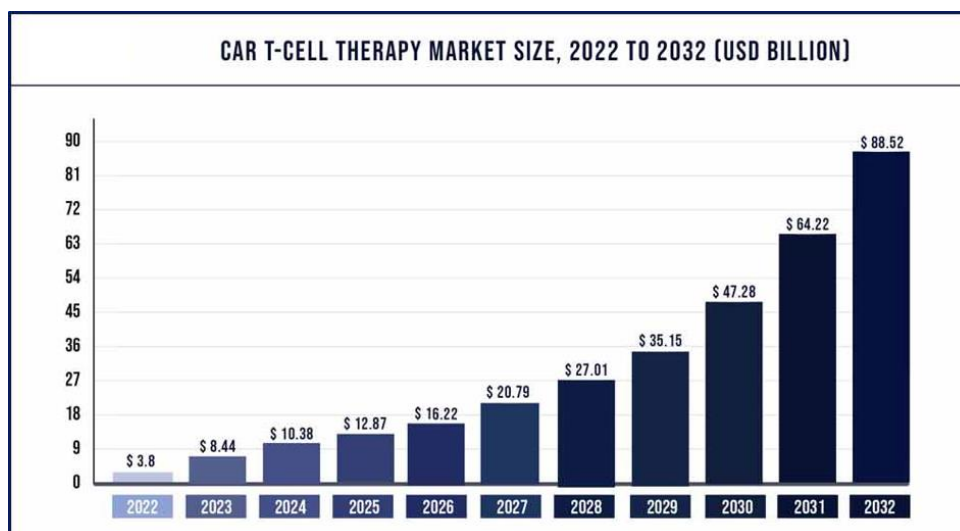


Figure 2. Global CAR T cell therapy market size from 2022 to 2032. Source: CAR T-Cell Therapy Market- Global Industry Analysis, Size, Share, Growth, Trends, Regional Outlook, and Forecast 2023-2032 by Towards Healthcare. Accessed August 2, 2023. <https://www.precedenceresearch.com/car-t-cell-therapy-market>

Despite this pipeline expansion, the field of CAR T cell therapy faces several challenges related to the biological activity of the engineered cell products on the one hand, and manufacturing complexities impeding broader clinical implementation on the other. While CAR T cell therapy has demonstrated remarkable clinical success in certain hematological cancers, its effectiveness in solid tumors remains limited (**Chapter 1**), necessitating new strategies to enhance CAR T cell persistence, improve tumor targeting and overcome immunosuppressive mechanisms in the tumor microenvironment (TME). In addition, the effects of CAR T cell therapy may be of limited durability, with a significant number of patients experiencing disease relapse after a period of time ^{5,6}. One common mechanism of such relapse is the loss of target antigen expression on the malignant cells, known as antigen escape, and described in 20–28% of patients with B cell lymphoma ^{7,8} and 16–68% with acute lymphoblastic leukemia ^{3,9}. As another challenge, CAR T cell therapy carries the risk of severe side effects, such as cytokine release syndrome (CRS) and immune effector cell-associated neurotoxicity syndrome (ICANS), which can be life-threatening in some cases ^{10–12}. Besides these acute adverse events, common long-term side effects include B cell aplasia, hypogammaglobulinemia, cytopenia and infections ^{13–17}. The use of integrating viral vectors in the CAR T cell manufacturing process (**Table 1**)

evokes safety concerns over the presence of replication-competent viruses and potential insertional oncogenesis, prompting regulatory agencies to require specific monitoring for replication-competent viruses throughout the entire production and treatment cycle, with patient follow-up of up to 15 years ^{18,19}.

The major challenge to CAR T cell therapy commercialization is the complex and costly manufacturing process driven by the “one batch - one patient” paradigm, which can result in a total treatment cost of hundreds of thousands of dollars per patient ²⁰. Manufacturing of autologous CAR T cells is a highly personalized process and requires i) collection of patient’s leukocytes *via* apheresis at a clinical site, ii) cryopreservation and shipping of the apheresed material to a specialized CAR T cell manufacturing site, iii) T cell isolation, transduction with a CAR transgene and expansion of CAR-modified cells, iv) formulation, cryopreservation and release testing of the CAR T cell product, v) cold chain shipment of CAR T cell formulation to a treatment site and patient infusion upon completion of lymphodepleting chemotherapy (**Figure 3**). Each of these steps requires specialized equipment, specific raw materials, trained staff and strict quality control measures, which has encouraged adoption of a centralized manufacturing process with limited tertiary care centers able to administer CAR T cell therapy. Currently, commercially available CAR T cell products have list prices ranging from \$373,000 to \$475,000, depending on the specific drug and indication (**Table 1**). On top of the drug acquisition cost, there are substantial ancillary costs of care, particularly for patients experiencing severe toxicities ^{21,22}. For instance, Jagannath *et al.* studied the per-patient US commercial healthcare costs (other than therapy acquisition cost) related to ciltacabtagene autoleucel (Carvykti) therapy in patients with r/r multiple myeloma administered in an inpatient setting ²³. The authors evaluated cost components such as apheresis, bridging therapy, conditioning therapy, management of adverse events (CRS and neurotoxicity) and post-infusion monitoring for 1 year of follow-up, estimating that average per-patient costs totaled around \$160,000. This high financial burden presents a significant challenge for healthcare providers, payers and insurers, inducing some resistance to therapy approval and reimbursement and restricting patient access to this novel treatment modality.

Another critical aspect of autologous CAR T cell therapy is the prolonged waiting time between apheresis and CAR T cell infusion, referred to as vein-to-vein time. With the

median turnaround times ranging from two to four weeks, some patients succumb to rapidly progressing disease without benefiting from CAR T cell administration ^{24–28}. In addition, vein-to-vein time can impact the clinical response of the infused patients. For instance, according to Kite’s analysis of patients treated with axicabtagene ciloleucel (Yescarta) in the U.S. between 2017 and 2020, the median time from leukapheresis to product release was 16 days, while real-world setting vein-to-vein time was 27 days ²⁹. Importantly, shorter leukapheresis to infusion time was associated with a favorable complete response (CR) rate and overall survival at 24-month follow-up (CR rates of 60% in patients infused in less than 40 days vs. 50% in those with a vein-to-vein time of \geq 40 days). Finally, autologous CAR T cell therapy carries the risk of manufacturing failure due to insufficient numbers of T cells in the apheresed material or suboptimal expansion/ cell dysfunction as a consequence of the disease burden and previous lines of treatment ^{8,30,31}.

Together, these manufacturing challenges contribute to the high cost of CAR T cell therapeutics, hesitation to use CAR T cells beyond end-stage patients and patient drop-off before receiving treatment. It is anticipated that addressing practical challenges related to CAR T cell manufacturing would make this treatment more affordable and readily available. Some of the strategies explored to improve the efficacy, safety and accessibility of CAR T cell therapy will be discussed in the following sections.

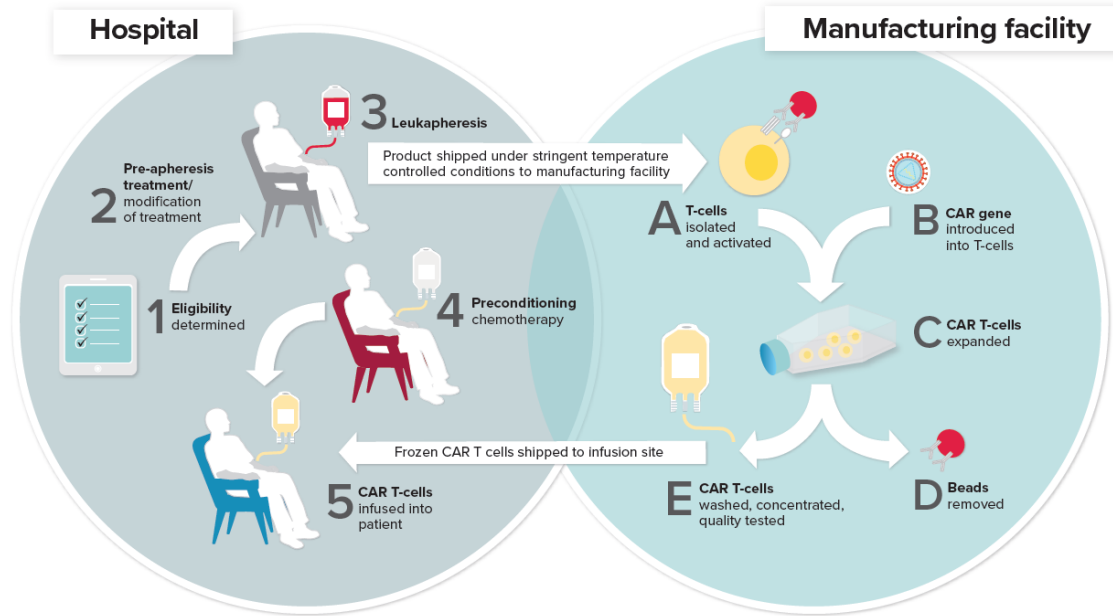


Figure 3. Schematic overview of an autologous CAR T cell manufacturing.

Table 1. Overview of approved CAR T cell therapeutics. r/r: relapsed or refractory, ALL: acute lymphoblastic leukemia, CAYA: children and young adults, LBCL: large B cell lymphoma, MCL: mantle cell lymphoma, MM: multiple myeloma.

Brand name Generic name	Company	Target antigen	Indications	Vector	Approximate cost per treatment	Pivotal trial	First FDA approval	Reference
Kymriah Tisagenlecleucel	Novartis	CD19	r/r ALL CAYA	Lentiviral	\$475,000	ELIANA (NCT02228096)	Aug 30, 2017	2,3,32
Yescarta Axicabtagene ciloleucel	Kite (Gilead)	CD19	r/r LBCL	Gamma-retroviral	\$373,000	ZUMA-1 (NCT02348216)	Oct 18, 2017	7,33
Tecartus Brexucabtagene autoleucel	Kite (Gilead)	CD19	r/r MCL	Gamma-retroviral	\$373,000	ZUMA-2 (NCT02601313)	Jul 24, 2020	9,34,35
Breyanzi Lisocabtagene maraleucel	Juno	CD19	r/r LBCL	Lentiviral	\$410,300	Transcend NHL001 (NCT02631044)	Feb 5, 2021	36
Abecma Idecabtagene vicleucel	Celgene	BCMA	r/r MM	Lentiviral	\$419,500	KarMMa (NCT03361748)	Mar 26, 2021	25
Carvykti Ciltacabtagene autoleucel	Janssen (J&J and Legend)	BCMA	r/r MM	Lentiviral	\$465,000	CARTITUDE-1 (NCT03548207)	Feb 28, 2022	37,38

2 Overcoming therapeutic limitations of engineered T cells

2.1 Optimization of T cell manufacturing protocols to increase T cell fitness

Among numerous strategies proposed to enhance CAR T cell therapeutic efficacy, many have focused on complex genetic engineering (**Chapter 1**), while less attention has been paid to culturing methods during *ex vivo* T cell manufacturing and their impact on the quality of engineered T cell products. Since the retrospective analysis of several clinical trials and preclinical studies has established a link between the characteristics of T cells in the infusion product and subsequent therapeutic responses^{39–46}, cell manufacturing protocols represent another area for potential optimization. Although the ideal T cell composition is not yet known, it has been recognized that the presence of less-differentiated T cells, such as naïve (T_N), stem cell memory (T_{SCM}) and central memory (T_{CM}) cells is associated with improved engraftment, long-term *in vivo* persistence and prolonged anti-tumor efficacy^{39,47–50}. In particular, T_N and T_{SCM} subsets, endowed with longevity, robust proliferation potential and the capacity to reconstitute the whole range of T cell phenotypes, can sustain long-lasting tumor control by supplying effector cells for the immune attack and replenishing the T cell pool with new stem and central memory cells. As such, transfusion of CAR T cells enriched in minimally differentiated subsets is favorable for therapeutic success.

For example, the adoptive transfer of defined T cell subsets in mouse models demonstrated that infusion of less differentiated CD62L-positive subpopulations resulted in improved T cell engraftment, *in vivo* expansion and persistence, translating to sustained tumor regression and extended mice survival^{39,40,47,51,52}. Consistently with the developmental hierarchy, minimally differentiated T_{SCM} subsets display more potent anti-tumor activity than T_{CM}, which in turn are more effective than effector memory T cells^{52–55}. In contrast, acquiring terminal effector properties during *in vitro* culture has been associated with decreased *in vivo* proliferation potential, upregulation of genes involved in apoptosis and replicative senescence and impaired anti-tumor efficacy upon adoptive transfer^{39,40}. Similarly, in clinical studies, transcriptomic profiling demonstrated that CAR T cells from CLL patients achieving complete remissions were enriched in memory-related genes, while T cells from non-responders showed upregulation of genes involved in

effector differentiation, glycolysis, exhaustion and apoptosis ⁴¹. Biomarker analysis of LBCL patients treated with axicabtagene ciloleucel in the ZUMA-1 study revealed that robust CAR T cell expansion early after infusion, associated with the number of CCR7⁺CD45RA⁺ stem cell-like T cells in the infused product and original apheresis material, correlated with durable responses ⁴⁴. Similarly, in the phase 1 clinical trial of BCMA-specific CAR T cells for multiple myeloma higher frequency of memory T cell subset defined by CD8⁺CD45RO⁻CD27⁺ immunophenotype in the premanufacturing leukapheresis product was associated with clinical response ⁴⁶. Given these preclinical and clinical observations, manufacturing procedures have evolved over time to generate CAR T cells enriched in less differentiated phenotypes with enhanced *in vivo* fitness.

As mentioned before, the manufacturing process starts with leukapheresis and enrichment of T cells. The cellular composition of the starting material is paramount for the phenotype of the engineered CAR T cell product. The presence of certain cell types, such as myeloid-derived suppressor cells, monocytes, granulocytes and erythrocytes at culture initiation, can impede T cell activation and expansion ^{56–58}. Thus, a washing step is first performed to remove anticoagulants added during the apheresis process and contaminating red blood cells and platelets ²⁰. Next, specific cell subsets can be enriched or depleted by magnetic selection. For instance, the separation of CD4⁺ T helper cells and CD8⁺ cytotoxic T cells has been used to engineer CAR T cell products with a defined CD4:CD8 ratio ^{36,59–62}. Preclinical experience has shown that combining these two cell subsets in a balanced ratio confers superior anti-tumor efficacy *in vivo*, indicating their synergistic activity ^{63,64}. In addition, CD4/CD8 preselection can improve the manufacturing feasibility and consistency of cell products derived from diverse starting patient material and help to identify optimal cell doses with highly potent anti-tumor activity and tolerable toxicity profile ^{61,62}. As an example, lisocabtagene maraleucel (Breyanzi), approved to treat patients with B cell lymphoma, is a CD19-directed CAR T cell therapy administered at equal target doses of CD8⁺ and CD4⁺ CAR T cells ³⁶. Of note, in the phase 2 clinical trial, this therapy demonstrated lower rates of adverse events such as CRS or neurotoxicity than other CAR T cell treatment forms ³⁶. Similarly, infusion of CD19 CAR T cells manufactured by enrichment of central memory subset was associated with decreased risk of CRS compared to therapy with a product derived from bulk CD8⁺ cells ⁶⁵.

Numerous approaches have focused on isolation and/or directing T cell expansion towards the enrichment of less differentiated CD62L⁺ subsets by regulation of T cell activation, application of specific cytokines, pharmacological inhibition of certain signaling pathways and shortening culture time. T cell activation is typically indispensable for efficient gene transfer by viral transduction²⁰. Optimal stimulation should enable sufficient T cell expansion without inducing terminal T cell differentiation or activation-induced cell death⁶⁶. T cells can be activated using soluble or immobilized monoclonal CD3 and CD28 antibodies or anti-CD3/CD28 antibody-coated paramagnetic beads to provide antigen-independent TCR signaling and co-stimulation^{3,7,20,32,33}. The latter approach has been shown to promote the generation of CAR T cells with a central memory phenotype, enhanced *in vivo* proliferative capacity and anti-tumor efficacy as compared to stimulation with soluble OKT3 (anti-CD3 Ab) and high-dose IL-2⁶⁷. Alternative stimulation reagents include TransAct™ (Miltenyi Biotec), which is based on colloidal polymeric nanomatrix conjugated with recombinant humanized CD3 and CD28 agonists⁶⁸ and the Expamer technology using anti-CD3/CD28 Fab fragments linked to polymerized Strep-Tactin backbone⁶⁹.

Following T cell activation and gene transfer, modified T cells are expanded to achieve clinically required doses in the presence of cytokines. Historically, IL-2 has been the most used supplement to support T cell proliferation in adoptive T cell transfer protocols⁷⁰. However, *ex vivo* T cell expansion with IL-2 promotes differentiation into terminal effector phenotypes and expansion of regulatory T cells, resulting in T cell products with limited *in vivo* persistence and reduced antitumor efficacy⁵². Consequently, supplementation with alternative γ -chain cytokines such as IL-7, IL-15 and IL-21 has gained considerable attention. It has been shown that replacing IL-2 with a combination of IL-7 and IL-15 promotes the survival and maintenance of minimally differentiated T cells such as T_N and T_{SCM}⁷¹⁻⁷⁴. Systemic comparison of CD19 CAR T cells expanded in the presence of IL-2 or IL7/IL-15 demonstrated enhanced proliferation and superior antitumor activity of IL7/IL-15-cultured cells compared to IL-2-expanded cells which were characterized by higher proportion of regulatory T cells and increased expression of exhaustion markers⁷⁵. Similarly, supplementation with IL-15 alone has been shown to increase anti-apoptotic properties, reduce expression of exhaustion markers and preserve T_{SCM} phenotype

compared to culture with IL-2⁷⁶. Moreover, IL-15-stimulated CAR T cells displayed decreased mTORC1 activity, reduced expression of glycolytic enzymes and enhanced mitochondrial fitness, translating to superior *in vivo* anti-tumor efficacy⁷⁶. In other studies, supplementation with IL-21 has been shown to promote outgrowth of naïve and memory T cells, while CAR T cells expanded with a combination of IL-21 and IL-2 demonstrated improved anti-tumor efficacy compared with cells cultured in IL-2 only^{77,78}.

Besides cytokine supplementation, several studies reported on pharmacological inhibition of specific signaling pathways involved in T cell terminal differentiation and exhaustion to modulate CAR T cell phenotype and functionality⁷⁹. One commonly investigated pathway is the PI3K-AKT-mTOR pathway, crucial for T cell activation, expansion and effector differentiation by promoting glycolytic metabolism and suppressing FOXO1, a transcriptional regulator of T cell memory⁸⁰. For instance, AKT inhibition during CAR T cell manufacturing promoted CD62L-expressing central memory phenotype and superior, compared to conventionally grown cells, anti-leukemic efficacy *in vivo*⁸¹. Similarly, PI3K blockade preserved less differentiated phenotypes with improved *in vivo* persistence, reduced expression of exhaustion markers and enhanced antitumor efficacy in CD33-specific⁸², mesothelin-specific⁸³ and CD19-directed CAR T cells^{84,85}. As another approach, inhibition of interleukin-2-inducible T cell kinase (ITK) with ibrutinib improved the yield and overall quality of CLL patient-derived CAR T cell products, displaying elevated cytokine release capacity *in vitro* and decreased expression of exhaustion markers such as PD-1, TIM-3 and LAG-3⁸⁶. Alternatively, the induction of the Wnt/ β -catenin signaling pathway by GSK β inhibition has been shown to arrest CD8⁺ T cell differentiation into effector cells, enabling the generation of potent CD8⁺ T_{SCM}⁸⁷. This strategy has been then used to obtain CD8⁺ T_{SCM}-enriched CD19 CAR T cell product by sorting CD8⁺CD62L⁺CD45RA⁺ naïve precursors and culturing them in the presence of IL7, IL-21 and GSK β inhibitor TWS119⁸⁸. Compared to cells manufactured with standard clinical protocol, T_{SCM}-enriched CAR T cells demonstrated enhanced metabolic fitness and long-lasting anti-tumor responses in a leukemia xenograft model.

Another important aspect in the optimization of CAR T cell manufacturing is shortening the manufacturing time, which would translate to reduced vein-to-vein time for the benefit of rapidly progressing patients, lower costs and support scaling-up. Recent efforts

have focused on reducing the duration of the CAR T cell expansion step, with several studies showing that shortened *ex vivo* culture time correlated with improved cell functionality. For example, Ghassemi *et al.* demonstrated that CAR T cells harvested after 3 days of culture exhibited superior anti-leukemic activity compared to cells expanded for 9 days in a murine xenograft model ⁸⁹. Next-day manufacturing with the FasT CAR T cell platform, where cells are activated, transduced and administered without expansion, has been recently evaluated in phase 1 clinical trial for B cell ALL (NCT03825718) ⁹⁰. CD19 CAR T cells were successfully manufactured and infused in all 25 enrolled patients, showing a tolerable safety profile and promising efficacy. Moreover, FasT CAR T cells demonstrated superior expansion capacity, less exhaustion and a younger cellular phenotype than conventionally produced CAR T cells *in vitro* ⁹⁰. In addition, the T-Charge™ platform from Novartis has been used to manufacture rapcabtagene autoleucel (YTB323), an autologous CD19-directed CAR-T cell therapy, in a phase 1/2 clinical study in patients with diffuse large B cell lymphoma (NCT03960840) ⁹¹. In this case, the *ex vivo* culture time was reduced to approximately 24 hours and it took less than two days to manufacture the final product, enriched in naïve and stem cell memory T cell subsets. According to a recent update, YTB323 infusion demonstrated a manageable safety profile and durable efficacy at dose level 2 with CR rates of 69% at 6 months ⁹¹. The same rapid manufacturing platform is currently used in phase 2 clinical trial of PHE885, an autologous BCMA-directed CAR T cell therapy for patients with r/r multiple myeloma (NCT05172596) ⁹². The feasibility of rapid (24 h) CAR T cell manufacturing without activation and expansion has been recently reported by Ghassemi *et al.*, demonstrating improved *in vivo* anti-leukemic activity of non-activated CAR T cells compared to their conventionally produced counterparts ⁹³.

Together, these new approaches seem highly promising for reducing the vein-to-vein time, however, since most of the CAR T cell expansion occurs in the patient's body, potential adverse events might be more difficult to predict, calling for further extensive monitoring in larger clinical studies. Finally, despite all the optimization efforts, the quality of CAR T cell product and clinical outcomes are constrained by the autologous starting material. Factors such as advanced patient age, disease type and prior therapies can have a negative impact on T cell function. Thus, one straightforward strategy to maximize T cell fitness would be to collect and preserve leukapheresis material early after diagnosis of

hematological malignancies, before any immunomodulating treatments that could deplete desirable T cell subsets. In addition, recently developed mathematical models trained on clinical data from CAR T cell therapies in hematological malignancies could accurately predict patient clinical response based on the transcriptional signatures of the pre-infusion products ⁹⁴. In the future, such predictive models could guide the optimization of CAR T cell manufacturing process and treatment regimen and identify patients who would benefit more from an allogeneic CAR T cell therapy approach.

2.2 Novel CAR designs to improve efficacy and mitigate toxicity

As introduced before, despite substantial clinical success in specific hematological malignancies, engineered T cell therapies face significant challenges related to short-lasting remission, limited efficacy in solid tumors and on-target off-tumor toxicities. To overcome these limitations, multiple CAR designs have been developed, focusing on improved antigen recognition, increasing resistance to immunosuppression and modulating CAR T cell activity and persistence with safety switches.

For instance, it was proposed that patient relapse due to antigen escape could be mitigated by engineering multispecific CAR T cells by co-expressing two independent CARs on the same T cell (dual-CAR) or expressing a single CAR chain with two scFv binding domains targeting two different antigens (tandem CAR). Dual CD19/CD123 CAR T cells demonstrated superior *in vivo* antileukemic activity compared to either of monospecific cells or a CD19 and CD123 CAR T cells pool ⁹⁵. In another study, CD19/CD20/CD22 trispecific CAR T cells, engineered by co-expressing individual CAR molecules on the same cell using a tricistronic transgene, demonstrated effective B cell ALL targeting *in vitro* and in animal models independent of CD19-expression ⁹⁶. In phase 1 clinical trial, bispecific CD19/CD22 CAR T cells showed good efficacy in 6 patients with r/r B cell ALL, though one relapse with loss of CD19 and diminished CD22 expression was observed 5 months after treatment (NCT03185494) ⁹⁷. Another phase 1 study evaluated CD19/CD22 dual targeting CAR T cells for the treatment of 15 patients with r/r B cell ALL, reporting 86% CR and one-year event-free survival of 32%, with relapses attributed mainly to lack of T cell persistence (NCT03289455) ⁹⁸. Although encouraging, these early studies highlight the

need to optimize antigen binding and CAR signaling to achieve a sustained response and might need to be combined with other approaches.

In solid tumors, the major challenges are related to immunosuppressive tumor microenvironment and lack of tumor-exclusive target antigens. TME is typically enriched with myeloid-derived suppressor cells, tumor-associated macrophages and regulatory T cells, which produce anti-inflammatory cytokines such as TGF- β , IL-10 and IL-4⁹⁹. To counteract these immunosuppressive effects, CAR T cells have been engineered to secrete cytokines such as IL-7, IL-12, IL-15, IL-18 and IL-21 and other molecules like dominant negative TGF- β receptor or CD40L that can increase T cell survival and antitumor activity and reshape TME by inducing innate immune responses and phenotype switches in immunosuppressive cells^{100–106}. In addition, due to the local production of these cytokines in the TME, toxicities observed in the systemic administration of these cytokines can be avoided¹⁰². For example, Chmielewski *et al.* developed CAR T cells with inducible IL-12 secretion upon CAR engagement in the tumor lesion, demonstrating improved control of antigen-positive tumor outgrowth compared to CAR T cells lacking the cytokine, as well as elimination of antigen-negative cancer cells¹⁰¹. The latter was attributed to the accumulation of activated macrophages at the tumor site, indicating that cytokine-armed CAR T cells can induce a bystander anti-tumor immune response, irrespective of antigen expression. Similarly, glypican 3 (GPC3)-specific CAR T cells armored with inducible IL-12 secretion showed enhanced anti-tumor efficacy in hepatocellular carcinoma xenograft models compared to their counterparts without cytokine release capacity¹⁰³. The IL-12 secretion was associated with increased IFN- γ production favoring CD8⁺ T cell infiltration and decreased frequency of regulatory T cells in established tumors. CAR T cells engineered with inducible IL-18 secretion demonstrated superior efficacy against established pancreatic cancer and disseminated human lung carcinoma that were refractory to CAR T cells without cytokine transgene¹⁰⁷. IL-18 CAR T cell treatment induced a global change in TME immune cell composition, with increased numbers of proinflammatory M1 macrophages and NKG2D⁺ NK cells and decreased frequency of regulatory T cells and M2 macrophages. GPC3-specific CAR T cells co-expressing IL-15 and IL-21 exhibited less differentiated phenotype, enhanced *in vivo* expansion, persistence and superior anti-tumor activity against hepatocellular carcinoma xenografts compared

to CAR T cells with single or no cytokine transgene ¹⁰⁴. Glypican 3-specific CAR T cells armored with IL-15 are evaluated in phase 1 clinical trials for the treatment of adult (NCT05103631) and pediatric (NCT04377932) GPC-3-positive solid tumors, while IL-15 and IL-21-armored CAR T cells are currently investigated in pediatric patients with solid tumors (NCT04715191). As another example, CAR T cells can be engineered to express a dominant-negative TGF- β receptor II (dnTGF- β RII) to act as a decoy receptor sequestering TGF- β within the TME and reducing its immunosuppressive effects. The co-expression of dnTGF- β RII in prostate-specific membrane antigen (PSMA)-directed CAR T cells was found to enhance T cell proliferation, *in vivo* persistence and anti-tumor efficacy in aggressive human prostate cancer mouse models ¹⁰⁵. Based on these results, a phase 1 clinical trial was initiated for patients with castration-resistant prostate cancer (NCT03089203) ¹⁰⁶.

Other approaches to reinvigorate T cell antitumor responses have focused on blocking immune checkpoints, such as programmed cell death protein 1 (PD-1), cytotoxic T-lymphocyte associated protein 4 (CTLA-4), lymphocyte activation gene 3 (LAG-3) and T cell immunoreceptor with immunoglobulin and ITAM domain (TIGIT) ¹⁰⁸. In preclinical models, a combination of CAR T cell therapy with anti-PD-1 antibodies was shown to enhance T cell persistence and anti-tumor activity and prevent cell exhaustion ^{109–111}. Several clinical studies have been initiated to evaluate such combination therapies, examples being FDA-approved axicabtagene ciloleucel in combination with anti-PD-L1 antibody atezolizumab for patients with r/r LBCL (NCT02926833) ¹¹² or mesothelin-targeted CAR T cells combined with anti-PD-1 antibody pembrolizumab in patients with mesothelioma (NCT04577326) ¹¹³. However, systemic administration of immune checkpoint inhibitors can lead to severe autoimmune side effects associated with uncontrolled T cell activation ^{114–116}. Other limitations include the short half-life of antibodies, requiring multiple infusions, and insufficient tumor penetration. As such, alternative strategies have been developed to block immune checkpoint signaling directly in the CAR T cells. To date, the most investigated approach has been the genetic knock-out of immune checkpoint receptors using CRISPR-Cas-9 or TALEN gene editing techniques (see **Chapter 1**). Preclinical reports demonstrated that deletion of PD-1, CTLA-4 and LAG-3 yielded CAR T cells less prone to checkpoint inhibition and exhaustion, which translated to enhanced anti-tumor efficacy and persistence *in vivo* ^{117–120},

encouraging clinical evaluation of such genetic disruption in multiple CAR T cell trials (**Chapter 1**). Alternatively, CAR T cells have been engineered to express PD-1 dominant negative receptors, which compete with endogenous receptors for PD-1 ligand binding but do not contain an intracellular signaling domain ^{110,121}. This approach showed long-term tumor suppression in a mouse model and is currently under investigation in a phase 1 clinical study for patients with malignant pleural mesothelioma (NCT04577326). In addition, armored CAR T cells have been modified to secrete PD-1-blocking single-chain variable fragments at the tumor site, showing similar or superior *in vivo* anti-tumor efficacy compared to a combination of CAR T cells with a checkpoint inhibitor ¹²². Other studies employed chimeric switch receptors that consist of the extracellular segments of an inhibitory receptor (*e.g.* PD-1, TIM-3, TIGIT) fused to the intracellular costimulatory domains such as CD28 or 4-1BB and can convert negative signals in the TME into activating signals, promoting T cell persistence and anti-tumor efficacy ^{123–126}.

Next to efficient tumor eradication, safety remains the paramount concern in the next-generation CAR T cell engineering. CAR T cell-associated adverse events could be mitigated by transient CAR expression using mRNA transfection, which restricts the cytotoxic half-life of CAR T cells, as extensively discussed in **Chapter 1**. Alternatively, novel CAR designs incorporating safety switches or suicide genes have been developed to allow for controlled deactivation or depletion of CAR T cells in case of life-threatening toxicities and to prevent long-term on-target off-tumor side effects once cancer has been cured. Several approaches utilizing these concepts have been reported in the literature ^{127–129}. As one example, CAR T cells engineered with inducible caspase 9 could be effectively eliminated by the administration of dimerizing drugs to mitigate GvHD ¹³⁰ and severe and steroid-refractory neurotoxicity in clinical trials ¹³¹. As an alternative to suicide gene activation which leads to an abrupt cessation of CAR T cell therapy, administration of tyrosine kinase inhibitors such as dasatinib can reversibly suppress T cell activation by inhibiting proximal TCR signaling kinases. This approach provides a temporary inhibition of T cell function and could allow for CAR T cell therapy to resume after toxicities have subsided ¹³².

Altogether, these examples illustrate the abundance of novel engineering strategies aiming at advancing CAR T cell therapy towards sustainable responses in a broader range of malignancies.

3 Overcoming manufacturing bottleneck to increase accessibility to T cell therapies

3.1 Non-viral T cell engineering

Despite the great promise of CAR T cell therapy, the complexity of the current viral vector-based manufacturing process and the associated prohibitive cost of commercial CAR T cell therapies have limited their widespread use, with clinical adoption rates lagging behind the number of regulatory approvals. In addition, as illustrated in the previous sections, constantly evolving CAR designs could eventually exceed the relatively limited cargo capacity of viral particles. As such, there is a pressing need for more flexible, safe and cost-effective approaches that would streamline production and logistics, translating to improved patient access to these novel immunotherapies. Much research has been directed towards developing non-viral strategies as a sustainable alternative for next-generation T cell engineering. Non-viral modalities include transient mRNA expression and gene editing, as discussed extensively in **Chapter 1**, as well as transposon-based methods. The latter are represented by DNA transposons such as Sleeping Beauty and piggyBac, which enable stable genomic integration and persistent expression of CAR transgenes in T cells¹³³. These delivery systems consist of a transposon plasmid encoding the gene of interest flanked by the inverted terminal repeats (ITR) and a transposase enzyme that recognizes the ITR sequences and mobilizes the transgene to an acceptor site in the genome *via* a cut-and-paste mechanism. The transposon can be encoded by DNA plasmid or minicircle DNA, while transposase is usually delivered in trans as DNA, mRNA, or protein^{134,135}. Compared to viral transduction, transposons offer larger cargo capacity, cost benefits and the potential to simplify and shorten the manufacturing procedure^{20,136,137}. For instance, Ziopharm Oncology has developed a Sleeping Beauty platform for point-of-care manufacturing of CD19-specific CAR T cells co-expressing membrane-bound IL-15 in less than two days¹³⁸. A limited number of clinical investigations in hematological malignancies initiated to date suggest that Sleeping Beauty is feasible, safe and able to generate stable CAR expression with efficiencies comparable to viral vectors^{139,140}. However, the development of lymphoma in 2 out of 10 patients treated with piggyBac-modified CD19 CAR T cells for r/r B cell malignancies in the CARTELL clinical study highlighted the need for caution in implementing these technologies^{138,141}. As an

alternative, mRNA transfection alleviates the risk of insertional mutagenesis associated with viral vectors and transposons systems and helps to reduce CAR T cell therapy side-effects such as cytokine release syndrome due to the transient nature of CAR expression^{142,143}. Several clinical trials using mRNA-modified CAR T cells are currently underway for the treatment of hematological malignancies and solid tumors, as illustrated in **Chapter 1**. In addition, advancements in gene editing technologies such as transcription activator-like effector nucleases (TALENs), zinc finger nucleases (ZFN) and CRISPR-Cas systems have paved the way for the development of novel complex T cell engineering designs combining CAR transgene insertion with a knock-out of immunosuppressive receptors^{144,145}. In particular, CRISPR-Cas variations have attracted much interest due to their relative simplicity, high editing efficiencies and compatibility with multiplex gene editing (**Chapter 1**)¹⁴⁶.

Several transfection techniques have been developed to enable intracellular delivery of CAR transgenes, gene editing nucleases, cytokine transgenes, *etc.*, as discussed in Chapter 1. To overcome the limitations of viral vector-based CAR T cell manufacturing, vast research efforts have been invested in developing alternative non-viral strategies that would offer a better safety profile, flexibility in cargo type and size, scalability and cost-effectiveness. Various approaches have been investigated, including membrane-permeabilization and carrier-mediated methods, each with its own advantages and drawbacks, as characterized in more detail in **Chapter 1**. Among those, electroporation represents the most used and clinically advanced technology, offering highly efficient T cell transfection in high throughput and compatibility with clinical-grade cell manufacturing platforms such as CliniMACS Prodigy[®] offered by Miltenyi or Lonza's Cocoon[®]^{137,147,148}. However, since electroporation has been associated with substantial cytotoxicity, alternative methods that would preserve cell viability and long-term functionality have been actively sought^{149–151}. These emerging techniques include microfluidic platforms^{149,152,153}, solvent-based membrane permeabilization¹⁵⁴, photoporation^{155–159}, nanostructures¹⁵⁰ and lipid^{160,161} and polymer nanocarriers^{162,163}. The former two technologies have already advanced towards clinical evaluation, while others remain in a more explorative stage of development. For example, SQZ Biotech markets Cell Squeeze[®] microfluidic platform for cost-effective cell engineering at very

high throughput (>10 billion cells per min). The platform has been used in ongoing phase 1 clinical trials evaluating two cancer vaccine candidates, SQZ-PBMC-HPV (NCT04084951) and SQZ-AAC-HPV (NCT04892043), for the treatment of HPV16+ solid tumors^{164–166}. Other microfluidic-based transfection systems currently developed by start-up companies include Hydropore™ microfluidic vortex shedding device by Indee Labs^{152,167}, the Poros™-EP platform from OpenCell Technologies¹⁶⁸ and the volume exchange for convective transfer (VECT) technology by CellFE¹⁶⁹. In addition, Avectas developed the Solupore® transfection platform, which is based on ethanol-mediated membrane permeabilization^{154,170}. With a portfolio including a research-grade device and a recently launched cGMP-compliant manufacturing system, the company aims to accelerate Solupore® translation into the clinic through strategic industrial collaborations.

Building on the previous experience demonstrating that nanoparticle-mediated photoporation enables successful delivery of various macromolecules into immortalized Jurkat cells and pre-activated primary human T cells^{156–159}, in this PhD thesis, we evaluated the applicability of photoporation for intracellular delivery in unstimulated primary human T cells. As discussed before, the ability to modify lymphocytes without a prior activation step is of particular interest for preserving minimally differentiated phenotypes endowed with enhanced *in vivo* activity and enabling rapid manufacturing of CAR T cell therapies towards reduced vein-to-vein time. Although gold nanoparticles (AuNPs) have been the most used nanosensitizers, they are known to fragment upon pulsed laser irradiation, raising concerns over potential genotoxicity due to intercalation in cellular DNA^{171–173}. Moreover, AuNPs are not biodegradable, which poses safety and regulatory hurdles for the clinical translation of photoporation. As such, in this thesis, we opted to work with two recent modifications of the photoporation technology, which either replace standard metallic NPs with biodegradable photosensitizers¹⁵⁸ (**Chapter 2**), or eliminate direct exposure of cells to the photothermal NPs¹⁵⁹ (**Chapter 3**).

In **Chapter 2**, we demonstrated that photoporation with biocompatible and biodegradable polydopamine NPs represents a viable alternative for efficient intracellular delivery of model dextran of 500 kDa in both unstimulated and expanded human T cells, with favorable delivery yields clearly exceeding those achieved previously by AuNP-mediated photoporation in the Jurkat cell line and stimulated primary T cells. Although

encouraging, in the context of adoptive T cell therapy, delivery efficiency and acute toxicity readouts alone are insufficient determinants of the therapeutic efficacy of engineered cell products, highlighting the need for a better understanding of the impact of the applied transfection method on cell phenotype and long-term functionality. Little is known about the potential functional consequences of plasma membrane disruption by nanoparticle-mediated photoporation in primary T cells, with previous studies investigating such cellular responses in Hela cells ^{174,175}. Therefore, taking advantage of our unstimulated T cell model, here we studied T cell propensity to activation after the photoporation treatment as a measure of T cell functionality. We showed that nanosensitizer size should be carefully tailored to cell size and phenotype to avoid excessive cell damage and minimize the impact on long-term T cell activity. In case of intolerable cell perturbation, apart from immediate cell loss detected with an ATP-based viability assay shortly after laser irradiation, the surviving population may carry some persistent phenotypical alterations, which manifest in reduced proliferation and aberrant cytokine production in prolonged *in vitro* culture. Therefore, future optimizations of photoporation parameters should ideally incorporate a functional parameter (*e.g.*, proliferation) next to the standard delivery efficiency and acute cytotoxicity readouts to ensure a minimal impact on the intrinsic T cell fitness. Since our experience indicate immediate cell lysis as a major toxicity mechanism, supplementation of the transfection buffer with osmoregulatory agents could potentially mitigate osmotic imbalance occurring during plasma membrane disruption to better preserve cell viability at harsh irradiation settings.

Moreover, it cannot be excluded that residues of PDNPs remaining in contact with T cells after laser exposure may have long-term functional implications. For metallic NPs, several phenomena in response to laser irradiation such as fragmentation, reshaping and welding have been described ^{171,176}. Similar effects remain to be elucidated for polymeric photosensitizers, with the majority of currently available reports focused on (chemo)-photothermal therapy with near-infrared laser irradiation for tumor ablation ¹⁷⁷⁻¹⁷⁹. To alleviate safety and regulatory concerns over cell exposure to NPs, in **Chapter 3** we showed that photo-responsive iron oxide NPs (IONPs) can be embedded within electrospun fibers to enable intracellular delivery of macromolecules without T cell

contact with free NPs. This system proved applicable for the effective delivery of model FD150 in both quiescent and pre-activated lymphocytes, with a minimal impact on T cell proliferation independently of the applied irradiation settings. Together, results presented in **Chapter 2** and **Chapter 3** attest to the photoporation applicability for intracellular delivery in a highly challenging model of unstimulated T cells, which are traditionally reluctant to carrier-mediated transfection methods. Since our protocols were optimized using FITC dextran of up to 500 kDa as a model cargo, as a next step, it is of interest to validate their efficacy in functional molecule delivery (*e.g.*, mRNA, CRISPR-Cas components) for a *bona fide* genetic modification of T lymphocytes. Once successful CAR T cell generation is achieved, the investigation of functional implications of the photoporation treatment may be strengthened by assessing antigen specific cytolytic activity of photoporated cells *in vitro* and in a relevant *in vivo* model. Nonetheless, *in vitro* analysis performed in the scope of this PhD thesis provides valuable insights for further development of photoporation technology towards effective manipulation of highly functional human T cells.

3.2 Shifting paradigm in T cell manufacturing: towards automation and decentralization

Considering the expanding landscape of T cell-based therapeutics in preclinical and clinical development, it is expected that the number of approved T cell therapies, and eligible patients, will increase continuously in the years to come. To meet this growing demand for adoptive immunotherapies, advances in T cell manufacturing are needed to increase production capacity and reduce manufacturing costs. One strategy that could provide a breakthrough in access to CAR T cell therapies is decentralized or point-of-care manufacturing, which can be achieved by developing a network of regional manufacturing facilities or implementing 'GMP-in-a-box' solutions at the hospital site ¹⁸⁰⁻¹⁸². The latter refers to the use of closed, automated and GMP-compliant manufacturing platforms, which could reduce the need for labor-intensive and contamination-prone procedures, improve manufacturing capacity and shorten vein-to-vein time while reducing logistical costs ^{148,183}. Examples of such platforms currently in use are CliniMACS Prodigy® (Miltenyi Biotec) and Cocoon® (Lonza), which can carry out a complete manufacturing process from T cell selection, transduction or transfection, expansion to harvest (**Figure 4A-B**) ¹⁴⁸. For

non-viral transfections, Miltenyi debuted the Prodigy Electroporator as an add-on feature to the traditional Prodigy system, while the Cocoon platform may be coupled with Lonza's 4D-Nucleofector. Other examples include ExPERT GTx™ electroporation system from MaxCyte that can transfect up to 20 billion cells in cGMP-compliant cartridges and a clinical-grade Solupore™ platform launched by Avestas (**Figure 4C**). The feasibility of point-of-care manufacturing with CliniMACS Prodigy has already been demonstrated in phase 1 clinical studies using bispecific CD19/CD20 CAR T cells for the treatment of r/r non-Hodgkin lymphoma and CLL (NCT03019055)¹⁸⁴, B-cell ALL and LBCL (NCT03233854)¹⁸⁵, and CD19-specific CAR T cells for CD19⁺ B cell malignancies (NCT03144583)¹⁸⁶. In addition, Sheba Medical Center in Israel reported successful dosing of first lymphoma patients with an autologous CD19 CAR T cell therapy produced using Lonza's Cocoon¹⁸⁷. In Belgium, Galapagos has partnered with Lonza to develop a novel decentralized model designed to manufacture CAR T cells at the point-of-care within 7 days of leukapheresis, with no cryopreservation¹⁸⁸. The proprietary platform combines Galapagos' end-to-end xCellit workflow management and monitoring software and Lonza's Cocoon cell manufacturing platform. Although promising, decentralized CAR T cell manufacturing will require updated regulatory frameworks to ensure its safe adoption¹⁸³.



Figure 4. Examples of GMP-compliant automated cell manufacturing platforms. (A) CliniMACS Prodigy® from Miltenyi Biotec. **(B)** Cocoon® platform from Lonza. **(C)** Solupore™ platform from Avestas.

3.3 Off-the-shelf CAR T cells

Given the inherent challenges of autologous CAR T cell therapy, such as variability in cellular starting material, T cell dysfunction, prolonged manufacturing time and high cost, considerable attempts have been made towards the development of ‘universal’, allogeneic CAR T cell therapies (**Chapter 1**). Such off-the-shelf CAR T cell products generated with cells obtained from healthy donors hold the potential to reduce vein-to-vein time and provide a treatment opportunity for heavily pretreated patients with low-quality lymphocytes that would otherwise fail during the manufacturing process^{189,190}. As another advantage, allogeneic CAR T cells can be produced at a much larger scale, with multiple doses per donor, hence reducing the production cost. However, generating universal CAR T cells comes with its own challenges, such as the risk of graft-versus-host-disease (GvHD) and immunological rejection leading to limited *in vivo* persistence of allogeneic CAR T cells. To overcome these issues, gene editing strategies with CRISPR-Cas or TALEN nucleases have been employed to disrupt endogenous T cell receptors and major histocompatibility complex genes, with a number of studies currently under clinical evaluation (**Chapter 1**)^{189,190}.

Alternatively, natural killer (NK) or unconventional $\gamma\delta$ T cells represent another source for allogeneic immunotherapy, as they exhibit innate antitumor activity but lower the risk of GvHD^{191–194}. As an example, cord blood-derived HLA-mismatched NK cells transduced with anti-CD19 CAR, IL-15 and inducible caspase 9 as safety switch have shown promising results in phase 1 clinical trial for patients with non-Hodgkin's lymphoma or chronic lymphocytic leukemia (NCT03056339)¹⁹⁵. In another study, allogeneic $\gamma\delta$ T cells engineered to express anti-CD20 CAR demonstrated a favorable safety profile, encouraging CR rates and sustained durability in patients with B cell lymphoma¹⁹⁶.

Conclusions and outlook

In the past decade, adoptive T cell therapy has established itself as a transformative modality for cancer treatment. With significant progress in understanding the biology of prototype CAR T cells and mechanisms of tumor resistance, advances in synthetic biology and gene editing technologies, future generations of T cell therapeutics will likely benefit from more sophisticated engineering designs combining various functionalities to unlock CAR T cell potential in a widening range of indications, including solid tumors. These engineering innovations must come hand in hand with the development of delivery technologies capable of accommodating such evolving CAR designs and compatible with scalable and cost-effective CAR T cell manufacturing. To overcome limitations associated with viral vector use in the current manufacturing process, various non-viral methods have been explored as a more sustainable alternative for next-generation CAR T cells. In this PhD thesis, we investigated the potential of photoporation as an emerging technology for intracellular delivery of macromolecules in human T cells. Using two photoporation modalities, namely polydopamine nanoparticle-sensitized photoporation and photothermal electrospun nanofibers, we showed effective model macromolecule delivery in both unstimulated and pre-activated T cells, providing important insights for the optimization of photoporation protocols to preserve T cell phenotype and functionality. To facilitate technology adoption, further research should demonstrate successful transfection of functional molecules such as mRNA or CRISPR-Cas9 components and expand the functional assessment of such engineered T cells to, *e.g.*, relevant cytolytic activity models. In addition, future efforts should be directed towards increasing the throughput and adoption of GMP-compliant protocols.

References

1. Siegel RL, Miller KD, Fuchs HE, Jemal A. Cancer statistics, 2022. *CA Cancer J Clin*. 2022;72(1):7-33.
2. Maude SL, Frey N, Shaw PA, et al. Chimeric Antigen Receptor T Cells for Sustained Remissions in Leukemia. *New England Journal of Medicine*. 2014;371(16):1507-1517.
3. Maude SL, Laetsch TW, Buechner J, et al. Tisagenlecleucel in Children and Young Adults with B-Cell Lymphoblastic Leukemia. *New England Journal of Medicine*. 2018;378(5):439-448.
4. Saez-Ibañez AR, Upadhaya S, Partridge T, Shah M, Correa D, Campbell J. Landscape of cancer cell therapies: trends and real-world data. *Nat Rev Drug Discov*. 2022;21(9):631-632.
5. Majzner RG, Mackall CL. Tumor antigen escape from car t-cell therapy. *Cancer Discov*. 2018;8(10):1219-1226.
6. Wang L. Clinical determinants of relapse following CAR-T therapy for hematologic malignancies: Coupling active strategies to overcome therapeutic limitations. *Curr Res Transl Med*. 2022;70(1).
7. Neelapu SS, Locke FL, Bartlett NL, et al. Axicabtagene Ciloleucel CAR T-Cell Therapy in Refractory Large B-Cell Lymphoma. *New England Journal of Medicine*. 2017;377(26):2531-2544.
8. Schuster SJ, Svoboda J, Chong EA, et al. Chimeric Antigen Receptor T Cells in Refractory B-Cell Lymphomas. *New England Journal of Medicine*. 2017;377(26):2545-2554.
9. Shah BD, Ghobadi A, Oluwole OO, et al. KTE-X19 for relapsed or refractory adult B-cell acute lymphoblastic leukaemia: phase 2 results of the single-arm, open-label, multicentre ZUMA-3 study. *The Lancet*. 2021;398(10299):491-502.
10. Brudno JN, Kochenderfer JN. Toxicities of chimeric antigen receptor T cells: Recognition and management. *Blood*. 2016;127(26):3321-3330.
11. Neelapu SS, Tummala S, Kebriaei P, et al. Chimeric antigen receptor T-cell therapy-assessment and management of toxicities. *Nat Rev Clin Oncol*. 2018;15(1):47-62.
12. Morris EC, Neelapu SS, Giavridis T, Sadelain M. Cytokine release syndrome and associated neurotoxicity in cancer immunotherapy. *Nat Rev Immunol*. 2022;22(2):85-96.
13. Shalabi H, Gust J, Taraseviciute A, et al. Beyond the storm — subacute toxicities and late effects in children receiving CAR T cells. *Nat Rev Clin Oncol*. 2021;18(6):363-378.
14. Cappell KM, Sherry RM, Yang JC, et al. Long-Term Follow-Up of Anti-CD19 Chimeric Antigen Receptor T-Cell Therapy. *J Clin Oncol*. 2020;38:3805-3815.
15. Cordeiro A, Bezerra ED, Hirayama A V., et al. Late Events after Treatment with CD19-Targeted Chimeric Antigen Receptor Modified T Cells. *Biology of Blood and Marrow Transplantation*. 2020;26(1):26-33.

16. Logue JM, Zucchetti E, Bachmeier CA, et al. Immune reconstitution and associated infections following axicabtagene ciloleucel in relapsed or refractory large B-cell lymphoma. *Haematologica*. 2021;106(4):978-986.
17. Brudno JN, Natrakul D, Lam N, Dulau-Florea A, Yuan CM, Kochenderfer JN. Acute and delayed cytopenias following CAR T-cell therapy: an investigation of risk factors and mechanisms. *Leuk Lymphoma*. 2022;63(8):1849-1860.
18. U.S. Food and Drug Administration. *Testing of Retroviral Vector-Based Human Gene Therapy Products for Replication Competent Retrovirus During Product Manufacture and Patient Follow-up; Guidance for Industry.*; 2020.
19. Cornetta K, Lin TY, Pellin D, Kohn DB. Meeting FDA Guidance recommendations for replication-competent virus and insertional oncogenesis testing. *Mol Ther Methods Clin Dev*. 2023;28:28-39.
20. Vormittag P, Gunn R, Ghorashian S, Veraitch FS. A guide to manufacturing CAR T cell therapies. *Curr Opin Biotechnol*. 2018;53:164-181.
21. Cliff ERS, Kelkar AH, Russler-Germain DA, et al. High Cost of Chimeric Antigen Receptor T-Cells: Challenges and Solutions. *American Society of Clinical Oncology Educational Book*. 2023;(43).
22. Keating SJ, Gu T, Jun MP, McBride A. Health Care Resource Utilization and Total Costs of Care Among Patients with Diffuse Large B Cell Lymphoma Treated with Chimeric Antigen Receptor T Cell Therapy in the United States. *Transplant Cell Ther*. 2022;28(7):404.e1-404.e6.
23. Jagannath S, Joseph N, Crivera C, et al. Component Costs of CAR-T Therapy in Addition to Treatment Acquisition Costs in Patients with Multiple Myeloma. *Oncol Ther*. 2023;11(2):263-275.
24. Raje N, Berdeja J, Lin Y, et al. Anti-BCMA CAR T-Cell Therapy bb2121 in Relapsed or Refractory Multiple Myeloma. *New England Journal of Medicine*. 2019;380(18):1726-1737.
25. Munshi NC, Anderson LD, Shah N, et al. Idecabtagene Vicleucel in Relapsed and Refractory Multiple Myeloma. *New England Journal of Medicine*. 2021;384(8):705-716.
26. Nastoupil LJ, Jain MD, Feng L, et al. Standard-of-Care Axicabtagene Ciloleucel for Relapsed or Refractory Large B-Cell Lymphoma: Results From the US Lymphoma CAR T Consortium. *Journal of Clinical Oncology*. 2020;38(27):3119-3128.
27. Pasquini MC, Hu ZH, Curran K, et al. Real-world evidence of tisagenlecleucel for pediatric acute lymphoblastic leukemia and non-Hodgkin lymphoma. *Blood Adv*. 2020;4(21):5414-5424.
28. Westin JR, Kersten MJ, Salles G, et al. Efficacy and safety of CD19-directed CAR-T cell therapies in patients with relapsed/refractory aggressive B-cell lymphomas: Observations from the JULIET, ZUMA-1, and TRANSCEND trials. *Am J Hematol*. 2021;96(10):1295-1312.
29. Gilead. Time to CAR T-cell Therapy May Impact Outcomes for Patients With Relapsed/Refractory Large B-cell Lymphoma in New CIBMTR Analysis.

30. Martinez-Cibrian N, Español-Rego M, Pascal M, Delgado J, Ortiz-Maldonado V. Practical aspects of chimeric antigen receptor T-cell administration: From commercial to point-of-care manufacturing. *Front Immunol*. 2022;13.
31. Jo T, Yoshihara S, Okuyama Y, et al. Risk factors for CAR-T cell manufacturing failure among DLBCL patients: A nationwide survey in Japan. *Br J Haematol*. Published online July 1, 2023.
32. Schuster SJ, Bishop MR, Tam CS, et al. Tisagenlecleucel in Adult Relapsed or Refractory Diffuse Large B-Cell Lymphoma. *New England Journal of Medicine*. 2019;380(1):45-56.
33. Locke FL, Ghobadi A, Jacobson CA, et al. Long-term safety and activity of axicabtagene ciloleucel in refractory large B-cell lymphoma (ZUMA-1): a single-arm, multicentre, phase 1–2 trial. *Lancet Oncol*. 2019;20(1):31-42.
34. Wang M, Munoz J, Goy A, et al. KTE-X19 CAR T-Cell Therapy in Relapsed or Refractory Mantle-Cell Lymphoma. *New England Journal of Medicine*. 2020;382(14):1331-1342.
35. Wang M, Munoz J, Goy A, et al. Three-Year Follow-Up of KTE-X19 in Patients With Relapsed/Refractory Mantle Cell Lymphoma, Including High-Risk Subgroups, in the ZUMA-2 Study. *Journal of Clinical Oncology*. 2023;41(3):555-567.
36. Abramson JS, Palomba ML, Gordon LI, et al. Lisocabtagene maraleucel for patients with relapsed or refractory large B-cell lymphomas (TRANSCEND NHL 001): a multicentre seamless design study. *The Lancet*. 2020;396(10254):839-852.
37. Berdeja JG, Madduri D, Usmani SZ, et al. Ciltacabtagene autoleucel, a B-cell maturation antigen-directed chimeric antigen receptor T-cell therapy in patients with relapsed or refractory multiple myeloma (CARTITUDE-1): a phase 1b/2 open-label study. *The Lancet*. 2021;398(10297):314-324.
38. Martin T, Usmani SZ, Berdeja JG, et al. Ciltacabtagene Autoleucel, an Anti-B-cell Maturation Antigen Chimeric Antigen Receptor T-Cell Therapy, for Relapsed/Refractory Multiple Myeloma: CARTITUDE-1 2-Year Follow-Up. *Journal of Clinical Oncology*. 2023;41(6):1265-1274.
39. Gattinoni L, Klebanoff CA, Palmer DC, et al. Acquisition of full effector function in vitro paradoxically impairs the in vivo antitumor efficacy of adoptively transferred CD8+ T cells. *Journal of Clinical Investigation*. 2005;115(6):1616-1626.
40. Klebanoff CA, Gattinoni L, Palmer DC, et al. Determinants of successful CD8 + T-cell adoptive immunotherapy for large established tumors in mice. *Clinical Cancer Research*. 2011;17(16):5343-5352.
41. Fraietta JA, Lacey SF, Orlando EJ, et al. Determinants of response and resistance to CD19 chimeric antigen receptor (CAR) T cell therapy of chronic lymphocytic leukemia. *Nat Med*. 2018;24(5):563-571.
42. Xu Y, Zhang M, Ramos CA, et al. Closely related T-memory stem cells correlate with in vivo expansion of CAR.CD19-T cells and are preserved by IL-7 and IL-15. *Blood*. 2014;123(24):3750-3759.
43. Rossi J, Paczkowski P, Shen YW, et al. *Preinfusion Polyfunctional Anti-CD19 Chimeric Antigen Receptor T Cells Are Associated with Clinical Outcomes in NHL*.

44. Locke FL, Rossi JM, Neelapu SS, et al. Tumor burden, inflammation, and product attributes determine outcomes of axicabtagene ciloleucel in large B-cell lymphoma. *Blood Adv.* 2020;4(19):4898-4911.
45. Deng Q, Han G, Puebla-Osorio N, et al. Characteristics of anti-CD19 CAR T cell infusion products associated with efficacy and toxicity in patients with large B cell lymphomas. *Nat Med.* 2020;26(12):1878-1887.
46. Cohen AD, Garfall AL, Stadtmauer EA, et al. B cell maturation antigen–specific CAR T cells are clinically active in multiple myeloma. *Journal of Clinical Investigation.* 2019;129(6):2210-2221.
47. Klebanoff CA, Gattinoni L, Torabi-Parizi P, et al. Central memory self/tumor-reactive CD8+ T cells confer superior antitumor immunity compared with effector memory T cells. *Proc Natl Acad Sci U S A.* 2005;102(27):9571-9576.
48. Gattinoni L, Klebanoff CA, Restifo NP. Paths to stemness: Building the ultimate antitumour T cell. *Nat Rev Cancer.* 2012;12(10):671-684.
49. Gattinoni L, Speiser DE, Lichterfeld M, Bonini C. T memory stem cells in health and disease. *Nat Med.* 2017;23(1):18-27.
50. Busch DH, Fräßle SP, Sommermeyer D, Buchholz VR, Riddell SR. Role of memory T cell subsets for adoptive immunotherapy. *Semin Immunol.* 2016;28(1):28-34.
51. Gattinoni L, Zhong XS, Palmer DC, et al. Wnt signaling arrests effector T cell differentiation and generates CD8 + memory stem cells. *Nat Med.* 2009;15(7):808-813.
52. Gattinoni L, Lugli E, Ji Y, et al. A human memory T cell subset with stem cell–like properties. *Nat Med.* 2011;17(10):1290-1297.
53. Hinrichs CS, Borman ZA, Cassard L, et al. Adoptively transferred effector cells derived from naïve rather than central memory CD8 + T cells mediate superior antitumor immunity. *Proceedings of the National Academy of Sciences.* 2009;106(41):17469-17474.
54. Hinrichs CS, Borman ZA, Gattinoni L, et al. Human effector CD8 T cells derived from naive rather than memory subsets possess superior traits for adoptive immunotherapy. Published online 2011.
55. Contreras A, Sen S, Tatar AJ, et al. Enhanced local and systemic anti-melanoma CD8+ T cell responses after memory T cell-based adoptive immunotherapy in mice. *Cancer Immunology, Immunotherapy.* 2016;65(5):601-611.
56. Stroncek DF, Ren J, Lee DW, et al. Myeloid cells in peripheral blood mononuclear cell concentrates inhibit the expansion of chimeric antigen receptor T cells. *Cytotherapy.* 2016;18(7):893-901.
57. Elavia N, Panch SR, McManus A, et al. Effects of starting cellular material composition on chimeric antigen receptor T-cell expansion and characteristics. *Transfusion (Paris).* 2019;59(5):1755-1764.

58. Wang H, Tsao ST, Gu M, et al. A simple and effective method to purify and activate T cells for successful generation of chimeric antigen receptor T (CAR-T) cells from patients with high monocyte count. *J Transl Med.* 2022;20(1).
59. Turtle CJ, Hanafi LA, Berger C, et al. *Immunotherapy of Non-Hodgkin's Lymphoma with a Defined Ratio of CD8 + and CD4 + CD19-Specific Chimeric Antigen Receptor-Modified T Cells.*
60. Teoh J, Brown LF. Developing lisocabtagene maraleucel chimeric antigen receptor T-cell manufacturing for improved process, product quality and consistency across CD19+ hematologic indications. *Cytotherapy.* 2022;24(9):962-973.
61. Shah NN, Highfill SL, Shalabi H, et al. *CD4/CD8 T-Cell Selection Affects Chimeric Antigen Receptor (CAR) T-Cell Potency and Toxicity: Updated Results From a Phase I Anti-CD22 CAR T-Cell Trial.* Vol 38.; 2020.
62. Gardner RA, Finney O, Annesley C, et al. Intent-to-treat leukemia remission by CD19 CAR T cells of defined formulation and dose in children and young adults. *Blood.* 2017;129(25):3322-3331.
63. Sommermeyer D, Hudecek M, Kosasih PL, et al. Chimeric antigen receptor-modified T cells derived from defined CD8+ and CD4+ subsets confer superior antitumor reactivity in vivo. *Leukemia.* 2016;30(2):492-500.
64. Tay RE, Richardson EK, Toh HC. Revisiting the role of CD4+ T cells in cancer immunotherapy—new insights into old paradigms. *Cancer Gene Ther.* 2021;28(1-2):5-17.
65. Hay KA, Hanafi LA, Li D, et al. Kinetics and biomarkers of severe cytokine release syndrome after CD19 chimeric antigen receptor–modified T-cell therapy. *Blood.* 2017;130(21):2295-2306.
66. Stock S, Schmitt M, Sellner L. Optimizing manufacturing protocols of chimeric antigen receptor t cells for improved anticancer immunotherapy. *Int J Mol Sci.* 2019;20(24).
67. Barrett DM, Singh N, Liu X, et al. Relation of clinical culture method to T-cell memory status and efficacy in xenograft models of adoptive immunotherapy. *Cytotherapy.* 2014;16(5):619-630.
68. Mock U, Nickolay L, Philip B, et al. Automated manufacturing of chimeric antigen receptor T cells for adoptive immunotherapy using CliniMACS prodigy. *Cytotherapy.* 2016;18(8):1002-1011.
69. Poltorak MP, Graef P, Tschulik C, et al. Expamers: a new technology to control T cell activation. *Sci Rep.* 2020;10(1).
70. Dwyer CJ, Knochelmann HM, Smith AS, et al. Fueling cancer immunotherapy with common gamma chain cytokines. *Front Immunol.* 2019;10(FEB).
71. Cieri N, Camisa B, Cocchiarella F, et al. IL-7 and IL-15 instruct the generation of human memory stem T cells from naive precursors. *Blood.* 2013;121(4):573-584.
72. Xu Y, Zhang M, Ramos CA, et al. Closely related T-memory stem cells correlate with in vivo expansion of CAR.CD19-T cells and are preserved by IL-7 and IL-15. *Blood.* 2014;123(24):3750-3759.

73. Gargett T, Brown MP. Different cytokine and stimulation conditions influence the expansion and immune phenotype of third-generation chimeric antigen receptor T cells specific for tumor antigen GD2. *Cytotherapy*. 2015;17(4):487-495.
74. Hoffmann JM, Schubert ML, Wang L, et al. Differences in expansion potential of naive chimeric antigen receptor T cells from healthy donors and untreated chronic lymphocytic leukemia patients. *Front Immunol*. 2018;8(JAN).
75. Zhou J, Jin L, Wang F, Zhang Y, Liu B, Zhao T. Chimeric antigen receptor T (CAR-T) cells expanded with IL-7/IL-15 mediate superior antitumor effects. *Protein Cell*. 2019;10(10):764-769.
76. Alizadeh D, Wong RA, Yang X, et al. IL15 enhances CAR-T cell antitumor activity by reducing mTORC1 activity and preserving their stem cell memory phenotype. *Cancer Immunol Res*. 2019;7(5):759-772.
77. Hinrichs CS, Spolski R, Paulos CM, et al. IL-2 and IL-21 confer opposing differentiation programs to CD8+ T cells for adoptive immunotherapy. *Blood*. 2008;111(11):5326-5333.
78. Singh H, Figliola MJ, Dawson MJ, et al. Reprogramming CD19-specific T cells with IL-21 signaling can improve adoptive immunotherapy of B-lineage malignancies. *Cancer Res*. 2011;71(10):3516-3527.
79. Zhang H, Passang T, Ravindranathan S, et al. The magic of small-molecule drugs during ex vivo expansion in adoptive cell therapy. *Front Immunol*. 2023;14.
80. Kim EH, Suresh M. Role of PI3K/Akt signaling in memory CD8 T cell differentiation. *Front Immunol*. 2013;4(FRB).
81. Klebanoff CA, Crompton JG, Leonard AJ, et al. Inhibition of AKT signaling uncouples T cell differentiation from expansion for receptor-engineered adoptive immunotherapy. *JCI Insight*. 2017;2(23).
82. Zheng W, O'Hear CE, Alli R, et al. PI3K orchestration of the in vivo persistence of chimeric antigen receptor-modified T cells. *Leukemia*. 2018;32(5):1157-1167.
83. Bowers JS, Majchrzak K, Nelson MH, et al. PI3K δ inhibition enhances the antitumor fitness of adoptively transferred CD8+ T cells. *Front Immunol*. 2017;8(SEP).
84. Stock S, Übelhart R, Schubert ML, et al. Idelalisib for optimized CD19-specific chimeric antigen receptor T cells in chronic lymphocytic leukemia patients. *Int J Cancer*. 2019;145(5):1312-1324.
85. Funk CR, Wang S, Chen KZ, et al. PI3K δ/γ inhibition promotes human CART cell epigenetic and metabolic reprogramming to enhance antitumor cytotoxicity. *Blood*. 2022;139(4):523-537.
86. Fan F, Yoo HJ, Stock S, et al. Ibrutinib for improved chimeric antigen receptor T-cell production for chronic lymphocytic leukemia patients. *Int J Cancer*. 2021;148(2):419-428.
87. Gattinoni L, Zhong XS, Palmer DC, et al. Wnt signaling arrests effector T cell differentiation and generates CD8 + memory stem cells. *Nat Med*. 2009;15(7):808-813.

88. Sabatino M, Hu J, Sommariva M, et al. Generation of clinical-grade CD19-specific CAR-modified CD8 1 memory stem cells for the treatment of human B-cell malignancies.
89. Ghassemi S, Nunez-Cruz S, O'Connor RS, et al. Reducing ex vivo culture improves the antileukemic activity of chimeric antigen receptor (CAR) T cells. *Cancer Immunol Res.* 2018;6(9):1100-1109.
90. Yang J, He J, Zhang X, et al. Next-day manufacture of a novel anti-CD19 CAR-T therapy for B-cell acute lymphoblastic leukemia: first-in-human clinical study. *Blood Cancer J.* 2022;12(7).
91. Barba P, Kwon M, Briones J, et al. YTB323 (Rapcabtagene Autoleucel) Demonstrates Durable Efficacy and a Manageable Safety Profile in Patients with Relapsed/Refractory Diffuse Large B-Cell Lymphoma: Phase I Study Update. *Blood.* 2022;140(Supplement 1):1056-1059.
92. Munshi N, Spencer A, Raab MS, et al. PB1983: TRIAL-IN-PROGRESS: PHASE II STUDY OF PHE885, A B-CELL MATURATION ANTIGEN-DIRECTED CHIMERIC ANTIGEN RECEPTOR T-CELL THERAPY, IN ADULTS WITH RELAPSED AND/OR REFRACTORY MULTIPLE MYELOMA. *Hemasphere.* 2022;6:1855-1856.
93. Ghassemi S, Durgin JS, Nunez-Cruz S, et al. Rapid manufacturing of non-activated potent CAR T cells. *Nat Biomed Eng.* 2022;6(2):118-128.
94. Kirouac DC, Zmurchok C, Deyati A, Sicherman J, Bond C, Zandstra PW. Deconvolution of clinical variance in CAR-T cell pharmacology and response. *Nat Biotechnol.* Published online 2023.
95. Ruella M, Barrett DM, Kenderian SS, et al. Dual CD19 and CD123 targeting prevents antigen-loss relapses after CD19-directed immunotherapies. *Journal of Clinical Investigation.* 2016;126(10):3814-3826.
96. Fousek K, Watanabe J, Joseph SK, et al. CAR T-cells that target acute B-lineage leukemia irrespective of CD19 expression. *Leukemia.* 2021;35(1):75-89.
97. Dai H, Wu Z, Jia H, et al. Bispecific CAR-T cells targeting both CD19 and CD22 for therapy of adults with relapsed or refractory B cell acute lymphoblastic leukemia. *J Hematol Oncol.* 2020;13(1).
98. Cordoba S, Onuoha S, Thomas S, et al. CAR T cells with dual targeting of CD19 and CD22 in pediatric and young adult patients with relapsed or refractory B cell acute lymphoblastic leukemia: a phase 1 trial. *Nat Med.* 2021;27(10):1797-1805.
99. Hawkins ER, D'souza RR, Klampatsa A. Armored CAR T-cells: The next chapter in T-cell cancer immunotherapy. *Biologics.* 2021;15:95-105.
100. Li L, Li Q, Yan ZX, et al. Transgenic expression of IL-7 regulates CAR-T cell metabolism and enhances in vivo persistence against tumor cells. *Sci Rep.* 2022;12(1).
101. Chmielewski M, Kopecky C, Hombach AA, Abken H. IL-12 Release by Engineered T Cells Expressing Chimeric Antigen Receptors Can Effectively Muster an Antigen-Independent Macrophage Response on Tumor Cells That Have Shut Down Tumor Antigen Expression. *Cancer Res.* 2011;71(17):5697-5706.

102. Chmielewski M, Abken H. CAR T cells transform to trucks: Chimeric antigen receptor-redirected T cells engineered to deliver inducible IL-12 modulate the tumour stroma to combat cancer. *Cancer Immunology, Immunotherapy*. 2012;61(8):1269-1277.
103. Liu Y, Di S, Shi B, et al. Armored Inducible Expression of IL-12 Enhances Antitumor Activity of Glypican-3-Targeted Chimeric Antigen Receptor-Engineered T Cells in Hepatocellular Carcinoma. *The Journal of Immunology*. 2019;203(1):198-207.
104. Batra SA, Rathi P, Guo L, et al. Glypican-3-specific CAR T cells coexpressing IL15 and IL21 have superior expansion and antitumor activity against hepatocellular carcinoma. *Cancer Immunol Res*. 2020;8(3):309-320.
105. Kloss CC, Lee J, Zhang A, et al. Dominant-Negative TGF- β Receptor Enhances PSMA-Targeted Human CAR T Cell Proliferation And Augments Prostate Cancer Eradication. *Molecular Therapy*. 2018;26(7):1855-1866.
106. Narayan V, Barber-Rotenberg JS, Jung IY, et al. PSMA-targeting TGF β -insensitive armored CAR T cells in metastatic castration-resistant prostate cancer: a phase 1 trial. *Nat Med*. 2022;28(4):724-734.
107. Chmielewski M, Abken H. CAR T Cells Releasing IL-18 Convert to T-Bethigh FoxO1low Effectors that Exhibit Augmented Activity against Advanced Solid Tumors. *Cell Rep*. 2017;21(11):3205-3219.
108. Al-Haideri M, Tondok SB, Safa SH, et al. CAR-T cell combination therapy: the next revolution in cancer treatment. *Cancer Cell Int*. 2022;22(1).
109. John LB, Kershaw MH, Darcy PK. Blockade of PD-1 immunosuppression boosts CAR T-cell therapy. *Oncoimmunology*. 2013;2(10):e26286.
110. Cherkassky L, Morello A, Villena-Vargas J, et al. Human CAR T cells with cell-intrinsic PD-1 checkpoint blockade resist tumor-mediated inhibition. *Journal of Clinical Investigation*. 2016;126(8):3130-3144.
111. Gargett T, Yu W, Dotti G, et al. GD2-specific CAR T Cells Undergo Potent Activation and Deletion Following Antigen Encounter but can be Protected from Activation-induced Cell Death by PD-1 Blockade. *Molecular Therapy*. 2016;24(6):1135-1149.
112. Jacobson CA, Locke FL, Miklos DB, et al. End of Phase 1 Results from Zuma-6: Axicabtagene Ciloleucef (Axi-Cel) in Combination with Atezolizumab for the Treatment of Patients with Refractory Diffuse Large B Cell Lymphoma. *Biology of Blood and Marrow Transplantation*. 2019;25(3):S173.
113. Adusumilli PS, Zauderer MG, Rivière I, et al. A phase I trial of regional mesothelin-targeted CAR T-cell therapy in patients with malignant pleural disease, in combination with the anti-PD-1 agent pembrolizumab. *Cancer Discov*. 2021;11(11):2748-2763.
114. Hofmann L, Forschner A, Loquai C, et al. Cutaneous, gastrointestinal, hepatic, endocrine, and renal side-effects of anti-PD-1 therapy. *Eur J Cancer*. 2016;60:190-209.
115. Kong X, Chen L, Su Z, et al. Toxicities associated with immune checkpoint inhibitors: a systematic study. *International Journal of Surgery*. 2023;109(6):1753-1768.

116. Zhou X, Yao Z, Bai H, et al. Treatment-related adverse events of PD-1 and PD-L1 inhibitor-based combination therapies in clinical trials: a systematic review and meta-analysis. *Lancet Oncol.* 2021;22(9):1265-1274.
117. Hu W, Zi Z, Jin Y, et al. CRISPR/Cas9-mediated PD-1 disruption enhances human mesothelin-targeted CAR T cell effector functions. *Cancer Immunology, Immunotherapy.* 2019;68(3):365-377.
118. Rupp LJ, Schumann K, Roybal KT, et al. CRISPR/Cas9-mediated PD-1 disruption enhances anti-Tumor efficacy of human chimeric antigen receptor T cells. *Sci Rep.* 2017;7(1):1-10.
119. Zhang Y, Zhang X, Cheng C, et al. CRISPR-Cas9 mediated LAG-3 disruption in CAR-T cells. *Front Med.* 2017;11(4):554-562.
120. Choi BD, Yu X, Castano AP, et al. CRISPR-Cas9 disruption of PD-1 enhances activity of universal EGFRvIII CAR T cells in a preclinical model of human glioblastoma. *J Immunother Cancer.* 2019;7(1).
121. Kiesgen S, Linot C, Quach HT, et al. Abstract LB-378: Regional delivery of clinical-grade mesothelin-targeted CAR T cells with cell-intrinsic PD-1 checkpoint blockade: Translation to a phase I trial. *Cancer Res.* 2020;80(16_Supplement):LB-378-LB-378.
122. Rafiq S, Yeku OO, Jackson HJ, et al. Targeted delivery of a PD-1-blocking scFV by CAR-T cells enhances anti-tumor efficacy in vivo. *Nat Biotechnol.* 2018;36(9):847-858.
123. Liu X, Ranganathan R, Jiang S, et al. A chimeric switch-receptor targeting PD1 augments the efficacy of second-generation CAR T cells in advanced solid tumors. *Cancer Res.* 2016;76(6):1578-1590.
124. Zhao S, Wang C, Lu P, et al. Switch receptor T3/28 improves long-term persistence and antitumor efficacy of CAR-T cells. *J Immunother Cancer.* 2021;9(12).
125. Hoogi S, Eisenberg V, Mayer S, Shamul A, Barliya T, Cohen CJ. A TIGIT-based chimeric co-stimulatory switch receptor improves T-cell anti-tumor function. *J Immunother Cancer.* 2019;7(1):243.
126. Liu H, Lei W, Zhang C, et al. CD19-specific CAR T cells that express a PD-1/CD28 chimeric switch-receptor are effective in patients with PD-L1⁺ B-cell lymphoma. *Clinical Cancer Research.* 2021;27(2):473-484.
127. Rafiq S, Hackett CS, Brentjens RJ. Engineering strategies to overcome the current roadblocks in CAR T cell therapy. *Nat Rev Clin Oncol.* 2020;17(3):147-167.
128. Akhoundi M, Mohammadi M, Sahraei SS, Sheykhasan M, Fayazi N. CAR T cell therapy as a promising approach in cancer immunotherapy: challenges and opportunities.
129. Hamieh M, Mansilla-Soto J, Rivière I, Sadelain M. Programming CAR T Cell Tumor Recognition: Tuned Antigen Sensing and Logic Gating. *Cancer Discov.* 2023;13(4):829-843.
130. Di Stasi A, Tey SK, Dotti G, et al. Inducible Apoptosis as a Safety Switch for Adoptive Cell Therapy. *New England Journal of Medicine.* 2011;365(18):1673-1683.
131. Foster MC, Savoldo B, Lau W, et al. Utility of a safety switch to abrogate CD19.CAR T-cell-associated neurotoxicity. *Blood.* 2021;137(23):3306-3309.

132. Mestermann K, Giavridis T, Weber J, et al. The tyrosine kinase inhibitor dasatinib acts as a pharmacologic on/off switch for CAR T cells. *Sci Transl Med*. 2019;11(499).
133. Muñoz-López M, García-Pérez JL. *DNA Transposons: Nature and Applications in Genomics*. Vol 11.; 2010.
134. Monjezi R, Miskey C, Gogishvili T, et al. Enhanced CAR T-cell engineering using non-viral Sleeping Beauty transposition from minicircle vectors. *Leukemia*. 2017;31(1):186-194.
135. Prommersberger S, Reiser M, Beckmann J, et al. CARAMBA: a first-in-human clinical trial with SLAMF7 CAR-T cells prepared by virus-free Sleeping Beauty gene transfer to treat multiple myeloma. *Gene Ther*. 2021;28(9):560-571.
136. de Macedo Abdo L, Barros LRC, Saldanha Viegas M, et al. Development of CAR-T cell therapy for B-ALL using a point-of-care approach. *Oncoimmunology*. 2020;9(1).
137. Lock D, Monjezi R, Brandes C, et al. Automated, scaled, transposon-based production of CAR T cells. *J Immunother Cancer*. 2022;10(9).
138. Hurton L V, Singh H, Switzer KC, et al. Very Rapid Production of CAR+ T-Cells upon Non-Viral Gene Transfer Using the Sleeping Beauty System. *Blood*. 2016;128(22):2807.
139. Magnani CF, Tettamanti S, Alberti G, et al. Transposon-Based CAR T Cells in Acute Leukemias: Where are We Going? *Cells*. 2020;9(6).
140. Moretti A, Ponzo M, Nicolette CA, Tcherepanova IY, Biondi A, Magnani CF. The Past, Present, and Future of Non-Viral CAR T Cells. *Front Immunol*. 2022;13(June):1-25.
141. Bishop DC, Clancy LE, Simms R, et al. Development of CAR T-cell lymphoma in 2 of 10 patients effectively treated with *piggyBac* -modified CD19 CAR T cells. *Blood*. 2021;138(16):1504-1509.
142. Liu C, Shi Q, Huang X, Koo S, Kong N, Tao W. mRNA-based cancer therapeutics. *Nat Rev Cancer*. Published online 2023.
143. Foster JB, Barrett DM, Karikó K. The Emerging Role of In Vitro-Transcribed mRNA in Adoptive T Cell Immunotherapy. *Molecular Therapy*. 2019;27(4):747-756.
144. Dimitri A, Herbst F, Fraietta JA. Engineering the next-generation of CAR T-cells with CRISPR-Cas9 gene editing. *Mol Cancer*. 2022;21(1).
145. Wagner DL, Koehl U, Chmielewski M, Scheid C, Stripecke R. Review: Sustainable Clinical Development of CAR-T Cells – Switching From Viral Transduction Towards CRISPR-Cas Gene Editing. *Front Immunol*. 2022;13(June):1-13.
146. Doudna JA. The promise and challenge of therapeutic genome editing. *Nature*. 2020;578(7794):229-236.
147. Alzubi J, Lock D, Rhiel M, et al. Automated generation of gene-edited CAR T cells at clinical scale. *Mol Ther Methods Clin Dev*. 2021;20:379-388.
148. Song HW, Somerville RP, Stroncek DF, Highfill SL. Scaling up and scaling out: Advances and challenges in manufacturing engineered T cell therapies. *Int Rev Immunol*. 2022;41(6):638-648.

149. DiTommaso T, Cole JM, Cassereau L, et al. Cell engineering with microfluidic squeezing preserves functionality of primary immune cells in vivo. *Proceedings of the National Academy of Sciences*. 2018;115(46):E10907-E10914.
150. Tay A, Melosh N. Transfection with Nanostructure Electro-Injection is Minimally Perturbative. *Adv Ther (Weinh)*. 2019;2(12):1900133.
151. Schmiderer L, Subramaniam A, Žemaitis K, et al. Efficient and nontoxic biomolecule delivery to primary human hematopoietic stem cells using nanostraws. *Proc Natl Acad Sci U S A*. 2020;117(35):21267-21273.
152. Jarrell JA, Twite AA, Lau KHWJ, et al. Intracellular delivery of mRNA to human primary T cells with microfluidic vortex shedding. *Sci Rep*. 2019;9(1):3214.
153. Sharei A, Zoldan J, Adamo A, et al. A vector-free microfluidic platform for intracellular delivery. *Proceedings of the National Academy of Sciences*. 2013;110(6):2082-2087.
154. O'Dea S, Annibaldi V, Gallagher L, et al. Vector-free intracellular delivery by reversible permeabilization. Omri A, ed. *PLoS One*. 2017;12(3):e0174779.
155. Raes L, Van Hecke C, Michiels J, et al. Gold Nanoparticle-Mediated Photoporation Enables Delivery of Macromolecules over a Wide Range of Molecular Weights in Human CD4+ T Cells. *Crystals (Basel)*. 2019;9(8):411.
156. Raes L, Stremersch S, Fraire JC, et al. Intracellular Delivery of mRNA in Adherent and Suspension Cells by Vapor Nanobubble Photoporation. *Nanomicro Lett*. 2020;12(1):1-17.
157. Raes L, Pille M, Harizaj A, et al. Cas9 RNP transfection by vapor nanobubble photoporation for ex vivo cell engineering. *Mol Ther Nucleic Acids*. 2021;25(September):696-707.
158. Harizaj A, Wels M, Raes L, et al. Photoporation with Biodegradable Polydopamine Nanosensitizers Enables Safe and Efficient Delivery of mRNA in Human T Cells. *Adv Funct Mater*. 2021;31(28):2102472.
159. Xiong R, Hua D, Van Hoeck J, et al. Photothermal nanofibres enable safe engineering of therapeutic cells. *Nat Nanotechnol*. 2021;16(11):1281-1291.
160. Billingsley MM, Singh N, Ravikumar P, Zhang R, June CH, Mitchell MJ. Ionizable Lipid Nanoparticle-Mediated mRNA Delivery for Human CAR T Cell Engineering. *Nano Lett*. 2020;20(3):1578-1589.
161. Billingsley MM, Hamilton AG, Mai D, et al. Orthogonal Design of Experiments for Optimization of Lipid Nanoparticles for mRNA Engineering of CAR T Cells. *Nano Lett*. 2022;22(1):533-542.
162. Smith TT, Stephan SB, Moffett HF, et al. In situ programming of leukaemia-specific T cells using synthetic DNA nanocarriers. *Nat Nanotechnol*. 2017;12(8):813-820.
163. Parayath NN, Stephan SB, Koehne AL, Nelson PS, Stephan MT. In vitro-transcribed antigen receptor mRNA nanocarriers for transient expression in circulating T cells in vivo. *Nat Commun*. 2020;11(1).

164. Park JC, Bernstein H, Loughhead S, et al. Cell Squeeze: driving more effective CD8 T-cell activation through cytosolic antigen delivery. *Immuno-Oncology and Technology*. 2022;16(C):100091.
165. Wang S, Yang Y, Zha Y, Li N. Microfluidic cell squeeze-based vaccine comes into clinical investigation. *NPJ Vaccines*. 2023;8(1):65.
166. Jimeno A, Baranda J, Iams WT, et al. Phase 1 study to determine the safety and dosing of autologous PBMCs modified to present HPV16 antigens (SQZ-PBMC-HPV) in HLA-A*02+ patients with HPV16+ solid tumors. *Invest New Drugs*. 2023;41(2):284-295.
167. Jarrell JA, Sytsma BJ, Wilson LH, et al. Numerical optimization of microfluidic vortex shedding for genome editing T cells with Cas9. *Sci Rep*. 2021;11(1):1-13.
168. Meacham JM, Durvasula K, Degertekin FL, Fedorov AG. Enhanced intracellular delivery via coordinated acoustically driven shear mechanoporation and electrophoretic insertion. *Sci Rep*. 2018;8(1).
169. Liu A, Islam M, Stone N, et al. Microfluidic generation of transient cell volume exchange for convectively driven intracellular delivery of large macromolecules. *Materials Today*. 2018;21(7):703-712.
170. Kavanagh H, Dunne S, Martin DS, et al. A novel non-viral delivery method that enables efficient engineering of primary human T cells for ex vivo cell therapy applications. *Cytotherapy*. 2021;23(9):852-860.
171. Bongiovanni G, Olshin PK, Yan C, Voss JM, Drabbels M, Lorenz UJ. The fragmentation mechanism of gold nanoparticles in water under femtosecond laser irradiation. *Nanoscale Adv*. 2021;3(18):5277-5283.
172. Ziefuss AR, Reich S, Reichenberger S, Levantino M, Plech A. In situ structural kinetics of picosecond laser-induced heating and fragmentation of colloidal gold spheres. *Physical Chemistry Chemical Physics*. 2020;22(9):4993-5001.
173. Tsoi M, Kuhn H, Brandau W, Esche H, Schmid G. Cellular uptake and toxicity of Au55 clusters. *Small*. 2005;1(8-9):841-844.
174. Houthaev G, De Smedt SC, Braeckmans K, De Vos WH. The cellular response to plasma membrane disruption for nanomaterial delivery. *Nano Converg*. 2022;9(1):6.
175. Fraire JC, Houthaev G, Liu J, et al. Vapor nanobubble is the more reliable photothermal mechanism for inducing endosomal escape of siRNA without disturbing cell homeostasis. *Journal of Controlled Release*. 2020;319(December 2019):262-275.
176. González-Rubio G, Guerrero-Martínez A, Liz-Marzán LM. Reshaping, Fragmentation, and Assembly of Gold Nanoparticles Assisted by Pulse Lasers. *Acc Chem Res*. 2016;49(4):678-686.
177. Liu Y, Ai K, Liu J, Deng M, He Y, Lu L. Dopamine-melanin colloidal nanospheres: An efficient near-infrared photothermal therapeutic agent for in vivo cancer therapy. *Advanced Materials*. 2013;25(9):1353-1359.

178. Poinard B, Lam SAE, Neoh KG, Kah JCY. Mucopenetration and biocompatibility of polydopamine surfaces for delivery in an Ex Vivo porcine bladder. *Journal of Controlled Release*. 2019;300(February):161-173.
179. Farokhi M, Mottaghitalab F, Saeb MR, Thomas S. Functionalized theranostic nanocarriers with bio-inspired polydopamine for tumor imaging and chemo-photothermal therapy. *Journal of Controlled Release*. 2019;309(July):203-219.
180. Harrison RP, Rafiq QA, Medcalf N. Centralised versus decentralised manufacturing and the delivery of healthcare products: A United Kingdom exemplar. *Cytotherapy*. 2018;20(6):873-890.
181. Harrison RP, Ruck S, Medcalf N, Rafiq QA. Decentralized manufacturing of cell and gene therapies: Overcoming challenges and identifying opportunities. *Cytotherapy*. 2017;19(10):1140-1151.
182. Abou-El-Enein M, Elsallab M, Feldman SA, et al. Scalable Manufacturing of CAR T Cells for Cancer Immunotherapy. *Blood Cancer Discov*. 2021;2(5):408-422.
183. Geethakumari PR, Ramasamy DP, Dholaria B, Berdeja J, Kansagra A. Balancing Quality, Cost, and Access During Delivery of Newer Cellular and Immunotherapy Treatments. *Curr Hematol Malig Rep*. 2021;16(4):345-356.
184. Shah NN, Johnson BD, Schneider D, et al. Bispecific anti-CD20, anti-CD19 CAR T cells for relapsed B cell malignancies: a phase 1 dose escalation and expansion trial. *Nat Med*. 2020;26(10):1569-1575.
185. Spiegel JY, Patel S, Muffly L, et al. CAR T cells with dual targeting of CD19 and CD22 in adult patients with recurrent or refractory B cell malignancies: a phase 1 trial. *Nat Med*. 2021;27(8):1419-1431.
186. Castella M, Caballero-Baños M, Ortiz-Maldonado V, et al. Point-of-care CAR T-cell production (ARI-0001) using a closed semi-automatic bioreactor: Experience from an academic phase i clinical trial. *Front Immunol*. 2020;11.
187. Lonza and Sheba Medical Center Use Cocoon® Platform and Show Successful Clinical Outcomes in Patients Treated with CAR-T Cell Immunotherapy. <https://www.lonza.com/news/2021-08-12-15-00>. Accessed 19/08/2023.
188. CellPoint and Lonza Enter Strategic Collaboration to Deliver CAR-T Cells to Patients at Point-of-Care. <https://www.prnewswire.com/news-releases/cellpoint-and-lonza-enter-strategic-collaboration-to-deliver-car-t-cells-to-patients-at-point-of-care-301318290.html>. Accessed 19/08/2023.
189. Depil S, Duchateau P, Grupp SA, Mufti G, Poirot L. 'Off-the-shelf' allogeneic CAR T cells: development and challenges. *Nat Rev Drug Discov*. 2020;19(3):185-199.
190. Khan A, Sarkar E. CRISPR/Cas9 encouraged CAR-T cell immunotherapy reporting efficient and safe clinical results towards cancer. *Cancer Treat Res Commun*. 2022;33.
191. Xie G, Dong H, Liang Y, Ham JD, Rizwan R, Chen J. CAR-NK cells: A promising cellular immunotherapy for cancer. *EBioMedicine*. 2020;59.

192. Pan K, Farrukh H, Chittepu VCSR, Xu H, Pan C xian, Zhu Z. CAR race to cancer immunotherapy: from CAR T, CAR NK to CAR macrophage therapy. *Journal of Experimental and Clinical Cancer Research*. 2022;41(1).
193. Kilgour MK, Bastin DJ, Lee SH, Ardolino M, McComb S, Visram A. Advancements in CAR-NK therapy: lessons to be learned from CAR-T therapy. *Front Immunol*. 2023;14.
194. Saura-Esteller J, de Jong M, King LA, et al. Gamma Delta T-Cell Based Cancer Immunotherapy: Past-Present-Future. *Front Immunol*. 2022;13.
195. Liu E, Marin D, Banerjee P, et al. Use of CAR-Transduced Natural Killer Cells in CD19-Positive Lymphoid Tumors. *New England Journal of Medicine*. 2020;382(6):545-553.
196. Neelapu SS, Stevens DA, Hamadani M, et al. A Phase 1 Study of ADI-001: Anti-CD20 CAR-Engineered Allogeneic Gamma Delta1 ($\gamma\delta$) T Cells in Adults with B-Cell Malignancies. *Blood*. 2022;140(Supplement 1):4617-4619.

SUMMARY AND CONCLUSIONS

Adoptive T cell therapies (ACT) hold significant potential to transform cancer treatment by harnessing the immune system to attack malignant cells. Among different ACT modalities, chimeric antigen receptor (CAR)-engineered T cell therapies that rely on *ex vivo* genetic modification to redirect T cell specificity with a synthetic receptor against tumor antigen have demonstrated remarkable clinical responses in patients with certain hematological malignancies. With six CAR T cell products approved by the FDA to date and over 800 ongoing clinical trials, CAR T cell therapeutics remain the most investigated form of adoptive cell transfer in the immune-oncology pipeline, with the global CAR T cell market projected to grow significantly over the next decade. Despite this great enthusiasm, several limitations remain to be addressed to unlock CAR T cell potential in a broad range of indications and larger patient cohorts.

As outlined in **Chapter 1**, CAR T cell therapy faces several challenges related to the biological activity of the engineered cell products, including poor efficacy in solid tumors, limited durability of patient responses and the risk of severe adverse events such as cytokine release syndrome and neurotoxicity. Hence, it has been recognized that further progress in CAR T cell therapy would require combinatorial engineering designs centering around multiple targeting, disruption of negative regulators of T cell function, extra functionalities like *de novo* cytokine production, or incorporation of safety switches. To realize such advanced engineering strategies, one critical aspect is the selection of suitable transfection technologies that can accommodate and effectively deliver evolving CAR constructs, gene editing components and/or complimentary molecules to modulate T cell potency upon re-infusion in patients. To date, CAR T cell manufacturing relies on gammaretroviral and lentiviral vectors for efficient transgene incorporation. However, their use comes with a set of drawbacks, such as safety concerns, high cost, regulatory hurdles and limited cargo capacity. To overcome these limitations, various non-viral approaches have been actively investigated as more flexible and sustainable alternatives for next-generation T cell engineering. As one particular area of interest, recent advances in such non-viral delivery technologies have paved the way for exploring RNA therapeutics as a safe and versatile tool to modulate T cell phenotype and functionality. Therefore, to

showcase the potential of non-viral delivery of RNA in therapeutic T cell engineering, we characterized different classes of RNA therapeutics and provided an extensive overview of established and upcoming non-viral T cell transfection techniques, including membrane permeabilization-based and carrier-based methods. We then elaborated on specific applications of RNA molecules in preclinical and clinical investigations, including transient expression of tumor antigen-specific receptors, immune checkpoint disruption and gene editing towards generating “off-the-shelf” CAR T cells.

Among alternative non-viral technologies, photoporation has recently emerged as a versatile physical delivery method, applicable to a broad range of cell types and cargo molecules. This technique relies on the combination of photo-responsive nanomaterials and pulsed laser irradiation to achieve transient plasma membrane permeabilization by distinct photothermal effects, allowing external molecules to enter the cytosol. Given the enhanced anti-tumor efficacy of CAR T cell products enriched in minimally differentiated phenotypes and the imperative of shortening the vein-to-vein time for the benefit of rapidly progressing patients, in this PhD thesis, we investigated the applicability of photoporation for intracellular delivery in unstimulated human T cells. In addition, in light of future technology translation, we sought to understand the impact of photoporation treatment on cell phenotype and functionality. To address safety and regulatory concerns related to most used gold nanoparticles (AuNPs) known to fragment under laser irradiation and intercalate with cellular DNA, in this PhD work, two recent modifications of photoporation technology have been employed, which either replace standard metallic NPs with biodegradable photosensitizers (**Chapter 2**), or eliminate direct contact between cells and NPs (**Chapter 3**).

In **Chapter 2**, we developed an alternative nanosensitizer based on biocompatible and biodegradable polydopamine nanoparticles (PDNPs), functionalized with bovine serum albumin (BSA) for increased colloidal stability. To account for size difference between unstimulated and expanded T cells, we synthesized and characterized PDNPs of nominal sizes of 150, 250 and 400 nm. Next, by extensive screening of PDNP concentrations and laser fluences, we identified optimal conditions that generated high delivery yields of model FITC-dextran 500 kDa in both T cell phenotypes. In unstimulated T cells, the maximal delivery yields were obtained with the smallest 150 nm PDNPs, while

intermediate 250 nm PDNPs turned out most optimal for the treatment of pre-activated and expanded T cells. For both cell models, delivery yields achieved with PDNP-sensitized photoporation clearly exceeded those described previously for AuNP-mediated photoporation in the Jurkat cell line and stimulated primary human T cells. Besides high delivery efficiency, intracellular delivery for therapeutic cell engineering requires the preservation of T cell function to maximize treatment efficacy. Therefore, for the optimized conditions, we investigated the propensity of quiescent T cells to become activated after PDNP-photoporation as a measure of T cell functionality. By analyzing cell proliferation, expression of surface activation markers and cytokine production, we found that T cell treatment with 150 and 250 nm PDNPs had a minimal impact on T cell activation propensity. In contrast, cells irradiated with 400 nm PDNPs showed diminished proliferation capacity and aberrant cytokine production, suggesting persistent phenotypic alterations after laser treatment. Altogether, our results demonstrated that PDNP-photoporation is a promising strategy for intracellular delivery in quiescent T cells, however nanosensitizer size should be carefully optimized to avoid excessive cell damage.

To alleviate any remaining concerns over cell exposure to free nanoparticles and pave the way for clinical translation of photoporation, we developed a photothermal system, in which light-responsive iron oxide nanoparticles (IONPs) are embedded in polycaprolactone nanofiber meshes fabricated by electrospinning. In this approach, laser irradiation of T cells sedimented on such photothermal electrospun nanofiber (PEN) substrates permits the effective transfer of photothermal effects for transient plasma membrane permeabilization, while direct contact between cells and NPs is avoided. In **Chapter 3**, we evaluated the applicability of this novel photoporation modality for intracellular delivery of model FITC-dextran 150 kDa in unstimulated and expanded human T cells. Using inductively coupled plasma tandem mass spectrometry, we first confirmed that no significant iron release from fibers occurred after laser activation of PEN substrates with laser fluences up to 0.36 J cm^{-2} . Next, we optimized photoporation protocols by varying IONP content in PEN substrates and laser fluences, demonstrating successful delivery of model FD150 in both resting and pre-activated T cells, with delivery efficiencies of 55-60%. As for PDNP-mediated photoporation, we studied the functional consequences of applying different irradiation settings by analyzing T cell activation after

PEN treatment. We found a short-term modulation of a limited subset of cytokines, however no impact on the expression of surface activation markers or long-term proliferation capacity of PEN-treated T cells.

Together, results presented in this PhD thesis attest to the applicability of PDNP-sensitized photoporation and PEN-photoporation for safe and effective intracellular delivery in unstimulated and pre-activated human T cells, providing relevant insights for further optimization of photoporation technology towards functional T cell engineering.

In **Chapter 4**, we presented a broader international context of this dissertation and indicated future directions in the field of engineered T cell therapy. First, we summarized the progress in developing T cell-based immunotherapies and pointed out the remaining challenges related to T cell biological activity upon adoptive transfer and manufacturing limitations restricting wider clinical adoption. Regarding the therapeutic efficacy of engineered T cells, we discussed the importance of optimizing manufacturing protocols to augment T cell fitness, providing a broader rationale for our interest in engineering T cells without prior activation step. As another strategy to increase T cell anti-tumor efficacy and mitigate toxicity, multiple novel genetic engineering designs have been developed, focusing on improved antigen recognition, resistance to immunosuppressive signals in the tumor microenvironment and modulating CAR T cell persistence with remote control switches. On the other hand, to overcome manufacturing bottlenecks and increase the accessibility to CAR T cell therapy, non-viral transfection technologies present a significant potential as a safe, flexible and cost-effective alternative to viral vector-based manufacturing. Such non-viral methods could be incorporated into closed and automated, GMP-compliant cell manufacturing platforms towards decentralized or point-of-care CAR T cell manufacturing, providing a breakthrough in patient access. Lastly, the emerging “off-the-shelf” allogeneic CAR T cell products generated with cells obtained from healthy donors could offer a new treatment opportunity for patients who could not benefit from autologous therapy due to, *e.g.*, poor quality of lymphocytes or rapidly progressing disease.

SAMENVATTING EN CONCLUSIES

Adoptieve T-celtherapieën (ACT) hebben een aanzienlijk potentieel om de behandeling van kanker te transformeren door het immuunsysteem in te zetten om kwaadaardige cellen aan te vallen. Onder verschillende ACT-modaliteiten, hebben chimere antigeenreceptor (CAR)-gemanipuleerde T-celtherapieën –berustende op *ex vivo* genetische modificatie om T-celspecificiteit te transformeren met een synthetische receptor tegen een tumorantigen – opmerkelijke klinische effectiviteit aangetoond bij patiënten met bepaalde hematologische maligniteiten. Met zes CAR T-celproducten die tot nu toe zijn goedgekeurd door de FDA en meer dan 800 lopende klinische onderzoeken, blijven CAR T-celtherapieën de meest onderzochte vorm van adoptieve celtransfer in de immuno-oncologische pijplijn, waarbij de wereldwijde CAR T-celmarkt naar verwachting beduidend zal groeien in de loop van het volgende decennium. Ondanks deze goede toekomstperspectieven, moeten er nog verschillende beperkingen worden aangepakt om het CAR-T-celpotentieel ten volste te benutten in een breed scala aan indicaties en grotere patiëntengroepen.

Zoals uiteengezet in Hoofdstuk 1, staan CAR T-celtherapieën voor verschillende uitdagingen die verband houden met de biologische activiteit van de gemanipuleerde celproducten, waaronder een slechte werkzaamheid bij solide tumoren, beperkte duurzaamheid van de respons in de patiënt, en risico op ernstige bijwerkingen zoals *cytokine-release-syndroom* en neurotoxiciteit. Daarom is de consensus dat verdere vooruitgang in combinatorische CAR-T-celtherapiedesigns vereist is die zich focussen op meerdere targets, verstoring van negatieve regulators van de T-celfunctie, extra functionaliteiten (*e.g., de novo* cytokineproductie) of integratie van veiligheidsschakelaars. Een cruciaal aspect in het realiseren van dergelijke geavanceerde engineeringstrategieën, is de selectie van geschikte transfectietechnologieën die evoluerende CAR-constructies, gen-modificerende-componenten en/of complementaire moleculen kunnen accommoderen en effectief kunnen leveren om de T-celpotentie te moduleren bij herinfusie bij patiënten. Tot op heden is de productie van CAR-T-cellen afhankelijk van gammaretrovirale en lentivirale vectoren voor een efficiënte afgifte van transgenen. Het gebruik ervan brengt echter een aantal nadelen met zich mee, zoals

bezorgdheid over de veiligheid, hoge kosten, hindernissen op het gebied van regelgeving en een beperkte laadcapaciteit. Om deze beperkingen te overwinnen, worden verschillende niet-virale benaderingen actief onderzocht als flexibelere en duurzamere alternatieven voor T-celtechnologieën van de volgende generatie. Vanwege de bijzonder grote interesse in dit gebied, hebben recente ontwikkelingen in dergelijke niet-virale afgiftetechnologieën de weg geëffend voor het verkennen van RNA-therapeutica als een veilig en veelzijdig hulpmiddel om het fenotype en de functionaliteit van T-cellen te moduleren. Om het potentieel van niet-virale levering van RNA in therapeutische T-celtechnologieën te demonstreren, beschouwen we daarom verschillende klassen van RNA-therapeutica en geven we een uitgebreid overzicht van reeds gevestigde en opkomende niet-virale T-celtransfectietechnieken, waaronder op membraanpermeabilisatie- en vehikel-gebaseerde transfectietechnieken. Vervolgens gingen we dieper in op specifieke toepassingen van RNA-moleculen in (pre)klinisch onderzoek, waaronder kortstondige expressie van tumorantigeen-specifieke receptoren, verstoring van het immuuncontrolepunt en genetische modificatie voor het genereren van *off-the-shelf* CAR T-cellen.

Onder alternatieve niet-virale technologieën, is fotoporatie recentelijk naar voren gekomen als een veelzijdige fysieke afleveringsmethode, toepasbaar op een breed gamma aan celtypen en af te leveren moleculen. Deze techniek is gebaseerd op de combinatie van fotogevoelige nanomaterialen en gepulseerde laserbestraling om voorbijgaande plasmamembraanpermeabilisatie te bereiken door verschillende fothermische effecten, waardoor externe moleculen het cytosol kunnen bereiken. Gezien de verbeterde antitumorwerking van CAR T-celproducten verrijkt wordt door minimaal gedifferentieerde fenotypes en de noodzaak om de ader-tot-adertijd te verkorten ten voordele van snel achteruitgaande patiënten, onderzochten we in dit proefschrift de toepasbaarheid van fotoporatie voor intracellulaire aflevering in niet-gestimuleerde menselijke T-cellen. Bovendien probeerden we, in het licht van toekomstige toepassingen, de impact van fotoporatiebehandeling op celfenotype en -functionaliteit te begrijpen. Om veiligheids- en regelgevingskwesaties aan te pakken die verband houden met de meest gebruikte gouden nanodeeltjes (AuNP's), waarvan bekend is dat ze fragmenteren onder laserbestraling en intercaleren met cellulair DNA, zijn in dit

doctoraatsproefschrift twee recente modificaties van fotoporatietechnologie gebruikt, die of standaard metalen NP's vervangen door biologisch afbreekbare fotosensitieve NP's (Hoofdstuk 2), of direct contact tussen cellen en NP's elimineren (Hoofdstuk 3).

In Hoofdstuk 2 hebben we een alternatieve nanosensitizer ontwikkeld op basis van biocompatibele en biologisch afbreekbare polydopamine nanodeeltjes (PDNP's), gefunctionaliseerd met runderserumalbumine (BSA) voor verhoogde colloïdale stabiliteit. Om rekening te houden met het verschil in grootte tussen niet-gestimuleerde en geëxpandeerde T-cellen, hebben we PDNP's met nominale afmetingen van 150, 250 en 400 nm gesynthetiseerd en gekarakteriseerd. Vervolgens identificeerden we door uitgebreide screening van PDNP-concentraties en laserenergiedichtheden optimale parameterinstellingen die hoge afleveringsopbrengsten genereerden van FITC-dextran 500 kDa modelmoleculen in beide T-celfenotypes. In niet-gestimuleerde T-cellen werden de maximale afleveringsopbrengsten verkregen met de kleinste 150 nm PDNP's, terwijl tussenliggende 250 nm PDNP's het meest optimaal bleken voor de behandeling van vooraf-geactiveerde en geëxpandeerde T-cellen. Voor beide celmodellen overtroffen de afleveringsopbrengsten die werden bereikt met PDNP-ge-sensibiliseerde fotoporatie duidelijk die eerder beschreven voor AuNP-gemedieerde fotoporatie in de Jurkat-cellijn en gestimuleerde primaire menselijke T-cellen. Naast een hoge afleveringsefficiëntie, vereist intracellulaire aflevering voor therapeutische celtechnologie het behoud van de T-celfunctie om de effectiviteit van de behandeling te maximaliseren. Daarom hebben we voor de geoptimaliseerde parameterinstellingen de neiging van T-cellen in rust om geactiveerd te worden na PDNP-fotoporatie onderzocht als een maat voor de T-celfunctionaliteit. Door celproliferatie, expressie van activeringsmerkers aan het celoppervlak en cytokineproductie te analyseren, ontdekten we dat T-celbehandeling met 150 en 250 nm PDNP's een minimale invloed had op de neiging tot T-celactivering. Daarentegen vertoonden cellen bestraald na behandeling met 400 nm PDNP's een verminderde proliferatiecapaciteit en afwijkende cytokineproductie, wat wijst op aanhoudende fenotypische veranderingen na laserbehandeling. Al met al toonden onze resultaten aan dat PDNP-fotoporatie een veelbelovende strategie is voor intracellulaire afgifte in rustende T-cellen, maar de grootte van de nanosensitizer moet zorgvuldig worden geoptimaliseerd om overmatige celbeschadiging te voorkomen.

Om eventuele resterende zorgen over blootstelling van cellen aan vrije nanodeeltjes weg te nemen en de weg vrij te maken voor klinische vertaling van fotoporatie, hebben we een fotothermisch systeem ontwikkeld, waarin op licht reagerende ijzeroxide-nanodeeltjes (IONP's) zijn ingebed in een netwerk van polycaprolacton nanovezels vervaardigd door elektrospinning. In deze benadering, maakt laserbestraling van T-cellen die zijn gesedimenteerd op dergelijke fotothermische elektrogeweven nanovezel (PEN)-substraten de effectieve overdracht van fotothermische effecten mogelijk voor kortstondige plasmamembraanpermeabilisatie, terwijl direct contact tussen cellen en NP's wordt vermeden. In Hoofdstuk 3 evalueerden we de toepasbaarheid van deze nieuwe fotoporatiemodaliteit voor intracellulaire afgifte van FITC-dextran 150 kDa (FD150) modelmoleculen in ongestimuleerde en geëxpandeerde menselijke T-cellen. Met behulp van inductief-gekoppelde plasma-tandemmassaspectrometrie hebben we eerst bevestigd dat er geen significante ijzerafgifte uit vezels optrad na laserirradiatie van PEN-substraten met laserfluenties tot $0,36 \text{ J cm}^{-2}$. Vervolgens hebben we fotoporatieprotocollen geoptimaliseerd door het IONP-gehalte in PEN-substraten en laserenergiedichtheden te variëren, wat een succesvolle aflevering van FD150 in zowel rustende als vooraf-geactiveerde T-cellen aantoont, met afleveringsefficiënties van 55-60%. Wat betreft PDNP-gemedieerde fotoporatie, bestudeerden we de functionele gevolgen van het toepassen van verschillende bestralingsinstellingen door T-celactivering na PEN-behandeling te analyseren. We vonden een kortetermijnmodulatie van een beperkte subset van cytokines, maar geen invloed op de expressie van oppervlakte-activatiemerkers of de proliferatiecapaciteit op lange termijn van met PEN behandelde T-cellen.

Samen getuigen de resultaten gepresenteerd in dit proefschrift over de toepasbaarheid van PDNP-geïmpregneerde fotoporatie en PEN-fotoporatie voor veilige en effectieve intracellulaire aflevering in niet-gestimuleerde en vooraf-geactiveerde menselijke T-cellen, wat relevante inzichten oplevert voor verdere optimalisatie van de fotoporatietechnologie richting functionele T-cel-engineering.

In Hoofdstuk 4 presenteren we een bredere internationale context van dit proefschrift en gaven we toekomstige richtingen aan op het gebied van gemanipuleerde T-celtherapie. Eerst hebben we de vooruitgang samengevat in de ontwikkeling van op T-cellen-

gebaseerde immunotherapieën en gewezen op de resterende uitdagingen met betrekking tot de biologische activiteit van T-cellen bij adoptieve overdracht en productiebeperkingen die een bredere klinische acceptatie beperken. Met betrekking tot de therapeutische werkzaamheid van gemanipuleerde T-cellen, bespraken we het belang van het optimaliseren van productieprotocollen om de T-celfitheid te vergroten, wat een bredere reden is voor onze interesse in het ontwikkelen van T-cellen zonder voorafgaande activeringsstap. Als een andere strategie om de anti-tumoreffectiviteit van T-cellen te vergroten en de toxiciteit te verminderen, zijn er meerdere nieuwe ontwerpen voor genetische manipulatie ontwikkeld, gericht op verbeterde antigenherkenning, weerstand tegen immunosuppressieve signalen in de micro-omgeving van de tumor en modulerende CAR T-celpersistentie met op-afstand-gecontroleerde-schakelaars. Aan de andere kant bieden niet-virale transfectietechnologieën een aanzienlijk potentieel als een veilig, flexibel en kosteneffectief alternatief voor productie op basis van virale vectoren om productieknelpunten te overwinnen en de toegankelijkheid tot CAR T-celtherapie te vergroten. Dergelijke niet-virale methoden kunnen worden opgenomen in gesloten en geautomatiseerde, GMP-conforme celproductieplatforms voor gedecentraliseerde of *point-of-care* CAR T-celproductie, wat een doorbraak betekent in de toegang voor patiënten. Ten slotte zouden de opkomende *off-the-shelf* allogene CAR T-celproducten, die zijn gegenereerd met cellen die zijn verkregen van gezonde donoren, een nieuwe behandelingsmogelijkheid kunnen bieden aan patiënten die geen baat kunnen hebben bij autologe therapie vanwege, bijvoorbeeld, een slechte kwaliteit van lymfocyten of snelle progressie van de pathologie.

CURRICULUM VITAE

PERSONALIA

Name	Berdecka
First names	Dominika
Nationality	Polish
Place of birth	Krakow, Poland
Date of birth	17/06/1991
Personal address	Savaanstraat 88/201 9000 Ghent
Email	dberdecka@gmail.com
Telephone	+32 487 84 78 55
Professional address	Laboratory for General Biochemistry and Physical Pharmacy, Faculty of Pharmaceutical Sciences, Ghent University Ottergemsesteenweg 460 9000 Gent Belgium
Telephone (professional)	+32 9 264 80 47 (secretary)
Email (professional)	dominika.berdecka@ugent.be
Websites	https://www.ugent.be/fw/pharmaceutics/ biochemphypharm/en/team/dominikaberdeca.htm https://www.researchgate.net/profile/ Dominika-Berdecka

EDUCATION AND RESEARCH EXPERIENCE

- 2016-2019 Early Stage Researcher Fellowship within Tendon Therapy Train
Marie Skłodowska-Curie Innovative Training Network
3B's Research Group, University of Minho, Portugal
- 2013-2015 Master of Science in Biochemistry
Jagiellonian University, Krakow, Poland
- Master thesis:
Optimization of in vitro culture of murine bone marrow-derived mesenchymal stem/ stromal cells (MSC) for the bioactive microvesicle isolation.
- Promotor: Prof. Ewa Zuba-Surma
- 2010-2013 Bachelor of Science in Biochemistry
Jagiellonian University, Krakow, Poland

LANGUAGES

- Polish Native language
- English Professional proficiency
- German Basic proficiency
- Portuguese Basic proficiency

INTERNATIONAL PEER-REVIEWED PUBLICATIONS

D. Berdecka, A. Harizaj, I. Goemaere, D. Punj, G. Goetgeluk, S. De Munter, H. De Keersmaecker, V. Boterberg, P. Dubruel, B. Vandekerckhove, S.C. De Smedt, W.H. De Vos, K. Braeckmans, Delivery of macromolecules in unstimulated T cells by photoporation with polydopamine nanoparticles, *Journal of Controlled Release*. 354 (2023) 680–693 (IF = 11.47)

R. Xiong, D. Hua, J. Van Hoeck, **D. Berdecka**, L. Léger, S. De Munter, J.C. Fraire, L. Raes, A. Harizaj, F. Sauvage, G. Goetgeluk, M. Pille, J. Aalders, J. Belza, T. Van Acker, E. Bolea-Fernandez, T. Si, F. Vanhaecke, W.H. De Vos, B. Vandekerckhove, J. van Hengel, K. Raemdonck, C. Huang, S.C. De Smedt, K. Braeckmans, Photothermal nanofibres enable safe engineering of therapeutic cells, *Nat Nanotechnol*. 16 (2021) 1281–1291 (IF = 40.50)

S.P.B. Teixeira, R.M.A. Domingues, P.S. Babo, **D. Berdecka**, M.S. Miranda, M.E. Gomes, N.A. Peppas, R.L. Reis, Epitope-Imprinted Nanoparticles as Transforming Growth Factor- β 3 Sequestering Ligands to Modulate Stem Cell Fate, *Adv Funct Mater.* 31 (2021)

A.I. Gonçalves, **D. Berdecka**, M.T. Rodrigues, A.D. Eren, J. de Boer, R.L. Reis, M.E. Gomes, Evaluation of tenogenic differentiation potential of selected subpopulations of human adipose-derived stem cells, *J Tissue Eng Regen Med.* 13 (2019) 2204–2217

R. Costa-Almeida, **D. Berdecka**, M.T. Rodrigues, R.L. Reis, M.E. Gomes, Tendon explant cultures to study the communication between adipose stem cells and native tendon niche, *J Cell Biochem.* 119 (2018)

I. Calejo, R. Costa-Almeida, A.I. Gonçalves, **D. Berdecka**, R.L. Reis, M.E. Gomes, Bi-directional modulation of cellular interactions in an in vitro co-culture model of tendon-to-bone interface, *Cell Prolif.* 51 (2018)

A. Labeledz-Maslowska, B. Lipert, **D. Berdecka**, S. Kedracka-Krok, U. Jankowska, E. Kamycka, M. Sekula, Z. Madeja, B. Dawn, J. Jura, E.K. Zuba-Surma, Monocyte chemoattractant protein-induced protein 1 (MCP1) enhances angiogenic and cardiomyogenic potential of murine bone marrow-derived mesenchymal stem cells, *PLoS One.* 10 (2015)

Submitted/In preparation

D. Berdecka, M. Minsart, T. Lu, D. Punj, R. De Rycke, M. Nikolić, E. Bolea-Fernandez, F. Vanhaecke, R. Xiong, S.C. De Smedt, P. Dubruel, W. H. De Vos and K. Braeckmans, Photothermal nanofibers enable macromolecule delivery in unstimulated human T cells. *Under revision in Applied Materials Today.*

D. Berdecka, S.C. De Smedt, W. H. De Vos and K. Braeckmans, Non-viral delivery of RNA for therapeutic T cell engineering. *Prepared for submission in Advanced Drug Delivery Reviews.*

CONFERENCES WITH POSTER PRESENTATIONS

2022 International Conference on Lymphocyte Engineering,
Munich, Germany

2022 International Graduate Symposium on Biopharmaceuticals,
Suzhou, China (online)

TEACHING AND SUPERVISION

- 2019-2023 Lab instructor for Pharmaceutical Bachelor Thesis (FaBaP)
- 2019-2020 Supervisor for Master thesis (Ghent University, Ghent)
Rebecca Vrielinck: Master in Pharmaceutical Care
Methods to enhance the permeability of cells and tissues
- 2020-2021 Supervisor for Master thesis (Ghent University, Ghent)
Julie Lavens: Master in Pharmaceutical Care
Nanofibrous scaffolds for bioactive compound delivery in cell therapy and tissue engineering
- 2021-2022 Supervisor for Bachelor thesis (Odisee Hogeschool, Ghent)
Cathérine Steyaert
Pharmacological supplementation to improve the quality of therapeutic cells engineered by photoporation

COURSES

- 2019 Light and Fluorescence Microscopy, Ghent University
- 2019 From Pictures to Numbers, University of Antwerp
- 2019 Leadership and Efficiency: Leadership Foundation,
Ghent University
- 2020 Research and Valorization: Research Data Management,
Ghent University
- 2020 Communication Skills: Delivering your presentation remotely,
Ghent University
- 2021 qPCR course, Biogazelle
- 2021 Cancer, CRIG